University of Southampton
Faculty of Physical Sciences and Engineering
Physics and Astronomy

Gauge/string duality for strong interactions

by

Konstantinos Christos Rigatos

A thesis submitted for the degree of
Doctor of Philosophy

February 3, 2022

UNIVERSITY OF SOUTHAMPTON

ABSTRACT

FACULTY OF PHYSICAL SCIENCES AND ENGINEERING

PHYSICS AND ASTRONOMY

Thesis for the degree of Doctor of Philosophy

GAUGE/STRING DUALITY FOR STRONG INTERACTIONS

by Konstantinos Christos Rigatos

In this thesis we focus on the study of strongly interacting systems using the gauge/gravity duality. We begin by providing an overview of the history of string theory and we briefly describe the basic properties of QCD and the $\mathcal{N} = 4$ super Yang-Mills. There are some warm up chapters, where we build our understanding on the basic facets of the AdS/CFT, namely field dynamics in AdS and some basic statements about conformal field theories. After that, we describe how it is possible to introduce fundamental degrees of freedom in the context of the AdS/CFT duality and we motivate the bottom-up holographic approach. We are using all probe-brane setups in the type IIA and type IIB theories that preserve eight supercharges in order to study the dynamics and mass spectra of spin-$\frac{1}{2}$ fields. We are allowing for higher dimensional interactions and we examine their effect on the spectrum. Using this knowledge, which stems from the formal top-down constructions, we proceed to use Dynamic AdS/Yang-Mills in order to obtain holographic predictions for models in which the Higgs is a composite state. We end this thesis by providing our proposals for future work.

Table of Contents

List of Figures

List of Tables

Declaration of Authorship

I, Konstantinos Christos Rigatos, declare that this thesis entitled *Gauge/string duality for strong interactions* and the work presented in it are my own and have been generated by me as the result of my own original research.

I confirm that:

1 This work was done wholly or mainly while in candidature for a research degree at this University;

2 Where any part of this thesis has previously been submitted for a degree or any other qualification at this University or any other institution, this has been clearly stated;

3 Where I have consulted the published work of others, this is always clearly attributed;

4 Where I have quoted from the work of others, the source is always given. With the exception of such quotations, this thesis is entirely my own work;

5 I have acknowledged all main sources of help;

6 Where the thesis is based on work done by myself jointly with others, I have made clear exactly what I have contributed myself;

7 Either none of this work has been published before submission, or parts of this work have been published as [1–4]. I have also collaborated in [5, 6] and single-authored [7, 8], the contents of which are not covered in this thesis.

Signed:

Date:

Acknowledgements

First and foremost, I would like to express my graditude to my supervisor Nick Evans for his guidance, patience and collaboration over the course of my PhD. Thank you for always being open to my questions and sharing your physics intuition. I have learned a lot from you. You truly are the Gandalf of physics. Thanks for introducing me to the music of Marillion and the football chats.

It is, also, a pleasure to thank James Drummond for our collaboration as well as many interesting discussions. Thank you for sharing your time enthusiastically.

Both Nick and James are great guys and they have suffered in silent from my stupid questions. Each of them had always a different way of guiding me to a proper way of phrasing and answering my physics concerns. I have benefited and learned a lot from both of you.

I am, also, very grateful to all my collaborators: many thanks to Johanna Erdmenger and Werner Porod for many stimulating discussions, to Hynek Paul for detailed explanations and practical help with Mathematica. It has been a pleasure to have worked with Dhritiman Nandan, Raimond Abt, and Theodoros Nakas. I want to thank Michele Santagata for our latest physics adventure and the many interesting discussion sessions we have had so far. Last, but certainly not least, I am grateful to Xinan Zhou for our common journey in the uncharted waters of holographic correlators.

I am very lucky to have friends back in Greece who have been very understanding and supporting during the time I have been away. Thanks to Kostas, George, Ermis, Stam, Dimosthenis and George, for always being available and willing to share a beer when I was getting back home. Additionally, I was very lucky to have met wonderful people during my time in Southampton that created a wonderful atmosphere. Thanks to Jack, Stefan, Michele, Hynek, Stanislav, Sami, Adam, Matt, Sam, Elena, Ross, Aaron and Federico.

Finally, none of this would have been possible without the unconditional love and support of my parents, Dora and Sotiris, and my sister, Artemis. To Andria, thank you for these amazing last six years, and for being a constant source of happiness in my life. To those people, sorry for not being the best version of myself in our relationships during the course of my PhD. A final special thanks from the depths of my heart for being very close no matter how far.

To anyone who is reading this thesis, my apologies...

Dedicated to my family

To ma, for teaching me the virtues of patience and perseverance

To sis, for always having something funny to say

To da, who would be the only family member able to understand it, but time took him too early

Part I

Introduction

Chapter 1

Prolegomena

Physics has seen tremendous advancements these past years. One of the most astounding achievements of modern theoretical physics is the development of quantum field theory (QFT). QFT is a well-defined mathematical framework that unifies successfully the fundamental principles of special relativity and those of quantum mechanics. The original motivation was the study of interactions amongst elementary particles, however, nowadays we have seen that its applications are ranging from cosmology to systems of condensed matter physics.

One of the most important approaches within physics is the so-called model building, namely the efforts that the community is making in order to construct models that successfully describe the different phenomena in nature. Within the framework of QFT the model building approach has led to the theoretical development of the standard model of particle physics. This is a non-Abelian gauge theory described by the group $SU(3) \times SU(2) \times U(1)$ providing us with a framework for three fundamental interactions of nature: the strong nuclear force, the weak nuclear force, and electromagnetism. The only fundamental interaction in nature that does not fall within the structure of the standard model is gravity. There have been extensive experimental studies for many years which has led to very high precision tests of the standard model and by now it is very well established both theoretically and experimentally.

The $SU(3)$ part of the standard model describes the strong nuclear force, namely the interactions of quarks and gluons. This theory is known by the name quantum chromodynamics (QCD) and hitherto is the most successful theory that we possess in order to describe the strong interactions in the nucleus. When approaching the high-energy regime of the theory, the interactions become weaker and this is a property of the theory that has been dubbed asymptotic freedom. On the other hand, when examining the low-energy limit, we find that QCD gets strongly coupled. This is the regime of the theory that involves the physics related to its bound-states, i.e hadrons.

For the high-energy/weak coupling limit of the theory we can use perturbation theory in order to perform our studies. The low-energy/strong coupling regime of the theory remains a very difficult and interesting problem until today. One approach that is being widely used to study QCD in the strong-coupling limit is to consider putting the theory on a discretized spacetime. This is called lattice

QCD [9] and is the most successful and accurate tool at our disposal for this purpose. While it has provided us with a wealth of results - mainly for the hadronic spectrum of the theory - there are two main disadvantages. To begin with, the results obtained are mainly numerical and analytic results are scarce, if any at all. This yields the question of how much intuition we can obtain based on numerics only. Additionally, lattice studies fail to provide results for dynamical quantities and finite chemical potential phenomena.

It is worthwhile noting that we can think the above situation a bit more broadly and generalize the above statement. In other words we can phrase this issue more widely in the sense that we do not have a well-developed, systematic and analytic method to perform studies in the strong-coupling limit of a general QFT.

The above provides us with a general and very interesting question that evades a well-understood, analytic answer for many years. As is usual in physics, we have come up with some ways to bypass the issue. One approach is to add symmetries to the QFT, such as conformal symmetry and/or supersymmetry. Integrability is another invaluable tool in the study of strongly coupled gauge theories, as theories that exhibit the homonymous property are solvable for any value of the gauge coupling. Another approach is to try and identify a second and distinct theory that appears to be different, but describes the same physics as the original one. This is what we call a duality.

For many years, one of the most typical approaches pertaining to the study of strongly coupled gauge theories has been to focus on their supersymmetric cousins. Supersymmetry is a symmetry that exchanges bosonic degrees of freedom and fermionic ones. Whether supersymmetry will be realized in nature as a physical symmetry or will remain an invaluable mathematical tool is still an open question. The hope is that future collider experiments will shed light on the matter and provide us with a conclusive answer. From a purely field theoretical perspective, supersymmetry imposes strong enough constraints that allows an analytic study of phenomena at strong coupling. Examples of the aforementioned constraints are a plethora of non-renormalization theorems [10, Chapter 8] and the supesymmetric localization approach [11]. Based on the two aforementioned properties we have been able to study precisely the moduli space of a theory and obtain correlation functions of certain operators respectively.

Furthermore, there exists another special class of QFTs that have additional symmetries and we call these conformal field theories (CFTs). CFTs have no intrinsic scale or mass and are more constrained, compared to theories without conformal symmetry, due to the fact of the extra symmetries that appear. In any given CFT we know the results for the two-point and three-point functions, since they are fixed by the presence of conformal symmetry. In recent years we have seen the revival of an old idea which is based on the use of first-principle consistency conditions in order to solve a theory. This is the conformal bootstrap program, which dates back to the original work of Polyakov [12] and independently by Ferrara, Gatto and Grillo [13] and Mack [14] and was reignited by Rattazzi, Rychkov, Tonni, and Vichi [15]. The most impressive result that the modern conformal bootstrap has offered is the very high-precision determination of operator product expansion (OPE) coefficients and the conformal dimensions of operators in the three-dimensional Ising model [16, 17].

At this point the most natural, perhaps, question is how far we can get with our studies and how much intuition we can obtain about phenomena at strong coupling if we consider the combination of the supersymmetry generators and the conformal algebra. The resulting theory is called a superconformal field theory (SCFT). At this point we would like to make a clarification. A SCFT does not contain just the supersymmetry and conformal symmetry generators, but also an extra ingredient, which is called conformal supercharge. This is necessary for the closure of the algebra. Now, it should be obvious that a SCFT is more constrained than what one might expect by combining supersymmetry and conformal symmetry, as it contains extra generators as we already mentioned. Owing to the nature of the SCFTs we can attempt to get a bit greedier in our studies and not just focus on a given theory to examine, but rather ask the question of whether or not we are able to uncover the phase space of consistent SCFTs and solve them. This has been a very rich area of research over the past years and much progress has been made when enough supersymmetry is present. We refer the interested reader to the excellent lectures [18, 19] - and references therein - for the current status of the above discussion.

An important related development came from the integrability side and it is the discovery of the Quantum Spectral Curve (QSC). The QSC describes the non-perturbative spectrum of anomalous dimensions of the single-trace operators of the theory. The QSC has been derived for the case of the four-dimensional $\mathcal{N} = 4$ SYM as well as the ABJM theory. For details and more developments, we suggest to the reader the recent review [20].

In addition to the above techniques, we can also use the idea of dualities, as we have already mentioned, which is very useful when examining strongly coupled QFTs. Before discussing the AdS/CFT duality, which is the main topic of this thesis, we want to mention one historic example. We are referring to the equivalence of the massive Thirring model and the sine-Gordon model. Both of them are two-dimensional QFTs. In the first case the fundamental degrees of freedom are fermi fields, while in the latter there are bosons. These two theories might seem to be very different at first, but it was proven that at a quantum level they are equivalent [21].

Another approach of studying gauge theories at their strong coupling limit came from string theory developments. Since the late nineties we have understood that string theory contains non-perturbative objects which have been named D-branes [22]. D-branes are higher-dimensional planes, in the ten-dimensional spacetime where string theory is defined, on which open strings can have their endpoints. If we take a number, N_c, of D3-branes, and examine the low-energy limit of the degrees of freedom of the open strings , we get a superconformal field theory in a four dimensional spacetime; the $\mathcal{N} = 4$ super Yang-Mills (SYM) theory. On the other hand, D3-branes are solitonic solutions of the type IIB theory with a well-defined metric and fluxes. In the low-energy limit, which consists of examining the near-horizon limit of the metric, we end-up having a supergravity theory in $AdS_5 \times S^5$, with AdS_5 denoting a five dimensional anti-de Sitter space and we have used S^5 to denote a five dimensional sphere.

Based on these two different descriptions of D3-branes, Maldacena suggested the identification of the resulting theories at low-energies [23]. This is the AdS/CFT correspondence and in its original form it relates the four dimensional $\mathcal{N} = 4$ SYM theory with an $SU(N_c)$ gauge group to type IIB supergravity

in $AdS_5 \times S^5$. It is important to point out that the field theory part of the duality is at strong coupling, while the gravitational description is a weakly coupled supergravity. Since the duality is strong/weak, this provides a very exciting and promising way to understand and study strongly coupled gauge theories by performing computations in a weakly coupled theory, which is under much better control. There are, of course, generalizations of the AdS/CFT that describe different field theories and are based on different D-branes and/or different compactification manifolds.

At this point let us remind the readers that QCD is weakly coupled in its high-energy limit. Thus, in order to derive the dual supergravity description we need the full non-perturbative formulation of string theory which is currently unknown. Be that as it may, progress can still be made in the study of strongly coupled gauge theories. The underlying reason is that many of these theories share similar features and common phenomena which are manifested universally in large classes of those theories.

After all these many years of studying the AdS/CFT, it is generally believed that the situation is more general and does not restrict itself to string theory. This has led to the more general notion of gauge/gravity duality. In other words, we believe that, with some caution, we can map the properties of any gauge theory to an appropriately constructed gravitational bulk description. This is directly related to the study of QCD and QCD-like theories and there have been many efforts to construct simple gravity descriptions of non-supersymmetric and non-conformal field theories that are of interest in the wider high-energy community.

It is worthwhile stressing that the results obtained using the notions above are qualitative. However, the use of gauge/gravity duality has provided a novel method of studying phenomena that were previously inaccessible.

In this thesis, we study various examples of strongly coupled gauge theories that have similar characteristic properties compared to QCD such as quark fields in the fundamental representation of the gauge group and chiral symmetry breaking. Our studies are both in the context of the formal supergravity settings, as well as with an eye towards phenomenological applications by using an appropriately constructed simple gravitational theory.

The structure of this thesis is the following: chapter 2 provides a historical retrospective of string theory. We also briefly mention some basic facts about QCD and the maximally supersymmetric Yang-Mills theory. In chapter 3 is a gentle introduction to the dynamics of fields in an AdS_5 spacetime. We begin by studying a scalar field and derive some central results such as the Breitenlohner-Freedman (BF) bound, the relation of the mass in the bulk to the conformal dimension of the field and the associated unitarity bound. We, furthermore, study extensively spin-1/2 fields which are the main focus of this thesis. In chapter 4 we review some basic facts about the conformal and superconformal symmetry that we feel are necessary in the context of the AdS/CFT. The content of Chapter 5 is an introduction to the main ideas of the AdS/CFT that are necessary ingredients for this thesis. It is by no means an exhaustive exposition to all the ideas behind AdS/CFT in general. Chapter 6 is the final addition to the presentation of the background material and it discusses how we can introduce quarks in the fundamental representation of the gauge group and chiral symmetry breaking in the AdS/CFT picture. It also contains the description of the simple five-dimensional gravity model that we will use for our

phenomenolly related studies.

In chapter 7 we present our original results for the study of fermionic dynamcis and their mass spectra in all possible supersymmetric brane setups. We also discuss the effect that the addition of double-trace interactions has on these systems, and comment on their possible interpretation as baryonic states. Chapter 8 contains our findings and analysis on composite Higgs models using gauge/gavity duality as a tool. Chapter 9 contains our final thoughts and some comments for future research. We have included some appendices at the end to supplement the material covered in this thesis.

We, finally, want to mention that perhaps surprisingly and unconventionally we refrain from attempting an introduction to string theory and/or theories of supergravity. The reason for doing so is that there are many excellent and extended resources that cover these topics and providing a short description of said matters here would be idle. We would like to mention our favourite books that cover these subjects thoroughly. For supergravity and some AdS/CFT topics we strongly suggest the book by Freedman and Van Proeyen [24]. For string theory we suggest the interested reader to go through the book by Becker, Becker, and Schwarz [25]. These have been the two books that we used extensively to get familiar with these topics.[1] We would also like to mention the book by Kiritsis [26] which also covers string theory subjects and a detailed exposition to the AdS/CFT.

[1] We strongly encourage any student reading this thesis to stop reading it and pick one of the aforementioned books for serious study and problem solving.
We also suggest "getting your hands dirty" in the sense of problem solving.

Part II

The saga begins

Chapter 2

Strings, QCD, super Yang-Mills and all that

Here we are loosely following [25, 26] to describe the history of string theory. The section on massive type IIA theory is based on the seminal work [27]. The section on the $\mathcal{N} = 4$ SYM is based on [28] mainly. For the QCD we have used the classic field theory books [29, 30].

2.1 Why strings?

The most natural question that arises when one encounters string theory for the very first time is "why was this theory developed?". A surprising, perhaps, answer is that it started as the wrong framework to a very interesting question. Let us try to explain this a little bit.

By the end of the sixties we had many great experimental data for a wealth of particles and their higher excited states (resonances), a situation which continued throughout the seventies.[1] Other than this amazing discovery it was also understood that some of them were fundamental, while others were composite states. It is only natural that many efforts were made by the community towards understanding as many aspects as possible.

Before the sixties, the work of [32] which showed that quantum mechanical bound states can be grouped together in what nowadays is known as Regge trajectories that each one has a distinct angular momentum. After the many particle discoveries, the community realized that many of the particles were following (almost) linear Regge trajectories, see for example [33]. This observation sparked the interest of constructing a theory describing these composite states with scattering amplitudes of appropriate form. This was achieved in [34] by using properties of the Eüler Γ-function, and this is known as the Veneziano scattering amplitude. The surprising realization came a bit later when it was explained how the said ampltiude has a physical interpretation in the context of describing one-dimensional objects; the strings [35, 36]. While this is a great achievement, at the time physicists were facing some troubles when dealing with strings. To begin with, there was a state of negative mass squared. Furthemore,

[1] A nice summary with the relevant dates can be found here [31].

the theory needed 26 dimensions for consistency. In addition to the above, the theory contained only bosons.

It was around that time that string theory lost its appeal, as the scientific community realized that QCD does a wonderful job describing the physics of strong nuclear interactions. This is what we meant in the beginning when we said that it started as an effort to address a very interesting problem, but ended up being the wrong answer.

Many people stopped examining string models, however, not all efforts stopped at that point. And that is an auspicious situation.

2.2 QCD

Before we continue with the history of string theory, we would like to have an overview of QCD, since it took over for the study of srong interactions. QCD [37–39] is the theory of the strong force. It describes the interactions amongst quarks and gluons. There is a colour charge associated with it and it has three values, namely red, green, and blue. Quarks do not appear free in nature, but rather in bound states only which we call hadrons. This is the phenomenon of confinement. There are two types of hadrons, the baryons and the mesons. Baryons are made by three quark states which have different colours and thus a baryon is a colour singlet (neutral) state of the theory. On the other hand, mesons consist of a quark and an anti-quark. They are also colour singlet states, which means that the quark carries a colour and the anti-quark the anti-colour, in such a way that a cancellation is achieved. Quarks also have six different flavours, which are: up, down, charm, strange, bottom, up. It is worthwhile noting that most of the ordinary hadronic matter is made out of the up and down flavours, as the other ones are much heavier. An example that comes to mind is the proton which is up-up-down and another one the neutron which is up-down-down. This does not mean that there are not exotic states, an example is the Λ-baryon which is up-down-strange.

The Lagrangian of the QCD theory is given by:

$$\begin{aligned} \mathcal{L} &= \bar{\psi}_q \left(i \not{D} - m_q \right) \psi_q - \frac{1}{4} F^a_{\mu\nu} F^{a\mu\nu} \,, \\ \not{D} &= \Gamma^\mu \partial_\mu - i g \Gamma^\mu A^a_\mu t^a \,, \\ F^a_{\mu\nu} &= \partial_\mu A^a_\nu - \partial_\nu A^a_\mu + g f^{abc} A^b_\mu A^c_\nu \,, \end{aligned} \tag{2.1}$$

where in the above ψ_q is a Dirac spinor that represents the quark field and transforms in the fundamental representation of the $SU(3)$. The gluons are the A^a_μ in the adjoint of the colour group, t^a are the eight generators of the group -the Gell-Mann matrices- and f^{abc} are the structure constants. We have also denoted by m_q the masses of the quark fields and g is gauge coupling. Latin indices are colour indices and the Greek letters are spacetime indices. Summation is implied for both types.

For small values of the coupling constant, $g \ll 1$, we can use a perturbative analysis to study the

β-function of the theory. The β-function is defined via [29]

$$\beta(g) = \frac{\partial g}{\partial \log \mu} = \mu \frac{\partial g}{\partial \mu} \,. \tag{2.2}$$

The behaviour of the β-function informs us about the properties of the gauge theory. We can distinguish three cases:

- $\beta > 0$: the coupling constant is small when approaching the low-energy regime of theory and it grows larger in high energies. Equivalently, particles are more attracted to each other as we decrease their relative distance. This behaviour describes Quantum Electro Dynamics (QED).
- $\beta < 0$: the theory exhibits the opposite behaviour from the previous case. The coupling constant is small in the high-energy regime of the theory and becomes much larger when approaching the low-energy description.
- $\beta = 0$: the coupling constant does not run and the theory is conformal.

At one-loop, an $SU(N_c)$ theory with N_f flavour degrees of freedom has a β-function given by:

$$\beta(g) = -\frac{g^3}{(4\pi)^2} \left(\frac{11}{3} N_c - \frac{2}{3} N_f \right) \,. \tag{2.3}$$

The β-function can be determined in terms of the gauge coupling and the expression becomes

$$g^2(\mu) = \frac{g^2(M)}{1 + \frac{g^2(M)}{(4\pi)^2} \left(\frac{11}{3} N_c - \frac{2}{3} N_f \right) \log \left(\frac{\mu^2}{M^2} \right)} \,, \tag{2.4}$$

with μ the scale we are probing and M a reference scale and it can be re-written in a more convenient way as

$$g^2(\mu) = \frac{(4\pi)^2}{\left(\frac{11}{3} N_c - \frac{2}{3} N_f \right) \log \left(\frac{\mu^2}{\Lambda_{QCD}} \right)} \,, \tag{2.5}$$

such that there is only one parameter. As we approach the high-energy limit of the theory, $\mu \to 0$, and quarks behave almost as free particles. This property is called asymptotic freedom [38, 39]. On the other hand, as we probe the small values of μ the coupling becomes very large and quarks are interacting very strongly leading to colour confinement. The QCD scale, Λ_{QCD}, is the scale where the coupling constant diverges and is estimated to be $\Lambda_{QCD} \sim 200$ MeV. Hadrons have a size of the order $\frac{1}{\Lambda_{QCD}}$ [30, 40].

We will base our description on [41]. Another important aspect of field theories is global symmetries. This is particularly true in the low-energy regime of the field theory, where the dynamics are characterized by the the symmetries of the vacuum of the theory. For QCD a good starting point is to consider the three lighest flavours amongst the set of six. These are the up, down, and strange. We can also assume that these types of quarks are massless and this is the so-called chiral limit of the theory. This modifies the Lagragian in the following way:

$$\mathcal{L} = i \bar{\psi}_{q,L} \not{D} \psi_{q,R} + i \bar{\psi}_{q,R} \not{D} \psi_{q,L} - \frac{1}{4} F^a_{\mu\nu} F^{a\mu\nu} \,, \tag{2.6}$$

and we have expressed it in terms of the chiral projections of the spinor fields. The Lagrangian possesses a global $SU(3)_L \times SU(3)_R$ flavour symmetry. This means that we can rotate independently the right-handed components of the left-handed ones and vice versa. It has, also, been argued that we can rotate the chiral projections $\psi_{q,L}$ and $\psi_{q,R}$ by the same phase without causing any changes in the Lagrangian. In other words, we can perform

$$\psi_{q,L} \to \psi'_{q,L} = e^{-i\phi}\psi_{q,L}\,, \qquad \psi_{q,R} \to \psi'_{q,R} = e^{-i\phi}\psi_{q,R}\,, \tag{2.7}$$

and leave the Lagrangian invariant. This is the $U(1)_B$ symmetry. A final symmetry is achieved when we perform a rotation on the chiral components that differs by a sign, that is we have

$$\psi_{q,L} \to \psi'_{q,L} = e^{-ia}\psi_{q,L}\,, \qquad \psi_{q,R} \to \psi'_{q,R} = e^{ia}\psi_{q,R}\,. \tag{2.8}$$

This is the $U(1)_A$ symmetry of the theory. So, we have in total a global symmetry that is $SU(3)_L \times SU(3)_R \times U(1)_B \times U(1)_A$. The $U(1)_A$ is anomalous; it is broken at the quantum level due to quark loops. This is thoroughly discussed in [30].

Of course, quarks are not massless and one has to consider a mass term which is written as

$$m_q\bar{\psi}_{q,L}\psi_{q,R} + m_q\bar{\psi}_{q,R}\psi_{q,L}\,, \tag{2.9}$$

when expressed in terms of the chiral projections. The mass terms mix the different chiral components and hence break the $SU(3)_L \times SU(3)_R$ explicitly. Under the assumption that the masses of the quarks are all equal we have an $SU(3)_V \times U(1)_B$ symmetry for the theory. The $U(1)_B$ is the part that rotates the left- and right-handed projections by the same phase. Under the further assumption that the masses are very small, the chiral symmetry is an approximate symmetry.

One of the most celebrated results in physics is the Higgs mechanism [42–44], which is a particular example of spontaneous symmetry breaking. In QCD, there exists a similar, although distinct, mechanism that spontaneously breaks chiral symmetry and gives dynamical masses to the quarks. The implications of spontaneous symmetry breaking are described in terms of the Nambu-Goldstone theorem. It states that when a global and continuous symmetry is broken spontaneously a number of massless scalar particles (the Nambu-Goldstone bosons) occur. The number of said particles is equal to the number of the broken generators. Note that the Nambu-Goldostone bosons have the same quantum numbers as the broken generators. While QCD has a Lagrangian description, chiral symmetry breaking is understood in terms of the formation of a chiral condensate in the vacuum of the theory. The chiral condensate is a bilinear that is not invariant under the chiral trnasformations but is under the $SU(3)_V$. This chiral condensate acquires a non-trivial vacuum expectation value

$$\langle\bar{\psi}_{q,L}\psi_{q,R} + \bar{\psi}_{q,R}\psi_{q,L}\rangle \neq 0\,. \tag{2.10}$$

2.3 Back to the stringy picture

We have already mentioned that string theory lost its edge compared to QCD, however, nowadays we know that string theory is a very rich subject and contains more than just strings as fundamental degrees of freedom. Below, we mention some historic landmark papers that helped us develop our understanding of the theory.

2.3.1 A new hope - More history

- Generalization of the Veneziano amplitude: the Veneziano amplitude was generalized to the description of N-particle scattering [45]. A further generalization came due to the works of [46, 47]. This has been named the Virasoro-Shapiro amplitude -after the people who worked on it- and it describes the scattering of closed strings.
- Another generalization of the Veneziano amplitude came in 1969, that included isospin factors [48]. This led to the introduction of the Chan–Paton factors that played a crucial role in the development of modern string theory.
- The RNS formalism: the works of [49, 50] showed how to consistenly remove the problematic tachyon from the spectrum of string theory and include fermionic fields. The RNS acronym stands for Ramond, Neveu, Schwarz.
- After that, Scherk and Schwarz [51] and in the independent work of Yoneya [52], studied the patterns that arise from vibrations of strings. They discovered that they match those of the graviton and thus, string theory describes more than originally thought. This led to the systematic study of bosonic string theory.
- Bosonic string theory was formulated in terms of the Polyakov action. The Polyakov action describes the worldsheet of a string, which can be studied in the context of a two-dimensional CFT. It was introduced in [53, 54], however, it is named after Polyakov as he used it to perform the quantization of the string [55].
- GSO projection [56]: this method was used in order to construct unitary, non-tachyonic, and consistent superstring theories.

2.3.2 Strings strike back - First superstring revolution

- Anomaly cancellation: The Green-Schwarz mechanism [57] showed that anomalies are cancelled consistently in the type I theory due to the contributions of a two-form field. This is the paper that paved the way for what is today known as the first superstring revolution.
- A year later in 1985 the heterotic string theory was discovered [58].
- The authors of [59] realized that by compactifying the six extra dimensions of critical string theory on a Calabi-Yau threefold we can obtain a theory with $\mathcal{N} = 1$ supersymmetry in four dimensions.

- Finally, we had the following picture by 1985
  - Type I theory [60]
  - Type IIA theory [60]
  - Type IIB theory [60]
  - $SO(32)$ heterotic [58]
  - $E_8 \times E_8$ heterotic [58]

  about superstring theories.
- In [61] the authors realized that the eleven-dimensional supergravity theory does not contrain strings, but rather branes.

2.3.3 Revenge of the strings - Second superstring revolution

We have seen that superstring theories can be seen as theories that unify the fundamental forces of nature. If that is the case, why do we have five of them? This was a main question that was puzzling the community. Also, how does eleven-dimensional supergravity fit in this framework? These questions and more were answered in the nineties, in the so-called second superstring revolution.

- In 1995, Witten [62] suggested that all the five superstring theories can be seen as different limits - under some duality transformations in some cases - of an eleven-dimensional theory, which has been dubbed M-theory. The low-energy limit of M-theory is eleven-dimensional supergravity.
- The picture now is better shaped and it resembles rougly a spider-web; a hexagon and on its edges the five superstring theories and the eleven-dimensional supergravity. All the theories are connected with different lines -very similar to the spider web- and each line is an equivalence or a duality.
  - S-duality: It was Sen who realized the manifestation of S-duality in the context of string theory [63]. Two very brief examples of how string theories are related amongst themselves under S-duality are
    - Type IIB string theory with a coupling constant g_s is equivalent to the same theory with a coupling $\frac{1}{g_s}$ under S-duality.
    - Type I string theory with a coupling constant g_s is equivalent to the $SO(32)$ heterotic theory a coupling $\frac{1}{g_s}$ under S-duality.
  - T-duality: this was first suggested in [64] in the context of bosonic string theory and refined much more in [65]. The statement is that the theory describing strings that propagate in a circular topology of radius R is dual to the theory in a circular topology of radius $\frac{1}{R}$. We note below two superstring examples of T-duality [66] that played a central role to the development of the unified picture:
    - Type IIA is T-dual to type IIB.

    - $E_8 \times E_8$ heterotic is T-dual to $SO(32)$ heterotic.
  - U-duality: this duality is the combination of target space duality (T-duality) that we mentioned earlier and the strong-weak coupling duality (S-duality) which we have, also, briefly described. U-duality was first suggested in [67]. Let us demonstrate its action with a simple example:
    - Consider the d-dimensional, torus-compactification of the IIB theory. The T-duality group is $SO(d,d;\mathbb{Z})$. The S-duality is described as the group $SL(2,\mathbb{Z})$. The U-duality group was suggested to be the result of the non-commuting action of both groups.
  - Mirror symmetry: this symmetry describes relations between two different Calabi-Yau manifolds. It is worthwhile pointing out, that while mirror symmetry today is an active branch of mathematical research it started within the context of string theory and more specifically its compactifications and T-duality. Mirror symmetry has become a vast subject and we cannot do justice to the literature, but we want to mention the historic references, we have done so far.
    - In [68, 69] the authors realized that given a four-dimensional, $\mathcal{N} = 2$ SCFT, it is not possible to uniquely determine the corresponding Calabi-Yau manifold that led to that theory after compactification.
    - The SYZ conjecture: in [70] the authors conjectured the relation of mirror symmery and T-duality.

- D-branes: in 1995 Polchinski published his inspirational work on D-branes [22]. This opened up many new areas of research and shaped differently our understanding of string theory.
- Since the pioneering work of Hanany and Witten [71] many examples of strongly coupled gauge theories of different dimensionality and with various amounts of supersymmetry have been realized in brane configurations involving magnetically charged five-branes, and D-branes in the context of (massive) IIA as well as IIB theories. For a review see [72].
- In 1997, Maldacena conjectured the AdS/CFT duality [23].

It should be apparent from the above brief enumeration of the major string results, string theory is not just a theory of strings. It has provided with much insight on the physics of field theories, the holographic principle, and many other disciplines as well as pure mathematics.

2.3.4 Supergravities as low-energy limits

In this subsection where we describe very briefly the main supergravity theories by giving their bosonic actions, and we are following the conventions and discussion of [25].

Eleven-dimensional supergravity

The existence of eleven-dimensional supergravity was predicted in [73] and its action was constructed subsequently in [74]. Nowadays, we know that this theory plays a major role in the web of string

dualities. It is the low-energy description of M-theory and after a dimensional reduction we can obtain type IIA. The bosonic content of the theory is the metric, G_{MN}, and a three-form potential, $A_{(3)}$, which generates a field strength as $F_{(4)} = dC_{(3)}$. The bosonic part of the action reads

$$S = \frac{1}{2\kappa_{11}^2}\int d^{11}x\sqrt{|G|}\left(R - \frac{1}{2}|F_{(4)}|^2\right) - \frac{1}{12\kappa_{11}^2}\int C_{(3)}\wedge C_{(3)}\wedge F_{(4)}\,. \tag{2.11}$$

The theory has 32 supercharges, or in other words $\mathcal{N}=1$ supersymmetry. The relation amongst the gravitational constant (κ_{11}), Newton's constant (G_{11}), and the Planck length (l_p) in eleven dimensions is given by

$$\kappa_{11}^2 = 8\pi G_{11} = 2^7\pi^8 l_p^9\,. \tag{2.12}$$

Type IIA theory

The most direct connection of eleven-dimensional supergravity and the low-energy effective descriptions of superstring theories is with the supegravity description of the type IIA theory. The proper way of arguing for that is to ssay that M-theory compactified on a circle of radius R_{11}, yields type IIA the ten-dimensional type IIA superstring theory with the coupling constant being given by $g_s = \frac{R_{11}}{\sqrt{\alpha'}}$. At the level of comparing directly the supergravity this means that type IIA supergravity is a dimensional reduction of the eleven-dimensional supergravity theory. In order to perform this dimensional reduction, we need to consider one dimension to be a circle, and then from the Fourier expansions of the various fields involved we need to keep only the zero modes. This is how the action of type IIA was originally constructed [75–77], and it is given by

$$\begin{aligned} S = \frac{1}{2\kappa^2}\int d^{10}x\sqrt{|G|}\left[e^{-2\Phi}\left(R + 4\partial_A\Phi\partial^A\Phi - \frac{1}{2}|H_{(3)}|^2\right)\right] - \frac{1}{2}\left(|F_{(2)}|^2 + |\tilde{F}_{(4)}|^2\right) \\ - \frac{1}{4\kappa^2}\int B_{(2)}\wedge F_{(4)}\wedge F_{(4)}\,, \end{aligned} \tag{2.13}$$

in the string frame. The various constants appearing in the above are given by

$$\begin{aligned} \kappa_{10}^2 &= 8\pi G_{10} = 2^6\pi^6 l_s^8 g_s^2\,, \\ \kappa^2 &= \frac{\kappa_{10}^2}{g_s^2}\,, \\ G_{11} &= 2\pi R_{11} G_{10}\,. \end{aligned} \tag{2.14}$$

The theory possesses $\mathcal{N}=2$ supersymmetry which translates to 32 supercharges. Finally, the various p-forms of the bosonic action are:

$$H_{(3)} = dB_{(2)}\,, \qquad \tilde{F}_{(4)} = dC_{(3)} + C_{(1)}\wedge H_{(3)}\,, \qquad F_{(2)} = dC_{(1)}\,. \tag{2.15}$$

Type IIB

While type IIA can be obtained by a direct dimensional reduction from eleven-dimensional supergravity, the same does not hold true for the type IIB theory. The basic principles that guided the community in

order to construct this theory came from supersymmetry considerations in addition to gauge invariance. The most challenging, perhaps, feature of the type IIB theory is the presence of the self-dual five-form. This hinders the formulation of a manifestly covariant action.

Here, before we proceed, we briefly demonstrate the problem with adding a self-dual, gauge invariant term that contains the five-form in the action. Assume that $A_{(5)} = \star A_{(5)}$. We have

$$\int A_{(5)} \wedge \star A_{(5)} = \int A_{(5)} \wedge A_{(5)} = -\int A_{(5)} \wedge A_{(5)} = 0\,, \tag{2.16}$$

where in the above we used first the self-duality condition, and then the standard differential geometry formula $A_{(p)} \wedge B_{(q)} = (-1)^{pq} B_{(q)} \wedge A_{(p)}$ for general p- and q-forms.

One possible way to circumvent this malady is to focus on the field equations instead, since they can be written covariantly, and the supersymmetry transformations, the variations of the dilatino and the gravitino. An alternative is to write an action that leads to the correct equations of motion and supplement the self-duality condition at the level of the equations of motion. The bosonic matter content of the theory consists of the metric, the two-form field in the NS-NS sector of the theory, the dilaton, the R-R fields $C_{(0)}$, $C_{(2)}$, and $C_{(4)}$. The action of type IIB supergravity is

$$\begin{aligned} S = \frac{1}{2\kappa^2}\int d^{10}x\sqrt{|G|}\left[e^{-2\Phi}\left(R + 4\partial_A\Phi\partial^A\Phi - \frac{1}{2}|H_{(3)}|^2\right)\right] - \frac{1}{2}\left(|F_{(1)}|^2 + |\tilde{F}_{(3)}|^2 + |\tilde{F}_{(5)}|^2\right) \\ - \frac{1}{4\kappa^2}\int C_{(4)} \wedge H_{(3)} \wedge F_{(3)}\,, \end{aligned} \tag{2.17}$$

with the various forms satisfying the following relations:

$$\begin{aligned} F_{(p+1)} = dC_{(p)}\,, \quad H_{(3)} = dB_{(2)}\,, \quad \tilde{F}_{(3)} = F_{(3)} - C_{(0)}H_{(3)}\,, \\ \tilde{F}_{(5)} = F_{(5)} - \frac{1}{2}C_{(2)} \wedge H_{(3)} + \frac{1}{2}B_{(2)} \wedge F_{(3)}\,, \end{aligned} \tag{2.18}$$

and the five-form obeys the self-duality condition

$$\tilde{F}_{(5)} = \star\tilde{F}_{(5)}\,. \tag{2.19}$$

Type I

The type I is obtained as an orientifold projection of the type IIB [78]. One has to perform a truncation of the type IIB spectrum to the states that are left-right symmetric and then add a twisted sector that contains open strings. The degrees of freedom of the theory that are coming from the closed-string states are described as an $\mathcal{N} = 1$ supergravity sector in ten dimensions. The massless open string sector -the low-energy open string sector- gives rise to an $\mathcal{N} = 1$ SYM theory with a gauge group $SO(32)$ in ten dimensions. The bosonic matter content of the theory consists of the metric, the dilaton, the R-R two-form $C_{(2)}$ and the $SO(32)$ gauge field, A_M which comes from the open-string twist. The action of

the theory is

$$S = \frac{1}{2\kappa^2}\int d^{10}x\sqrt{|G|}\left[e^{-2\Phi}\left(R + 4\partial_A\Phi\partial^A\Phi\right)\right] - \frac{1}{2}|\tilde{F}_{(3)}|^2 - \frac{\kappa^2}{g^2}e^{-\Phi}\,\mathrm{tr}\left(|F_{(2)}|^2\right)\,, \tag{2.20}$$

where the trace in the above is taken over the 32-dimensional fundamental representation of the gauge group, $A = A_M dx^M$ is the Yang–Mills gauge field generating the field strength $F_{(2)} = dA + A\wedge A$, and we also have

$$\tilde{F}_{(3)} = dC_{(2)} + \frac{l_s^2}{4}\,\mathrm{tr}\left(\omega\wedge d\omega + \frac{2}{3}\omega\wedge\omega\wedge\omega - A\wedge dA + \frac{2}{3}A\wedge A\wedge A\right)\,, \tag{2.21}$$

where in the above ω is the spin-connection. Finally, the coupling g that appears in the type I action is related to the ten-dimensional Yang-Mills gauge coupling via

$$\frac{g_{YM}^2}{4\pi} = \frac{g^2 g_s}{4\pi} = (2\pi l_s)^6 g_s\,. \tag{2.22}$$

Heterotic theories

At the level of superstring theories the massless spectrum of the $SO(32)$ heterotic theory is exactly the same as the one of type I, and the difference when considering the $E_8\times E_8$ theory is just a change of the gauge group. For higher energy excitations there are more significant differences, however, we are not concerned with these here as the supergravity spectra contain only the low-energy degrees of freedom. The action is

$$S = \frac{1}{2\kappa^2}\int d^{10}x\sqrt{|G|}e^{-2\Phi}\left[R + 4\partial_A\Phi\partial^A\Phi - \frac{1}{2}|\tilde{H}_{(3)}|^2 - \frac{\kappa^2}{30g^2}\,\mathrm{tr}_G\left(|F_{(2)}|^2\right)\right]\,, \tag{2.23}$$

where in the above tr_G denotes the trace in the adjoint and we also have

$$\tilde{H}_{(3)} = dB_{(2)} + \frac{l_s^2}{4}\,\mathrm{tr}\left(\omega\wedge d\omega + \frac{2}{3}\omega\wedge\omega\wedge\omega - A\wedge dA + \frac{2}{3}A\wedge A\wedge A\right)\,, \tag{2.24}$$

Massive IIA

Massive type IIA supergravity is a modification of type IIA by a R-R scalar (zero form) [27]. One can regard the theory as first performing a T-duality to type IIA, hence landing on type IIB, and then a specific orientifold projection thereof. This makes O8-orientifold planes appear and consistency requirements yield the presence of D8-branes. The term that has to be added to the part of the action describing the R-R p-form fields is precisely

$$\frac{1}{2}F_0^2\,, \tag{2.25}$$

which yields the following modifications

$$H_{(3)} = dB_{(2)}\,,\qquad \tilde{F}_{(4)} = dC_{(3)} + C_{(1)}\wedge H_{(3)} + \frac{1}{2}F_0 B_{(2)}\wedge B_{(2)}\,,\qquad F_{(2)} = dC_{(1)} + F_0 B_{(2)}\,. \tag{2.26}$$

2.4 The maximally supersymmetric Yang-Mills theory

The Lagrangian for the $\mathcal{N}=4$ SYM in four-dimensions is unique and given by [28]:

$$\begin{aligned}\mathcal{L}=\mathrm{tr}\Bigg(&-\frac{1}{2g^2}F_{MN}F^{MN}+\frac{\theta}{8\pi^2}F_{MN}\hat{F}^{MN}-\sum_a i\bar{\lambda}^a\bar{\sigma}^M D_M\lambda_a-\sum_i D_M X^i D^M X^i\\&+\sum_{a,b,i} g\left(C_i^{ab}\lambda_a[X^i,\lambda_b]+\bar{C}_{i,a,b}\bar{\lambda}^a[X^i,\bar{\lambda}^b]\right)+\frac{g^2}{2}\sum_{i,j}[X^i,X^j]\Bigg)\,,\end{aligned}\tag{2.27}$$

where in the above $a=1,..,4$, $i=1,...,6$, θ is the instanton angle, and we also have

$$F_{MN}=\partial_M A_N-\partial_N A_M+i[A_M,A_N]\,,\quad \hat{F}_{MN}=\frac{1}{2}\epsilon_{MNRS}F^{RS}\,,\quad D_M\lambda=\partial_M\lambda+i[A_M,\lambda]\,.\tag{2.28}$$

We have denoted by λ the left Weyl fermions (gauginos), by X the six real scalar fields and we have in addition to these the gauge field A. The remaining quantities are related to the Clifford structures. The gauge field is a singlet under the $SU(4)_R$, which is the R-symmetry while the Weyl fermi fields are in the **4**. The six real scalars are in the **6** of the R-symmetry.

It is easy to see that the theory is scale invariant. From dimensional analysis we have

$$[X]=1\,,\quad [A_M]=1\,,\quad [\lambda]=\tfrac{3}{2}\,,\tag{2.29}$$

where we are using mass/energy dimensions and the coupling and the instanton angle have dimension zero. Now, it is also quite clear that all the terms in the Lagrangian are dimension 4. Another remarkable property of the theory is that the β-functions vanishes to all orders in perturbation theory; having assumed no instanton effects. However, even contributions that originate from instantons lead to finite contributions. The $\mathcal{N}=4$ SYM is regarded to be a UV finite theory.

It is worthwhile noting here that the theory can be obtained as a dimensional reduction of the ten-dimensional $\mathcal{N}=1$ SYM on a torus. The Lagrangian of $\mathcal{N}=1$ SYM is

$$\mathcal{L}=-\frac{1}{2g_{YM}^2}\,\mathrm{tr}\left(F_{MN}F^{MN}-2i\bar{\lambda}\not{D}\lambda\right)\,,\tag{2.30}$$

with M,N the ten-dimensional spacetime indices, λ the ten-dimensional Majorana-Weyl spinor which has 16 real components.

The most straightforward way, in our knowledge, that one can see this dimensional reduction is the following: the ten-dimensioanl SYM theory has 16 supercharges. In that theory there are no fields with spin higher than 1. The resulting four-dimensioanl theory, after dimensional reduction, should also have 16 supercharges and no matter of spin higher than 1. The only theory fullfilling all the requirements is the $\mathcal{N}=4$ SYM. This counting of supercharges across dimensions can be found in almost every modern textbook on supergravity and/or supersymmetry. As always we suggest [24].

The above argument, however nice and quick, is not a proof. Now we attempt to justify even further.

We are dimensionally reducing the bosonic part of the ten-dimensional geometry. We have

$$F_{MN} = F_{\mu\nu} + F_{\mu i} + F_{ij} \,. \tag{2.31}$$

In the above we have decomposed in a natural way. The first piece is pure Minkowski, while the second has a Minkowski and a torus contribution, and the final bit is purely on the torus. There are no other possibilities for the two-form. A silent assumption is that the fields themselves are independent of x^i; the torus directions. The field strength pieces are equal to

$$F_{\mu\nu} = \partial_\mu A_\nu - \partial_\nu A_\mu - i[A_\mu, A_\nu] \,, \quad F_{\mu i} = \partial_\mu A_i - i[A_\mu, A_i] \,, \quad F_{ij} = -i[A_i, A_j] \,. \tag{2.32}$$

Again we only wrote the definition of the field strength and imposed that the gauge field does not depend on the torus directions. Collecting the above we have

$$F_{MN}F^{MN} = F_{\mu\nu}F^{\mu\nu} + (\partial_\mu A_i - i[A_\mu, A_i]) \left(\partial^\mu A^i - i[A^\mu, A^i]\right) - [A_i, A_j][A^i, A^j] \,. \tag{2.33}$$

From the four-dimensional point of view, the A_i components are just scalar fields and we re-write them as X_i. Observe at this point as well, that the term appearing in the middle is just the covariant derivative of a scalar in the adjoint of the group. Hence, we have

$$F_{MN}F^{MN} = F_{\mu\nu}F^{\mu\nu} + (D_M X_i)^2 - [X_i, X_j]^2 \,, \tag{2.34}$$

which is the bosonic matter content of the $\mathcal{N} = 4$. Supersymmetry guarantees that the reduction of the spinor should also work. The tentative reader will observe now that this is a handwavy argument and the formal way to prove the reduction is to actually perform it and obtain the Yukawa couplings and the fermionic bit of the $\mathcal{N} = 4$. We fully agree, and we remind that this section only meant to serve as a gentle introduction to the basic concepts of the thesis.

Part III

Foundations

Chapter 3

Fields in a five dimensional AdS space

The purpose of this section is to familiarize ourselves with the dynamics of fields in an AdS spacetime and to establish the basic relations between the mass and the classical dimension of a bulk mode. We will also derive two very central results with respect to the AdS/CFT duality. The first one is the BF bound and the second one the unitarity bound for the conformal dimension of a scalar field.

We are using the Poincaré parameterization of the AdS_5 spacetime here, which is given by

$$ds^2 = G_{AB}\ dx^A dx^B = \frac{L^2}{U^2}\left(\eta_{\mu\nu}dx^\mu dx^\nu + dU^2\right)\,, \tag{3.1}$$

with the conformal boundary of AdS being given as we approach $U \to 0$. The hypersurface defined by $U \to 0$ is isomorphic to the four-dimensional Minkowski metric.[1] Henceforth, we set the overall scale of the AdS manifold to one; $L = 1$.

Some relevant references are the following: the scalar case has been analyzed in many places in the literature. We suggest the extraordinary book [24].[2] For the fermions, the computation has been performed originally in [81] and later in [82]. We explain in more detail several aspects here. The vector field results can be found in the MIT lecture notes as well as the lecture notes by Zaffaroni. In section 3.1.5 we are following the seminal work of [83].

3.1 Scalar fields

We want to consider a massive scalar field whose dynamics is described by the action

$$S[\Phi] = \frac{1}{2}\int [dx]\ \sqrt{|G|}\left[G^{MN}\nabla_M\Phi\nabla_N\Phi - m^2\Phi^2\right]\,, \tag{3.2}$$

where in the above $[dx] = d^4x dU$ and $\sqrt{|G|}$ is the square root of the absolute value of the determinant of the metric and also $\Phi = \Phi(x^\mu, U)$. From the above expression, it is a straightforward exercise to

[1] Had we considered a Euclidean signature AdS_5 metric, the hypersurface $U \to 0$ would be isomorphic to the flat $\mathbb{R}^4$ spacetime.

[2] There is also excellent online material demonstrating the computational procedure. The MIT lectures on string theory [79] would be one place for that. Another online resource is the lecture notes by Alberto Zaffaroni at EPFL [80].

obtain the equations of motion for the scalar field in the bulk, given by

$$\begin{aligned}&\left(\Box - m^2\right)\Phi = 0\,, \implies \\ &\left(\frac{1}{\sqrt{|G|}}\partial_A\left(\sqrt{|G|}\; G^{AB}\;\partial_B\right) - m^2\right)\Phi = 0\,.\end{aligned} \tag{3.3}$$

We can expand explicitly the above equations of motion in the following way:

$$U^5\frac{\partial}{\partial U}\left(U^{-3}\frac{\partial}{\partial U}\Phi\right) + U^2\frac{\partial^2}{\partial x^\mu \partial x_\mu}\Phi - m^2\Phi = 0\,. \tag{3.4}$$

We proceed by assuming a decomposition along the Minkowski subspace of the five-dimensional manifold as a plane-wave, $e^{ik^\mu x_\mu}$, and absorb the dependence of the fifth dimension into a scalar function, $\varphi(U)$. In what follows k^2 is the momentum.[3] We now substitute the ansatz $\Phi = e^{ik^\mu x_\mu}\varphi(U)$ into the equations of motion given by equation (3.4) above and obtain an ordinary second-order differential equation for the function φ given by

$$\ddot{\varphi} - \frac{3}{U}\dot{\varphi} - \left(k^2 + \frac{m^2}{U^2}\right)\varphi = 0\,, \tag{3.5}$$

where in the above we have suppressed the dependence of the φ on the radial coordinate U to simplify notation and we have used a dot to denote derivative with respect to the coordinate U.

The above equation admits simple analytic solutions in terms of Bessel functions in the following way:

$$\varphi = U^2\left(J_{\sqrt{m^2+4}}(-i\;k\;U) + Y_{\sqrt{m^2+4}}(-i\;k\;U)\right)\,, \tag{3.6}$$

with $J_n(x)$ being the Bessel function of the first kind and $Y_n(x)$ is the Bessel function of the second kind.

As a final exercise and in order to make the physics of the equation given by equation (3.5) more transparent we can manipulate it in a simple manner and bring it in a Schrödinger form. To do so, we need to eliminate the first derivative and in order to achieve that we begin by considering $\varphi(U) = \mathcal{A}(U)\psi(U)$. Inserting that into equation (3.5) we obtain

$$\mathcal{T}_1\ddot{\psi} + \mathcal{T}_2\dot{\psi} + \mathcal{T}_3\psi = 0\,, \tag{3.7}$$

where the prefactors are explicitly given by

$$\begin{aligned}\mathcal{T}_1 &= \mathcal{A}\,,\\ \mathcal{T}_2 &= 2\dot{\mathcal{A}} - \frac{3}{U}\mathcal{A}\,,\\ \mathcal{T}_3 &= \ddot{\mathcal{A}} - \frac{3}{U}\dot{\mathcal{A}} - \left(k^2 + \frac{m^2}{U^2}\right)\mathcal{A}\,.\end{aligned} \tag{3.8}$$

[3] More specifically we have $k^2 = -\omega^2 + \vec{k}^2$.

What we want to solve is the simple equation $\mathcal{T}_2 = 0$, which is

$$2\dot{\mathcal{A}} - \frac{3}{U}\mathcal{A} = 0 \rightarrow \mathcal{A} = U^{3/2}\,, \tag{3.9}$$

where we have taken the constant of integration to be equal to one.

We use this solution for $\mathcal{A}$ into the equations of motion and we obtain

$$-\ddot{\psi} + \underbrace{\left[\vec{k}^2 + \frac{1}{U^2}\left(m^2 + \frac{15}{4}\right)\right]}_{V(U)}\psi = \omega^2\psi\,. \tag{3.10}$$

The above equation, equation (3.10), is a Schrödinger equation with a potential $V(U)$ and of energy ω^2. An instability is signalled via a state of negative energy. This, in turn, implies an imaginary value for ω. It is worthwhile noting that the differential equation always has solutions irregardless of the value of ω. Be that as it may, not all of them are normalizable and hence physically acceptable. A normalizable solution, and thus physical, to the wave equation in AdS_5 is one with finite energy; this is closely related to the normalizability and finiteness of the wavefunction in ordinary quantum mechanics ($\int dU|\psi|^2 =$ finite) and this justifies the previous exercise with re-writing the scalar equations of motion in the more familiar Schrödinger form. Henceforth, we will set the momentum along the spatial directions to zero; $\vec{k} = 0$.

3.1.1 The mass-dimension formula

The dynamics of the field is described by equation (3.4) as we have already seen. We focus on the U-dependence of the massive scalar and we consider a solution of the form, $\Phi = U^{\Delta}$. We substitute this solution into the equations of motion and obtain -after a straightforward algebraic manipulation

$$\begin{aligned} &U^{\Delta}\left(-m^2 + \Delta(\Delta - 4)\right) = 0\,, \implies \\ &m^2 = \Delta(\Delta - 4)\,. \end{aligned} \tag{3.11}$$

This describes the relation between the classical dimension and the bulk mass of a massive scalar field propagating in AdS_5.

We realize at this point the above relation does not make much sense, however it will become much more apparent to the reader after the introductory section to the AdS/CFT. There we will see that U is a dual energy scale.

3.1.2 A quick and dirty derivation of the BF bound

Recall that we arrived at a problem of the form

$$-\ddot{\psi} + V(U) = \omega^2\psi\,, \tag{3.12}$$

with the potential being given by he expression

$$V(U) = \frac{1}{U^2}\left(m^2 + \frac{15}{4}\right) . \tag{3.13}$$

This type of problem has been studied extensively and it has been argued that it admits stable solutions when the condition $V > -\frac{1}{4}$ is satisfied, see [84, Chapter 4]. From that inequality we can readily solve for the mass and obtain a bound such that the solution remains stable, which is given by:

$$m^2 > -4 . \tag{3.14}$$

The above result is the BF bound [85, 86].

Note also that the BF bound can be obtained by equation (3.11) and the requirement that Δ is real.

3.1.3 The stress tensor

We have already derived the BF bound, however, we would like to sketch the basic steps of a more formal derivation of that result. We are following [79]. We begin by recalling that there exists a fundamental property for a field configuration which determines whether or not that particular field is physical. This property is the normalizability of the field configuration. When working in a Minkwoski signature, a field is considered to be a normalizable solution, if it has finite energy.[4]

Here we want to examine what the precise relation is between the notion of a normalizable wave-function in a quantum mechanical sense (the norm of the wave-function is a finite result) and a normalizable solution to wave equation in an AdS spacetime (such that the solution is of finite energy).

Energy flux

We want to impose that there is no energy flux out of the boundary of AdS such that the energy is conserved.

As a first step we note that if an isometry is generated by a Killing vector, ξ^M, there exists an associated current, given by $j^N = T^{MN}\xi_M$, that is conserved; $\nabla_N j^N = 0$. Here, we have denoted by T_{MN} the stress-energy tensor. We have a timelike Killing vector $\xi \equiv \xi^0 = \partial_t$. We start by giving the definition of the energy-momentum tensor which is

$$T_{AB} = \nabla_A\Phi\nabla_B\Phi - \frac{1}{2}G_{AB}\left(G^{MN}\nabla_M\Phi\nabla_N\Phi - m^2\Phi^2\right) . \tag{3.15}$$

Requiring that there is no energy loss is equivalent to

$$\int_{\partial AdS}\sqrt{h}n_M J^M = \int_{\partial AdS}\sqrt{h}n_M\xi^N T_{MN} , \tag{3.16}$$

[4] On the other hand, when considering a quantum field theory in Euclidean space, normalizability is the statement that the Euclidean action evaluated on that particular field configuration is finite.

with the normal vector given by $n^M = U\delta^M_u$. We insert the expression for the stress tensor and obtain

$$0 = \int d^3x dt U^{-3} T_{tU}\Big|_{U=0} = \int dt U^{-3} \partial_t \Phi \partial_t \Phi\Big|_{U=0} . \tag{3.17}$$

Now we can split the above into two terms and perfom integration by parts

$$\frac{1}{2}\int dt U^{-3} \left(\partial_t \Phi \partial_U \Phi - \Phi \partial_t \partial_U \Phi\right)\Big|_{U=0} , \tag{3.18}$$

and as a next step we can consider the Fourier transformation $\Phi = \int dw \phi e^{iwt}$ and obtain

$$\frac{1}{2}\int dt dw_1 dw_2 U^{-3} i w_1 e^{i(w_1+w_2)t} \left(\phi_1 \partial_U \phi_2 - \phi_2 \partial_U \phi_1\right)\Big|_{U=0} . \tag{3.19}$$

As a final step we wish to re-write the expression in terms of the ψ. A useful trick is to note that reality implies $\phi_2(w2) = \phi_2^*(-w2)$ and hence we arrive at

$$\frac{1}{2}\int dt dw_1 dw_2 i w_1 e^{i(w_1+w_2)t} \left(\psi_1^* \partial_U \psi_2 - \psi_2 \partial_U \psi_1^*\right) = 0 , \tag{3.20}$$

which yields the boundary condition

$$\psi_1^* \partial_U \psi_2 - \psi_2 \partial_U \psi_1^* = 0 \tag{3.21}$$

Finite energy

By considering the Killing vector $\xi \equiv \xi^0 = \partial_t$ and a surface of constant time with a normal vector the energy is the integral

$$\begin{aligned} E &= \int d^3x dU \sqrt{h} n^M \xi^N T_{MN} \\ &= \int d^3x dU U^{-3} T_{tt} \\ &= \int dt dU U U^{-3} \left(\frac{1}{2}\left(\partial_t \Phi\right)^2 - \frac{1}{2}\left(\partial_U \Phi\right)^2 - U^{-2} m^2 \Phi\right) . \end{aligned} \tag{3.22}$$

From this expression one can show that

$$E = w^2 \int dU |\psi|^2 . \tag{3.23}$$

The algebraic manipulations that are needed are just integration by parts, swapping the fields as we did previously and using the equations of motion.

The important aspect here is that the finiteness of the energy is equivalent to the normalization of the wave-function.

3.1.4 Returning to the study of the BF bound

We are now at a position to derive one of the most central results in AdS supergravity theories and by extension the AdS/CFT duality. This is the celebrated Breitenlohner-Freedman bound and it pertains the stability of the AdS vacuum solution.

Our starting point is the Schrödinger equation, which we re-state here for convenience

$$\left(-\partial_U^2 + \frac{1}{U^2}\mathcal{A}\right)\psi = -\mathcal{B}^2\psi\,, \tag{3.24}$$

with $\mathcal{A}$ being given by

$$\mathcal{A} = m^2 + \frac{15}{4}\,. \tag{3.25}$$

The task at hand, now, is to seek solutions of negative-energy. For the problem described by equation (3.24), these negativeenergy solutions correspond to real values of the parameter $\mathcal{B}$; $\mathcal{B} \in \mathbb{R}$. We know that the above admits solutions in terms of Bessels given by

$$\psi = \sqrt{U}\left(c_1 J_{\mathcal{C}}(i\mathcal{B}U) + c_2 Y_{\mathcal{C}}(i\mathcal{B}U)\right)\,, \tag{3.26}$$

having defined $\mathcal{C} = \frac{1}{2}\sqrt{1+4\mathcal{A}}$. It is easy to observe that there is a special value, $\mathcal{A} = -\frac{1}{4}$, which makes $\mathcal{C}$ vanish. We can note that we can fix one of the integration constants in terms of the other just by looking the limit $U \to \infty$ which gives

$$J_{\mathcal{C}}(i\mathcal{B}U) \sim \frac{2}{i\mathcal{B}U}\cosh\left(\mathcal{B}U\right)\,, \qquad Y_{\mathcal{C}}(i\mathcal{B}U) \sim \frac{2}{i\mathcal{B}U}\sinh\left(\mathcal{B}U\right)\,, \tag{3.27}$$

and by therefore the solution can be written as

$$\psi = c\,\sqrt{U}\left(J_{\mathcal{C}}(i\mathcal{B}U) + Y_{\mathcal{C}}(i\mathcal{B}U)\right)\,. \tag{3.28}$$

In the $U \to 0$ limit we obtain

$$\psi = c\sqrt{U}\,\left(\frac{1}{\Gamma(\mathcal{C}+1)}\left(\frac{i\mathcal{B}U}{2}\right)^{\mathcal{C}} - i\frac{\Gamma(\mathcal{C})}{\pi}\left(\frac{2}{i\mathcal{B}}\right)^{\mathcal{C}}\right)\,. \tag{3.29}$$

Let us now go back to the boundary condition we derived earlier given by equation (3.21) and evaluate it for the solutions equation (3.29) assuming that we have two different energies. We obtain

$$\left(\frac{\mathcal{B}_2}{\mathcal{B}_1}\right)^{\mathcal{C}} + \left(\frac{\mathcal{B}_1}{\mathcal{B}_2}\right)^{\mathcal{C}} = 0 \tag{3.30}$$

And now we can see that

- For $\mathcal{A} > -\frac{1}{4}$ which means that $\mathcal{C} \in \mathbb{R}$, equation (3.30) can never be satisfied no matter what the values of $\mathcal{B}_1$ and $\mathcal{B}_2$ are; recall that these are real.

- For $\mathcal{A} < -\frac{1}{4}$ which means that $\mathcal{C}$ is imaginary one can show[5] that the condition given by equation (3.30) can be satisfied. This means that there are **NEGATIVE** energy states that respect the boundary conditions. Let us remind the reader that negative energy in AdS means an instability.

The punchline of the above is that **ANY** finite-energy, normalizable state satisfies

$$m^2 > -4\,, \tag{3.31}$$

which we have already seen as the BF bound [85, 86].

3.1.5 Saturating the unitarity bound

Before we start this section, we want to point out that the main result will make much more sense after the reader finishes section 4.1.3. We are following [83] and working for convenience in a Euclidean signature.

Recall that the action for a massive scalar in the bulk is

$$S = \int [dx]\ \sqrt{G}\left(G^{AB}\partial_A\phi\partial_B\phi + m^2\phi^2\right)\,, \tag{3.32}$$

which we have already seen. We can expand the action in terms of partial derivatives and then consider the ansatz for the bulk scalar mode $\phi = e^{-ikx}U^{\Delta}$. We plug the ansatz into the action and the result reads

$$S = \frac{1}{2}\int [dx]\ \left(\Delta^2 + m^2 - k^2U^2\right)U^{2\Delta-5}\,. \tag{3.33}$$

Now we can perform the U-integral and observe that the leading term as $U \to 0$ is

$$S \sim \lim_{U\to 0}\frac{\Delta^2+m^2}{2(2\Delta-4)}U^{2\Delta-4}\,. \tag{3.34}$$

The above result, and thus the action, is finite if and only if the inequality $2\Delta - 4 > 0$ is satisfied. This yields the bound on the weight of the operator to be

$$\Delta > 2\,. \tag{3.35}$$

Recall, however, that the solutions obtained previously for the two possible values of the conformal dimension are given by

$$\Delta_{\pm} = 2 \pm \sqrt{m^2+4}\,, \tag{3.36}$$

and it should be clear now that evaluating the above action for an ansatz of the form $\phi = U^{\Delta_-}$ and performing the U-integration will always lead to a divergent answer. It should also be clear that for $\phi = U^{\Delta_+}$ the result is finite. However, the bound obtained by equation (3.35) is over restricted. This is just a statement now, but we will prove it to be true in section 4.1.3 directly from a CFT computation.

[5] this required extensive use of Mathematica and a lot of patience.

Let us examine how we can remedy that and obtain the right answer. Consider the modified action [83]

$$\tilde{S} = \frac{1}{2}\int [dx]\ \sqrt{G}\phi\left(-\nabla^2 + m^2\right)\phi\,. \tag{3.37}$$

This new action leads to the same equations of motion as the previous one we examined. It differs only by a boundary term, which is divergent. We can work out what the precise value is. The strategy is to proceed as we did previously. We expand the action fully by considering $\phi = e^{ikx}\phi$ and we obtain

$$\tilde{S} = \frac{1}{2}\int [dx]\ U^{-5}\phi\left(-U^5\partial_U\left(U^{-3}\partial_U\right) + k^2U^2 + m^2\right)\phi\,, \tag{3.38}$$

and now we can consider the power scaling $\phi = U^\Delta$ and obtain

$$\tilde{S} = \frac{1}{2}\int [dx]\ U^{2\Delta-5}\left(\Delta(4-\Delta) + m^2 + U^2k^2\right)\,. \tag{3.39}$$

The first direct observation we can make is to assume that Δ takes either of the values $\Delta_\pm$. This leads $\Delta(4-\Delta) = -m^2$ and hence the first part of the action vanishes. Now we can perform the U-integral, as we did previously, and observe that the leading term as $U \to 0$ is

$$\tilde{S} \sim \lim_{U\to 0}\frac{k^2}{2(2\Delta-2)}U^{2\Delta-2}\,. \tag{3.40}$$

The above result, and thus the action, is finite if and only if the inequality $2\Delta - 2 > 0$ is satisifed. This yields the bound on the conformal dimension of the operator to be

$$\Delta > 1\,. \tag{3.41}$$

This is precisely what we find in section 4.1.3 by performing a pure CFT computation. It is worthwhile pointing out that if the mass satisfies

$$-4 < m^2 < -3\,, \tag{3.42}$$

then both solutions for $\Delta_\pm$ satisfy equation (3.41) and so both of them can correspond to a normalizable solution and hence an operator in the boundary field theory. There is much more discussion behind this result and we strongly encourage the readers to study [83].

3.2 Spin-1/2 fields

The action for a free, massive spinor is given by,

$$S = \int [dx]\ \sqrt{|G|}\bar{\Psi}\left(\not{D} - m\right)\Psi\,, \tag{3.43}$$

from which we can obtain very straightforwardly the equations of motion for the spinor Ψ. They read

$$\left(\not{D} - m\right)\Psi = 0\,. \tag{3.44}$$

In order to proceed with our computations we find it very helpful to find an appropriate choice of basis, thus, using the vielbein formalism - for which it holds that $G_{MN} = e^{(A)}{}_M\, e^{(B)}{}_N\, \eta_{(A)(B)}$ - [6] in the geometry of equation (3.1), it is straightforward to evaluate the following quantities:

$$e^{(A)}{}_\mu = \left(\frac{1}{U}\right) \delta^A{}_\mu, \qquad e^{(A)}{}_U = \left(\frac{1}{U}\right) \delta^A{}_U. \tag{3.45}$$

The vielbein basis $\left\{e^{(A)} \,\middle|\, e^{(A)} = e^{(A)}{}_M\, dx^M\right\}$,[7] satisfies the following relation

$$ds^2 = G_{MN}\, dx^M\, dx^N = \eta_{(A)(B)}\, e^{(A)}\, e^{(B)}\,. \tag{3.47}$$

We also compute and present below the non-trivial components of the spin-connection. We remind the definition for torsion-free theories, which is definition is

$$\omega_M^{(A)(B)} = e^{(A)}{}_N\, \Gamma^N_{ML}\, e^{(B)L} + e^{(A)}{}_N\, \partial_M\, e^{(B)N}, \tag{3.48}$$

where $e^{(A)M} = e^{(A)}{}_N\, g^{NM} = \eta^{(A)(B)} e_{(B)}{}^M$. Using equation (3.48) we obtain the following components

$$\omega_\nu^{(U)(\mu)} = -\omega_\nu^{(\mu)(U)} = \frac{1}{U}\delta^\mu_\nu\,. \tag{3.49}$$

The Dirac operator[8] on a curved manifold is given by

$$\not{D} = e^M_{(A)}\Gamma^{(A)} \left(\partial_M + \omega_M^{(B)(C)}\Sigma_{(B)(C)}\right) \tag{3.50}$$

where the Γ-matrices satisfy the Clifford algebra $\{\Gamma^{(A)}, \Gamma^{(B)}\} = 2\eta^{(A)(B)}$, and the $\Sigma_{(B)(C)}$ is the relativistic spin-matrix.[9]

Firstly, let us compute the first term of the sum which is very straightforward. The result is

$$U\Gamma^u\partial_U + U\Gamma^\mu\partial_\mu\,. \tag{3.51}$$

[6] Indices between brackets will be used solely to denote vielbein indices.

[7] the dual basis $\left\{e_{(A)} \,\middle|\, e_{(A)} = e_{(A)}{}^M\, \partial_M\right\}$ is defined via

$$e^{(A)}\left(e_{(B)}\right) = e^{(A)}{}_M\, dx^M \left(e_{(B)}{}^N\, \partial_N\right) = e^{(A)}{}_M\, e_{(B)}{}^N\, \delta^M{}_N = \delta^{(A)}{}_{(B)}\,, \tag{3.46}$$

[8] by definition the Dirac operator is just the covariant derivative of the curved spacetime with its index contracted with the γ-matrix.

[9] we are using the standard definition $\Sigma_{(A)(B)} = \frac{1}{4}[\Gamma_{(A)}, \Gamma_{(B)}]$.

The second part of the operator is equal to

$$\begin{aligned} e^{M}_{(A)}\Gamma^{(A)}\omega^{(B)(C)}_{M}\Sigma_{(B)(C)} &= U\ \delta^{M}_{(A)}\Gamma^{(A)}\left(\omega^{(U)(\mu)}_{\nu}\Sigma_{(U)(\mu)}+\omega^{(\mu)(U)}_{\nu}\Sigma_{(\mu)(U)}\right)\,, \\ &= \Gamma^{M}\left(\Sigma_{(U)(\mu)}+\Sigma_{(\mu)(U)}\right)\,, \\ &= \frac{1}{2}\Gamma^{M}\left(\Gamma_{(U)}\Gamma_{(\mu)}-\eta_{(U)(\mu)}\right)\,, \\ &= -\frac{1}{2}\Gamma^{M}\Gamma_{M}\Gamma_{U}\,, \\ &= -2\Gamma_{U}=-2\Gamma^{U}\,. \end{aligned} \tag{3.52}$$

Finally, we have obtained the result

$$\not{D} = U\ \Gamma^{U}\partial_{U}+U\ \Gamma^{\mu}\partial_{\mu}-2\Gamma^{U}\,. \tag{3.53}$$

We would like to derive a second-order differential equation of a scalar function of a single variable, which is easy to solve, as we did for the case of a scalar field. To do so, we start by acting by acting on the first order equations of motion with a differential operator; more specifically this operator is part of the Dirac operator. The next step is to use the Clifford algebra, and the linear equations of motion to simplify the resulting terms of the equations.

From the standard fermionic action for a spinor with a bulk fermion mass, we obtain the Dirac equation below

$$\begin{aligned} &(\not{D}_{\rm AdS}-m)\Psi=0\,,\implies \\ &\left(U\ \Gamma^{U}\partial_{U}+U\ \Gamma^{\mu}\partial_{\mu}-2\Gamma^{U}-m\right)\Psi=0\,, \end{aligned} \tag{3.54}$$

where we have used the shorthand: $\Psi=\Psi(x^{\mu},U)$. We act from the left on the above equation with $U\ \Gamma^{U}\partial_{U}+U\ \Gamma^{\mu}\partial_{\mu}$ and after expanding all terms we obtain the following expression

$$\left(U^{2}\partial^{2}_{U}-U\partial_{U}+U^{2}\partial^{\mu}\partial_{\mu}+3U\Gamma^{U}\Gamma^{\mu}\partial_{\mu}-mU\Gamma^{U}\partial_{U}-mU\Gamma^{\nu}\partial_{\nu}\right)\Psi\,, \tag{3.55}$$

where we have used the fact that Γ^{U} anti-commutes with any Γ-matrix in order to cancel the term $U^{2}\Gamma^{U}\Gamma^{\mu}\partial_{U}\partial_{\mu}\Psi$ against $U^{2}\Gamma^{\nu}\Gamma^{U}\partial_{U}\partial_{\nu}\Psi$.

Now we can use the first-order equation of motion, equation (3.54), to re-express the terms $3\Gamma^{U}\Gamma^{\mu}\partial_{\mu}$ and $-mU(\Gamma^{U}\partial_{U}+\Gamma^{\mu}\partial_{\mu})$ as $(6+3m\Gamma^{U}-3U\partial_{U})\Psi$ and $-(m^{2}+2m\Gamma^{U})\Psi$ respectively. Now, we have only terms of the form that we wanted and it is time to decompose the spinor according to the symmetries of the problem we study. This decomposition is quite obvious and we write the ansätz $\Psi=\Psi(x^{\mu},U)=e^{ik^{\mu}x_{\mu}}\psi(U)$, where the wave-vector is related to the mass of the flucutation via $k^{2}=-M^{2}$ and we obtain the following expression

$$\left(U^{2}\partial^{2}_{U}-4U\partial_{U}+U^{2}M^{2}-m^{2}+6+m\Gamma^{U}\right)\psi=0\,, \tag{3.56}$$

with the shorthand $\psi(U)=\psi$.

The above equation, equation (3.56), can be solved analytically. The general solutions are given by

$$\begin{aligned}\psi_+ &\sim U^{5/2}\left(J_{m-1/2}(M\ U)+Y_{m-1/2}(M\ U)\right)\,,\\ \psi_- &\sim U^{5/2}\left(J_{m+1/2}(M\ U)+Y_{m+1/2}(M\ U)\right)\,,\end{aligned} \tag{3.57}$$

where the $\pm$ denotes the eignevalue of the projector -the Γ^U matrix- and, $J_n(x), Y_n(x)$ are the Bessel functions of the first and the second kind respectively, and we have written the solutions up to the integration constants which will play an important role and will be translated subsequently.

Now, we want to examine the asymptotics of the solutions as we approach the conformal boundary $U \to 0$

$$\begin{aligned}\psi_+|_{U\to 0} &\sim U^{5/2}\left(U^{m-1/2}+U^{-m+1/2}\right)\,,\\ \psi_-|_{U\to 0} &\sim U^{5/2}\left(U^{m+1/2}+U^{-m-1/2}\right)\,,\end{aligned} \tag{3.58}$$

At this point some comments and clarifications are in order. In holography, we associate the diverging part of a solution with the boundary field theory source, which is set to zero in order to study the field theoretic spectrum, and the convergent solution has an interpretation as the field theory operator. However, in the case of the spin-1/2 states we have seen that we have two quantities that we want to determine, yet there are four solutions; namely the four constants of integration in equation (3.57). The crucial point to understand is that the solutions are not independent. In other words, we have not described two different sets of sources and operators, but rather we have introduced a double copy of the source and the operator. This is because we acted on the first-order differential equation with a differential operator, in order to promote it to a simpler problem. Therefore, the expectation is that two of the constants will be identified as the boundary source and the boundary operator and the other two will be related to them such that the dimensions match.

We describe, now, how to reduce the number of the integration constants from four to two. This is of utmost importance as these constants have a physical interpration.

The startning point is the first-order Dirac equation in pure AdS. This is written as

$$\left(U\ \Gamma^U\partial_U + U\ \Gamma^\mu\partial_\mu - 2\Gamma^U - m\right)\Psi(x^\mu,U)=0\,. \tag{3.59}$$

We decompose the spinor as $\Psi(x^\mu,U)=e^{ik\cdot x}(\psi_+\alpha_+ + \psi_-\alpha_-)$ where the $\alpha_\pm$ are eigenstates of the projector Γ^U and have values ± 1. They are related to one another via

$$\alpha_- = \frac{i\not{k}}{M}\alpha_+\,. \tag{3.60}$$

We can substitue the above decomposition in the Dirac equation and obtain a set of first-order coupled differential equations. Taking into consideration that the Γ^u-eigenspinors are linearly independent the

resulting equations read

$$\begin{aligned}\psi_+ &= \frac{1}{U\ M}\left(U\partial_U\psi_- - (-2+m)\psi_-\right)\,,\\ \psi_- &= \frac{1}{U\ M}\left(-U\partial_U\psi_+ + (2+m)\psi_+\right)\,,\end{aligned} \tag{3.61}$$

We can plug the asymptotic expansions,

$$\begin{aligned}\psi_+|_{U\to 0} &= c_1 U^{m+2} + c_2 U^{-m+3}\,,\\ \psi_-|_{U\to 0} &= c_3 U^{m+3} + c_4 U^{-m+2}\,,\end{aligned} \tag{3.62}$$

in the above expressions, see equation (3.61), and solve the resulting relations to relate two of the constants to other two. The final form of the asymptotics reads -we specify $m = 5/2$ for simplicity

$$\begin{aligned}\psi_+|_{U\to 0} &= c_1 U^{9/2} + c_4 \frac{M}{4} U^{1/2}\,,\\ \psi_-|_{U\to 0} &= c_1 \frac{M}{6} U^{11/2} + c_4 U^{-1/2}\,,\end{aligned} \tag{3.63}$$

and the identification is $c_1 = \mathcal{O}$ and operator of UV conformal dimension $9/2$ and $c_4 = \mathcal{J}$ is the dimension $1/2$ source.

3.3 A quick comment on vectors and their scaling dimension

Below we quickly describe what happens with fields of other spins in an AdS spacetime. We will be very concise with our presentation as the necessary ingredients for this thesis have already been presented. We feel, however, that some comments are in order for the sake of completeness. Since we have worked out the spin-1/2 field computation in gory detail, here we will proceed more quickly. Starting from the Proca action the equations of motion for the one-form field are given by

$$\frac{1}{\sqrt{|G|}}\partial_M\left(\sqrt{|G|}G^{MN}G^{RS}F_{NS}\right) - m^2 A_M = 0\,. \tag{3.64}$$

In order to keep our presentation simple, let us imagine that the AdS has a Euclidean signature and we can put the momentum in the time direction only. We also want to examine polarizations of the vector field that are neither in the time nor the radial direction. Expanding out the equations of motion yields

$$U^2\partial_z^2 A_S - U\partial_U A_S + U^2\partial_t^2 A_S - m^2 A_S = 0\,. \tag{3.65}$$

Here is where the things can go horribly wrong and this is quite an educational example. If we substitute as an ansatz now $U^{\tilde{\Delta}}$ into the equation we derived above we will get a wrong answer. The reason is that in contrast to the scalar field example, here we have a vector index. Consider working for example with A^M instead of A_M. The expression would be shifted by different powers of U. We can however, remember that there is physical meaning in the orthonormal basis. All we need to do is to consider shifting the expression by considering the change $\frac{1}{U}A_{(M)} = A_M$, where again we have denoted by $_{(A)}$ indices in the one-form basis. Inserting this expression into the equations of motion will bring them in

a more appropriate basis. Then we can consider a power-law of the form $A_{(M)} = U^{\Delta}$ and study the resulting equation. The answer we obtain is

$$\Delta = 2 \pm \sqrt{1 + m^2}\,. \tag{3.66}$$

The above is the correct answer [79, 80].

Chapter 4

Symmetries in field theory

Here we wish to review some basic facts about symmetries in field theory that we feel are necessary for a proper presentation of the material of the next sections. There are many great places in the literature that analyze these issues thoroughly, however we are basing our presentation to our favourite resources which we mention here. Since we do not cover supersymmetry here, we would like suggest either [10] or [24] as excellent resources.[1]

4.1 Conformal symmetry

Our discussion here mainly follows [87, 88].

The transformations of the conformal group are such that the metric can at most pick up a position dependent overall factor. Another way of phrasing this, perhaps a more intuitive way, is that conformal transformations preserve angles. Let us consider as a starting point a metric in a general d-dimensional space $\mathbb{R}^{a,b}$ such that the dimension is $d = a + b$ with a signature (a, b) that is given by

$$ds^2 = G_{MN} dx^M dx^N \,. \tag{4.1}$$

A conformal tranformation is defined as the mapping $\Phi : \mathbb{R}^{a,b} \to \mathbb{R}^{a,b}$ and explicitly we have that $\Phi : G_{MN}(x) \to G'_{MN}(x') = \Omega(x) G_{MN}(x)$, having denoted by $\Omega(x)$ the scale factor of the conformal transformation. Note, however, under a general coordinate transformation $x \to x'$, the metric transforms as

$$G_{MN} \to G'_{MN}(x') = \frac{\partial x^R}{\partial x'^M} \frac{\partial x^S}{\partial x'^N} G_{RS}(x) \tag{4.2}$$

and hence the flat metric under a conformal transformation obeys the following

$$\eta'_{MN} = \frac{\partial x^R}{\partial x'^M} \frac{\partial x^S}{\partial x'^N} \eta_{RS} = \Omega(x) \eta_{MN} \,. \tag{4.3}$$

[1] There are two approaches in the study of supersymmetric field theories. One is the use of the superspace. In that approach the distinct physical fields are collectively grouped into superfields. The second approach, which is utilized in [24], is the use of field components that describe the physical states of the theory.

The goal is to find the infinitesimal generators and to do so we examine the following coordinate tranformation

$$x^M \to x'^M = x^M + \epsilon^M(x)\,. \tag{4.4}$$

Now, we are going to derive the conformal Killing vector equation and subsequently we will demonstrate its solution. To begin with, we compute the following

$$\frac{\partial x^R}{\partial x'^M} = \frac{\partial\left(x'^R + \epsilon^R\right)}{\partial x'^M} = \delta^R_M + \frac{\partial \epsilon^R}{\partial x'^M}\,. \tag{4.5}$$

It is quite easy to see that to linear order in ϵ we have for the last term

$$\frac{\partial \epsilon^R}{\partial x'^M} = \frac{\partial \epsilon^R}{\partial x^C}\frac{\partial x^C}{\partial x'^M} = \frac{\partial \epsilon^R}{\partial x^C}\left(\frac{\partial x'^C}{\partial x'^M} - \frac{\partial \epsilon^C}{\partial x'^M}\right) = \frac{\partial \epsilon^R}{\partial x^M} + \mathcal{O}(\epsilon^2)\,. \tag{4.6}$$

We can use equations (4.5) and (4.6) to manipulate equation (4.3) and we derive

$$\begin{aligned}
\left(\delta^R_M + \partial_M \epsilon^R\right)\left(\delta^S_N + \partial_N \epsilon^S\right)\eta_{RS} = \Lambda(x)\eta_{MN}\,,\to \\
\eta_{MN} + \partial_N \epsilon_M + \partial_M \epsilon_N + \mathcal{O}(\epsilon^2) = \Lambda(x)\eta_{MN}\,,\to \\
\left(\Lambda(x) - 1\right)\eta_{MN} = \partial_M \epsilon_N + \partial_N \epsilon_M\,,\to \\
\Lambda(x) - 1 = \frac{2}{d}\left(\partial\cdot\epsilon\right)\,,
\end{aligned} \tag{4.7}$$

where in the last line we just traced with η^{MN}. Recall, however, that

$$\left(\Lambda(x) - 1\right)\eta_{MN} = \partial_M \epsilon_N + \partial_N \epsilon_M \tag{4.8}$$

and we can use the last line of equation (4.7) to derive

$$\partial_M \epsilon_N + \partial_N \epsilon_M = \frac{2}{d}\left(\partial\cdot\epsilon\right)\eta_{MN}\,, \tag{4.9}$$

which is the conformal Killing vector equation.

4.1.1 Solving the conformal Killing vector equation

The starting point of this section is the conformal Killing vector equation, given by

$$\partial_M \epsilon_N + \partial_N \epsilon_M = \frac{2}{d}\left(\partial\cdot\epsilon\right)\eta_{MN}\,. \tag{4.10}$$

We act on the above equation with the operator $\partial_A\partial_B$ and we obtain

$$\partial_A\partial_B\left(\partial_M \epsilon_N + \partial_N \epsilon_M\right) = \frac{2}{d}\eta_{MN}\partial_A\partial_B\left(\partial\cdot\epsilon\right)\,. \tag{4.11}$$

In the above epression, equation (4.11), we consider different cases separately:

- We have $A = M$ and $B = N$ which yields

$$\begin{aligned} 2\Box\left(\partial\cdot\epsilon\right) &= \frac{2}{d}\Box\left(\partial\cdot\epsilon\right) \rightarrow \\ \Box\left(\partial\cdot\epsilon\right) &= 0\,. \end{aligned} \tag{4.12}$$

  Note that the above is trivially satisfied if $d = 1$.

- We consider $B = M$ and we obtain

$$\begin{aligned} \Box\partial_A\epsilon_M + \partial_A\partial_M\left(\partial\cdot\epsilon\right) &= \frac{2}{d}\partial_A\partial_M\left(\partial\cdot\epsilon\right) \\ \left(\frac{2}{d}-1\right)\partial_A\partial_M\left(\partial\cdot\epsilon\right) &= \Box\partial_A\epsilon_M \end{aligned} \tag{4.13}$$

  From the above equation we obtain

$$\left(\frac{2}{d}-1\right)\partial_A\partial_M\left(\partial\cdot\epsilon\right) = \frac{1}{2}\Box\left(\partial_A\epsilon_M + \partial_M\epsilon_A\right)\,, \tag{4.14}$$

  and we can use equation (4.11) to furher write

$$\left(\frac{2}{d}-1\right)\partial_A\partial_M\left(\partial\cdot\epsilon\right) = \frac{1}{d}\eta_{AM}\Box\left(\partial\cdot\epsilon\right)\,. \tag{4.15}$$

  It is easy to see that using equation (4.12) we obtain

$$\left(\frac{2}{d}-1\right)\partial_A\partial_M\left(\partial\cdot\epsilon\right) = \frac{1}{d}\eta_{AM}\Box\left(\partial\cdot\epsilon\right) = 0\,, \tag{4.16}$$

  and hence

$$\partial_A\partial_M\left(\partial\cdot\epsilon\right) = 0\,. \tag{4.17}$$

  Note that the above holds for $d \neq 2$, while for the two-dimensional case it is satisfied trivially. As a remark we mention that for $d = 2$ it is quite straightforward to show that after a careful manipulation the conformal Killing vector equations become the Cauchy-Riemann equations. After this brief remark, we return to the final result we obtained above. Just by examining the general form of $\partial_A\partial_M\left(\partial\cdot\epsilon\right) = 0$ we an conclude that $\partial\cdot\epsilon$ can contain a constant term and a linear term in x^M. Therefore, without loss of generality we can write the solution as

$$\partial\cdot\epsilon = d\left(\lambda - 2b_A x^A\right)\,. \tag{4.18}$$

  So now, having an expression for $\partial\cdot\epsilon$ we an insert it into the expression for $\Box\left(\partial_M\epsilon_N + \partial_N\epsilon_M\right)$ and derive

$$\partial_M\epsilon_N + \partial_N\epsilon_M = 2\eta_{MN}\left(\lambda - 2b_A x^A\right)\,. \tag{4.19}$$

  The next step is to act on the above with a derivative, ∂_A. From that result we rename $A \leftrightarrow N$

and hence we obtain the following two formulae

$$\begin{aligned}\partial_A\partial_M\epsilon_N + \partial_A\partial_N\epsilon_M &= -4\eta_{MN}b_A\,,\\ \partial_N\partial_M\epsilon_A + \partial_N\partial_A\epsilon_M &= -4\eta_{MA}b_N\,,\end{aligned} \tag{4.20}$$

we subtract the two expression and the result is

$$\partial_M\left(\partial_A\epsilon_N - \partial_N\epsilon_A\right) = 4\left(\eta_{MA}b_N - \eta_{MN}b_A\right)\,, \tag{4.21}$$

and now we proceed as we did previously. Namely, we can observe that $\partial_A\epsilon_N - \partial_N\epsilon_A$ can contain a constant and a linear term in x^M and thus we write

$$\partial_A\epsilon_N - \partial_N\epsilon_A = 2\omega_{AN} + 4\left(\eta_{MA}b_N - \eta_{MN}b_A\right)x^M = 2\omega_{AN} + 4\left(x_Ab_N - x_Nb_A\right)\,. \tag{4.22}$$

From the above, we can see that the combination $x_Ab_N - x_Nb_A$ is antisymmetric under $A \leftrightarrow N$ and therefore ω_{AN} has to be antisymmetric as well. Let us re-write for convenience what we have derived so far

$$\partial_A\epsilon_N - \partial_N\epsilon_A = 2\omega_{AN} + 4\left(x_Ab_N - x_Nb_A\right)\,, \partial_A\epsilon_N + \partial_N\epsilon_A \quad = 2\left(\lambda - 2b\cdot x\right)\eta_{AN}\,, \tag{4.23}$$

and we can simply sum the above to obtain

$$\partial_A\epsilon_N = \left(\omega_{AN} + \lambda\eta_{AN}\right) + 2\left(-b_R\eta_{AN} + b_N\eta_{AR} - b_A\eta_{NR}\right)x^R\,, \tag{4.24}$$

from which we see that ϵ_N can contain terms up to order $\mathcal{O}(x^2)$. We write the solution

$$\epsilon_N = a_N + \mathcal{E}_{NR}x^R + \mathcal{F}_{NRS}x^Rx^S\,, \tag{4.25}$$

and it is quite straightforward to see that $\mathcal{F}_{NRS} = \mathcal{F}_{NSR}$ in order to respect the symmetries of x^Rx^S. We act on ϵ_N with a derivative and we obtain

$$\partial_A\epsilon_N = \mathcal{E}_{NA} + 2\mathcal{F}_{NRA}x^R\,. \tag{4.26}$$

Finally, we can compare the above to equation (4.24) and deduce that

$$\begin{aligned}\mathcal{E}_{NA} &= \omega_{AN} + \lambda\eta_{AN}\,,\\ \mathcal{F}_{NRA} &= -b_R\eta_{AN} + b_N\eta_{AR} - b_A\eta_{NR}\,,\end{aligned} \tag{4.27}$$

and therefore the final solution that we get is

$$\epsilon_M = \alpha_M + \lambda x_M + \omega_{NM}x^N + b_Mx^2 - 2b\cdot x\; x_M\,. \tag{4.28}$$

4.1.2 Conformal symmetry in $d \geq 3$

Given a general coordinate trnaformation of the form $x \to x' = x'(x)$ we can define the way it acts on functions $\Phi(x)$ such that $\Phi'(x') \equiv \Phi(x)$. Any infinitesimal coordinate transformation assumes the form

$$x'^M = x^M + \epsilon_A \frac{\delta x^M}{\delta \epsilon_A}\,, \tag{4.29}$$

with ϵ_A being a small parameter. The generator, G_A, of the above transformation is given by

$$\delta_\epsilon \Phi = \Phi'(x) - \Phi(x) = -\epsilon_A \; G_A \; \Phi(x)\,, \tag{4.30}$$

and keeping in mind that $\Phi'(x') \equiv \Phi(x)$ we obtain

$$\epsilon_A \; G_A \; \Phi(x) = \Phi(x) - \Phi\left(x - \epsilon_A \frac{\delta x^M}{\delta \epsilon_A}\right)\,, \tag{4.31}$$

and we linearize in the small parameter to obtain

$$G_A \Phi(x) = -\frac{\delta x^M}{\delta \epsilon_A} \partial_M \Phi(x)\,. \tag{4.32}$$

In the above general framework consider for example a translation of the form $x^M \to x^M + \omega^M$. In this case, the index A in the ω_A of the above expression is just a a spacetime index and the result just yields a δ^M_N. Hence, the generator of translations, which we denote by P_M as is common in the literature, just takes the simple form $P_M = -\partial_M$. Likewise, we can think of infinitesimal Lorentz transformations of the form $x^M \to x^M + \omega_{RN}\eta^{RN}x^N$, with ω_{RN} being antisymmetric. In this case, the A index in ω_A of our last equation is equal to $A = RN$. We obtain

$$\frac{\delta x^M}{\delta \omega_{RN}} = \frac{1}{2}\left(\eta^{RM}x^N - \eta^{NM}x^R\right)\,, \tag{4.33}$$

and we obtain $\Lambda_{MN} = x_M\partial_N - x_N\partial_M$. Moving on the dilatations it is easy to see that the generator is given by $D = -x^M\partial_M$. And similarly we obtain from the infinitesimal special conformal trnasformation its corresponding generator. We state the results explicitly below[2]

$$\begin{aligned} P_M &= -\partial_M\,, \qquad \Lambda_{MN} = x_M\partial_N - x_N\partial_M\,, \\ D &= -x^M\partial_M\,, \qquad K_M = -2x_M x^N\partial_N + x^2\partial_M\,. \end{aligned} \tag{4.34}$$

[2]we are working with anti-hermitian generators. This gets rid of the i-factors in many places and follows the same convention of [24].

It is quite straightforward to check that these satisfy the following commutation relations

$$\begin{aligned}
[D, P_M] &= P_M \,, \\
[D, K_M] &= -K_M \,, \\
[K_M, P_N] &= 2\left(\eta_{MN} D - \Lambda_{MN}\right) \,, \\
[K_P, \Lambda_{MN}] &= \eta_{PM} K_N - \eta_{PN} K_M \,, \\
[P_P, \Lambda_{MN}] &= \eta_{PM} P_N - \eta_{PN} P_M \,, \\
[\Lambda_{MN}, \Lambda_{PS}] &= \eta_{NP}\Lambda_{MS} + \eta_{MS}\Lambda_{NP} - \eta_{MP}\Lambda_{NS} - \eta_{NS}\Lambda_{MP} \,,
\end{aligned} \tag{4.35}$$

and any unspecified commutator vanishes.[3]

For any CFT in $d \geq 3$ the above is the complete description of the conformal group. It contains Lorentz transformations, translations, dilatations and special conformal transformations. The conformal group has dimension equal to

$$d + 1 + \frac{1}{2}d(d-1) + d = \frac{1}{2}(d+1)(d+2) \,, \tag{4.36}$$

where the contributions above are due to the presence of translations, dilatation, Lorentz tranformations and special conformal transformations respectively. This is isomorphic to the group $SO(a+1, b+1)$. We have described how to obtain the generators of the Lie algebra $\mathfrak{so}(a+1, b+1)$ and what commutation relations they satisfy. It is quite interesting to make some brief comments on the structure described above. The first two commutators dictate how translations and special conformal generators transform under the generator of dilatations. That generator, denoted by D above, defines an abelian Lie algebra that is isomorphic to $\mathfrak{so}(1,1)$ and every generator has a specified weight under its action. This weight is the scaling dimension and it's quite easy to see from the explicit form of the generators that that the generator of translations has weight equal to 1, while the special conformal transformation generator has weight equal to -1. The commutation relations in the fourth and fifth lines inform us that translations, which are generated by P_M, and special conformal transformations, generated by K_M, transform under the vector representation of the $\mathfrak{so}(a,b)$ algebra. This works as it should, since we have described these generators by a vector. The last line is the deinition of the Lorentz Lie algebra, $\mathfrak{so}(a,b)$. The thrid line is needed in order to close the algebra.

4.1.3 Unitarity bounds

Here we wish to discuss the unitarity bounds for the CFTs we have considered so far. We will be working in Euclidean signature, which is equivalent to setting $b = 0$ in the above discussion, in order to follow closely [88, 89]. This will also be very convenient. We refrain from demonstrating all the details of radial quantization in order to keep the presentation brief. There are many excellent places in the literature that discuss this in depth, see for example [87]. In this section, we will state below some basic facts that we will need and then derive some very important results.

To begin with, we state that in this context the generator of the dilations, D, can be thought of as the Hamiltonian of the system. As mentioned above, we will not go into much detail but we will sketch a

[3] We prove these relations in appendix A.1.

nice way of thinking about this. Consider the space $\mathbb{R}^b$ parameterized by

$$ds^2 = dr^2 + r^2 d\Omega_{d-1} = r^2 \left(\frac{1}{r^2} dr^2 + d\Omega_{d-1} \right) , \tag{4.37}$$

with $d\Omega_{d-1}$ being a $d-1$ dimensional sphere. We can consider the change of variables $t = \log r$ in order to obtain

$$\frac{1}{r^2} dr^2 + d\Omega_{d-1} = dt^2 + d\Omega_{d-1} , \tag{4.38}$$

which describes the space $\mathbb{R} \times S^{d-1}$. On the $\mathbb{R}^d$ space the theory should be invariant under a rescaling and hence the study of a CFT defined on $\mathbb{R}^d$ is equivalent to the study of the theory on $\mathbb{R} \times S^{d-1}$. Essentially, doing the above we have taken circles of constant radius in $\mathbb{R}^d$ and mapped them to slices of constant t defined on $\mathbb{R} \times S^{d-1}$. So, the dilation operator corresponds to time translations on the $\mathbb{R} \times S^{d-1}$ theory and thus we can identify it with the Hamiltonian.

Any CFT that contains operators that do not respect the bounds that we will derive is either non-unitary (in Lorentzian signature) or non-positive (in Euclidean signature). This is to say, that physical CFTs should have a bounded from below energy spectrum. We have already seen that translation generators have weight equalt to 1 and conformal transformation generators have weight -1. Since our CFT has to be bounded from below, there has to be a state of lowest energy (which is called highest weight state) that satisfies

$$K_M \, |[Y]_\Delta\rangle = 0 . \tag{4.39}$$

The highest weight state is also called a primary state. The label Δ denotes its scaling dimension and it forms a representation with respect to the $\mathfrak{so}(d)$ Lorentz group. In order for it to be unique, we should also require that it is a primary of the $\mathfrak{so}(d)$ representation. The Y index refers to the representation under the Lorentz group. Our main interest in this thesis is the four dimensional case for which we have $\mathfrak{so}(4) \cong \mathfrak{su}(2) \oplus \mathfrak{su}(2)$ and thus the respective representations carry two labels, one for each of the $\mathfrak{su}(2)$ spins, namely $[Y] = [j_1, j_2]$.

We can create non-highest weight states, which we call descendants, just by acing on the primary with the P_M generator in the following way:

$$P_{M_1} P_{M_2} \cdots P_{M_n} \, |[Y]_\Delta\rangle \ . \tag{4.40}$$

In order to work out the expressions for the unitarity bounds in our CFTs we need to introduce hermitian conjugation. While there is a formal way of deriving the results see [87, 88] here we just state them without proof for brevity. The relations that we need are stated below

$$\begin{aligned} \Lambda_{MN}^\dagger &= \Lambda_{MN} , \qquad & P_M^\dagger &= K_M , \\ K_M^\dagger &= P_M , & D^\dagger &= D . \end{aligned} \tag{4.41}$$

Scalar fields

With the above information at hand we are in a position to compute the unitarity bound for a scalar, $[Y] = 0$. We normalize such that the primary has unit norm $\langle [0]_\Delta | [0]_\Delta \rangle = 1$ and we can now compute the norm of a descendant of level one

$$\begin{aligned}
\left\| \alpha^M P_M \left| [0]_\Delta \right\rangle \right\|^2 &= \bar{\alpha}^M \alpha^N \left\langle [0]_\Delta \left| K_M P_N \right| [0]_\Delta \right\rangle \,, \\
&= \bar{\alpha}^M \alpha^N \left\langle [0]_\Delta \left| [K_M, P_N] + P_N K_M \right| [0]_\Delta \right\rangle \,, \\
&= \bar{\alpha}^M \alpha^N \left\langle [0]_\Delta \left| [K_M, P_N] \right| [0]_\Delta \right\rangle \,, \\
&= 2\bar{\alpha}^M \alpha^N \left\langle [0]_\Delta \left| \delta_{MN} D - \Lambda_{MN} \right| [0]_\Delta \right\rangle \,, \\
&= 2|\alpha|^2 \Delta \,,
\end{aligned} \tag{4.42}$$

where we have used the fact that is a highest weight state and has zero spin. Thus, we conclude that $\Delta \geq 0$.

A natural question is whether we can constrain the scaling dimension more by considering higher-level descendants. Let us do the level-2 computation.

$$\begin{aligned}
\left\| \alpha^{MN} P_M P_N \left| [0]_\Delta \right\rangle \right\|^2 &= \alpha^{MN} \bar{\alpha}^{PS} \left\langle [0]_\Delta \left| K_S K_P P_M P_N \right| [0]_\Delta \right\rangle \,, \\
&= 2\alpha^{MN} \bar{\alpha}^{PS} \left(\left\langle [0]_\Delta \left| K_S \left([K_P, P_M] + P_M K_P \right) P_N \right| [0]_\Delta \right\rangle \right) \,, \\
&= 2\alpha^{MN} \bar{\alpha}^{PS} \left(\left\langle [0]_\Delta \left| K_S [K_P, P_M] P_N + K_S P_M \left([K_P, P_N] + P_N K_P \right) \right| [0]_\Delta \right\rangle \right) \,, \\
&= 2\alpha^{MN} \bar{\alpha}^{PS} \left(\left\langle [0]_\Delta \left| K_S [K_P, P_M] P_N + K_S P_M [K_P, P_N] \right| [0]_\Delta \right\rangle \right) \,, \\
&= 2\alpha^{MN} \bar{\alpha}^{PS} \left(\left\langle [0]_\Delta \left| K_S \left(\delta_{PM} D + \Lambda_{MP} \right) P_N + K_S P_M \left(\delta_{PN} D + \Lambda_{PN} \right) \right| [0]_\Delta \right\rangle \right) \,, \\
&= 2\alpha^{MN} \bar{\alpha}^{PS} \left(\left\langle [0]_\Delta \left| K_S \left(\delta_{PM} D + \Lambda_{MP} \right) P_N + K_S P_M \delta_{PN} D \right| [0]_\Delta \right\rangle \right) \,,
\end{aligned} \tag{4.43}$$

having used the fact that we are considering a scalar.

We can now proceed to examine the last term of the above expression. It is equal to

$$\begin{aligned}
\left\langle [0]_\Delta \left| \delta_{PN} K_S P_M D \right| [0]_\Delta \right\rangle &= \left\langle [0]_\Delta \left| \delta_{PN} K_S \left([P_M, D] + D P_M \right) \right| [0]_\Delta \right\rangle \,, \\
&= \left\langle [0]_\Delta \left| \delta_{PN} K_S [P_M, D] \right| [0]_\Delta \right\rangle + \left\langle [0]_\Delta \left| \delta_{PN} K_S D P_M \right| [0]_\Delta \right\rangle \,, \\
&= - \left\langle [0]_\Delta \left| \delta_{PN} K_S P_M \right| [0]_\Delta \right\rangle + \left\langle [0]_\Delta \left| \delta_{PN} \left([K_S, D] + D K_S \right) P_M \right| [0]_\Delta \right\rangle \,, \\
&= - \left\langle [0]_\Delta \left| \delta_{PN} K_S P_M \right| [0]_\Delta \right\rangle + \left\langle [0]_\Delta \left| \delta_{PN} K_S P_M \right| [0]_\Delta \right\rangle + \left\langle [0]_\Delta \left| \delta_{PN} D K_S P_M \right| [0]_\Delta \right\rangle \,, \\
&= \left\langle [0]_\Delta \left| \delta_{PN} D K_S P_M \right| [0]_\Delta \right\rangle \,, \\
&= 2\Delta^2 \delta_{MS} \delta_{PN} \,.
\end{aligned} \tag{4.44}$$

We can likewise manipulate the rest of the terms. We have

$$\begin{aligned}\langle [0]_\Delta | K_S \left(\delta_{PM} D + \Lambda_{MP}\right) P_N | [0]_\Delta \rangle &= \langle [0]_\Delta | K_S \delta_{PM} D P_N | [0]_\Delta \rangle + \langle [0]_\Delta | K_S \Lambda_{MP} P_N | [0]_\Delta \rangle \ , \\ &= \langle [0]_\Delta | \delta_{PM} K_S D P_N | [0]_\Delta \rangle + \langle [0]_\Delta | K_S \left([\Lambda_{MP}, P_N] + P_N \Lambda_{MP}\right) | [0]_\Delta \rangle \ , \\ &= \langle [0]_\Delta | \delta_{PM} K_S D P_N | [0]_\Delta \rangle + \langle [0]_\Delta | K_S [\Lambda_{MP}, P_N] | [0]_\Delta \rangle \ , \\ &= \langle [0]_\Delta | \delta_{PM} K_S D P_N | [0]_\Delta \rangle + \langle [0]_\Delta | K_S \left(\delta_{PN} P_M - \delta_{MN} P_P\right) | [0]_\Delta \rangle \ , \\ &= \langle [0]_\Delta | \delta_{PM} K_S D P_N | [0]_\Delta \rangle + \langle [0]_\Delta | \delta_{PN} K_S P_M | [0]_\Delta \rangle \\ &- \langle [0]_\Delta | \delta_{MN} K_S P_P | [0]_\Delta \rangle \end{aligned} \tag{4.45}$$

Now, everything is quite simple and we can proceed as we did in the level-1 case as all the expressions are very similar. We have

$$\begin{aligned}\langle [0]_\Delta | \delta_{PM} K_S D P_N | [0]_\Delta \rangle &= \langle [0]_\Delta | \delta_{PM} \left([K_S, D] + D K_S\right) P_N | [0]_\Delta \rangle \ , \\ &= \langle [0]_\Delta | \delta_{PM} K_S P_N | [0]_\Delta \rangle + \langle [0]_\Delta | \delta_{PM} D K_S P_N | [0]_\Delta \rangle \ , \\ &= \delta_{MP} \delta_{SN} 2\Delta + \delta_{MP} \Delta_{SN} 2\Delta^2 \end{aligned} \tag{4.46}$$

The remaining terms are equal to

$$\langle [0]_\Delta | \delta_{PN} K_S P_M | [0]_\Delta \rangle = 2\delta_{PN} \delta_{SM} \Delta \tag{4.47}$$

and we also have

$$- \langle [0]_\Delta | \delta_{MN} K_S P_P | [0]_\Delta \rangle = -2\delta_{MN} \delta_{SP} \Delta \tag{4.48}$$

So, now we can return to the original expression of interest, namely the norm of the level-2 descendant. We just gather all the pieces we have computed so far and we factorize the expression, which yields

$$\begin{aligned}\left\| \alpha^{MN} P_M P_N | [0]_\Delta \rangle \right\|^2 &= 4\alpha^{MN} \bar{\alpha}^{PS} \left(\delta_{MP} \delta_{NS} \Delta(\Delta+1) + \delta_{MS} \delta_{NP} \Delta(\Delta+1) - \delta_{MN} \delta_{PS} \Delta\right) \ , \\ &= 4\Delta \left(2\left(\Delta+1\right) \bar{\alpha}^{MN} \alpha_{MN} - \bar{\alpha}^M_M \alpha^N_N\right) \end{aligned} \tag{4.49}$$

Allow us now to set $\alpha^{MN} = \delta^{MN}$ to obtain

$$4\Delta \left(2\left(\Delta+1\right) d - d^2\right) \tag{4.50}$$

and using the level-1 constrain, namely $\Delta \geq 0$, we conclude that the level-2 norm computation bounds the scaling expression to be

$$\Delta \geq \frac{d}{2} - 1 \tag{4.51}$$

which is the result we should obtain, see the review [90]. Observe that for $d = 4$ the result nicely agrees with what we derived in AdS_5 section 3.1.5.

One may wonder whether computing the norms of higher-level descendants will constrain the bound even further, however such is not the case. The proofs for this statement are quite involved and non-trivial and we refer the reader to the works of [91, 92]. Let us briefly mention that one can consider

the general case of an operator with arbitrary spin, use representation theory and obtain the bounds for the scaling dimensions. This goes beyond the scope of this thesis and we refer the interested reader to the lectures of [88, 89], where they can see the derivation and work out the details on their own.

The identity

Le us start with this example albeit trivial. Any CFT contains an identity field, which we denote by 1, which is a scalar state and has scaling dimension $\Delta = 0$. From the computations performed previously we know that its descendants have to be null. This holds true for any level and it is quite straightforward to verify the claim.

$$P_M \, 1 = \partial_M \, 1 = 0 \,, \tag{4.52}$$

in other words the identity field is invariant under translations.

Free massless scalar

The action for the theory is

$$\int d^d x \partial_M \Phi \partial^M \Phi \,, \tag{4.53}$$

and it is easy to compute that the dimension of the field is $\Delta = \frac{d}{2} - 1$. Since there are no interactions in the theory the scaling dimension does not obtain any quantum corrections. The free massless scalar saturates the unitarity bound computed above adn therefore we expect a null-vector in its representation which we have and is obvious from the equations of motion

$$P_M P^M \Phi = \partial_M \partial^M \Phi = 0 \,. \tag{4.54}$$

4.2 Superconformal symmetry

We being by mentioning some very useful references discussing aspects of the superconformal algerba. These are [89, 93–97].

In order to simplify matters and to follow [89, 94, 98] we will complixify the algebra. In order to impose the reality conditions whenever necessary we will specify the hermitian conjugate. In a four dimensional theory we have $\mathfrak{so}(4, \mathbb{C}) \cong \mathfrak{sl}(2, \mathbb{C}) \oplus \mathfrak{sl}(2, \mathbb{C})$ and similarly $\mathfrak{so}(6, \mathbb{C} \cong \mathfrak{sl}(4, \mathbb{C})$ for the conformal group. Note that in this section we will use lower case letters to avoid stifling the notation.

We employ a bi-spinor notation for the conformal algebra, which is a common practice, and we have

$$\begin{aligned} (\sigma^\mu)_{\alpha\dot{\alpha}} &= (i \; 1, \, \vec{\sigma}) \;, \\ (\bar{\sigma}^\mu)^{\dot{\alpha}\alpha} &= (-i \; 1, \, \vec{\sigma}) \;, \end{aligned} \tag{4.55}$$

where $\vec{\sigma}$ is a vector of the usual Pauli matrices. For the lowering and raising of the indices we use

$$X^a = \epsilon^{ab} X_b \;, \qquad X_a = \epsilon_{ab} X^b \;, \tag{4.56}$$

where $\epsilon_{12} = 1$, $\epsilon^{12} = -1$.

4.2.1 Four dimensional theories

The Lorentz generators $\Lambda_{\mu\nu}$ fall in the two adjoint representations of $\mathfrak{sl}(2,\mathbb{C})$, which are denoted by $\Lambda_\alpha{}^\beta$ and $\Lambda^{\dot\alpha}{}_{\dot\beta}$. The generators of the momenta and special conformal transformations are bispinors under the Lorentz group. We write

$$\begin{aligned} P_{\alpha\dot\alpha} &= (\sigma^\mu)_{\alpha\dot\alpha} P_\mu \ , \quad \Lambda_\alpha{}^\beta \ \ = -\frac{1}{4}(\bar\sigma^\mu)^{\dot\alpha\beta}(\sigma_\nu)_{\alpha\dot\alpha}\Lambda_{\mu\nu} \ , \\ K^{\dot\alpha\alpha} &= (\bar\sigma^\mu)^{\dot\alpha\alpha} K_\mu \ , \quad \Lambda^{\dot\alpha}{}_{\dot\beta} \ = -\frac{1}{4}(\bar\sigma^\mu)^{\dot\alpha\alpha}(\sigma_\nu)_{\alpha\dot\beta}\Lambda_{\mu\nu} \ . \end{aligned} \tag{4.57}$$

The conformal algebra in the notation we have chosen is, see [98, Appendix A]

$$\begin{aligned} [\Lambda_\alpha{}^\beta, \Lambda_\gamma{}^\delta] &= \delta_\gamma{}^\beta \Lambda_\alpha{}^\delta - \delta_\alpha{}^\delta \Lambda_\gamma{}^\beta \ , \\ [\Lambda^{\dot\alpha}{}_{\dot\beta}, \Lambda^{\dot\gamma}{}_{\dot\delta}] &= -\delta^{\dot\alpha}{}_{\dot\delta}\Lambda^{\dot\gamma}{}_{\dot\beta} + \delta^{\dot\gamma}{}_{\dot\beta}\Lambda^{\dot\alpha}{}_{\dot\delta} \ , \\ [\Lambda_\alpha{}^\beta, P_{\gamma\dot\gamma}] &= \delta_\gamma{}^\beta P_{\alpha\dot\gamma} - \frac{1}{2}\delta_\alpha{}^\beta P_{\gamma\dot\gamma} \ , \\ [\Lambda^{\dot\alpha\dot\beta}, P_{\gamma\dot\gamma}] &= \delta^{\dot\alpha}{}_{\dot\gamma} P_{\gamma\dot\beta} - \frac{1}{2}\delta^{\dot\alpha}{}_{\dot\beta} P_{\gamma\dot\gamma} \ , \\ [\Lambda_\alpha{}^\beta, K^{\dot\gamma\gamma}] &= -\delta_\alpha{}^\gamma K^{\dot\gamma\beta} + \frac{1}{2}\delta_\alpha{}^\beta K^{\dot\gamma\gamma} \ , \\ [\Lambda_\alpha{}^\beta, K^{\dot\gamma\gamma}] &= -\delta^{\dot\gamma}{}_{\dot\beta} K^{\dot\alpha\gamma} + \frac{1}{2}\delta^{\dot\alpha}{}_{\dot\beta} K^{\dot\gamma\gamma} \ , \\ [D, P_{\alpha\dot\alpha}] &= P_{\alpha\dot\alpha} \ , \\ [D, K^{\dot\alpha\alpha}] &= -K^{\dot\alpha\alpha} \ , \\ [K^{\dot\alpha\alpha}, P_{\beta\dot\beta}] &= 4\delta_\beta{}^\alpha \delta^{\dot\alpha}{}_{\dot\beta} D + 4\delta_\beta{}^\alpha \Lambda^{\dot\alpha}{}_{\dot\beta} + 4\delta^{\dot\alpha}{}_{\dot\beta}\Lambda_\beta{}^\alpha \ . \end{aligned} \tag{4.58}$$

At this point we wish to discuss the introduction of the supercharges $\mathcal{Q}^i{}_\alpha$ and $\bar{\mathcal{Q}}_{i\dot\alpha}$, with the index $i = 1, \cdots, \mathcal{N}$ denotng the amount of supersymmetry that we consider in a given theory. The algebra possesses an R-symmetry $\mathfrak{u}(\mathcal{N})$, as well, acting on the i, j indices. The generators of the R-symmetry are knonw to satisfy the $\mathfrak{u}(\mathcal{N})$ algebra which is described in terms of the commutator

$$[\mathcal{R}^i{}_j, \mathcal{R}^k{}_\ell] = \delta^k{}_j \mathcal{R}^i{}_\ell - \delta^i{}_\ell \mathcal{R}^k{}_j \ . \tag{4.59}$$

Now we are at a position to combine the superalgebra with the conformal algebra. As in the purely bosonic case, here we can also think of the composition of inversion with a supercharge and an inversion. The result of this operation is a new fermionic generator which is known as conformal supercharge and we denote these conformal supercharges by $\mathcal{S}_i{}^\alpha$ and $\bar{\mathcal{S}}^{i\dot\alpha}$. Note that the genrators of the R-symmetry, $\mathcal{R}^i{}_j$, in this case are included in the algebra.[4] We describe below the superconformal algebra in terms

[4] This is to be contrasted with the situation in supersymmetric gauge theories where the R-symmetry is an outer automorphism.

of commutators and anti-commutators

$$
\begin{aligned}
[\Lambda_\alpha{}^\beta, \mathcal{Q}^i{}_\gamma] &= \delta_\gamma{}^\beta \mathcal{Q}^i{}_\alpha - \frac{1}{2}\delta_\alpha{}^\beta \mathcal{Q}^i{}_\gamma \ , \\
[\Lambda^{\dot\alpha}{}_{\dot\beta}, \bar{\mathcal{Q}}_{i\dot\gamma}] &= \delta^{\dot\alpha}{}_{\dot\gamma} \bar{\mathcal{Q}}_{i\dot\beta} - \frac{1}{2}\delta^{\dot\alpha}{}_{\dot\beta} \bar{\mathcal{Q}}_{i\dot\gamma} \ , \\
[\Lambda_\alpha{}^\beta, \mathcal{S}_i{}^\gamma] &= -\delta_\alpha{}^\gamma \mathcal{S}_i{}^\beta + \frac{1}{2}\delta_\alpha{}^\beta \mathcal{S}_i{}^\gamma \ , \\
[\Lambda^{\dot\alpha}{}_{\dot\beta}, \bar{\mathcal{S}}^{i\dot\gamma}] &= -\delta^{\dot\gamma}{}_{\dot\beta} \bar{\mathcal{S}}^{i\dot\alpha} + \frac{1}{2}\delta^{\dot\alpha}{}_{\dot\beta} \bar{\mathcal{S}}^{i\dot\gamma} \ , \\
[D, \mathcal{Q}^i{}_\alpha] &= \frac{1}{2}\mathcal{Q}^i{}_\alpha \ , \\
[D, \bar{\mathcal{Q}}_{i\dot\alpha}] &= \frac{1}{2}\bar{\mathcal{Q}}_{i\dot\alpha} \ , \\
[D, \mathcal{S}_i{}^\alpha] &= -\frac{1}{2}\mathcal{S}_i{}^\alpha \ , \\
[D, \bar{\mathcal{S}}^i{}_{\dot\alpha}] &= -\frac{1}{2}\bar{\mathcal{S}}^i{}_{\dot\alpha} \ , \\
[\mathcal{R}^i{}_j, \mathcal{Q}^k{}_\alpha] &= \delta_j{}^k \mathcal{Q}^i{}_\alpha - \frac{1}{4}\delta^i{}_j \mathcal{Q}^k{}_\alpha \ , \\
[\mathcal{R}^i{}_j, \bar{\mathcal{Q}}_{k\dot\alpha}] &= -\delta_k{}^i \bar{\mathcal{Q}}_{j\dot\alpha} + \frac{1}{4}\delta^i{}_j \bar{\mathcal{Q}}_{k\dot\alpha} \ , \\
[\mathcal{R}^i{}_j, \mathcal{S}_k{}^\alpha] &= -\delta^i{}_k \mathcal{S}_j{}^\alpha + \frac{1}{4}\delta^i{}_j \mathcal{S}_k{}^\alpha \ , \\
[\mathcal{R}^i{}_j, \bar{\mathcal{S}}^{k\dot\alpha}] &= \delta^k{}_j \bar{\mathcal{S}}^{i\dot\alpha} - \frac{1}{4}\delta^i{}_j \bar{\mathcal{S}}^{k\dot\alpha} \ , \\
[P_{\alpha\dot\alpha}, \mathcal{S}_i{}^\beta] &= -2\delta_\alpha{}^\beta \bar{\mathcal{Q}}_{i\dot\alpha} \ , \\
[P_{\alpha\dot\alpha}, \bar{\mathcal{S}}^{i\dot\beta}] &= -2\delta_{\dot\alpha}{}^{\dot\beta} \mathcal{Q}^i{}_\alpha \ , \\
[K^{\dot\alpha\alpha}, \mathcal{Q}^i{}_\beta] &= 2\delta_\beta{}^\alpha \bar{\mathcal{S}}^{i\dot\alpha} \ , \\
[K^{\dot\alpha\alpha}, \bar{\mathcal{Q}}_{i\dot\beta}] &= 2\delta_{\dot\beta}{}^{\dot\alpha} \mathcal{S}_i{}^\alpha \ , \\
\{\mathcal{Q}^i{}_\alpha, \bar{\mathcal{Q}}_{j\dot\alpha}\} &= \frac{1}{2}\delta^i{}_j P_{\alpha\dot\alpha} \ , \\
\{\bar{\mathcal{S}}^{i\dot\alpha}, \mathcal{S}_j{}^\alpha\} &= \frac{1}{2}\delta^i{}_j K^{\dot\alpha\alpha} \ , \\
\{\mathcal{Q}^i{}_\alpha, \mathcal{S}_j{}^\beta\} &= \delta^i{}_j \Lambda_\alpha{}^\beta + \frac{1}{2}\delta^i{}_j \delta_\alpha{}^\beta D - \delta_\alpha{}^\beta \mathcal{R}^i{}_j \ , \\
\{\bar{\mathcal{S}}^{i\dot\alpha}, \bar{\mathcal{Q}}_{j\dot\beta}\} &= \delta^i{}_j \bar{\Lambda}^{\dot\alpha}{}_{\dot\beta} + \frac{1}{2}\delta^i{}_j \delta^{\dot\alpha}{}_{\dot\beta} D + \delta^{\dot\alpha}{}_{\dot\beta} \mathcal{R}^i{}_j \ .
\end{aligned}
\tag{4.60}
$$

From the above commutators we can conclude that the supercharges have $+\frac{1}{2}$ scaling dimension, while the conformal supercharges have weight $-\frac{1}{2}$.[5]

While this looks horribly complicated, the structure of the algebra is actually quite simple. In order to make this apparent we can just break it down to much simpler superalgebras. We can observe that the

[5]Recall that supercharges square to generators of momenta.

algebra can be understood as supermatrices that assume the following form

$$\left(\begin{array}{c|c} \text{conformal algebra} & \text{supercharges} \\ (\Lambda_{\mu\nu}, P_\mu, K_\mu, D) & \left(\mathcal{Q}^i{}_\alpha, \bar{\mathcal{S}}^{i\dot{\alpha}}\right) \\ \hline \text{supercharges} & \text{R-symmetry} \\ \left(\bar{\mathcal{Q}}_{i\dot{\alpha}}, \mathcal{S}_i{}^\alpha\right) & \left(\mathcal{R}^i{}_j\right) \end{array}\right)$$

Let use quickly point out that for the case of the $\mathcal{N}=4$ the generator $\mathcal{R}^i{}_i$ commutes with all the elements belonging in the algebra.[6] This can be very easily seen from the previous commutations relations and by noting that the (i,j) contraction in the Kronecker-δ, $\delta^i{}_j$, yields $\mathcal{N}$ as a result. Therefore, for $\mathcal{N}=4$ the commutators vanish. Hence, in this case the $\mathcal{R}^i{}_i$ can be removed from the algebra. We state below the real form of the superconformal algebras for various ammounts of $\mathcal{N}$ taking into account the fact that $\mathcal{R}^i{}_i$ can be moded out in the $\mathcal{N}=4$ theory. We have

$$\begin{aligned} \mathcal{N} = \{1,\,2,\,3\}\text{superconformal algebra} &\cong \mathfrak{su}(2,2|\mathcal{N})\ , \\ \mathcal{N}=4\text{ superconformal algebra} &\cong \mathfrak{psu}(2,2|4)\ . \end{aligned}$$

Before moving on to te next sections, let us state the representations of the bosonic subalgebra in which the supercharges transform:

$$\begin{aligned} \mathcal{N}=1\ &:\ \ \mathcal{Q}\in[1,0]^{(-1)}_{\frac{1}{2}}\ , \qquad \bar{\mathcal{Q}}\in[0,1]^{(1)}_{\frac{1}{2}}\ , \\ \mathcal{N}=2\ &:\ \ \mathcal{Q}\in[1,0]^{(1,-1)}_{\frac{1}{2}}\ , \qquad \bar{\mathcal{Q}}\in[0,1]^{(1,1)}_{\frac{1}{2}}\ , \\ \mathcal{N}=3\ &:\ \ \mathcal{Q}\in[1,0]^{(1,0,-1)}_{\frac{1}{2}}\ , \quad \bar{\mathcal{Q}}\in[0,1]^{(0,1,1)}_{\frac{1}{2}}\ , \\ \mathcal{N}=4\ &:\ \ \mathcal{Q}\in[1,0]^{(1,0,0)}_{\frac{1}{2}}\ , \qquad \bar{\mathcal{Q}}\in[0,1]^{(0,0,1)}_{\frac{1}{2}}\ . \end{aligned} \tag{4.61}$$

Here, we labelled representations by $[Y]^{(R)}_{\Delta}$, with Y denoting the specific Lorentz representation - which is specified by the doublet of Dynkin labels of the two $\mathfrak{su}(2)$'s of the theory - Δ is the scaling dimension and (R) stands for the representation of the R-symmetry. It is determined by the $\mathcal{N}-1$ Dynkin labels of $\mathfrak{su}(\mathcal{N})$ and the overall $\mathfrak{u}(1)$ charge, with the only exception being the $\mathcal{N}=4$ theory. The last entry is the $\mathfrak{u}(1)$-charge.

Finally, we state how the hermicity property acts on the generators of the algebra:

$$\begin{aligned} (\Lambda_\alpha{}^\beta)^\dagger &= \Lambda_\beta{}^\alpha\ , \quad (\mathcal{Q}^i{}_\alpha)^\dagger = \mathcal{S}_i{}^\alpha\ , \\ (\Lambda^{\dot{\alpha}}{}_{\dot{\beta}})^\dagger &= \Lambda^{\dot{\beta}}{}_{\dot{\alpha}}\ , \quad (\bar{\mathcal{Q}}_{i\dot{\alpha}})^\dagger = \bar{\mathcal{S}}^{i\dot{\alpha}}\ , \\ (P_{\alpha\dot{\alpha}})^\dagger &= K^{\dot{\alpha}\alpha}\ , \quad (\mathcal{R}^i{}_j)^\dagger = \mathcal{R}^j{}_i\ , \\ D^\dagger &= D\,. \end{aligned} \tag{4.62}$$

[6] In other words it is central.

The hermitian conjugation: an aside

It is worthwhile stressing that the way we have defined the action of the † is essentially by considering it as an anti-automorphism of the algebra [89]. In other words, hermitian conjugation acts as

$$\langle X^\dagger, Y^\dagger \rangle = \Big(\langle Y^\dagger, X^\dagger \rangle \Big)^\dagger \,, \tag{4.63}$$

where in the above $\langle ., . \rangle$ is either a commutator or an anticommutator. This is consistent with the structure of the superconformal algebra as we explicitly show in appendix A.2.

4.2.2 Unitary representations

We have already seen that the generators of special conformal trnasformations have weight equal to -1 and that the conformal supercharges have scaling dimension given by $-\frac{1}{2}$. As we did in the purely bosonic, here we also wish to consider theories that have a bounded from below energy spectrum. Hence, we require that there exists a state that is annihilated by the action of the special conformal trnasformations generator as well as the conformal supercharges, and we write

$$K^{\dot\alpha\alpha} \, |[Y]^{(R)}_\Delta\rangle = 0 \,, \qquad \mathcal{S}_k{}^\alpha \, |[Y]^{(R)}_\Delta\rangle = 0 \,, \qquad \bar{\mathcal{S}}^{k\dot\alpha} \, |[Y]^{(R)}_\Delta\rangle = 0 \,. \tag{4.64}$$

In the above notation we have written (R) to denote colelctively all labels related to the R-symmetry of the theory. Following the nomenclature of the CFTs, this state is called a superconformal primary state. From that we cna build representations that contain its descendants which can be obtained by the action of the supercharges and the translation generators. Any representation of the superconformal algebra contains a finite number of conformal primaries. Recall that $\{\mathcal{Q}, \bar{\mathcal{Q}}\} \sim P_\mu$ and thus certain combinations of the supercharges can be re-expressed in terms of the operator P_μ, which is just a derivative. So, the number of combinations of supercharges that we can apply on a primary state, without generating derivatives, is always a finite number. A very useful trick is to decompose the superconformal multiplet into its bosonic part (the conformal multiplets).

Let us consider a simple example, a four-dimensional $\mathcal{N} = 1$ superconformal field theory. Starting from the conformal primary we can consider the level-1 descendants

$$\mathcal{Q}_\alpha \, |[j_1, j_2]^{(r)}_\Delta\rangle \qquad \text{and} \qquad \bar{\mathcal{Q}}_{\dot\alpha} \, |[j_1, j_2]^{(r)}_\Delta\rangle \,, \tag{4.65}$$

and we can of course continue acting with more supercharges on these states. Doing so allows us to obtain all the $2^4 = 16$ conformal primaries within the $\mathcal{N} = 1$ superconformal multiplet. We depict this procedure schematically in the following diamond, see figure 4.1 We are now ready to discuss some unitarity bounds. In general, unitarity imposes on the theory

$$\Delta \geq \Delta_A = f(j_1, j_2, (R)) \,, \tag{4.66}$$

where by (R) we collectively denote all the R-symmetry structure of the field theory. The situation regarding unitarity bounds and allowed region in the supersymmetric case is much richer compared to

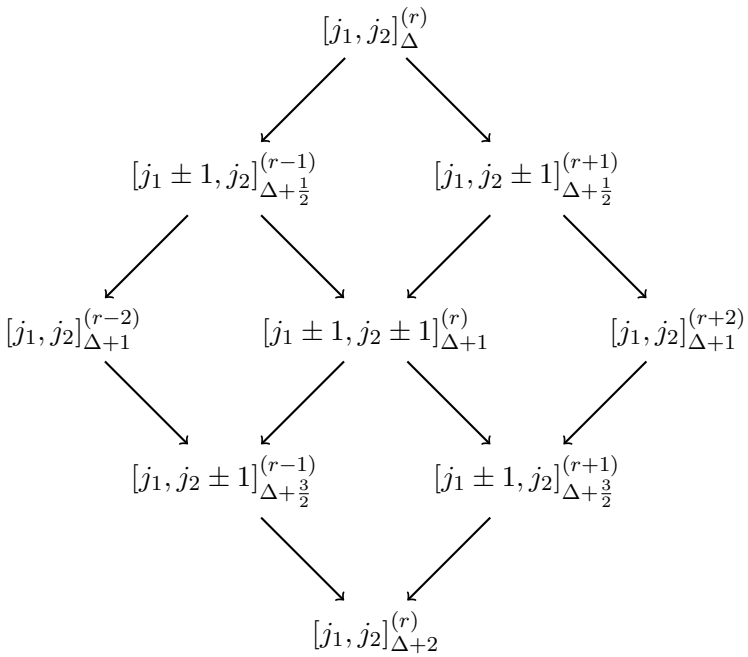

Figure 4.1: In this long multiplet, the superconformal primary is state depicted at the top. The arrows show schematically the action of the supercharges. An arrow down and to the left stands for the $\mathcal{Q}$ action, while an arrow downand to the right denotes the action of $\bar{\mathcal{Q}}$.

the purely bosonic CFTs. States in representations that are above the unitarity bound live in the allowed region of the theory and they form long multiplets. There exist states that saturate the unitarity bound, namely their weight satisfies $\Delta = \Delta_A$, and these are unitary. They do have, however, extra null vectors. Below the unitarity bound there exists the forbidden region of the theory. Be that as it may, there is the possibility of additional short representations which exist for discrete values of their conformal dimension. States that satisfy this criterio are described by $\Delta = \Delta_B$. The corresponding operators are denoted by $\mathcal{L}$ that stands for long representations, and $\mathcal{A}$ if $\Delta = \Delta_A$ or $\mathcal{B}$ if $\Delta = \Delta_B$. While this might seem at first very counter-intuitive recall the case of non-supersymmetric CFTs. We have seen that in a four-dimensional CFT the unitarity bound for a scalar is given by the restriction $\Delta \geq 1$. We have also seen that $\Delta = 0$ gives a unitary representation, the identity field. In a four-dimensional SCFT we have two different sets of supercharges, namely $\mathcal{Q}$ and $\bar{\mathcal{Q}}$, and two spins, j_1 and j_2, and therefore we can act on the superconformal multiplets either with $\mathcal{Q}$ or $\bar{\mathcal{Q}}$ or both leading to various short multiplets.

For the sake of completeness and clarity we will explicitly work out a unitarity bound for a type-$\mathcal{B}$ operator in a four-dimensional $\mathcal{N} = 1$. Similar manipulations can be performed in the other cases as well and by considering the action of more supercharges. The interested reader can find a catalogue of results in [94, Table 10, page 29]. Note that with the conventions used here the comparison should be obvious.

We begin by considering the norm $\left\| \mathcal{Q}^1{}_\alpha \, |[0, j_2]^{(r)}_{\Delta}\rangle \right\|^2$. Note that we do not imply summaton over the repeated index. We wish to compute this norm similarly to what we did in the CFT case. We have

$$\left\| \mathcal{Q}^1{}_\alpha \, |[0, j_2]^{(r)}_{\Delta}\rangle \right\|^2 = \langle [0, j_2]^{(r)}_{\Delta}| \, \mathcal{S}_1{}^\alpha \mathcal{Q}^1{}_\alpha \, |[0, j_2]^{(r)}_{\Delta}\rangle \tag{4.67}$$

$$= \langle [0, j_2]^{(r)}_{\Delta} | \, \tfrac{1}{2} D - \mathcal{R}^1{}_1 + \Lambda_1{}^1 \, | [0, j_2]^{(r)}_{\Delta} \rangle \tag{4.68}$$

$$= \langle [0, j_2]^{(r)}_{\Delta} | \, \tfrac{1}{2} D - \mathcal{R}^1{}_1 \, | [0, j_2]^{(r)}_{\Delta} \rangle \ , \tag{4.69}$$

having used the fact that $\mathcal{B}_1$ is a scalar and a primary. Now we need to remember,

$$[\mathcal{R}^1{}_1, \mathcal{Q}^k{}_\alpha] = \delta_1{}^k \mathcal{Q}^1{}_\alpha - \tfrac{1}{4} \mathcal{Q}^k{}_\alpha = \tfrac{3}{4} \mathcal{Q}^k{}_\alpha \ , \tag{4.70}$$

since in this case k can only have one value. Recall at this stage that $\mathcal{Q} \in [1, 0]^{(-1)}_{\frac{1}{2}}$ and hence $\mathcal{Q}$ has $r = -1$. Therefore we can write $\mathcal{R}^1{}_1 = -\frac{3}{4} r$. From the above it is quite straightforward to obtain

$$\frac{1}{2} \Delta + \frac{3}{4} r = 0 \, , \tag{4.71}$$

which of course yields

$$\Delta = -\frac{3}{2} r \, , \tag{4.72}$$

which is the result we should obtain.

4.2.3 Theories with eight supercharges

Theories that possess $\mathcal{N} = 2$ supersymmetry behave very similarly to the previous ones. In this case, the R-symmetry representation of the SCFT is specified by an $\mathfrak{su}(2)$ label, let us call it R, and also the $\mathfrak{u}(1)$ charge which we denote by r. The conditions on short multiplets are rather different but follow the same logic as the one outlined above. In order to be precise we comment on the difference compared to the previous case with a simple example. We will look again the unitarity bound for the $\mathcal{B}_1$ operator of the $\mathcal{N} = 2$ theory. This time we wish to compute the norm $\left\| \mathcal{Q}^1{}_\alpha \, | [0, j_2]^{(R;r)}_{\Delta} \rangle \right\|^2$. Observe that as we had mentioned we include all possible R-symmetries in the labelling. This is not essential. The important part that we need to account for in the commutator since in $\mathcal{N} = 2$ theories, the index k can have two different values. We have

$$[\mathcal{R}^1{}_1, \mathcal{Q}^k{}_\alpha] = \begin{cases} \frac{3}{4} \mathcal{Q}^k{}_\alpha \ , & k = 1 \ , \\ -\frac{1}{4} \mathcal{Q}^k{}_\alpha \ , & k = 2 \ . \end{cases} \ . \tag{4.73}$$

Remember that for the theories under examination here, $\mathcal{Q} \in [1; 0]^{(1;-1)}_{\frac{1}{2}}$ and thus $\mathcal{Q}$ has $r - 1$ and $R = 1$. Therefore, we can write $\mathcal{R}^1{}_1 = \frac{1}{2} R - \frac{3}{4} r$. While this normalization appears to be a bit peculiar we chose it such that we use the same conventions of [94]. It is quite easy to see now that the unitarity bound is

$$\Delta = R - \frac{1}{2} r \, , \tag{4.74}$$

as expected. Likewise one is able to continue with the other operators of the SCFT and from the shortening conditions derive the unitarity bounds. The interested reader can find these result in [94, Table 13, page 33].

Free multiplets

The matter multiplets of an $\mathcal{N}=2$ theory are called hypermultiplets. Hypermultiplets are not chiral due to the presence of the $SU(2)_R$, which is the R-symmetry. The $\mathcal{N}=2$ hypermultiplet consists of two complex scalar fields, ϕ and $\tilde{\phi}^*$, which can be conveniently groupped into a single Φ^I that transforms as a doublet under the R-symmetry. It also contains two Weyl fermions, ψ_α and $\tilde{\psi}_\alpha$, that are singlets under the $SU(2)_R$. The fields of the hypermultiplet can be combined into two $\mathcal{N}=1$ chiral multiplets and it can be depicted as in figure 4.2 [99]. In $\mathcal{N}=2$ theories we can also have vector multiplets. An

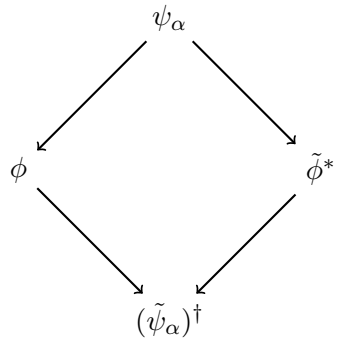

Figure 4.2: The $\mathcal{N}=2$ hypermultiplet in terms of free fields.

$\mathcal{N}=2$ vector multiplet contains two Weyl fermions, λ^1 and λ^2, that can be collectively written as λ^I. In this case, λ^I transforms as a doublet under the R-symmetry. The vector multiplet also contains a complex scalar field, ϕ, and a one-form potential, A_μ, both of which are R-symmetry singlets. We depict the $\mathcal{N}=2$ vector multiplet in figure 4.3. The fields of the $\mathcal{N}=2$ vector multiplet combine themselves into an $\mathcal{N}=1$ vector and an $\mathcal{N}=1$ chiral multiplets [99].

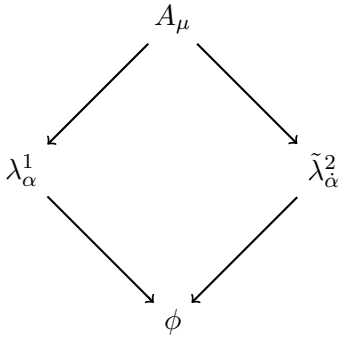

Figure 4.3: The $\mathcal{N}=2$ vector multiplet in terms of free fields.

Chapter 5

The AdS/CFT duality

In this section we will introduce the basic ideas for the AdS/CFT correspondence. It was originally suggested by Maldacena and it relates the physics of D3-branes in the type IIB theory with a superconformal field theory that lives in a four-dimensional spacetime, namely the $\mathcal{N} = 4$ SYM. It is worthwhile pointing out that a formal proof of the duality is still lacking, however, there are numerous tests by now and all of them suggest its validity. Most of the results we have obtained are in the low-energy regime where string theory can be very well approximated by classical supergravity.

Nowadays, after many careful studies and applications, we believe that the story is much more general and that the duality is really between a gravitational theory that is living on D+1 dimensions and non-gravitational QFTs in D dimensional spacetimes. In the classical approximation on the gravity side the calculations become tractable and they yield information and a wealth of data for the field theories in their strong coupling limit. If we look at it from a different perspective, it is fascinating how much we can understand for gravitational theories just by performing a field theory computation.

Any two theories related to one another by the duality must have the same symmetries. This does not mean that the duality is just that, namely a match of symmetries. It includes, as well, a great deal of dynamics.

There are by now many great review articles on the nuts and bolts of the AdS/CFT. We follow closely the discussions of [41, 100] in our presentation here.

5.1 Three-branes and IIB supergravity

Let us imagine that we introduce a large number of D3-branes into a ten-dimensional spacetime. From the string theory point of view there excitations and interactons of the strings that are of different type. The first type is the interactions of the closed string states in the type IIB background. We can also have interactions of open strings that live on the world-volume of the D3. We also expect that there will be some interactions amongst open and closed strings (i.e two open strings can join to form a

closed string). Effectively the theory can be described by the action

$$S = S_{open} + S_{closed} + S_{interactions} \,. \tag{5.1}$$

This will be the low-energy description of the theory. In this context by low we mean that all states have energies that are much smaller than the string scale. It is most convenient to send the string scale to infinity or equivalently to consider sending the string length to zero, $\alpha' \to 0$, while at the same time we keep all other parameters fixed. In this limit, the low-energy approximation, only massless string excitations. The theory describing the closed string sector will become free. This can be seen easily since the closed string coupling is proportional to the Newton constant in ten-dimensions, which in turn is proportional to $(\alpha')^2$. In the low-energy approximation the interaction term we have written above vanishes. Hence, we are left with only two theories that are completely decoupled. The open string sector of the theory and the closed string sector which is described by free supergravity.

D-branes are hypersurfaces, higher-dimensional surfaces, on which open strings can start and end. There can be additional degrees of freedom associated with the open-strings ends which are called Chan-Paton charges. We can stack a number of D-branes one on top of the other and we can label strings by doing so. We call the number of D-branes N. Each string will have two labels, one for each brane that is attached. These labels run from one to the number of branes. It has been shown that this gives rise to a $U(N)$ gauge theory with coupling given by $g_{YM} = \sqrt{g_s}$, with g_s being the string coupling. In low energies the massless string modes are the N^2 degrees of freedom in the adjoint of the gauge group. Note that it is possible to break this gauge symmetry by removing one brane away from the stack. Imagine having 2 D-branes described by a $U(2)$ group. Then we move away one brane from the stack and we have the breaking $U(2) \to U(1) \times U(1)$. This is not the end of the story for the D-branes, as Polchinski demonstrated that they also carry charges and therefore they can source potentials.

Back to the low-energy description of the open string sector. The theory describing the open string is a $U(N)$ gauge theory which can factorize into $SU(N) \times U(1)$, with the $U(1)$ being related to the centre of mass of the stack of the D3s. In order to find the field content one can reduce the ten-dimensional $\mathcal{N} = 1$ gauge multiplet to four dimensions. The result of this computation is the the $\mathcal{N} = 4$ SYM in four dimensions [56, 101]. The field content consists of a massless gauge field, four massless Weyl fermi fields, and six massless scalars. All of the fields transform in the adjoint representation of the gauge group.

From a different perspective, we can consider the embedding of a stack of D3 branes into a ten-dimensional theory. Since branes carry tension they can act as a stress-energy tensor term in the gravitational theory and they can source some supergravity fields. A consequence of this embedding is that the spacetime is warped. This has been thoroughly considered and it has been shown that D3-branes are solitonic solutions of the type IIB supergravity [102] with a metric given by

$$ds^2 = \mathcal{H}^{-1/2} \eta_{\mu\nu} dx^\mu dx^\nu + \mathcal{H}^{1/2} \left(dy^2 + y^2 d\Omega_5^2 \right) , \tag{5.2}$$

where in the above $d\Omega_5^2$ denotes a five-dimensional sphere and the warp factor is

$$\mathcal{H} = 1 + \frac{R^2}{y^2}\,, \tag{5.3}$$

with $R^2 = 2\alpha'\sqrt{\pi g_s N}$. It is easy to see that in the limit $y \gg R$ the metric returns to that of a flat Minkowski spacetime in ten dimensions while in the $y \ll R$ limit, which is called the near-horizon limit, we get

$$ds^2 = R^2 \left(\frac{1}{U^2} \left(\eta_{\mu\nu} dx^\mu dx^\nu + dU^2 \right) + d\Omega_5^2 \right)\,, \tag{5.4}$$

having performed the change of variables

$$U \equiv \frac{R^2}{y}\,. \tag{5.5}$$

The metric in the near-horizon limit is that of $\mathrm{AdS}_5 \times \mathrm{S}^5$. There exists another ingredient in the D3-brane description. We have already mentioned that D3-branes carry charge and they can source supergravity fields. More specifically the D3 branes source an antisymmetric four-form field $C_{(4)}$ in the IIB theory and the D3-brane solution has a self-dual five-form given by $F_{(5)} = dC_{(4)}$ that satisfies

$$\int_{S^5} dC_{(4)} = N\,. \tag{5.6}$$

So far we have encountered two different pictures describing the same physics system. In both descriptions we have two theories that are decoupled. The statement of the AdS/CFT is the identification of the two different pictures. Specifically, the $\mathcal{N} = 4$ SYM theory with an $SU(N)$ gauge group[1] in a four-dimensional spacetime is dual to the D3-brane solution of the type IIB theory.

5.2 Symmetry matching

Let us briefly check that the symmetries of the duality match and thus the statement makes sense. The isometry group of the AdS_5 submanifold of the ten-dimensional geometry is $SO(2,4)$ and the group of isometries of the five-sphere is $SO(6)$. Note that $SO(6)$ is isomorphic to $SU(4)$. From the field theory perspective, the $\mathcal{N} = 4$ SYM has an R-symmetry group, global internal symmetry, that is also $SU(4)$. The theory is also conformal and lives in four dimensions. The conformal group in four dimensions is $SO(2,4)$.

5.3 The holographic coordinate

We started from a ten-dimensional string theory and after compactifying five of its dimensions on a sphere we are left, in the gravity side of the duality, with an additional coordinate of the non-compact space as compared to the gauge theory description. Therefore, the duality has beend described as being a holographic duality [104]. This means that all the information of the higher dimensional theory, the gravity theory in five dimensions, is encoded in the degrees of freedom of the four dimensional

[1] the duality has been extended to describe other gauge groups such as $SO(N)$ and $USp(N)$ in [103].

field theory. We would like to have a better understanding of the effect of the holographic coordinate in the field theory side of the duality. In order to address this matter, we focus on the actions of dilatations which is a subgroup of the $SO(2,4)$. Under dilatations, the action describing a massless scalar is invariant. This can be easily seen by looking at the scalar action

$$S = \int d^4x \, (\partial\phi)^2 \ , \tag{5.7}$$

and realizing that dilatations

$$x \to e^A x \, , \qquad \phi \to e^{-A}\phi \, , \tag{5.8}$$

for some arbitrary parameter A, leave it invariant. Based on power counting we can deduce that the field has weight one and x has dimension minus one. We are using energy dimensions in the counting. On the other hand, the gravitational part of the duality should also possess such a symmetry and for the metric to be invariant we have to require in addition to the above that

$$y \to e^{-A} y \, . \tag{5.9}$$

Hence, it is evident that the holographic non-compact coordinate carries energy dimensions unlike the rest of the non-compact ones. In other words, it behaves as a field theory scalar in some sense. This leads to interpreting the holographic direction as the representation of the renormalization scale of the field theory.

5.4 Fields and operators

The AdS/CFT duality has been developed more and refined and the authors of [105, 106] established a map among fileds and operators. This allows the extraction of physical quantities from the correspondence. The way that the map works is by matching certain gauge invariant operators of the $\mathcal{N} = 4$ SYM that are in irreducible representations of the $SU(4)$ to modes in the dual gravity picture that live in the same representations and have been obtained after the Kaluza-Klein reduction on the S^5.

The mathematical formulation is the following statement

$$\langle e^{\int d^dx \phi_0(\vec{x})\mathcal{O}(\vec{x})} \rangle_{CFT} = \mathcal{Z}_{string}|_{\phi(\infty,\vec{x})=\phi_0(\vec{x})} \, , \tag{5.10}$$

which is stating that the generating functional of correlation functions of particular gauge invariant operators in the CFT with sources $\phi_0(\vec{x})$ coincides with the string partition function where the fields are valued at the boundary of the $AdS_5 \times S^5$. Simply put, the boundary values of the fields that live in the gravity part of the duality are interpreted as sources of operators in the field theory picture.

Let us exemplify the above by considering a supergravity massive scalar field in AdS_5. The action describing this is

$$S = \int d^4x dU \sqrt{-G} \left(G^{MN} \partial_M \phi \partial_N \phi - m^2 \phi^2 \right) \, . \tag{5.11}$$

We have seen how to solve the equations of motion and that they can be brought to the form

$$\phi(U) \sim U^{\Delta} A + U^{4-\Delta} B \,, \tag{5.12}$$

with the conformal dimension being given by $\Delta = 2 + \sqrt{4 + R^2 m^2}$. The supergravity field does not transform under field theory dilatations and hence does not carry a mass dimension. On the other hand, the holographic coordinate U has an inverse mass dimension. This implies that both A and B have to carry appropriate dimensions. It is easy to see that B has dimension $4 - \Delta$, while A carries dimension equal to Δ. Now let us briefly look at the behaviour of $\phi(\epsilon)$ when sending $\epsilon \to \infty$. It is clear from equation (5.12) that the second part, the one proportional B is dominant. Following [105] we can identify B with the source of an operator $\mathcal{O}$ and A with its VEV; $A = \langle \mathcal{O} \rangle$.

5.5 Tests of the duality

We can now mention some of the tests that have been made in the context of the AdS/CFT. Equation (5.10) is a suggestion that the duality might be tested by comparing correlation functions of the $\mathcal{N} = 4$ SYM with classical correlators in the supergravity. Note that this is not possible for any correlation function, since weakly coupled supergravity is mapped to the strongly coupled $\mathcal{N} = 4$ theory. For very specific correlators that obey non-renormalization theorems and hence are independent of the coupling constant a direct comparison is possible. This has been done for the case of two-point correlators and three-point correlation functions [107, 108]. More recently the case of four-point correlators was also studied [109, 110]. The operators in the correlation functions discussed above have a special property, they are $\frac{1}{2}$-BPS, which means that they are annihilated by half of the supercharges. Another very important test that has been performed was the calculation of the conformal trace anomaly [111]. Finally, there are numerous very rigorous tests of the AdS/CFT correspondence that stem from integrability [112]. Perhaps the most impressive one is the match of the spectrum of scaling dimensions with the energies of string states using the dilatation operator [113].

5.6 RG flows and the holographic duality

While the AdS/CFT duality is remarkable on its own, it would be very desirable to bring it a bit closer to the field theories that are of interest in the wider high-energy community such as QCD or more generally QCD-like theories. This requires to finding ways to generalize the gravitational description to non-conformal field theories with less supersymmetry. The ideal situation would be to have no superchages at all. In order to obtain field theories with a running for the gauge coupling, and hence a renormalization group flow, it is mandatory to deform appropriately the AdS space. Recall that the AdS_5 space possesses an $SO(2,4)$ symmetry which is reflected as a conformal symmetry in the field theory dual picture and therefore corresponds to a fixed point of the renormalization group.

One way of achieving the desired result is to turn on supergravity modes in the bulk that will backreact on the metric. The scalar field analysis performed above is only in the limit in which it is safe to ignore the backreaction to the ambient geometry. Switching on a supergravity field appropriately still leads to

the same UV description and hence we are able to determine the operator that is necessary for the deformation. In the IR the theory will be deformed indicating the loss of conformality.

Such deformations have already been considered in the past and the simplest one is the multi-centered D3-brane solution of supergravity. These geometries are described as a stack of parallel D3-branes, but the branes are separated in transverse subspace to their world-volume. The result is

$$ds^2 = \mathcal{H}^{-1/2}\eta_{\mu\nu}dx^\mu dx^\nu + \mathcal{H}^{1/2}\left(dy^2 + y^2 d\Omega_5^2\right) , \tag{5.13}$$

but in this case the warp factor is given by

$$\mathcal{H} = 1 + \sum\left(\frac{1}{|y - y_0|}\right) , \tag{5.14}$$

where in the above y_0 is the position of the D3-branes. We can expand the warp factor in terms of sherical harmonics of the five dimensional sphere that are labelled by their $SO(6)$ represenations in the following way [114]

$$\mathcal{H} \sim \frac{R^4}{y^4}\left(1 + Ay^4 + B\frac{1}{y^2}\mathcal{Y}_{20} + C\frac{1}{y^4}\mathcal{Y}_{50} + \cdots\right) , \tag{5.15}$$

and the deformation parameters of the geometry, $A, B, C, \cdots$ all have a field theory interpretation as deforming the original gauge theory. Specifically, they are VEVs of operators that have been determined by a careful examination and analysis of the symmetries in each case [115, 116].

The field theory interpretation of A has been worked out in [117, 118]. It corresponds to stepping away from the near-horizon limit of the spacetime. It is a singlet under the R-symmetry and carries dimension -4. It is an irrelevant operator that affects the UV of the theory. Its field theory form is that it is an interaction term $\sim \mathrm{tr}\, F^4$. B has dimension 2 such that it cancels that of y in the expression and lives in the $\mathbf{20'}$ of the $SO(6)$. In the field theory there exists such an operator which is given by $\mathrm{tr}\, \phi^2$. Using similar arguments one can see that C corresponds to $\mathrm{tr}\, \phi^4$ in the field theory. These operators are relevant and hence become important in the IR of the theory.

As a final comment, we mention that these multi-centered solutions have been obtained as supergravity renormalization group flows in [119].

Chapter 6

Flavour degrees of freedom and holography

The basic statement and properties of the AdS/CFT duality are very-well understood and studied. Be that as it may, the boundary field theory is very different from the non-supersymmetric, asymptotically free gauge theories that are of interest in the wide high-energy community, such as QCD for example. One major difference between the $\mathcal{N} = 4$ SYM theory and those theories is that in the latter ones, the matter fields transform in the fundamental representation of the gauge group.

Introducing fundamental matter into the AdS/CFT framework was one of the major issues that the community addressed in the very early days of the duality. After many years of research and much effort towards a better holographic description of QCD-like theories, we have established two main approaches:

- Top-down: models that fall into this category have their starting point directly in string theory. For example, starting with the original proposal by Maldacena and the duality between a stack of D3 branes and the $\mathcal{N} = 4$ SYM, when working in a top-down way, we try to introduce additional branes or other sources such that we modify the bulk appripriately in order to accommodate the desired features in the boundary field theory. Different setups have been investigated these many years, starting with the embedding of probe-branes [120] to introduce the necessary fundamental fields -quarks- and then considering the meson-like states and their mass-spectra [121]. Chiral symmetry breaking has also been discussed in this context[122], as well as more involved constructions for confinement and Seiberg dualities. The major drawback in working with top-down models is the inherent mathematical complexity in the computations.
- Bottom-up: when utilizing this approach -which has been also dubbed as AdS/QCD- we draw inspiration from the top-down studies, but the bulk geometry and fields are such that they encapsulate the required phenomenological properties of the gauge theory without caring about embedding these models into string theory [123]. It should be clear that when using this approach we lose the mathematical rigour of the previous constructions. The main advantage is that we have a more useful model for phenomenological purposes.

Our discussion here follows [41] as well as the original papers on the flavour degress of freedom.

6.1 D7-branes in the $AdS_5\times S^5$ background

We have stated previously that all the fields in the $\mathcal{N}=4$ SYM theory tranform in the adjoint representation of the group. Geometrically this is explained as all the open string states start and end on one of the N_c branes from the stack of coincident D3-branes that form the $AdS_5\times S^5$ geometry. Let us briefly remind the reader that the stack of N_c D3-branes has a $U(N_c)$ gauge group description. Thus, the wave-function of a string is a superposition of N_c^2 different states; a string from brane-1 to brane-2, from 1 to 3, and so on. Therefore we have the representation of the $U(N_c)$ group that contains N_c^2, which is the adjoint.

The addition of fundamental degrees of freedom requires us to consider that the string has one end in the stack of the D3-branes and another end is on another brane. For simplicity we consider the case of a D7-brane.[1] Doing this, we generate just the N_c possible string configurations per brane, while the other string ends on the D7.

If we denote an open string mode with one end on the Dp brane and the other end on the Dq-brane as $p-q$-string, we have the following string sectors:

- $3-3$ sector: this generates the $\mathcal{N}=4$ adjoint multiplet.
- $3-7$ sector: this sector is responsible for the fields that transform in the $\mathcal{N}=2$ fundamental hypermultiplet.
- $7-7$ sector: these strings generate the bound states that are comprised of the fundamental degrees of freedom and transform in the adjoint of the $\mathcal{N}=2$ theory. These are the "mesons" of the theory.

It is worthwhile mentioning that one possible way to simplify the analysis, is to consider the limit where the number of flavour degrees of freedom is much smaller compared to the number of colours; $N_f \ll N_c$. This is the probe-limit (or in the field theory language the quenched approximation), and in this limit there is no backreaction to the background geometry due to the presence of the flavour degrees of freedom.

6.1.1 The geometry of the D7 brane

Let us imagine that we want to embed in the $\{x^0,x^1,x^2,x^3,x^4,x^5,x^6,x^7\}$ directions a probe D7 brane in the background that is generated by the stack of D3 branes. We want to ask the question of what is the geometry that the probe, flavour brane realizes. To begin with, let us recall the $AdS_5\times S^5$ geometry, which can be written as

$$ds^2=\frac{r^2}{R^2}\eta_{\mu\nu}dx^\mu dx^\nu+\frac{R^2}{r^2}\left(d\rho^2+\rho^2 d\Omega_3^2+dw_5^2+dw_6^2\right), \tag{6.1}$$

[1] The other options are the D3,D5, and D9. The D9 is spacetime filling and we cannot separate it from the D3-branes, hence we cannot describe massive fields in the fundamental representation. The other two options lead to very interesting defect field theories.

where in the above $r^2 = \rho^2 + w_5^2 + w_6^2$.

Since we are interested in describing massive quarks, we want to separate the D7 from the colour branes in the $\{x^8, x^9\}$ plane by some finite distance. We can consider that $w_6 = 0$ and $w_5 = L(\rho)$. In order to obtain the induced geometry on the probe brane, and now we need to compute the pullback which can be done by using

$$G_{\hat{A}\hat{B}} = G_{MN} \frac{\partial X^M}{\partial \xi^{\hat{A}}} \frac{\partial X^N}{\partial \xi^{\hat{B}}} \,. \tag{6.2}$$

We can work in the static gauge, and the result is simply given by

$$ds^2 = \frac{r^2}{R^2} \eta_{\mu\nu} dx^\mu dx^\nu + \frac{R^2}{r^2} \left(1 + (\partial_\rho L)^2\right) d\rho^2 + \frac{R^2}{r^2} \rho^2 d\Omega_3^2 \,. \tag{6.3}$$

The action for the D7 is given by [124]

$$S_{D7} \sim \int d^4 d\rho \rho^3 \sqrt{1 + (\partial_\rho L)^2} \,, \tag{6.4}$$

having neglected some uninteresting factors arising from the integration over the S^3 coordinates and the tension of the brane. We can obtain the equations of motion for the $L(\rho)$ function, given by

$$\partial_\rho \left(\rho^3 \frac{\partial_\rho L}{\sqrt{1 + (\partial_\rho L)^2}} \right) = 0 \,. \tag{6.5}$$

Equation (6.5) is known as the embedding equation. Its solution describes the profile of the D7 brane in the ten-dimensional spacetime. It is quite obvious that the above can be solved by an arbitrary constant. In turn, this implies that the D7 lies flat in spacetime. The fact that the solution is an arbitrary constant with no dependence on ρ -which corresponds to the renormalization group scale- is the gravity manifestation of the non-renormalization of the mass, which is a characteristic feature of supersymmetric gauge theories.

Let us consider the limit $\rho \to \infty$ and $\partial_\rho L \to 0$ in the above equation. In this limit, it becomes

$$\partial_\rho \left(\rho^3 \partial_\rho L \right) = 0 \,, \tag{6.6}$$

which is solved by

$$L = m + \frac{c}{\rho^2} \,. \tag{6.7}$$

As we have already mentioned m is related to the quark mass, and more specifically the relation is $m = 2\pi\alpha' \, m_q$. In order to agree with the statement of the AdS/CFT duality, the extra ingredient of the solution, c, should be related to the VEV of an operator that possesses the same symmetries as the mass and is of dimension 3; recall that ρ carries energy dimension. Thus, c is a measure of the quark condensate $\bar{q}_L q_R$. Furthermore, any solution with $c \neq 0$ is not regular in AdS space and must be excluded, as it would correspond to a VEV for the operator which is not allowed by supersymmetry considerations. An elaborate discussion on the relation between and equation (6.7) is given in [125] in

the context of holographic renormalization [126].

6.1.2 Meson spectroscopy: a brief, scalar example

We would like to demonstrate how to obtain the mass spectrum of scalar mesons resulting from the string fluctuations around the supersymmetric embedding of the D7-brane, as an illustrative example. In this example we follow the seminal work of [121].

We have already mentioned that the ninth and tenth dimensions are transverse to both the background branes and the D7-probe. We separate the different branes by a finite, constant distance -L- in those directions and consider the fluctuations:

$$X^8 = 0 + 2\pi\alpha'\phi_1\,, \qquad X^9 = L + 2\pi\alpha'\phi_2\,, \tag{6.8}$$

where in the above, $\phi_{1,2}$ are the fluctuations that we wish to study.

The Lagrangian describing the dynamics of the these scalar fields is given by

$$\mathcal{L} \simeq \sqrt{-P[G]_{\hat{A}\hat{B}}}\left(1 + 2(R\pi\alpha')\frac{G^{\hat{C}\hat{D}}}{r^2}\left(\partial_{\hat{C}}\phi_1\partial_{\hat{D}}\phi_1 + \partial_{\hat{C}}\phi_2\partial_{\hat{D}}\phi_2\right)\right)\,, \tag{6.9}$$

the indices are all defined on the probe D7-brane and we have implicitly used the static.

In order to determine the supergravity mode solutions and the mass spectrum for the above equations we need to study the equations of motion resulting from the above. It is clear that the two independent fluctuations have the same equations of motion given by:

$$\partial_{\hat{A}}\left(\frac{\rho^3\sqrt{\tilde{G}}}{\rho^2+L^2}G^{\hat{A}\hat{B}}\partial_{\hat{B}}\mathcal{X}\right) = 0\,, \tag{6.10}$$

where in the above $\tilde{G}$ is the determinant of the metric on S^3 and by $\mathcal{X}$ we denote either of the fluctuations. This can be fully expanded to give

$$\frac{1}{\rho^3}\partial_\rho\left(\rho^3\partial_\rho\mathcal{X}\right) + \frac{R^4}{\left(\rho^2+L^2\right)^2}\partial^\mu\partial_\mu\mathcal{X} + \frac{1}{\rho^2}\nabla^i\nabla_i\mathcal{X} = 0\,, \tag{6.11}$$

with ∇_i the covariant derivative on the S^3.

We can use separation of variables to make an ansatz for the modes of the following form:

$$\mathcal{X} = e^{ik^\mu x_\mu}f(\rho)\mathcal{Y}^\ell\,, \tag{6.12}$$

with $k^2 = -M^2$ being the mass of the fluctuation and $\mathcal{Y}^\ell$ being the spherical harmonics on the S^3 for which we know the eigenvalues

$$\nabla^i\nabla_i\mathcal{Y}^\ell = -\ell(\ell+2)\mathcal{Y}^\ell\,. \tag{6.13}$$

Taking the above into consideration and inserting the ansatz equation (6.12) into the equations of

motion equation (6.11), we obtain

$$\partial_\rho^2 f + \frac{3}{\rho}\partial_\rho f + \left(\frac{R^4 M^2}{(\rho^2+L^2)^2} - \frac{1}{\rho^2}\right) f = 0\,. \tag{6.14}$$

The above equation can be solved in terms of hypergeometric functions. Before presenting the solution, we feel that it is necessary to briefly present the the criteria of validity for the solution. We require that the resulting function is real-valued, regular, small in amplitude and normalizable. Taking all these into consideration leads to the mode solution

$$f(\rho) = \frac{\rho^\ell}{(\rho^2+L^2)^{n+\ell+1}}\ {}_2F_1\left(-(n+\ell+1)\,, -n, \ell+2, -\frac{\rho^2}{L^2}\right)\,, \tag{6.15}$$

with the masses of the states being described by

$$M = \frac{2L}{R^2}\sqrt{(n+\ell+1)\,(n+\ell+2)}\,. \tag{6.16}$$

In the above, n is a quantum number associated with the nodes of the mode solution equation (6.15) and ℓ is the quantum number associated with the angular momentum on the internal manifold. We see that the spectrum is gapped, discrete and the mass scale is set by L; the relavant distance of the probe D7 with respect to the background stack of D3s.

It is, also, quite interesting to investigate the behaviour of the solution at infinity. This particular limit is associated to the high-energy properties of the field theory. In this regime we can ignore te mass of the quarks, and the theory becomes a CFT. In other words, as we approach the ultraviolet (UV) the theory under examination flows to the one described by $L = 0$. As we approach $\rho \to \infty$, the behaviour of the mode solutions equation (6.15) is related to the UV operator with the lowest conformal dimension, Δ. This has the quantum number of a meson state [105, 106, 121].

If the kinetic term of the fields were canonically normalized, the behaviour would be given by $1/\rho^\Delta$ for the normalizable part and $1/\rho^{-4+\Delta}$ for the non-normalizable one. However, in this case the kinetic terms are not canonically normalized and the UV behaviour is given by $\rho^{-\Delta+k}$ and $\rho^{\Delta-4+k}$, for a given value of k. In this case, all we need to do it to subtract the exponents and we can obtain the conformal dimension. To that end, let us briefly state a very useful relation in the $\rho \to \infty$ of the hypergeometric function

$${}_2F_1\left(A, B, C, -\frac{\rho^2}{L^2}\right) \sim \frac{\mathcal{Z}_1}{\rho^{2A}} + \frac{\mathcal{Z}_2}{\rho^{2B}}\,, \tag{6.17}$$

where we have neglected to write explicitly some unimportant factors of Γ-functions.[2] Under the assumption that $B > C$, the first term of the expansion corresponds to the non-normalizable part and the second one is the normalizable piece.

With this at hand we can obtain a formula for the conformal dimension of the operator, which is

$$\Delta = 2 + B - A\,, \tag{6.18}$$

[2]They can be obtained very straightforwardly by expanding in any computer software.

which is the particular case of interest yields

$$\Delta = \ell + 3\,. \tag{6.19}$$

Of course, it is possibe to continue this line of investigation for the other operators that appear in the setup. We refrain from doing so, as this was meant to be just an illustrative example and there exists a wonderful analysis in [121] of all bosonic states.

6.1.3 Chiral symmetry breaking and dilaton flows

We can take another step towards the more faithful holographic description of asymptotically free gauge theories, by finding a gravitational way to mimic the running of the coupling in the gauge theory. This can be achieved by considering a dilaton flow. A dilaton flow allows the dilaton field of the theory to obtain a non-trivial profile that depends on the radial coordinate. As an effect, the AdS space gets distorted.

The breaking of chiral symmetry in the field theory picture

In order to describe chiral symmetry and its breaking, let us consider the case of massless QCD with three flavours of quarks, which is described by the Lagrangian

$$\mathcal{L} = -\frac{1}{4}F^a_{MN}F^{a,MN} + \bar{\psi}_L \not{D}\psi_L + \bar{\psi}_R \not{D}\psi_R\,, \tag{6.20}$$

where we have written the left and right chiral projections of the Dirac spinor, ψ.

In this massless limit that we have considered, it is easy to see that the transformations[3]

$$\psi_L \to e^{-i\theta_L\cdot\lambda}\psi_L\,, \qquad \psi_R \to e^{-i\theta_R\cdot\lambda}\psi_R\,, \tag{6.21}$$

leave the theory invariant. In the above λ^a, with $a = 1, \cdots, 8$ are the $SU(3)$ generators and the $\theta_{L,R}$ are parameters related to the $SU(3)$ left and right-subgroups. Hence, the statement is that the Lagrangian of the theory is invariant under the $SU(3)_L \times SU(3)_R$. We want to stress that the $U(1)_A$ that would make the theory invariant under the $U(3)_L \times U(3)_R$ is anomalous [127, 128]. The exception to that picture is only in the limit of small number of flavours, $N_f \ll N_c$, in which case the traingle diagram that is the underlying reason for the anomaly is suppressed when performing the $1/N_c$ expansion of the theory. Thus, in the large-N_c limit there is also a $U(1)_A$ symmetry.

There are two ways to break this chiral symmetry. The first one is an explicit breaking of the symmetry, which amounts to considering a mass term, $m\bar{\psi}\psi$. The other way is its spontaneous breaking. In this case the strong dynamics of the theory triggers a VEV for the operator

$$\langle\bar{\psi}\psi\rangle \neq 0\,. \tag{6.22}$$

[3]We can also express these tranformation rules as vector and axial ones by considering $\theta_V = \frac{1}{2}(\theta_L + \theta_R)$ and $\theta_A = \frac{1}{2}(\theta_L - \theta_R)$. In other words the theory is invariant under the $SU(3)_V \times SU(3)_A$.

In both cases described above, the flavour symmetry is broken down to a single $SU(3)_V$.

The gravitational picture

The above symmetry breaking picture can be realized holographically. We keep in mind the large-N_c limit and we will discuss the breaking of a simple $U(1)_A$ symmetry.[4] The fields transform

$$\psi_L \to e^{i\alpha}\psi_L\,, \qquad \psi_R \to e^{i\alpha}\psi_R\,. \tag{6.23}$$

There are, by now, some very famous examples of non-supersymmetric and confining supergraviy backgrounds [118, 131, 132]. In this section we are focusing on the Constable-Myers solution [118]. This background is a particular example of a dilaton flow. From the point of view of the supergravity theory, in order to obtain solutions like that, we simply search for a solution of the type IIB equations with the dilaton being a non-trivial function depending on the holographic radial coordinate.

We will be working in the Einstein frame. The geometry describing the Constable-Myers solution is given by [118]

$$ds^2 = h^{-\frac{1}{2}}\left(\frac{w^4+b^4}{w^4-b^4}\right)^{\frac{\delta}{4}}\eta_{\mu\nu}dx^\mu dx^\nu + h^{\frac{1}{2}}\left(\frac{w^4+b^4}{w^4-b^4}\right)^{\frac{2-\delta}{4}}\frac{w^4-b^4}{w^4}\sum_{i=1}^{6}dw_i^2\,, \tag{6.24}$$

where in the above, the parameter b determines the geometric deformation via

$$\delta = \frac{R^4}{2b^4}\,, \tag{6.25}$$

with R begin the AdS radius and we also have

$$h = \left(\frac{w^4+b^4}{w^4-b^4}\right)^{\delta} - 1\,, \qquad w^2 = \sum_{i=1}^{6} w_i^2\,. \tag{6.26}$$

In this coordinate system, the dilaton and the four-from have the expressions,

$$e^{2\phi} = e^{2\phi_0}\left(\frac{w^4+b^4}{2^4-b^4}\right)^{\Delta}\,, \qquad C_{(4)} = -\frac{1}{4h}dx^0\wedge dx^1\wedge dx^2\wedge dx^3\,, \tag{6.27}$$

with

$$\Delta^2 + \delta^2 = 10\,. \tag{6.28}$$

It is quite clear, just by performing an expansion for large-w, that the geometry above returns to the familiar $AdS_5\times S^5$. Hence, the field theory in the UV of the theory is still the $\mathcal{N}=4$ SYM. In the IR, however, owing to the deformation due to the dilaton flow, conformal invariance is broken. The scale is set by the parameter b, which is equivalent to the Λ_{QCD} in the gauge theory [41],

$$\Lambda_b = \frac{b}{2\pi\alpha'}\,. \tag{6.29}$$

[4] There is also an approach that realizes the non-abelian chiral symmetry breaking [129, 130].

The R-symmetry, $SO(6)$, of the geometry is not broken and hence the equivalent gauge theory deformation must not break the R-symmetry of theory. By looking at the b and the way it enters with the radial direction in the AdS description we can easily conclude that it is an operator of dimension 4. The natural candidate is the uncharged under the R-symmetry, dimension 4, $\mathrm{tr}\, F^2$ operator in the field theory. The interpretation of this geometry is that it describes the $\mathcal{N} = 4$ theory, but with a source that is forcing it go away from the supersymmetric vacuum.

6.2 Early bottom-up models

We now turn our focus to the bottom-up approach of modelling QCD and QCD-like theories using a simple holographic framework. These models have been dubbed AdS/QCD in the literature, and the starting point is a much simpler gravity description in terms of an AdS_5 geometry [123]. On its boundary, we wish to have a QCD(- like) gauge theory. For unit radius the metric describing this class of models is given by

$$ds^2 = r^2 \eta_{\mu\nu} dx^\mu dx^\nu + \frac{1}{r^2} dr^2 \,. \tag{6.30}$$

In order to reflect all the phenomenology properties of the QCD(-like) gauge theories, the bulk must contain fields appropriately, such that they correspond to the necessary operator-source combination in the field theory language.

We want to introduce a scalar field of dimension $\Delta = 3$ - or equivalently $M^2 = -3$ - in order to account for the quark mass and the condensate. We also need two massless gauge fields, of dimension $\Delta = 1$, that correspond to current operators of the $SU(N_f)_{L,R}$.[5] Collecting all these different pieces of information, we are able to write an action in the bulk that encodes the basic properties of a QCD-like gauge theory, given by [41]:

$$S = \int d^4x dr \sqrt{-\det G_{MN}} Tr \left((D_M X)^\dagger (D^M X) + 3X^\dagger X - \frac{1}{4g_5^2} \left(F_{L,MN} F_L^{MN} + F_{R,MN} F_R^{MN} \right) \right) , \tag{6.31}$$

with the covariant derivative being given by

$$D_M X = \partial_M X - i L_M X + i X R_M \,, \tag{6.32}$$

and the field strength

$$F_{\mathcal{I},MN} = \partial_M \mathcal{I}_N - \partial_N \mathcal{I}_M - i[\mathcal{I}_M, \mathcal{I}_N] \,, \tag{6.33}$$

where $\mathcal{I} = \{L, R\}$ and $\mathcal{I}^M = \mathcal{I}^{a,M} t^a$. The choice for the scalar field is

$$X(\vec{x}, r) = L(r) e^{2i\pi^a(\vec{x}) t^a} \,, \tag{6.34}$$

which is inspired from the effective chiral Lagrangian approach [133]. Fluctuations in the $\vec{x}$ coordinates of the scalar describe the pion fields of the theory. The radial coordinate in the energy scale and is mapped to the renormalization scale of the field theory.

[5] The relation of a general massive p-form $M^2 = (\Delta - p)(\Delta + p - 4)$ [80].

There is still one issue that we have not yet addressed. Since we have an AdS_5 spacetime in the bulk, it is implied that there is a conformal symmetry in the field theory. However, QCD(-like) theories are not invariant under the conformal group, and thus this is an undesired property that we need to take care of. There are two ways to achieve that [41]:

- Hard wall models [123, 134]: by hard wall what we mean is that we impose a boundary at some fixed point $r = r_{fixed}$ into the spacetime. This has as an effect the breaking of the $SO(2,4)$ isometry and hence the conformal symmetry of the field theory. The model is valid in the region $r_{fixed} < r < \infty$, or in other words by introducing the hard wall we cut out a chunk of the bulk geometry. The boundary that we have imposed, r_{fixed}, acts as the QCD scale, Λ_{QCD}, in the sense that it is the only scale in the system that we are able to use to set dimensionful parameters. It is worthwhile noting that a drawback of these models is that the Regge trajectories of the excited meson states are not of the right form, rather they are described by $M_n^2 \sim n^2$.

- Soft wall models [135]: An alternative method to the above that fixes the issue of conformal invariance of the field theory is the introduction of a soft wall in the model. The soft wall means that we are introducing a non-trivial dilaton, $\phi(r)$, in the bulk description. The introduction of the dilaton modifies the action in the following way:

  $$S = \int d^4dr \sqrt{-\det G_{MN}} e^{\phi(r)} Tr\left((D_M X)^\dagger (D^M X) + 3X^\dagger X - \frac{1}{4g_5^2}\left(F_{L,MN}F_L^{MN} + F_{R,MN}F_R^{MN}\right)\right),$$

  Chossing a dilaton profile of the form $\phi(r) \sim 1/r^2$ not only breaks the conformal symmetry of the boundary field theory, but also a $r \to 0$ yields the correct Regge trajectories; $M_n^2 \sim n$.

6.3 Dynamic AdS/Yang-Mills

Finally, we are at a position to explain the Dynamic AdS/Yang-Mills model -originally it was called Dynamic AdS/QCD- that was originally developed in [136], which we used to make predictions for Beyond the Standard Model setups in chapter 8. The Dynamic AdS/Yang-Mills model can be seen as a hybrid between the two approaches described so far, as it is based on the bottom-up AdS/QCD models but is heavily infuenced by the top-down D3/D7 models.

We work in a five-dimensional spacetime as we did previously. The bulk geometry in this case is given by

$$ds^2 = \left(\rho^2 + L^2\right)\eta_{\mu\nu}dx^\mu dx^\nu + \frac{1}{\rho^2 + L^2}d\rho^2\,, \tag{6.35}$$

where in the above $L = L(\rho)$. This metric is heavily inspired by the D3/probe-D7 and we see that as in that case here as well the scalar field $L(\rho)$ enters the metric. We can define a new "variable", as $r = \sqrt{\rho^2 + L^2}$, which is identified as the renormalization scale of the field theory - once more in accord with the D3/probe-D7 setup.

The action describing the dynamics of the bulk fields is given by:

$$S = \int d^4 d\rho \rho^3 Tr \left((D_M X)^\dagger (D^M X) + \frac{\Delta m^2}{\rho^2} |X|^2 + \frac{1}{2g_5^2} \left(F_{L,MN} F_L^{MN} + F_{R,MN} F_R^{MN} \right) \right) , \tag{6.36}$$

with

$$X = L(\rho) e^{2i\pi^a t^a} . \tag{6.37}$$

Since we have already discussed the basic properties and the action of AdS/QCD models, the action of the Dynamic AdS/Yang-Mills model might seem as being the same as the previous ones. However, such is not the case. Other than the difference in the metric which is used in all contractions, a closer look at the metric reveals the choice $\sqrt{-g} = \rho^3$ rather than the expected result $\sqrt{-g} = (\rho^2 + L^2)^{3/2}$ by using the metric equation (6.35). This is because the ρ^3 factor has been imported directly from the top-down D3/probe-D7 description. This is an important feature as it guarantees the soft-wall behaviour in the infrared of the theory. For $L \neq 0$ the radial "coordinate" cannot have access to the very deep infrared. In other words, $r > L$ for arbitrarily low values of the holographic coordinate ρ. In the $L \to 0$ limit the metric returns to pure AdS_5 and the theory becomes conformal. A third very interesting feature is the appearance of a term proportional to $|X|^2 = L^2$ which is inherited directly from the action of the D3/probe-D7 with a dilaton flow. This allows the scalar field to have a radially dependent bulk mass. In the field theory, the dimension of the operator $\bar{q}q$ depends on the energy. In the limit $\Delta m^2 = 0$, the bulk scalar mass is once again $M^2 = -3$.

In chapter 8 we use this holographic model to obtain predictions -meson masses and decay constants- for a number of phenomenologically interesting models in the context of Beyond the Standard Model physics. A detailed discussion on meson dynamics can be found in [136] where this model was originally suggested as well as in [137, 138] and the most extended description can be found in [139]. Below, we briefly want to comment on some basic aspects that we believe deserve a detailed explanation and provide a more thorough understanding of the general framework. Our main focus is the fermionic sector which was left unexplored in the past.

We wish to understand what value the g_5 coupling has, and hence we need to know how to evaluate the vector two-point function in the framework of Dynamic AdS/Yang-Mills. Then, we match the result to the vector-vector correlator computed in perturbative QCD. Below we briefly describe this general procedure. We are following [123, 140] in our brief description. A detailed computation can be found, [139, see for example the discussion around page 73 and Appendix E]. The first step of the approach is to find the solutions to the equations of motion for the vector gauge field. Then we need to evaluate the action on that particular solution. This computation yields the vector-vector correlator of the theory, and the result is given by [140]

$$\Pi_{VV} \left(q^2 \right) = \frac{1}{g_5^2} \log(q^2) . \tag{6.38}$$

The above has to be compared to the result obtained from perturbative QCD considerations, which is [141]

$$\Pi_{VV} \left(q^2 \right) = \frac{N_f N_c}{24\pi^2} \log(q^2) . \tag{6.39}$$

By matching the two expressions above, we can immediately see that

$$g_5^2 = \frac{24\pi^2}{N_c N_f}\,. \tag{6.40}$$

6.3.1 Solving the embedding and deriving the vacuum

We want to find the vacuum configuration of the model. In order to do that, we are setting all fields to zero except for the scalar $L(\rho)$. We want to study its solution. The action for the scalar field, $L(\rho)$, is given by

$$S = \int d^4x d\rho \rho^3 \left((\partial_\rho L)^2 + \Delta m^2 \frac{L^2}{\rho^2} \right) . \tag{6.41}$$

For the limiting value $\Delta m^2 = 0$, the ultraviolet solution to the equations of motion is given by $L = m + c/\rho^2$, with m being the quark mass and $c = \langle \bar{q}q \rangle$ the chiral condensate. If we move away from the limiting case and we assume $\Delta m^2 \neq 0$, then we are allowing the scalar to have a mass that is a function of ρ, $\Delta m^2 = \Delta m^2(\rho)$. In turn, this implies that the clasical dimension of the $\langle \bar{q}q \rangle$ gets a correction; the anomalous dimension.

If we correct the conformal dimension of a field theory operator from Δ to $\Delta - \gamma$, then the mass of the bulk scalar field gets a shift from M^2 to $M^2 + \Delta m^2$, and thus obtaining

$$(\Delta - \gamma)(\Delta - \gamma - 4) = M^2 + \Delta m^2\,, \tag{6.42}$$

and keeping in mind that $M^2 = \Delta(\Delta - 4)$, we obtain the following

$$\Delta m^2 = \gamma^2 - 2\gamma(\Delta - 2)\,. \tag{6.43}$$

For the $\langle \bar{q}q \rangle$, we have $\Delta = 3$ and the final relation, equation (6.43), becomes $\Delta m^2 = \gamma(\gamma - 2)$. The profile of the non-trivial function we have introduced, $\Delta m^2(\rho)$, can be imposed simply by using the result of the perturbative anomalous dimension for the gauge theory at one-loop level, which is

$$\gamma = \frac{3C_2(R)}{2\pi}\alpha_s\,. \tag{6.44}$$

In the above we have denoted by α_s the two loop-perturbative running of the gauge coupling. Also, R stands for the specific representation under examination of the quarks. Under the assumption that $\gamma \ll 1$ we can expand the result and to leading order we get:

$$\Delta m^2 = -2\gamma\,, \tag{6.45}$$

and furthermore we obtain

$$\Delta m^2(r) = -\frac{3C_2(R)}{2\pi}\alpha_s\,, \tag{6.46}$$

where in the above $r = \sqrt{\rho^2 + L^2}$ and we remind the reader that is mapped to the RG scale, μ. We should stress at this point that beyond the weak-coupling regime, the perturbative result for the

anomalous dimension is not rigorous. However, as we shall see, extending the validity of the result to the non-perturbative regime gives reasonable results.

The equation of motion for the bulk AdS scalar reads

$$\partial_\rho(\rho^3\partial_\rho L) - \rho\Delta m^2 L = 0\,, \tag{6.47}$$

where we have implicitly assumed that Δm^2 is an arbitrary constant. For the case of a constant and non-zero Δm^2 the solution to the equation of motion is

$$L = \frac{m}{\rho^\gamma} + \frac{c}{\rho^{2-\gamma}}\,. \tag{6.48}$$

Finally, we want to comment on a more general situation. Now, we are allowing Δm^2 to be a non-trivial function of ρ, but only at the level of the equations of motion. However, in this case the general solution of equation (6.47) cannot be found analytically and we are forced to resort to numerics. In order to do so, we need to impose initial conditions for the problem under examination. We choose said conditions to be given by

$$L(\rho = \rho_{IR}) = \rho_{IR}\,, \qquad \partial_\rho L|_{\rho=\rho_{IR}} = 0\,. \tag{6.49}$$

It is quite obvious that these boundary conditions are inspired -or perhaps a bit more accurately almost directly imported- from the D3/probe-D7 system. Recall that in the latter case they are given by $L(\rho = 0)$ =constant and $\partial_\rho L = 0$. The difference is that in this bottom-up model that we are utilizing here, they are imposed at the RG scale as is related to the ρ-coordinate. In other words, the initial conditions we set in our description enforce the masses to be less than the energy scale.

In chapter 8, we will see many examples of solutions to the embedding equation we described above, with different groups and different matter fields. However, we feel it necessary for illustrational purposes to present here an example as well. We choose to study the vacuum configuration of an $SU(3)$ theory with 3 flavours of quarks in the fundamental representation of the gauge group and the result is shown in figure 6.1. Chiral symmetry breaking should be obvious, as the quark mass mass starts from zero and gets a non-zero value as we move deep into the infrared of the theory.

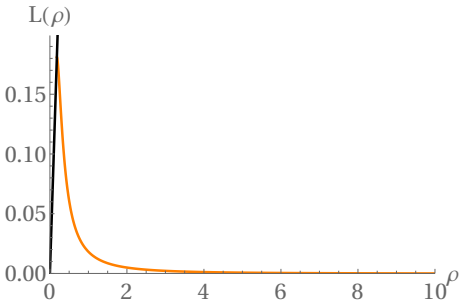

Figure 6.1: The $SU(3)$ theory with $N_f = 3$ flavours in the fundamental representation. The boundary condition that we imposed on the β-function is $\alpha(0) = 0.4$.

6.3.2 Chiral symmetry breaking and the Breitenlohner-Freedman bound

One central aspect of the QCD(-like) theories that we wish to examine is whether chiral symmetry breaking can be triggered as the running of the gauge coupling passes through its critical value. An immediate question we address to answer here is how this feature is manifested in the gravitational bulk model we are considering. We have seen that chiral symmetry breaking occurs when the coupling constant passes though a critical value. This forces the chirally symmetric ground state of the system to become unstable. Let us consider the situation in the bulk theory. In flat spacetime, a field that has a negative mass-squared is not a stable state. We have already seen that this is also true in AdS spacetimes, with the extra feature that some negative values are allowed and below a specific threshold the theory becomes unstable.

Scalar fields in AdS_5, as we have seen, must satisfy the BF-bound given by

$$M^2 < -4\,. \tag{6.50}$$

What happens if the mass of the $\bar{q}q$ scalar operator is driven below this bound? The theory will become unstable around the initial global minimum. In our bottom-up model, the instability occurs when the mass of the $L(\rho)$ scalar is driven below that point. This relates to a specific value of Δm^2 which is $\Delta m^2 = -1$. We can recall that the scaling dimension of the field is $\Delta = 3$ and we arrive at the value $\gamma = 1$ when the instability occurs.

Here we encounter an important aspect of the model. If we were to violate the BF-bound and the scalar $L(\rho)$ to become unstable, while at the same time mapping the renormalization group scale, μ, with the AdS radial coordinate, ρ, without any modifications we would have obtained a theory with a scalar field that has an unbounded from below potential and hence the model would not make sense. This is why the identification, $\mu = \sqrt{\rho^2 + L(\rho)^2}$, saves the model from undesired features. For finite values of the field L the deep IR of the theory is never accessed and we can retain stable AdS solutions but for different vacuum configurations, which are related to the fact that $\langle \bar{q}q \rangle \neq 0$.

In terms of the $L - \rho$ plane we can consider the circular region given by

$$L^2 + \rho^2 \leq \mu_0^2\,, \tag{6.51}$$

where μ_0 is the scale of chiral symmetry breaking. This can never be reached by the field. The vacuum solution of the embedding function has a profile that increases from the IR to meet the BF bound close to the condiiton $L = \rho$, which is the mass-shell condition. Below that point, the fields are decoupled from the theory. Of course we keep in mind that in our bottom-up model we have kept only the lowest order terms of the DBI expansion. If all terms were considered, the situation would have been corrected and the matching $\rho = L$ woud be exactly at μ_0.

Part IV

Research

Part V

The top-down approach

Chapter 7

Worldvolume fermions in probe-brane systems[1]

7.1 Why bother with fermions at all?

It has long been a matter of interest whether strongly coupled gauge theories can generate light or even massless fermionic bound states (baryons), since these might form the basis for a composite model of standard model fermions [142]. A related problem is to generate the experimentally observed top quark mass in composite Higgs models, in which the Higgs particle is a pseudo-Nambu Goldstone boson. This requires baryonic top partners [143, 144] that are light relative to the typical hadronic scale in the strongly coupled sector. The AdS/CFT correspondence [23, 105, 106] has provided a new window on strongly interacting gauge dynamics that may potentially be useful as a new approach to Beyond the Standard Model (BSM) physics. It motivates us here to look afresh at a mechanism for generating light or massless baryons in top-down holographic models, in which the use of a top-down string theory D-brane construction provides control over the field content of the dual gauge theory. As a starting point for new BSM analyses, we begin by carefully fixing the details of top-down gauge/gravity duality models required for investigating fermionic modes. Somewhat removed from the phenomenological BSM models mentioned, we study a rigorously understood top-down construction of an $\mathcal{N} = 2$ gauge theory with massive quarks. In this theory, the meson states and their supersymmetric partners, the mesinos, can be analytically computed -in some brane setups- and lie at a scale determined by the quark mass. We will, also, determine how higher dimension operators may be used to generate abnormally light mesino states. There are two sets of mesino states corresponding to different representations of the supersymmetry algebra. One of them is very similar to a QCD baryon multiplet since the lowest mass entry in this multiplet consists of a product of three elementary fermion fields (of course a true baryon at large N_c is made of N_c quarks and must be represented by a baryon vertex in the dual [103]).

[1]Research presented in this chapter is based on two papers. The first [1] was in collaboration with Raimond Abt, as well as my supervisor Nick Evans and Johanna Erdmenger. My main contribution was to derive the second-order equations of motion and perform the numerical analysis of the mass spectrum and the effect of the double-trace deformations. In [3] my main contributions were the derivations of the results in the D2/D6 setup and probe branes in the D3 background, the study of the large-N_c limit and the derivation of the avoided level-crossing.

Let us consider the vanilla D3/probe D7-brane system [41, 120, 121] as simple illustrative example. It provides a clean holographic description of a strongly coupled gauge theory with quark matter for which an easily calculable dual description exists. The gauge theory is an $\mathcal{N} = 2$ supersymmetric theory with hypermultiplets added to the base $\mathcal{N} = 4$ super Yang Mills theory. The gravity dual in the quenched approximation consists of probe D7-branes embedded in $AdS_5 \times S^5$ space that wrap a subspace which asymptotically near the boundary is $AdS_5 \times S^3$ [120]. The quark mass and condensate are explicitly present in the model as holographic modes and determine the near-boundary behaviour of the embedding functions. The meson spectrum, corresponding to fluctuations of the brane about their vacuum configuration, was computed in [121]. The fermionic spectrum in the *massless* theory was fully derived in [82]. In the same paper, a phenomenological bottom-up rule was used to guess the equations of motion for the fluctuations in the massive case, reproducing the expected spectrum, with further results in [41]. A full derivation of the equations of motion for the massive case has been completed in the unpublished notes [145]. Therefore, one of the first tasks we set ourselves here is to provide an explicit derivation of these equations and to check the supersymmetric degeneracy of the spectrum. The results in [146] are also a useful related reference.

So far, the model considered does not give rise to light baryons since the masses of the baryon-like mesinos are tied to the meson spectrum by supersymmetry. To proceed, one possible addition to the theories are higher dimension operators. Witten's double trace prescription [147] allows such operators to be introduced easily as modifications of the UV boundary conditions on the holographic solutions. Previously this has been done in the D3/D7 system for Nambu-Jona-Lasinio type four-fermion operators in [148]. Here, instead, we consider adding operators of "mesino squared" form which naively will generate a shift in the mesino mass in the effective description of the low-energy hadrons. We show that as the coupling of these operators is raised, the mesino masses can be driven to light values relative to the rest of the spectrum. For small values of the coupling of this operator, the shift in the mesino mass is small and linear, but above a critical value of the coupling the shift in the mesino mass is suddenly sharp and much larger. Inspite of this, the mesino mass can only be pushed to zero for asymptotically large values of the coupling, presumably reflecting that fermionic states cannot become tachyonic and condense. Our approach provides at least one (tuned) mechanism for generating light composite fermions in strongly coupled gauge theories. We also study the radially excited states of the mesinos and show that their masses are bounded from below and do not become light along with the lowest state whose mass approaches zero.

7.2 A more formal elaboration

The AdS/CFT correspondence [23, 105, 106] asserts that certain field theories are dual (equivalent) to string theory in an AdS space. The original proposal was generalized shortly after its discovery to a more general notion of gauge/gravity dual pairs in various dimensions, by considering different Dp-branes [149]. The prescription is, tersely, to consider a stack of N_c Dp-branes that coincide and take the limit in which the brane modes decouple from the bulk. We are left with a super Yang-Mills (SYM) theory with a $U(N_c)$ gauge group on the $(p+1)$-dimensional worldvolume of the Dp branes. This SYM theory is dual to string theory in the near-horizon limit of the background induced by the stack of

Dp-branes. For any Dp-brane with $p \neq 3$, the holographic gauge description is a non-conformal theory, since the Yang-Mills coupling carries dimensions. The energy scale of the gauge theory is mapped to the radial coordinate in the gravity side which is orthogonal to the branes. The absence of conformal invariance manifests itself in the bulk by the non-trivial radial profile of the dilaton as well as the spacetime curvature. The supergravity approximation holds when the string coupling is weak and the curvature small. It gives a theory which is trustworthy for an intermediate regime of energies, where the dual gauge theory is always strongly coupled. For the case $p = 3$, the supergravity description is valid for all energy regimes as the dilaton is just a constant. A classic review of the AdS/CFT with a detailed exposition to the above as well as other basic ideas is [100].

In its original form, the AdS/CFT relates Type IIB string theory in $AdS_5 \times S^5$ to the four-dimensional $\mathcal{N} = 4$ SYM. All matter fields transform in the adjoint representation of the gauge group. For the supergravity descriptions of confining gauge theories [150], it is possible to calculate the spectra of glueball states by considering the corresponding spectra of supergravity modes such that the classical solutions to equations of motion are normalisable. There is extensive work on glueball spectra and we cannot do justice to the literature so we mention indicatively some of the main papers [151–154].

One of the main questions that the community tried to understand since the early days of the duality was how to add fields that transform in the fundamental representation of the gauge group, such that the duality contains matter in appropriate group representations, and thus taking the duality a step closer to the more interesting quantum field theories and thus making the correspondence more physical and appealing. An early variant of the AdS/CFT describing a field theory with matter in the fundamental representation related the conformal $Sp(2N_c)$ with $\mathcal{N} = 2$ theory to D3-branes near singularities in F-theory; string theory in $AdS_5 \times S^5/\mathbb{Z}_2$ [155–157].

In a landmark paper [120], Karch and Katz showed that adding D7 branes in the probe limit - such that the D-branes do not backreact to the background geometry - is the appropriate way to add matter fields transforming the fundamental representation of the gauge group in the original setup with the D3-branes that generate the $AdS_5 \times S^5$ background. The addition of N_f D7 branes in the $AdS_5 \times S^5$ background is equivalent to coupling N_f hypermultiplets in the fundamental representation of the original SYM theory. The probe (or in the field theory language the quench) limit corresponds to having $N_f/N_c \to 0$. The stretched strings between the two different branes are the fields that we consider as dynamical quarks, specifically the lightest string states that stretch between the two different types of branes. Adding the D7 branes reduces the supercharges by half compared to the original setup and the resulting four-dimensional $\mathcal{N} = 2$ theory has quark-antiquark bound states (mesons) and in the decoupling limit the exercise of studying the dynamics and the masses of these states is equivalent to computing the classical equations of motion of open strings. The seminal paper exploring these ideas is [121] where the analysis was performed for the D3-probe D7 system.

A number of directions have been undertaken in order to construct gravity dual descriptions of QCD-like theories. Chiral symmetry breaking has been described in [122, 129, 158, 159] and the meson spectra of brane intersections with eight supercharges have been computed in [160, 161]. For more details on flavour physics and mesons in the context of the gauge/gravity duality see the review [41]. The

aforementioned works are all in the probe (in gravity terms) or the quench limit (in the field theory language) of the correspondence such that the branes do not backreact to the geometry. Considerable efforts have been made beyond this approximation. For an excellent review on unquenched flavours in the AdS/CFT see [162].

While much effort has been put and progress has been made towards the understanding of the bosonic sectors of adjoint matter fields comprised out of the fundamental quarks (meson fields), much less attention has been given to their supersymmetric partners. There are some reasons for this.

To begin with, in cases with any amount of supersymmetry the spectra of fermionic states can be derived using representation theory. This counting had been performed in [121] for the fermionic superpartners of the bosonic meson states in the D3/probe-D7 setup. It is worthwhile mentioning that while it is possible to obtain the mass spectra precisely due to the preserved amount of supersymmetry, if one follows this approach then there is no access to the dynamics of world-volume fermions as the equations of motion are missing.

In addition to that, these fermionic superpartners should be formally interpreted as fermionic meson states in the sense they are fermionic fields in the adjoint representation of the $\mathcal{N} = 2$. Such a state has no counterpart neither in the real-world QCD theory nor in any non-supersymmetric version of QCD-like theories. In other words, it can be characterized as a purely supersymmetric effect.

A final hindrance was the form of the fermionic completion to the DBI action. Before the work of [163–165] that particular part of the action was written in superspace [166, 167]. In spite of the compact form of the action and the elegance of the superspace techniques, using the superspace as the target space of the theory obscures how the background fields enter the fermionic terms of the action. Hence, with that particular formulation of the action at our disposal any explicit computations or considerations involving the world-volume fermions cannot be performed. The work of [163–165] resolved precisely that issue and presented an action for world-volume fermions written in terms of the spacetime.

Since the technology developed enough and made explicit computations involving world-volume fermions possible the first explicit results in probe-brane holography started appearing. This was initiated in [82] where the author considered the D3/probe-D7 intersection in the limit where the flavour branes have collapsed on the background ones. In field theory terms, this corresponds to massless quarks. From that effective bottom-up approach a replacement rule was invoked at the level of the equations of motion that yields the correct mass spectra even for the case of the massive embedding of the flavour brane. A follow-up to that work was presented in [168] where the authors followed the same line of reasoning but for all possible probe-brane setups in the D3 background. Another very interesting result was derived in [146], where the authors obtained the spectrum of bosonic and fermionic excitations of 1/2-BPS Wilson loops for a D3-brane in the $AdS_5 \times S^5$ background.

With a formal understanding of the massive embedding in the D3/probe-D7 intersection being a motivation as well as some phenomenological applications of holography and the use of fermions in bottom-up models, the authors in [1] studied the top-down massive picture in all probe brane systems in the presence of the D3 background and obtained the expressions for the supergravity states dual to these fermions and the corresponding mass spectra. The work of [169] is also a top-down approach that

investigates the D4-D8 setup in Type IIA supergravity and it pertains to the Sakai-Sugimoto model [129]. It is worthwile pointing out that the authors in [1, 169] are using different approaches to finding the mass eigenvalues. In [1] the authors also considered the effect of adding multi-trace operators to these fermionic states following Witten's prescription [147]. After a careful numerical analysis they observed an avoided level-crossing as one approaches from a higher excited state the lower one in the KK tower.

Another point made by the authors in that paper was that, after analysing the holographic dictionary, they observed that some of the aforementioned fermionic states are made of three elementary Fermi fields; two fields transforming in the fundamental representation (quarks) and one in the adjoint of the gauge group (a gaugino). Hence, the observation that the lowest lying state of that particular supermultiplet resembles qualitatively—by means of the same structure—the baryon operators in real-life QCD.

In this work we continue in a natural line of the aforementioned research and we study all possible probe-branes intersections in Type IIA/B supergravity theories that have been shown to preserve eight supercharges; $\mathcal{N}=2$ SUSY in a four-dimensional language. Since the bosonic mass spectra are explicitly known in these cases [160, 161] the interest lies in the deeper understanding of the dynamics of fermionic open-string states and unveiling potential computational subtleties in the derivation that did not appear in the study of probe-branes in the presence of the D3-background. We obtain the equations of motion explicitly for each case starting from the fermionic action as was derived in [163–165] .

We show the expected supersymmetric degeneracy for the mass eigenvalues. For the case of the D3-background there are analytic solutions that have been previously obtained [1] and we report these here for completeness. All the other backgrounds do not admit analytic solutions for the eigenstates of the equations of motion and the mass eigenvalues. For these cases we work in two different ways. To begin with, we perform a careful numerical analysis and obtain the mass eigenvalues directly from the fermionic equations of motion. We see that in each case they are the same as the corresponding results anticipated from the analysis of the bosonic meson states and their equations of motion.

Furthermore, we were able to derive a map such that we bring the equations of motion describing world-volume fermions in our brane intersections to the relevant equations of motion describing bosonic degrees of freedom in these setups. Here some comments are in order. Due to the two eigenvalues of the spinor spherical harmonics we have two sets of supergravity fields. We denote those associated with the positive eigenvalues by $\mathcal{G}$. These are the superpartners of the gauge fields on the probe-brane which have a non-trivial profile only on the internal manifold. More explicitly, these gauge fields are decomposed as $A_\mu = 0, \quad A_\rho = 0, \quad A_i = a(\rho)e^{ik^\mu x_\mu}\mathcal{Y}_i^{\ell\pm}$. From the negative eigenvalue of the spinor spherical harmonic we obtain modes which we generically denote by $\mathcal{F}$ and they are the superpartners of the scalar fields obtained as fluctuations of the transverse coordinates.

For both types of the fermionic modes described above we were able to map the equations of motion associated with the positive eigenvalue of the projection Γ-matrix defined along the holographic radial

coordinate ($\Gamma^\rho \Psi^\pm = \pm \Psi^\pm$) to the associated bosonic equations of motion. The map is given by

$$\psi^{\oplus}_{\mathcal{G}_\ell}(\varrho) = \frac{1}{(1+\varrho^2)^{\frac{3}{16}(7-p)}} f_{\ell+1}(\varrho), \qquad \psi^{\oplus}_{\mathcal{F}_\ell}(\varrho) = \frac{1}{(1+\varrho^2)^{\frac{3}{16}(7-p)}} f_{\ell}(\varrho), \tag{7.1}$$

where in the above we denote by $\oplus$ superscript the supergravity modes obtained by considering the projection $\Gamma^\rho \Psi^\oplus = \Psi^\oplus$ and we reserve the $\ominus$ for the negative eigenvalue of the projection.

While at this point the reader might be concerned that we were able to map only the equations of motion related to one of the Γ^ρ eigenvalues, there is nothing out of place in doing so. We are able to deduce the eigenstates and mass eigenvalues from either of the equations of motion. The reasoning behind this is simple: we start with two coupled first-order equations of motion that describe a source and the relevant operator. Then, we derive the second-order equations of motion starting from the first-order ones. In doing so we act with an appropriately chosen differential operator and we create a double-copy of the operator and the source [1, 170]. Hence, the equations of each eigenvalue of the Γ^ρ matrix contains a copy of the source and a copy of the operator. By requiring normalizable open-string modes in the UV in either of the equations we are setting the source to zero and hence each second-order differential equation yields the correct answer individually. This procedure is made more precise and explained thoroughly in section 7.4.1. We also, further support and refine the argument that these states describe effectively baryons as we show that in large-N_c limit their mass scales as

$$M^2 \sim N_c^2 \,, \tag{7.2}$$

when we fix the quantum number n which counts the nodes of the state and the angular quantum number ℓ. This scaling in large-N_c limit of the theory is a purely field theory expectation [171]. The results described by equations (7.1) and (7.2) constitute the two main points of this work. The third main result is the explanation of the avoided level crossing, which is explained in section 7.8.

Furthermore, the authors of [1] observed an avoided level crossing when examining the inclusion of multi-trace interactions without giving an analytic explanation for the effect. We revisit that computation and give an analytic justification to the observed avoided level crossing by bringing the equations of motion in a Schrödinger form and examining the solutions of the supergravity modes. Interestingly, such a crossing has been shown to occur when considering instanton configurations in the probe-brane setup [172].

At this point, we would like to clarify that we do not claim that we have solved the true string baryonic vertex. In the large-N_c limit a baryon is made of N_c fundamental fields (quarks) and has to be appropriately described in the gravity side. The description is well known [103]. Witten has shown that in the base $\mathcal{N} = 4$ SYM theory a baryonic vertex is obtained by a wrapped D5-brane over the S^5. Since we have not considered the addition of the five-branes in our basic D3/probe-D7 model, we do not approach baryons directly in this work. However, we believe that the spectrum we obtain in section 7.6 should be obtained from the full string construction in the limit where the boundary gauge theory is in the conformal window. This result was obtained in an effective, bottom-up way in [82], however a 10-dimensional derivation was lacking, which we provide here.

7.3 Background spacetime and probe-brane geometries

In this section we wish to establish notation and conventions, as well as set the stage for the analysis of the forthcoming sections. The analysis presented below in section 7.3.1 and section 7.3.2 has been performed a number of times in the past [124, 160, 161], however we do find it convenient and useful to quote once more the basic results here.

7.3.1 The background geometry

We will be considering the brane junctions of a Dp-brane and a Dk-brane (under the assumption that $p \leq k$) along a number d of common spatial dimensions such that the system is 1/2-BPS. We will denote this intersection by $\{d, p, k\}$. The lower dimensional brane is treated as the background one, while we treat the other one as the probe. Taking into consideration the above physical constraints, one can verify that there are three possibilities for consistent intersections: $\{p, p, p+4\}$, $\{p-1, p, p+2\}$, and $\{p-2, p, p\}$.

The supergravity background geometry that describes a stack of N_c coincident Dp-branes is given by

$$ds^2 = \frac{1}{\sqrt{H_p}} dx^\mu dx_\mu + \sqrt{H_p}\; d\vec{Z} \cdot d\vec{Z}\,, \tag{7.3}$$

written in the string frame. The μ is taking values over a $(p+1)$-dimensional Minkowski spacetime parallel to the branes, while the Z-coordinates parametrize the $(9-p)$-dimensional transverse space. In the above, $p \leq 4$, while the expression of the harmonic function H_p is of the following form

$$H_p = 1 + \left(\frac{R}{r}\right)^{7-p}, \tag{7.4}$$

with R being given by

$$R^{7-p} = 2^{5-p}\pi^{(5-p)/2}\; g_s\; N_c\; \Gamma\left(\frac{7-p}{2}\right)(\alpha')^{(7-p)/2}, \tag{7.5}$$

where in the above N_c is the number of the background Dp-branes, g_s is the string coupling constant, and α' is the inverse string tension. We will be working in the decoupling limit where the open string modes decouple from the closed string modes, thus, $\alpha' \to 0$ and

$$\lim_{\alpha'\to 0} g_{YM}^2 = \lim_{\alpha'\to 0} (2\pi)^{p-2}\; g_s\; \alpha'^{(p-3)/2} = \textit{fixed}\,. \tag{7.6}$$

Taking the near-horizon limit, the geometry of equation (7.3) takes the form

$$ds^2 = \left(\frac{r}{R}\right)^{\frac{7-p}{2}} dx^\mu dx_\mu + \left(\frac{R}{r}\right)^{\frac{7-p}{2}}\; d\vec{Z} \cdot d\vec{Z}, \tag{7.7}$$

while the dilaton and the Ramond-Ramond (R-R) potential can be expressed in terms of the r-coordinate

as follows

$$e^{\phi} = \left(\frac{R}{r}\right)^{\frac{(7-p)(3-p)}{4}}\,, \qquad\qquad C_{(p+1)} = \left(\frac{r}{R}\right)^{7-p} dx^0 \wedge \ldots \wedge dx^p\,. \tag{7.8}$$

For probe embeddings a particular useful re-parametrization of the near-horizon geometry is to choose spherical coordinates and re-express the spacetime. This can be achieved as follows: consider the introduction of the probe Dk-brane in this background which extends along the directions

$$X^{\hat{A}} = \{t, x^1, x^2, \cdots, x^d, Y^1, Y^2, \cdots, Y^{k-d}\}. \tag{7.9}$$

The hatted capital Latin indices denote the coordinates of the probe Dk-brane. It is worthwhile stressing that the set of Y-coordinates describes directions that are transverse to the background Dp-brane, which means that they coincide with some of the Z-coordinates. The rest of the Z-coordinates which are transverse to both background and probe branes will be denoted with $\vec{w}$, namely

$$\vec{w} = \{w^1, w^2, \cdots, w^{9-p-k+d}\}, \tag{7.10}$$

with $w^m = Z^{k-d+m}$, and $m = 1, 2, \cdots, 9-p-k+d$. In order to introduce spherical coordinates on the world-volume of the Dk-brane that is transverse to the Dp-brane, we define

$$\begin{aligned}
Y^1 &= \rho\, \cos\theta_1\,, \\
Y^2 &= \rho\, \sin\theta_1\, \cos\theta_2\,, \\
&\vdots \\
Y^{k-d-1} &= \rho\, \sin\theta_1\, \sin\theta_2 \cdots \sin\theta_{k-d-2}\, \cos\theta_{k-d-1}\,, \\
Y^{k-d} &= \rho\, \sin\theta_1\, \sin\theta_2 \cdots \sin\theta_{k-d-2}\, \sin\theta_{k-d-1}\,,
\end{aligned} \tag{7.11}$$

which results to

$$\left(Y^1\right)^2 + \left(Y^2\right)^2 + \cdots + \left(Y^{k-d}\right)^2 = \rho^2\,, \tag{7.12}$$

and

$$\left(dY^1\right)^2 + \left(dY^2\right)^2 + \cdots + \left(dY^{k-d}\right)^2 = d\rho^2 + \rho^2 d\Omega^2_{k-d-1}\,. \tag{7.13}$$

In the above relation

$$d\Omega^2_{k-d-1} = d\theta_1^2 + \sum_{i=2}^{k-d-1} \left(\prod_{j=1}^{i-1} \sin^2\theta_j\right) d\theta_i^2\,, \tag{7.14}$$

is the line element of the unit $(k-d-1)$-dimensional sphere.

Consequently, decomposing the Z-coordinates in the Y and w-coordinates, which are parallel and transverse to the Dk-brane, respectively, we are led to

$$ds^2 = \left(\frac{r}{R}\right)^{\frac{7-p}{2}} \sum_{\mu,\nu=0}^{p} \eta_{\mu\nu}\, dx^\mu\, dx^\nu + \left(\frac{R}{r}\right)^{\frac{7-p}{2}} \left(d\rho^2 + \rho^2\, d\Omega^2_{k-d-1} + \sum_{m,n=1}^{9-p-k+d} \delta_{mn}\, dw^m\, dw^n\right)\,, \tag{7.15}$$

where $r^2 = \rho^2 + \sum_{m=1}^{9-p-k+d} (w^m)^2$.

7.3.2 The geometries on the probe branes

Let us start by considering the embedding of D$(p+4)$ branes, with $0 \leq p \leq 4$. We embed the flavour probe-brane in the $x^{p+5} x^{p+6} \cdots x^9$-plane at a constant position $|\vec{w}| = L \neq 0$. The induced geometry on the probe can be written as

$$ds^2 = \left(\frac{r}{R}\right)^{\frac{7-p}{2}} ds^2\left(\mathbb{M}^{(1,p)}\right) + \left(\frac{R}{r}\right)^{\frac{7-p}{2}} d\rho^2 + \left(\frac{R}{r}\right)^{\frac{7-p}{2}} \rho^2 \, d\Omega_3^2 \,, \tag{7.16}$$

where $\mathbb{M}^{(1,p)}$ denotes the $(1+p)-$dimensional Minkowski spacetime. The boundary gauge theory is a $(p+1)$-dimensional SYM theory coupled to a matter hypermultiplet in the fundamental representation of the gauge group and the quark mass is proportional to the distance L that separates the two different branes. In case of $p = 3$ the induced geometry in the UV limit ($r = \rho \to \infty$) spans an $AdS_5 \times S^3$ spacetime.

Now, we want to consider the supersymmetric embedding of D$(p+2)$ branes, with $1 \leq p \leq 4$. In this case the dual gauge theory is $(p+1)$-dimensional with the fundamental hypermultiplet confined on a p-dimensional surface. The induced geometry is equal to

$$ds^2 = \left(\frac{r}{R}\right)^{\frac{7-p}{2}} ds^2\left(\mathbb{M}^{(1,p-1)}\right) + \left(\frac{R}{r}\right)^{\frac{7-p}{2}} d\rho^2 + \left(\frac{R}{r}\right)^{\frac{7-p}{2}} \rho^2 \, d\Omega_2^2 \,. \tag{7.17}$$

In case of $p = 3$ the induced geometry in the UV limit spans an $AdS_4 \times S^2$ geometry.

Finally, we want to consider embedding probe Dp-branes in the background of geometry of Dp-branes with $2 \leq p \leq 4$. The matter field of fundamental hypermultiplet propagate in a co-dimension two defect; the hypermultiplet is confined on a $(p-1)$-dimensional surface. The geometry on the probe brane can be written as

$$ds^2 = \left(\frac{r}{R}\right)^{\frac{7-p}{2}} ds^2\left(\mathbb{M}^{(1,p-2)}\right) + \left(\frac{R}{r}\right)^{\frac{7-p}{2}} d\rho^2 + \left(\frac{R}{r}\right)^{\frac{7-p}{2}} \rho^2 \, d\Omega_1^2. \tag{7.18}$$

In case of $p = 3$ the induced geometry in the UV limit spans an $AdS_3 \times S^1$ spacetime.

7.3.3 Vielbeins & spin-connection components

An appropriate choice of basis will be proven very helpful for the forthcoming calculations, thus, using the vielbein formalism - for which it holds that $g_{MN} = e^{(A)}{}_M \, e^{(B)}{}_N \, \eta_{(A)(B)}$ - [2] in the geometry of equation (7.15), it is straightforward to evaluate the following quantities:

$$e^{(A)}{}_\mu = \left(\frac{r}{R}\right)^{\frac{7-p}{4}} \delta^A{}_\mu, \qquad e^{(A)}{}_\rho = \left(\frac{R}{r}\right)^{\frac{7-p}{4}} \delta^A{}_\rho, \tag{7.19}$$

$$e^{(A)}{}_{\bar{i}} = \rho \left(\frac{R}{r}\right)^{\frac{7-p}{4}} \bar{e}^{(A)}{}_{\bar{i}} \,, \quad i = 1, \ldots, k-d-1 \,, \tag{7.20}$$

[2] Indices between brackets will be used solely to denote vielbein indices.

$$e^{(A)}{}_{\widetilde{m}} = \left(\frac{R}{r}\right)^{\frac{7-p}{4}} \delta^{A}{}_{\widetilde{m}}\,, \quad m = 1, \ldots, 9-p-k+d\,, \tag{7.21}$$

where the indices with bar correspond to the spherical coordinates $\{\theta_1, \ldots, \theta_{k-d-1}\}$, while the indices with tilde correspond to the coordinates $\{w^1, \ldots, w^{9-p-k+d}\}$. In addition, the quantity $\bar{e}^{(A)}{}_{\bar{i}}$ represents the vielbein of S^{k-d-1}; its explicit expression is given in appendix C.2. The vielbein basis $\left\{e^{(A)} \,|\, e^{(A)} = e^{(A)}{}_M\, dx^M\right\}$ satisfies the following relation[3]

$$ds^2 = g_{MN}\, dx^M\, dx^N = \eta_{(A)(B)}\, e^{(A)}\, e^{(B)}\,. \tag{7.23}$$

We also present below the non-zero components of the spin-connection. We remind the readers that for torsion-free theories the definition is

$$\omega_M^{(A)(B)} = e^{(A)}{}_N\, \Gamma^N_{ML}\, e^{(B)L} + e^{(A)}{}_N\, \partial_M\, e^{(B)N}, \tag{7.24}$$

where $e^{(A)M} = e^{(A)}{}_N\, g^{NM} = \eta^{(A)(B)} e_{(B)}{}^M$. Using equation (7.24) we obtain the following spin-connection components:

$$\omega_\mu^{(A)(B)} = \frac{7-p}{4} \frac{r^{\frac{3-p}{2}}}{R^{\frac{7-p}{2}}} \left[\rho(\delta^A_\mu\, \delta^B_\rho - \delta^B_\mu\, \delta^A_\rho) + w^{\widetilde{m}}(\delta^A_\mu\, \delta^B_{\widetilde{m}} - \delta^B_\mu\, \delta^A_{\widetilde{m}})\right], \tag{7.25}$$

$$\omega_\rho^{(A)(B)} = \frac{(7-p)}{4} \frac{w^{\widetilde{m}}}{r^2} (\delta^A_{\widetilde{m}}\, \delta^B_\rho - \delta^B_{\widetilde{m}}\, \delta^A_\rho)\,, \tag{7.26}$$

$$\begin{aligned}\omega_{\bar{k}}^{(A)(B)} &= \bar{\omega}_{\bar{k}}^{(A)(B)} + \left[\frac{(7-p)\rho^2}{4r^2} - 1\right] (\delta^A_\rho\, \bar{e}^{(B)}{}_{\bar{k}} - \delta^B_\rho\, \bar{e}^{(A)}{}_{\bar{k}}) \\ &\quad + \frac{(7-p)\rho\, w^{\widetilde{m}}}{4r^2} (\delta^A_{\widetilde{m}}\, \bar{e}^{(B)}{}_{\bar{k}} - \delta^B_{\widetilde{m}}\, \bar{e}^{(A)}{}_{\bar{k}})\,,\end{aligned} \tag{7.27}$$

$$\omega_{\widetilde{m}}^{(A)(B)} = \frac{(7-p)}{4r^2} \left[\rho(\delta^A_\rho\, \delta^B_{\widetilde{m}} - \delta^B_\rho\, \delta^A_{\widetilde{m}}) + w^{\widetilde{n}}(\delta^A_{\widetilde{n}}\, \delta^B_{\widetilde{m}} - \delta^B_{\widetilde{n}}\, \delta^A_{\widetilde{m}})\right], \tag{7.28}$$

where the quantity $\bar{\omega}_{\bar{k}}^{(A)(B)}$ constitutes the spin-connection of S^{k-d-1}; its explicit expression is given in appendix C.2 as well.

7.3.4 The Dirac operator

The Dirac operator for fermionic fields on a generic curved manifold is defined by

$$\not{D} = \Gamma^N\, e_{(N)}{}^M \left(\partial_M + \frac{1}{8}\, \omega_M^{(K)(L)}\, [\Gamma_K, \Gamma_L]\right) = \Gamma^N\, e_{(N)}{}^M \left(\partial_M + \frac{1}{4}\, \omega_M^{(K)(L)}\, \Gamma_{KL}\right). \tag{7.29}$$

In what follows, we compute the Dirac operator for the general case that we consider here; the embedding of a probe Dk-brane in the background generated by Dp-branes. Note that for a probe Dk the index

[3]The dual basis $\left\{e_{(A)} \,\middle|\, e_{(A)} = e_{(A)}{}^M\, \partial_M\right\}$ is defined through the relation

$$e^{(A)}\left(e_{(B)}\right) = e^{(A)}{}_M\, dx^M \left(e_{(B)}{}^N\, \partial_N\right) = e^{(A)}{}_M\, e_{(B)}{}^N\, \delta^M{}_N = \delta^{(A)}{}_{(B)}\,. \tag{7.22}$$

M in equation (7.29) should be replaced by $\hat{M}$, which runs over the probe brane coordinates. After a straightforward computation we are led to

$$\begin{aligned}\not{D}_{Dk} =& \frac{R^{\frac{7-p}{4}}}{r^{\frac{7-p}{4}}}\,\Gamma^{\mu}\partial_{\mu} + \frac{r^{\frac{7-p}{4}}}{R^{\frac{7-p}{4}}}\,\Gamma^{\rho}\partial_{\rho} + \frac{1}{\rho}\frac{r^{\frac{7-p}{4}}}{R^{\frac{7-p}{4}}}\not{D}_{S^{k-d-1}} \\ &+ \frac{1}{R^{\frac{7-p}{4}}}\left[\frac{7-p}{8}\frac{\rho}{r^{\frac{p+1}{4}}}(2d+2-k) + \frac{1}{2}\frac{r^{\frac{7-p}{4}}}{\rho}(k-d-1)\right]\Gamma^{\rho} \\ &+ \frac{7-p}{8}\frac{1}{R^{\frac{7-p}{4}}}\frac{1}{r^{\frac{p+1}{4}}}\,(2d+1-k)\sum_{m=1}^{9-p-k+d} w^{m}\,\Gamma_{\widetilde{m}}\,,\end{aligned} \tag{7.30}$$

with

$$\not{D}_{S^{k-d-1}} = \Gamma^{N}\,\bar{e}_{(N)}{}^{\bar{k}}\left(\partial_{\bar{k}} + \frac{1}{4}\bar{\omega}_{\bar{k}}^{(K)(L)}\,\Gamma_{KL}\right). \tag{7.31}$$

We have already mentioned that the consistent intersections - characterized by the set of numbers $\{d,p,k\}$ - between the background Dp- and probe Dk-branes, are: $\{p,p,p+4\}$, $\{p-1,p,p+2\}$, and $\{p-2,p,p\}$. One can easily verify that in all cases $2d+1-k=p-3$, thus, equation (7.30) can be written as

$$\begin{aligned}\not{D}_{Dk} =& \frac{R^{\frac{7-p}{4}}}{r^{\frac{7-p}{4}}}\,\Gamma^{\mu}\partial_{\mu} + \frac{r^{\frac{7-p}{4}}}{R^{\frac{7-p}{4}}}\,\Gamma^{\rho}\partial_{\rho} + \frac{1}{\rho}\frac{r^{\frac{7-p}{4}}}{R^{\frac{7-p}{4}}}\not{D}_{S^{k-d-1}} \\ &+ \frac{1}{R^{\frac{7-p}{4}}}\left[\frac{(7-p)(p-2)}{8}\frac{\rho}{r^{\frac{p+1}{4}}} + \frac{1}{2}\frac{r^{\frac{7-p}{4}}}{\rho}(k-d-1)\right]\Gamma^{\rho} \\ &- \frac{(7-p)(3-p)}{8}\frac{1}{R^{\frac{7-p}{4}}}\frac{1}{r^{\frac{p+1}{4}}}\sum_{m=1}^{9-p-k+d} w^{m}\,\Gamma_{\widetilde{m}}\,.\end{aligned} \tag{7.32}$$

7.4 Dynamics and spectra from string fluctuations

7.4.1 D0 branes: supersymmetric matrix quantum mechanics

In the background generated by a stack of D0-branes there is a unique way to arrange the flavour branes which we demonstrate in table 7.1. The fermionic action [163–165] is given by

	x^0	x^1	x^2	x^3	x^4	x^5	x^6	x^7	x^8	x^9
Background D0-brane	—	•	•	•	•	•	•	•	•	•
Probe D4-brane	—	—	—	—	—	•	•	•	•	•

Table 7.1: The brane intersection. In the above notation — denotes that a brane extends along that particular direction, while • means that the coordinate is transverse to the brane.

$$S_{D4} = \frac{T_{D4}}{2}\int d^{5}\xi\,\sqrt{-\hat{g}}\,\bar{\Psi}\,\mathcal{P}_{-}\left[\not{D}_{D4} - \frac{e^{\phi}}{8\cdot 2!}F_{AB}\left(\Gamma^{\hat{M}}\Gamma^{AB}\Gamma^{(10)}\Gamma_{\hat{M}} + 3\,\Gamma^{AB}\Gamma^{(10)}\right) - \frac{1}{2}\Gamma^{M}\partial_{M}\phi\right]\Psi \tag{7.33}$$

In the above, $(T_{Dk})^{-1} = (2\pi)^{k}(a')^{\frac{k+1}{2}}\,g_s$ is the brane tension, $\mathcal{P}_{-}$ is a κ-symmetry projector ensuring κ-symmetry invariance of the action, and F_{AB} represents the components of the 2-form R-R field

strength. With the use of equation (7.8) and setting $p = 0$ it is straightforward to determine both the dilaton field

$$e^{\phi} = \left(\frac{R}{r}\right)^{\frac{21}{4}}, \tag{7.34}$$

and the 2-form R-R field strength

$$F_{(2)} = dC_{(1)} = -\frac{7r^5}{R^7}\, e^{(0)} \wedge \left(\rho\, e^{(\rho)} + \sum_{i=1}^{5} w^i\, e^{(w^i)}\right). \tag{7.35}$$

In addition, $\Gamma^{(10)} \equiv \Gamma^{01\cdots p\,\rho\,\theta_1\cdots\theta_{k-d-1}\,w^1\cdots w^{9-p-k+d}}$ is the ten-dimensional chiral operator, $\hat{g}_{\hat{M}\hat{N}} = P[g]_{\hat{M}\hat{N}}$ is the pullback of the background metric g_{MN} on the worldvolume, while $\hat{g}$ constitutes the determinant of the aforementioned metric.

Varying equation (7.33) with respect to the conjugate spinor $\bar{\Psi}$, we readily obtain the equation of motion of the spinor Ψ (Ψ is a ten-dimensional spinor of positive chirality $\Gamma^{(10)}\Psi = \Psi$), namely

$$\not{D}_{D4}\Psi - \frac{e^{\phi}}{8\cdot 2!}F_{AB}\left(\Gamma^{\hat{M}}\Gamma^{AB}\Gamma^{(10)}\Gamma_{\hat{M}} + 3\Gamma^{AB}\Gamma^{(10)}\right)\Psi - \frac{1}{2}(\Gamma^M\partial_M\phi)\Psi = 0\,. \tag{7.36}$$

Using equation (7.34) and equation (7.35) together with the properties of Γ^M matrices, we can evaluate

$$\frac{e^{\phi}}{8\cdot 2!}F_{AB}\left(\Gamma^{\hat{M}}\Gamma^{AB}\Gamma^{(10)}\Gamma_{\hat{M}} + 3\Gamma^{AB}\Gamma^{(10)}\right)\Psi = -\frac{7}{4R^{7/4}}\frac{\rho}{r^{1/4}}\,\Gamma^{0\rho}\Psi = \frac{7}{4R^{7/4}}\frac{\rho}{r^{1/4}}\,\Gamma_{0\rho}\Psi\,, \tag{7.37}$$

while by setting $p = d = 0$ and $k = 4$ in equation (7.30) we are led to

$$\begin{aligned}\not{D}_{D4}\Psi = \Bigg\{&\left(\frac{R}{r}\right)^{\frac{7}{4}}\Gamma^{\mu}\partial_{\mu} + \left(\frac{r}{R}\right)^{\frac{7}{4}}\Gamma^{\rho}\partial_{\rho} + \frac{1}{\rho}\left(\frac{r}{R}\right)^{\frac{7}{4}}\not{D}_{S^3} + \frac{1}{R^{\frac{7}{4}}}\left(-\frac{7}{4}\frac{\rho}{r^{\frac{1}{4}}} + \frac{3r^{\frac{7}{4}}}{2\rho}\right)\Gamma^{\rho}\\ &-\frac{21}{8}\frac{1}{R^{\frac{7}{4}}}\frac{1}{r^{\frac{1}{4}}}\sum_{i=1}^{5} w^i\,\Gamma_{w^i}\Bigg\}\Psi\,.\end{aligned} \tag{7.38}$$

For the spherical piece we can utilize the spinor spherical harmonics [173]

$$\not{D}_{S^3}\Psi^{\ell^{\pm}} = \pm\left(\ell + \frac{3}{2}\right)\Psi^{\ell^{\pm}}\,. \tag{7.39}$$

It is also important to notice that the above calculations have been performed in the vielbein basis $\{e^{(M)}\}$ (see for example the expression of the R-R field strength) instead of the usual $\{dx^M\}$. Thus, we should recognise that $\Gamma^M\partial_M\phi$ is in fact $\Gamma^N e_{(N)}{}^M\partial_M\phi$. From equation (7.8) and after a straightforward calculation, we get

$$\Gamma^M\partial_M\phi \to \Gamma^N e_{(N)}{}^M\partial_M\phi = -\frac{21}{4}\frac{1}{R^{\frac{7}{4}}}\frac{1}{r^{\frac{1}{4}}}\left(\rho\,\Gamma^{\rho} + \sum_{i=1}^{5} w^i\,\Gamma_{w^i}\right). \tag{7.40}$$

Consequently, substituting equations (7.37) and (7.40) in equation (7.36) and imposing the projection

$\Gamma_{0\rho}\Psi = -\Psi$, we are led to the following first-order equation of motion

$$\left\{\left(\frac{R}{r}\right)^{\frac{7}{4}}\Gamma^{\mu}\partial_{\mu} + \left(\frac{r}{R}\right)^{\frac{7}{4}}\Gamma^{\rho}\partial_{\rho} + \frac{1}{R^{\frac{7}{4}}}\left[\frac{7}{4}\frac{\rho}{r^{\frac{1}{4}}} \pm \left(\ell+\frac{3}{2}\right)\frac{r^{\frac{7}{4}}}{\rho}\right] + \frac{1}{R^{\frac{7}{4}}}\left(\frac{7}{8}\frac{\rho}{r^{\frac{1}{4}}} + \frac{3}{2}\frac{r^{\frac{7}{4}}}{\rho}\right)\Gamma^{\rho}\right\}\Psi^{\ell^{\pm}} = 0\,. \quad (7.41)$$

In what follows we consider that $\sum_{i=1}^{5}(w^i)^2 = L^2$, which by its turn leads to $r^2 = \rho^2 + L^2$. L constitutes the distance between the D0- and the D4-branes in the $x^5x^6x^7x^8x^9$-hyperplane of the 10-dimensional spacetime. Acting with the operator $\left(\frac{R}{r}\right)^{7/4}\Gamma^{\mu}\partial_{\mu} + \left(\frac{r}{R}\right)^{7/4}\Gamma^{\rho}\partial_{\rho}$ on the l.h.s. of equation (7.41), and then using the Clifford algebra and the first-order equation of motion equation (7.41), it is possible to re-express some of the terms appropriately such that we derive an ordinary, second-order differential equation of the following form

$$\left(\mathcal{A}_1^{\pm}\partial_{\varrho}^2 + \mathcal{A}_2^{\pm}\partial_{\varrho} + \mathcal{A}_3^{\pm}\bar{M}^2 + \mathcal{A}_4^{\pm}\Gamma^{\varrho} + \mathcal{A}_5^{\pm}\right)\psi^{\ell^{\pm}}(\varrho) = 0\,, \quad (7.42)$$

where we have used the decomposition $\Psi^{\ell^{\pm}}(x^{\lambda},\rho) = e^{i\,k_{\lambda}x^{\lambda}}\,\psi^{\ell^{\pm}}(\rho)$ and the relation $M^2 = -\eta^{\mu\nu}k_{\mu}k_{\nu}$.[4] In addition, we have also used the dimensionless quantities $\varrho = \rho/L$, $\bar{M}^2 = M^2R^7/L^5$. The $\mathcal{A}$ factors which appropriately describe the second-order equation are shown below:

$$\begin{aligned}
&\mathcal{A}_1^{\pm} = 1, \quad \mathcal{A}_2^{\pm} = \frac{3}{\varrho} + \frac{21}{4}\frac{\varrho}{\varrho^2+1}, \quad \mathcal{A}_3^{\pm} = \frac{1}{(\varrho^2+1)^{7/2}}\,,\\
&\mathcal{A}_4^{\pm} = \frac{7}{4}\frac{1\pm 2\ell\pm 3}{\varrho^2+1} \mp \frac{1}{\varrho^2}\left(\ell+\frac{3}{2}\right) + \frac{21}{8}\frac{\varrho^2}{(\varrho^2+1)^2}\,, \quad (7.43)\\
&\mathcal{A}_5^{\pm} = \frac{7}{4}\frac{1}{\varrho^2+1}\left(5\mp 3\mp 2\ell\right) - \frac{63}{64}\frac{\varrho^2}{(\varrho^2+1)^2} - \frac{1}{\varrho^2}\left(\ell^2+3\ell+\frac{3}{2}\right)\,.
\end{aligned}$$

In the above equations, the plus sign in the $\mathcal{A}$ factors denotes the positive eigenvalue of the spinorial harmonics ($\mathcal{G}$ operators) and the negative sign superscript is related to the negative eigenvalue ($\mathcal{F}$ operators). Moreover, the projection $\Gamma^{\rho}\Psi = \pm\Psi$ (or $\Gamma^{\varrho}\psi = \pm\psi$) generates two additional second-order differential equations when it is applied to equation (7.42). The spinor which under the aforementioned projection remains invariant will be denoted by $\Psi^{\oplus}$ (or $\psi^{\oplus}$), while $\Psi^{\ominus}$ (or $\psi^{\ominus}$) will represent the spinor which under the same projection goes to minus itself. Therefore, we can distinguish the following cases:

1 Positive spinorial harmonics eigenvalues:

- Positive Γ^{ϱ}-projection:

$$\left(\mathcal{A}_1^{+}\partial_{\varrho}^2 + \mathcal{A}_2^{+}\partial_{\varrho} + \mathcal{A}_3^{+}\bar{M}^2 + \mathcal{A}_4^{+} + \mathcal{A}_5^{+}\right)\psi^{\oplus}_{\mathcal{G}_{\ell}}(\varrho) = 0 \Rightarrow$$

[4] This particular decomposition results to

$$\Gamma^{\mu}\Gamma^{\nu}\partial_{\mu}\partial_{\nu}\Psi^{\ell^{\pm}} = -k_{\mu}k_{\nu}\Gamma^{\mu}\Gamma^{\nu}\Psi^{\ell^{\pm}} = -k_{\mu}k_{\nu}\left(2\eta^{\mu\nu}\mathbb{I}_{32} - \Gamma^{\nu}\Gamma^{\mu}\right)\Psi^{\ell^{\pm}} = 2M^2\,\Psi^{\ell^{\pm}} + k_{\mu}k_{\nu}\Gamma^{\nu}\Gamma^{\mu}\Psi^{\ell^{\pm}} \overset{\mu\leftrightarrow\nu}{\Longrightarrow}$$

$$-k_{\mu}k_{\nu}\Gamma^{\mu}\Gamma^{\nu}\Psi^{\ell^{\pm}} = 2M^2\,\Psi^{\ell^{\pm}} + k_{\nu}k_{\mu}\Gamma^{\mu}\Gamma^{\nu}\Psi^{\ell^{\pm}} \Rightarrow -k_{\mu}k_{\nu}\Gamma^{\mu}\Gamma^{\nu}\Psi^{\ell^{\pm}} = M^2\,\Psi^{\ell^{\pm}} \Rightarrow$$

$$\Gamma^{\mu}\Gamma^{\nu}\partial_{\mu}\partial_{\nu}\Psi^{\ell^{\pm}} = M^2\,\Psi^{\ell^{\pm}}\,.$$

$$\left[\partial_\varrho^2+\left(\frac{3}{\varrho}+\frac{21}{4}\frac{\varrho}{\varrho^2+1}\right)\partial_\varrho+\frac{\bar{M}^2}{(\varrho^2+1)^{7/2}}-\frac{1}{\varrho^2}(\ell^2+4\ell+3)\right.$$
$$\left.+\frac{21}{2}\frac{1}{\varrho^2+1}+\frac{105}{64}\frac{\varrho^2}{(\varrho^2+1)^2}\right]\psi^{\oplus}_{\mathcal{G}_\ell}(\varrho)=0\,. \quad (7.44)$$

- Negative Γ^{ϱ}-projection:

$$\left(\mathcal{A}_1^+\partial_\varrho^2+\mathcal{A}_2^+\partial_\varrho+\mathcal{A}_3^+\bar{M}^2-\mathcal{A}_4^++\mathcal{A}_5^+\right)\psi^{\ominus}_{\mathcal{G}_\ell}(\varrho)=0\Rightarrow$$

$$\left[\partial_\varrho^2+\left(\frac{3}{\varrho}+\frac{21}{4}\frac{\varrho}{\varrho^2+1}\right)\partial_\varrho+\frac{\bar{M}^2}{(\varrho^2+1)^{7/2}}-\frac{1}{\varrho^2}(\ell^2+2\ell)\right.$$
$$\left.-\frac{7}{2}\frac{1+2\ell}{\varrho^2+1}-\frac{231}{64}\frac{\varrho^2}{(\varrho^2+1)^2}\right]\psi^{\ominus}_{\mathcal{G}_\ell}(\varrho)=0\,. \quad (7.45)$$

2 Negative spinorial harmonics eigenvalues:

- Positive Γ^{ϱ}-projection:

$$\left(\mathcal{A}_1^-\partial_\varrho^2+\mathcal{A}_2^-\partial_\varrho+\mathcal{A}_3^-\bar{M}^2+\mathcal{A}_4^-+\mathcal{A}_5^-\right)\psi^{\oplus}_{\mathcal{F}_\ell}(\varrho)=0\Rightarrow$$

$$\left[\partial_\varrho^2+\left(\frac{3}{\varrho}+\frac{21}{4}\frac{\varrho}{\varrho^2+1}\right)\partial_\varrho+\frac{\bar{M}^2}{(\varrho^2+1)^{7/2}}-\frac{1}{\varrho^2}(\ell^2+2\ell)\right.$$
$$\left.+\frac{21}{2}\frac{1}{\varrho^2+1}+\frac{105}{64}\frac{\varrho^2}{(\varrho^2+1)^2}\right]\psi^{\oplus}_{\mathcal{F}_\ell}(\varrho)=0\,. \quad (7.46)$$

- Negative Γ^{ϱ}-projection:

$$\left(\mathcal{A}_1^-\partial_\varrho^2+\mathcal{A}_2^-\partial_\varrho+\mathcal{A}_3^-\bar{M}^2-\mathcal{A}_4^-+\mathcal{A}_5^-\right)\psi^{\ominus}_{\mathcal{F}_\ell}(\varrho)=0\Rightarrow$$

$$\left[\partial_\varrho^2+\left(\frac{3}{\varrho}+\frac{21}{4}\frac{\varrho}{\varrho^2+1}\right)\partial_\varrho+\frac{\bar{M}^2}{(\varrho^2+1)^{7/2}}-\frac{1}{\varrho^2}(\ell^2+4\ell+3)\right.$$
$$\left.+\frac{7}{2}\frac{5+2\ell}{\varrho^2+1}-\frac{231}{64}\frac{\varrho^2}{(\varrho^2+1)^2}\right]\psi^{\ominus}_{\mathcal{F}_\ell}(\varrho)=0\,. \quad (7.47)$$

It is straightforward to see that applying $p=0$ in equation (C.9) yields the corresponding bosonic equation of motion for the D0/D4-brane system, namely, it is

$$\partial_\varrho^2 f_\ell(\varrho)+\frac{3}{\varrho}\partial_\varrho f_\ell(\varrho)+\left[\frac{\bar{M}^2}{(1+\varrho^2)^{7/2}}-\frac{\ell(\ell+2)}{\varrho^2}\right]f_\ell(\varrho)=0\,. \quad (7.48)$$

One can easily verify that the transformation

$$\psi^{\oplus}_{\mathcal{G}_\ell}(\varrho) = \frac{1}{(1+\varrho^2)^{21/16}}\, f_{\ell+1}(\varrho)\,, \tag{7.49}$$

maps equation (7.44) to equation (7.48) for $\ell \to \ell+1$, while the transformation

$$\psi^{\oplus}_{\mathcal{F}_\ell}(\varrho) = \frac{1}{(1+\varrho^2)^{21/16}}\, f_{\ell}(\varrho)\,, \tag{7.50}$$

maps equation (7.46) to equation (7.48). Notice that the above transformations can be obtained from equation (7.1) by setting $p = 0$. In contrast, equation (7.45) and equation (7.47) cannot be mapped to equation (7.48). This particular behaviour is anticipated due to the structural difference of the two separate equations of motion obtained by the application of the two different projection eigenvalues of the Γ^ρ matrix. In order to demonstrate their difference, we simply plot the mode-solutions from which we obtain the correct mass squared eigenvalues, see figure 7.1 and figure 7.2. At this point, it is important to mention that the quantum number n counts the nodes of the functions $\psi^{\oplus,\ominus}_{\mathcal{G}_\ell}$ and $\psi^{\oplus,\ominus}_{\mathcal{F}_\ell}$; it is clear that in both figure 7.1 and figure 7.2 the quantum number n is zero. From these plots it is also very clear how we must shift appropriately the quantum number ℓ such that all the states are part of the same massive supermultiplet as dictated in [121]. We have employed this shift in the ℓ quantum number in all the tables with our numerical results such that we keep our presentation short. While

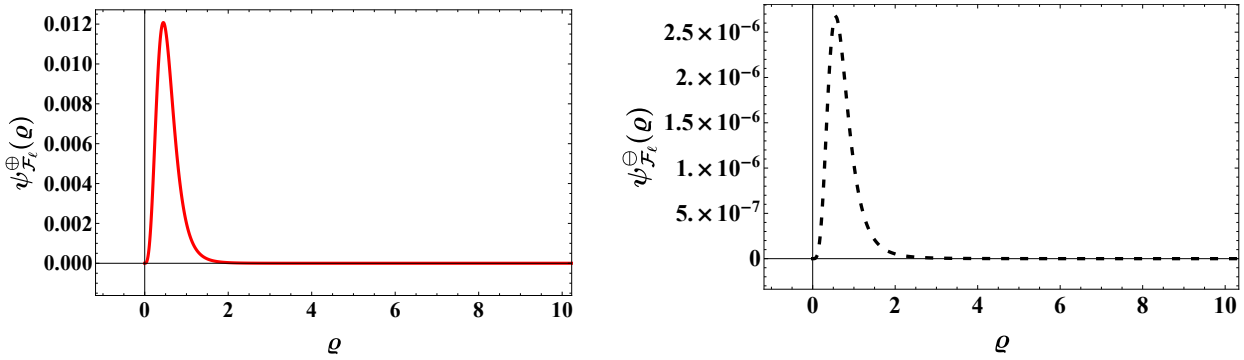

(a) **(b)**

Figure 7.1: (a) The solution obtained from the positive eigenvalue of the Γ^ϱ projector, while (b) refers to the negative eigenvalue of the Γ^ϱ projector. Both of them are dual to the field theory $\mathcal{F}$ modes for quantum numbers $n = 0, \ell = 3$.

we have provided appropriate transformations such that we analytically map the fermionic degrees of freedom to the bosonic ones, equations (7.49) and (7.50), here we demonstrate the numerical approach that we used to determine the mass eigenvalues directly from the second order equations of motion for the D0/D4 brane junction. The same numerical approach was of course used to compute the solutions in figure 7.1 and figure 7.2.

- We are shooting from the $\Lambda_{\rm IR}$ to the $\Lambda_{\rm UV}$ by fine-tuning $\bar{M}^2$ such that the mode solutions are normalizable in the UV and small in amplitude [121].
- We use $\Lambda_{\rm IR} = 10^{-7}$ and $\Lambda_{\rm UV} = 10$. We have checked the stability of our numerical solutions under variations of $\Lambda_{\rm IR}$ and $\Lambda_{\rm UV}$.

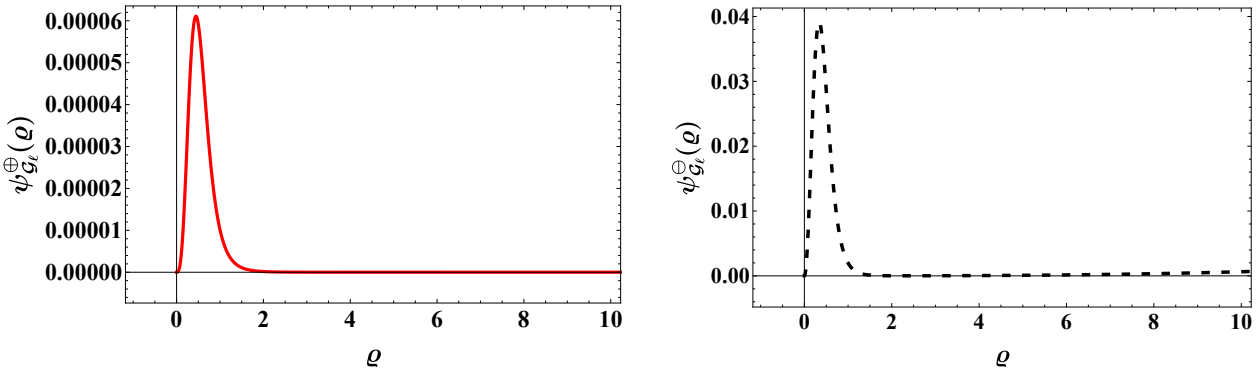

(a) **(b)**

Figure 7.2: (a) The solution obtained from the positive eigenvalue of the Γ^{ϱ} projector, while (b) refers to the negative eigenvalue of the Γ^{ϱ} projector. Both of them are dual to the field theory $\mathcal{G}$ modes for quantum numbers $n = 0, \ell = 2$.

- For the initial conditions we use

$$\begin{aligned} &\psi_{\mathcal{G},+}(\varrho)|_{\varrho\to 0} = \varrho^{\ell+1}, \qquad &&\partial_{\varrho}\psi_{\mathcal{G},+}(\varrho)|_{\varrho\to 0} = (\ell+1)\varrho^{\ell}\,, \\ &\psi_{\mathcal{G},-}(\varrho)|_{\varrho\to 0} = \varrho^{\ell}, \qquad &&\partial_{\varrho}\psi_{\mathcal{G},-}(\varrho)|_{\varrho\to 0} = \ell\varrho^{\ell-1}\,, \end{aligned} \tag{7.51}$$

$$\begin{aligned} &\psi_{\mathcal{F},+}(\varrho)|_{\varrho\to 0} = \varrho^{\ell}, \qquad &&\partial_{\varrho}\psi_{\mathcal{F},+}(\varrho)|_{\varrho\to 0} = \ell\varrho^{\ell-1}\,, \\ &\psi_{\mathcal{F},-}(\varrho)|_{\varrho\to 0} = \varrho^{\ell+1}, \qquad &&\partial_{\varrho}\psi_{\mathcal{F},-}(\varrho)|_{\varrho\to 0} = (\ell+1)\varrho^{\ell}\,. \end{aligned} \tag{7.52}$$

We show explicitly the first few numerical values of the masses in table 7.2. The numerical values for n and ℓ describe the $\mathcal{F}$ operators and one needs to shift appropriately the ℓ to read off the value of the $\mathcal{G}$ states. We have also explicitly checked that we obtain the same spectrum from equation (7.48). In

		n			
		0	1	2	3
ℓ	0	18.164	62.390	132.57	228.71
	1	52.188	115.60	204.53	319.13
	2	102.53	185.35	293.52	422.96
	3	168.85	271.32	398.78	551.65

Table 7.2: Numerical results of the parameter $\bar{M}^2$ for the D0/D4 brane junction.

order to perform the numerical analysis for the bosonic degrees of freedom we used as initial conditions $f(\varrho)|_{\varrho\to 0} = \varrho^{\ell}$ and $\partial_{\varrho} f(\varrho)|_{\varrho\to 0} = \ell\varrho^{\ell-1}$ [160, 161] and the other parameters are the same as previously.

As a final project within the D0/D4 brane setup, we are demonstrating explicitly that the $\bar{M}^2$ value can be obtained from either the positive or the negative eigenvalues of the Γ^{ϱ} matrix. This statement holds true of course for both the string modes dual to the $\mathcal{F}$ and $\mathcal{G}$ modes. In order to do so, we predict the mass of the $n = 0,\ \ell = 2$ for the supergravity modes dual to the $\mathcal{G}$ operators (the ones associated with the positive eigenvalue of the spinor spherical harmonics) and the $n = 0,\ \ell = 3$ state of the fluctuation dual to the $\mathcal{F}$ operators (related to the negative eigenvalue of the spinor harmonics). Note that these

particular $\mathcal{F}$ and $\mathcal{G}$ states should have the same mass, since we are shifting ℓ by one. We present our results for the $\mathcal{F}$ modes in figure 7.3 and we proceed to the results related to the $\mathcal{G}$ modes, which are shown in figure 7.4.

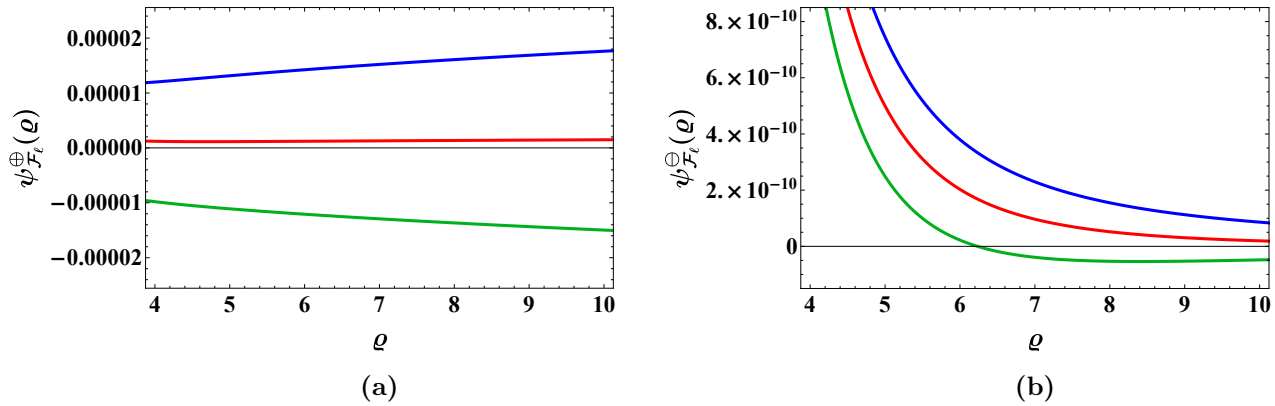

(a) **(b)**

Figure 7.3: For both (a) and (b), the masses are $\bar{M}^2 = 169$ (blue), 169.0736 (red), 169.1 (green) (from top to bottom). The parameters n and ℓ are the same as in figure 7.1, namely $n = 0$, $\ell = 3$. We have zoomed in to the plots in order to show the behaviour near the UV cut-off. Clearly the red line, which is the correct solution, can be uniquely determined from either positive or negative Γ^{ϱ}-projections.

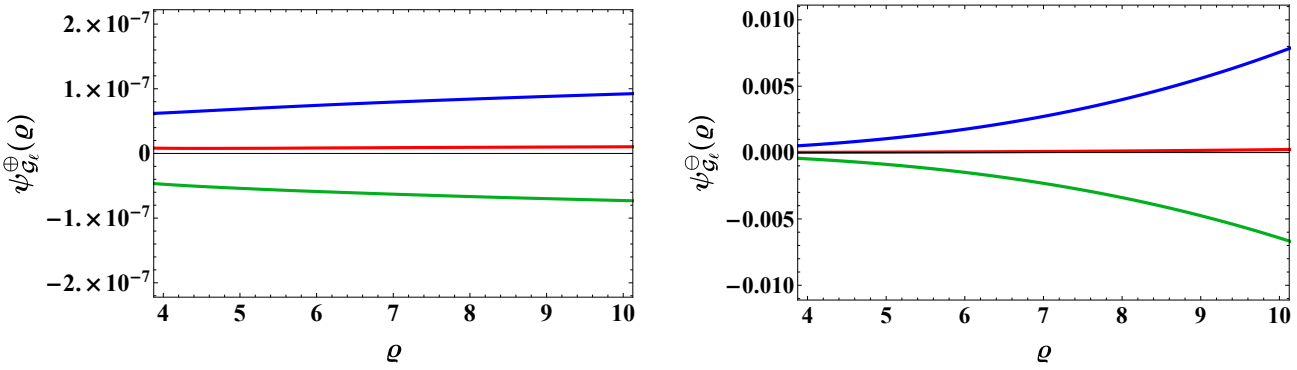

(a) **(b)**

Figure 7.4: For both (a) and (b), the masses are $\bar{M}^2 = 169$ (blue), 169.0736 (red), 169.1 (green) (from top to bottom). The parameters n and ℓ are the same as in figure 7.2, namely $n = 0$, $\ell = 2$. We have zoomed in to the plots in order to show the behaviour near the UV cut-off. Clearly the red line, which is the correct solution, can be uniquely determined from either positive or negative Γ^{ϱ}-projections.

7.4.2 The general procedure

In this section, we present the necessary mathematical machinery for computing the equation of motion and solve for the mass eigenvalues of the world-volume fermions in all possible probe-brane setups. The main task at hand, in order to determine the equations of motion and solve for the mass eigenvalues, is to derive a second-order ordinary differential equation of a scalar function depending on the holographic radial coordinate. To do so, we:

- Compute the vielbein and the spin-connection components of the background geometry from equations (7.19) to (7.21) and equations (7.25) to (7.28).
- Compute the dilaton field and the R-R field strength from equation (7.8). In addition, we

re-express the R-R field strength components in the vielbein basis.

- Write the curved Γ-matrices in terms of flat ones. It is also worthwhile commenting that we do not need an explicit representation of these matrices as we will be dealing only with projectors. These can be computed by means of the Clifford algebra and general properties that the generators of the algebra satisfy.

- Obtain the equation of motion for the ten-dimensional spinor Ψ by varying the fermionic DBI action with respect to the conjugate spinor $\bar{\Psi}$.

- Determine the first-order differential equation of the spinor using the explicit expression of the Dirac operator given by equation (7.30) or equation (7.32). For the spherical piece we can utilize the spinor spherical harmonics [173]

$$\not{D}_{S^{k-d-1}}\Psi^{\ell\pm} = \pm\left(\ell + \frac{k-d-1}{2}\right)\Psi^{\ell\pm}\,, \tag{7.53}$$

while, for the bulk piece, we use separation of variables for the Minkowski coordinates and the radial coordinate by making a plane-wave ansatz, with the wave-vector satisfying $k^\mu k_\mu = -M^2$ and M being the mass of the fluctuation.

It is also important to stress here that performing the calculations in the vielbein basis $\{e^{(M)}\}$, instead of the usual $\{dx^M\}$, will affect all spacetime derivatives in the spinor equation of motion. Thus, in the Dp/Dk-brane systems in which the dilaton field ϕ does not vanish, we should keep in mind that $\Gamma^M\partial_M\phi$ in the $\{dx^M\}$ basis will become $\Gamma^N e_{(N)}{}^M\partial_M\phi$ in the $\{e^{(M)}\}$ basis. From equation (7.8) and after a straightforward calculation, we find that

$$\Gamma^N e_{(N)}{}^M\partial_M\phi = -\frac{(7-p)(3-p)}{4}\frac{1}{R^{\frac{7-p}{4}}}\frac{1}{r^{\frac{p+1}{4}}}\left(\rho\,\Gamma^\rho + \sum_{m=1}^{9-p-k+d} w^m\,\Gamma_{\widetilde{m}}\right). \tag{7.54}$$

Subtracting now equation (7.54) from equation (7.32) we get

$$\begin{aligned}\not{D}_{Dk}\Psi^{\ell\pm} - \frac{\Gamma^N e_{(N)}{}^M\partial_M\phi}{2}\,\Psi^{\ell\pm} = \Bigg\{&\frac{R^{\frac{7-p}{4}}}{r^{\frac{7-p}{4}}}\,\Gamma^\mu\partial_\mu + \frac{r^{\frac{7-p}{4}}}{R^{\frac{7-p}{4}}}\,\Gamma^\rho\partial_\rho \pm \frac{1}{\rho}\frac{r^{\frac{7-p}{4}}}{R^{\frac{7-p}{4}}}\left(\ell+\frac{m}{2}\right)\\ &+\frac{1}{R^{\frac{7-p}{4}}}\left[\frac{7-p}{8}\frac{\rho}{r^{\frac{p+1}{4}}} + \frac{m}{2}\frac{r^{\frac{7-p}{4}}}{\rho}\right]\Gamma^\rho\Bigg\}\Psi^{\ell\pm}\,,\end{aligned} \tag{7.55}$$

where we have defined $m \equiv k-d-1$.

- Once we obtain the first-order equation of motion that the spinor satisfies we act with the differential operator

$$\frac{R^{\frac{7-p}{4}}}{r^{\frac{7-p}{4}}}\,\Gamma^\mu\partial_\mu + \frac{r^{\frac{7-p}{4}}}{R^{\frac{7-p}{4}}}\,\Gamma^\rho\partial_\rho\,, \tag{7.56}$$

on this first-order equation of motion. Then, by using some basic identities of the Clifford algebra and after some tedious algebra we derive a second-order ordinary differential equation of the

following schematic form

$$\left(\mathcal{A}_1\,\partial_\varrho^2+\mathcal{A}_2\,\partial_\varrho+\mathcal{A}_3\,\bar{M}^2+\mathcal{A}_4\,\Gamma^\varrho+\mathcal{A}_5\right)\psi(\varrho)=0\,, \tag{7.57}$$

where we have also used the dimensionless quantities

$$\varrho=\frac{\rho}{L}\,,\qquad\qquad \bar{M}^2=\frac{M^2R^{7-p}}{L^{5-p}}\,. \tag{7.58}$$

In the above, $L^2=\sum_{m=1}^{9-p-k+d}(w^m)^2$ constitutes the distance between the Dp- and the Dk-branes. $\mathcal{A}$'s are the coefficients of interest that we compute explicitly for each case we consider.

7.4.3 Fermions in the D1-background

The branes in the D1-background are arranged in the following way, see table 7.3. The fermionic action

	x^0	x^1	x^2	x^3	x^4	x^5	x^6	x^7	x^8	x^9
Background D1-brane	—	—	•	•	•	•	•	•	•	•
Probe D3-brane	—	•	—	—	—	•	•	•	•	•
Probe D5-brane	—	—	—	—	—	—	•	•	•	•

Table 7.3: The supersymmetric brane intersections. In the above notation — denotes that a brane extends along that particular direction, while • means that the coordinate is transverse to the brane.

is given by [5]

$$S_{Dk}=\frac{T_{Dk}}{2}\int d^{k+1}\xi\sqrt{-\hat{g}}\,\bar{\Psi}\,\mathcal{P}_-\left[\not{D}_{Dk}+\frac{e^\phi}{8\cdot 3!}F_{ABC}\left(\Gamma^{\hat{M}}\Gamma^{ABC}\Gamma_{\hat{M}}+2\,\Gamma^{ABC}\right)-\frac{1}{2}\Gamma^M\partial_M\phi\right]\Psi\,. \tag{7.59}$$

Varying equation (7.59) with respect to the conjugate spinor $\bar{\Psi}$, we readily obtain the equation of motion of the spinor Ψ, namely it is

$$\not{D}_{Dk}\Psi+\frac{e^\phi}{8\cdot 3!}F_{ABC}\left(\Gamma^{\hat{M}}\Gamma^{ABC}\Gamma_{\hat{M}}+2\,\Gamma^{ABC}\right)\Psi-\frac{1}{2}(\Gamma^M\partial_M\phi)\Psi=0\,, \tag{7.60}$$

where the dilaton field is determined from equation (7.8) with $p=1$, thus

$$e^\phi=\left(\frac{R}{r}\right)^3\,. \tag{7.61}$$

As it is depicted in table 7.3, there are two possibilities for the probe Dk-branes. We can either have $k=3$ or $k=5$, with $d=0$ and $d=1$, respectively. The R-R field strength field strength in the D1/Dk-brane setup is a 3-form and it is given by

$$F_{(3)}=dC_{(2)}=\frac{6r^{5/2}}{R^{9/2}}\,e^{(0)}\wedge e^{(1)}\wedge\left(\rho\,e^{(\rho)}+\sum_{i=1}^{8-k+d}w^i\,e^{(w^i)}\right)\,. \tag{7.62}$$

[5] We have written the action using single spinor notation rather than the two-component one. In order to do so we have manipulated appropriately some Pauli matrices as explained in Appendix of paper [165].

Having in our disposal the components of the R-R field strength as well as the expression of the dilaton field it is straightforward to calculate that

$$\frac{e^{\phi}}{8\cdot 3!}F_{ABC}\left(\Gamma^{\hat{M}}\Gamma^{ABC}\Gamma_{\hat{M}}+2\,\Gamma^{ABC}\right)\Psi=\frac{3}{2R^{3/2}}\frac{\rho}{\sqrt{r}}\,\Gamma^{01\rho}\Psi=-\frac{3}{2R^{3/2}}\frac{\rho}{\sqrt{r}}\,\Gamma_{01\rho}\Psi\,, \tag{7.63}$$

while by setting $p=1$ in equation (7.55) we get

$$\begin{aligned}\not{D}_{Dk}\Psi^{\ell\pm}-\frac{\Gamma^{M}\partial_{M}\phi}{2}\,\Psi^{\ell\pm}=&\left(\frac{R}{r}\right)^{\frac{3}{2}}\Gamma^{\mu}\partial_{\mu}\Psi^{\ell\pm}+\left(\frac{r}{R}\right)^{\frac{3}{2}}\Gamma^{\rho}\partial_{\rho}\Psi^{\ell\pm}\pm\frac{1}{\rho}\left(\frac{r}{R}\right)^{\frac{3}{2}}\left(\ell+\frac{m}{2}\right)\Psi^{\ell\pm}\\&+\frac{1}{R^{\frac{3}{2}}}\left(\frac{3}{4}\frac{\rho}{\sqrt{r}}+\frac{m}{2}\frac{r^{\frac{3}{2}}}{\rho}\right)\Gamma^{\rho}\Psi^{\ell\pm}\,,\end{aligned} \tag{7.64}$$

where $m=k-d-1$. Substituting equations (7.63) and (7.64) in equation (7.60) and imposing the projection $\Gamma_{01\rho}\Psi=-\Psi$, we are led to the following first-order equation of motion

$$\left\{\left(\frac{R}{r}\right)^{\frac{3}{2}}\Gamma^{\mu}\partial_{\mu}+\left(\frac{r}{R}\right)^{\frac{3}{2}}\Gamma^{\rho}\partial_{\rho}+\frac{1}{R^{\frac{3}{2}}}\left[\frac{3}{2}\frac{\rho}{\sqrt{r}}\pm\left(\ell+\frac{m}{2}\right)\frac{r^{\frac{3}{2}}}{\rho}+\left(\frac{3}{4}\frac{\rho}{\sqrt{r}}+\frac{m}{2}\frac{r^{\frac{3}{2}}}{\rho}\right)\Gamma^{\rho}\right]\right\}\Psi^{\ell\pm}=0\,. \tag{7.65}$$

In what follows we consider that $\sum_i (w^i)^2=L^2$, which by its turn leads to $r^2=\rho^2+L^2$. In both cases, L constitutes the distance between the D1- and the Dk-branes. Applying the procedure which was described in section 7.4.2 to equation (7.65), we construct the following second-order differential equation

$$\left(\mathcal{A}_1^{\pm}\partial_{\varrho}^2+\mathcal{A}_2^{\pm}\partial_{\varrho}+\mathcal{A}_3^{\pm}\bar{M}^2+\mathcal{A}_4^{\pm}\Gamma^{\varrho}+\mathcal{A}_5^{\pm}\right)\psi^{\ell\pm}(\varrho)=0\,, \tag{7.66}$$

where

$$\begin{aligned}&\mathcal{A}_1^{\pm}=1,\quad \mathcal{A}_2^{\pm}=\frac{m}{\varrho}+\frac{9}{2}\frac{\varrho}{\varrho^2+1},\quad \mathcal{A}_3^{\pm}=\frac{1}{(\varrho^2+1)^3}\,,\\&\mathcal{A}_4^{\pm}=\frac{3}{2}\frac{1\pm 2\ell\pm m}{\varrho^2+1}\mp\frac{1}{\varrho^2}\left(\ell+\frac{m}{2}\right)+\frac{3}{2}\frac{\varrho^2}{(\varrho^2+1)^2}\,,\\&\mathcal{A}_5^{\pm}=\frac{3}{4}\frac{1}{\varrho^2+1}\left(3m\mp 2m+1\mp 4\ell\right)-\frac{15}{16}\frac{\varrho^2}{(\varrho^2+1)^2}-\frac{1}{\varrho^2}\left(\ell^2+m\ell+\frac{m}{2}\right).\end{aligned} \tag{7.67}$$

Employing the projection $\Gamma^{\varrho}\psi^{\ell\pm}=\psi^{\ell\pm}$ and adopting the same notation as in section 7.4.1 we are led to

$$\begin{aligned}\Bigg[\partial_{\varrho}^2+\left(\frac{m}{\varrho}+\frac{9}{2}\frac{\varrho}{\varrho^2+1}\right)\partial_{\varrho}+\frac{\bar{M}^2}{(\varrho^2+1)^3}-\frac{1}{\varrho^2}\left(\ell^2+(m+1)\ell+m\right)\\+\frac{9}{4}\frac{1+m}{\varrho^2+1}+\frac{9}{16}\frac{\varrho^2}{(\varrho^2+1)^2}\Bigg]\psi^{\oplus}_{\mathcal{G}_\ell}(\varrho)=0\,,\end{aligned} \tag{7.68}$$

$$\begin{aligned}\Bigg[\partial_{\varrho}^2+\left(\frac{m}{\varrho}+\frac{9}{2}\frac{\varrho}{\varrho^2+1}\right)\partial_{\varrho}+\frac{\bar{M}^2}{(\varrho^2+1)^3}-\frac{1}{\varrho^2}\left(\ell^2+(m-1)\ell\right)\\+\frac{9}{4}\frac{1+m}{\varrho^2+1}+\frac{9}{16}\frac{\varrho^2}{(\varrho^2+1)^2}\Bigg]\psi^{\oplus}_{\mathcal{F}_\ell}(\varrho)=0\,,\end{aligned} \tag{7.69}$$

for positive and negative spinorial harmonics, respectively. As we already mentioned, $m = k - d - 1$, which by its turn implies that for $k = 5$ we have $m = 3$, while for $k = 3$ we have $m = 2$. The corresponding bosonic equations of motion for the D1/D5 and D1/D3-brane systems can be determined from equation (C.9) and equation (C.10), respectively. Hence, setting $p = 1$ in the aforementioned relations, we get

$$\partial_\varrho^2 f_\ell(\varrho) + \frac{3}{\varrho}\partial_\varrho f_\ell(\varrho) + \left(\frac{\bar{M}^2}{(1+\varrho^2)^3} - \frac{\ell(\ell+2)}{\varrho^2}\right) f_\ell(\varrho) = 0\,, \tag{7.70}$$

$$\partial_\varrho^2 f_\ell(\varrho) + \frac{2}{\varrho}\partial_\varrho f_\ell(\varrho) + \left(\frac{\bar{M}^2}{(1+\varrho^2)^{(7-p)/2}} - \frac{\ell(\ell+1)}{\varrho^2}\right) f_\ell(\varrho) = 0\,, \tag{7.71}$$

respectively. One can easily verify that the transformation

$$\psi^{\oplus}_{\mathcal{G}_\ell}(\varrho) = \frac{1}{(1+\varrho^2)^{9/8}}\, f_{\ell+1}(\varrho)\,, \tag{7.72}$$

maps equation (7.68) either to equation (7.70), when we have the D1/D5 setup, or to equation (7.71), when we have the D1/D3 setup. In exactly the same sense, the transformation

$$\psi^{\oplus}_{\mathcal{F}_\ell}(\varrho) = \frac{1}{(1+\varrho^2)^{9/8}}\, f_\ell(\varrho)\,, \tag{7.73}$$

maps equation (7.69) either to equation (7.70) (D1/D5 setup), or to equation (7.71) (D1/D3 setup). The differential equations which result from equation (7.66) with the projection $\Gamma^\varrho \psi^{\ell\pm} = -\psi^{\ell\pm}$, namely the differential equations for the $\psi^{\ominus}$ spinor, cannot be mapped to the corresponding bosonic equations of motion, although they provide us with the same mass eigenvalues $\bar{M}$. The reason behind this is the degeneracy which results from the projection matrix Γ^ρ. Notice as well that the above transformations can be obtained from equation (7.1) by setting $p = 1$.

The above equations of motion cannot be solved analytically (as in the case of bosonic mesons) and we have to resort to numerical analysis. We show explicitly the first few numerical values of the masses in table 7.4. The numerical values for n and ℓ describe the $\mathcal{F}$ operators and one needs to shift appropriately the ℓ to read off the value of the $\mathcal{G}$ states.

		n			
		0	1	2	3
ℓ	0	14.830	49.711	104.53	179.30
	1	42.793	92.952	162.67	252.03
	2	84.366	150.11	235.27	339.96
	3	139.43	220.76	319.85	441.55

		n			
		0	1	2	3
ℓ	0	6.2638	34.138	82.315	150.64
	1	27.082	69.506	131.62	213.50
	2	61.893	119.84	197.26	294.26
	3	110.21	183.75	276 .58	387.88

Table 7.4: Numerical results of the parameter $\bar{M}^2$ for the D1/Dk brane intersections. The left table pertains to the D1/D5 and the right one depicts results for the D1/D3 brane intersection.

7.4.4 Open-string fluctuations in the D2-background

The D2-background has been extensively studied in the past in the probe-limit [160] as well as beyond the quenched approximation [174]. The relevant orientation of the branes in order for the boundary

theory to preserve eight supercharges is shown in table 7.5. The fermionic action is given by [163–165]

	x^0	x^1	x^2	x^3	x^4	x^5	x^6	x^7	x^8	x^9
Background D2-brane	—	—	—	•	•	•	•	•	•	•
Probe D2-brane	—	•	•	—	—	•	•	•	•	•
Probe D4-brane	—	—	•	—	—	—	•	•	•	•
Probe D6-brane	—	—	—	—	—	—	—	•	•	•

Table 7.5: The BPS brane intersections. In the above notation — denotes that a brane extends along that particular direction, while • means that the coordinate is transverse to the brane.

$$S_{Dk} = \frac{T_{Dk}}{2}\int d^{k+1}\xi\sqrt{-\hat{g}}\,\bar{\Psi}\,\mathcal{P}_-\left[\not{D}_{Dk} + \frac{e^{\phi}}{8\cdot 4!}F_{ABCD}\left(\Gamma^{ABCD} - \Gamma^{\hat{M}}\Gamma^{ABCD}\Gamma_{\hat{M}}\right) - \frac{1}{2}\Gamma^M\partial_M\phi\right]\Psi\,. \tag{7.74}$$

Varying equation (7.74) with respect to the conjugate spinor $\bar{\Psi}$, we readily obtain the equation of motion of the spinor Ψ, namely it is

$$\not{D}_{Dk}\Psi + \frac{e^{\phi}}{8\cdot 4!}F_{ABCD}\left(\Gamma^{ABCD} - \Gamma^{\hat{M}}\Gamma^{ABCD}\Gamma_{\hat{M}}\right)\Psi - \frac{1}{2}(\Gamma^M\partial_M\phi)\Psi = 0\,, \tag{7.75}$$

where the dilaton field and the R-R field strength, which in this case constitutes a 4-form, can be determined from equation (7.8) with $p=2$, thus we have

$$e^{\phi} = \left(\frac{R}{r}\right)^{\frac{5}{4}}\,, \tag{7.76}$$

$$F_{(4)} = dC_{(3)} = -\frac{5\sqrt{r}}{R^{5/2}}\,e^{(0)}\wedge e^{(1)}\wedge e^{(2)}\wedge\left(\rho\,e^{(\rho)} + \sum_{i=1}^{7-k+d} w^i\,e^{(w^i)}\right)\,, \tag{7.77}$$

respectively. As it is depicted in table 7.5, there are three possibilities for the probe Dk-branes, $k=\{2,4,6\}$ with $d=\{0,1,2\}$ respectively. Having in our disposal the components of the R-R field strength as well as the expression of the dilaton field it is straightforward to calculate that

$$\frac{e^{\phi}}{8\cdot 4!}F_{ABCD}\left(\Gamma^{ABCD} - \Gamma^{\hat{M}}\Gamma^{ABCD}\Gamma_{\hat{M}}\right)\Psi = \frac{5}{4}\frac{\rho}{R^{5/4}\,r^{3/4}}\Gamma_{012\rho}\Psi\,, \tag{7.78}$$

while by setting $p=2$ in equation (7.55) we get

$$\begin{aligned}\not{D}_{Dk}\Psi^{\ell^{\pm}} - \frac{\Gamma^M\partial_M\phi}{2}\,\Psi^{\ell^{\pm}} &= \left(\frac{R}{r}\right)^{\frac{5}{4}}\Gamma^{\mu}\partial_{\mu}\Psi^{\ell^{\pm}} + \left(\frac{r}{R}\right)^{\frac{5}{4}}\Gamma^{\rho}\partial_{\rho}\Psi^{\ell^{\pm}} \pm \frac{1}{\rho}\left(\frac{r}{R}\right)^{\frac{5}{4}}\left(\ell + \frac{m}{2}\right)\Psi^{\ell^{\pm}} \\ &\quad + \frac{1}{R^{\frac{5}{4}}}\left(\frac{5}{8}\frac{\rho}{r^{\frac{3}{4}}} + \frac{m}{2}\frac{r^{\frac{5}{4}}}{\rho}\right)\Gamma^{\rho}\Psi^{\ell^{\pm}}\,.\end{aligned} \tag{7.79}$$

Substituting equations (7.78) and (7.79) in equation (7.75) and imposing the projection $\Gamma_{012\rho}\Psi = \Psi$, we are led to the following first-order equation of motion

$$\left\{\left(\frac{R}{r}\right)^{\frac{5}{4}}\Gamma^{\mu}\partial_{\mu} + \left(\frac{r}{R}\right)^{\frac{5}{4}}\Gamma^{\rho}\partial_{\rho} + \frac{1}{R^{\frac{5}{4}}}\left[\frac{5}{4}\frac{\rho}{r^{\frac{3}{4}}} \pm \left(\ell + \frac{m}{2}\right)\frac{r^{\frac{5}{4}}}{\rho}\right] + \frac{1}{R^{\frac{5}{4}}}\left(\frac{5}{8}\frac{\rho}{r^{\frac{3}{4}}} + \frac{m}{2}\frac{r^{\frac{5}{4}}}{\rho}\right)\Gamma^{\rho}\right\}\Psi^{\ell^{\pm}} = 0\,. \tag{7.80}$$

Applying the procedure which was described in section 7.4.2 to equation (7.80), we construct the following second-order differential equation

$$\left(\mathcal{A}_1^{\pm}\partial_{\varrho}^2 + \mathcal{A}_2^{\pm}\partial_{\varrho} + \mathcal{A}_3^{\pm}\bar{M}^2 + \mathcal{A}_4^{\pm}\Gamma^{\varrho} + \mathcal{A}_5^{\pm}\right)\psi^{\ell^{\pm}}(\varrho) = 0\,, \tag{7.81}$$

where

$$\begin{aligned}
&\mathcal{A}_1^{\pm} = 1, \quad \mathcal{A}_2^{\pm} = \frac{m}{\varrho} + \frac{15}{4}\frac{\varrho}{\varrho^2+1}, \quad \mathcal{A}_3^{\pm} = \frac{1}{(\varrho^2+1)^{5/2}}\,,\\
&\mathcal{A}_4^{\pm} = \frac{5}{4}\frac{1 \pm 2\ell \pm m}{\varrho^2+1} \mp \frac{1}{\varrho^2}\left(\ell + \frac{m}{2}\right) + \frac{5}{8}\frac{\varrho^2}{(\varrho^2+1)^2}\,,\\
&\mathcal{A}_5^{\pm} = \frac{5}{8}\frac{1}{\varrho^2+1}\left(3m \mp 2m + 1 \mp 4\ell\right) - \frac{55}{64}\frac{\varrho^2}{(\varrho^2+1)^2} - \frac{1}{\varrho^2}\left(\ell^2 + m\ell + \frac{m}{2}\right)\,.
\end{aligned} \tag{7.82}$$

Employing the projection $\Gamma^{\rho}\,\psi^{\ell^{\pm}} = \psi^{\ell^{\pm}}$ and using equations (7.81) and (7.82) one can readily obtain the fermionic second-order ordinary differential equation for $\psi^{\ell^{\pm}}(\varrho)$. In case of positive spinorial harmonics (ℓ^+), we get the differential equation of $\psi^{\oplus}_{\mathcal{G}_\ell}(\varrho)$, while for negative spinorial harmonics (ℓ^-), the differential equation of $\psi^{\oplus}_{\mathcal{F}_\ell}(\varrho)$ is obtained. The corresponding bosonic equations of motion for the D2/Dk-brane setups ($k = \{2,4,6\}$), can be determined from equations (C.9) and (C.11) by setting $p = 2$. For all possible D2/Dk-brane systems the transformation

$$\psi^{\oplus}_{\mathcal{G}_\ell}(\varrho) = \frac{1}{(1+\varrho^2)^{15/16}}\,f_{\ell+1}(\varrho)\,, \tag{7.83}$$

maps the fermionic function $\psi^{\oplus}_{\mathcal{G}_\ell}(\varrho)$ to the bosonic function $f_{\ell+1}(\varrho)$, while the transformation

$$\psi^{\oplus}_{\mathcal{F}_\ell}(\varrho) = \frac{1}{(1+\varrho^2)^{15/16}}\,f_{\ell}(\varrho)\,, \tag{7.84}$$

maps the fermionic function $\psi^{\oplus}_{\mathcal{F}_\ell}(\varrho)$ to the bosonic function $f_{\ell}(\varrho)$. Notice as well that the above transformations can be obtained from equation (7.1) by setting $p = 2$.

The above equations of motion cannot be solved analytically (as in the case of bosonic mesons). We show explicitly the first few numerical values of the masses in table 7.6. The numerical values for n and ℓ describe the $\mathcal{F}$ operators and one needs to shift appropriately the ℓ to read off the value of the $\mathcal{G}$ states. It is important to stress at this point that, in cases where the dimensionality of the background and the probe brane is the same, the quantum number ℓ—contrary to the rest of the cases—should be greater than zero as dictated by the normalizability of the mode solution in the UV; observe for example the bottom table in table 7.6.

		n			
		0	1	2	3
ℓ	0	11.509	37.185	76.982	130.93
	1	33.403	70.419	121.15	185.66
	2	66.197	114.96	177.34	253.38
	3	109.75	170.30	244.10	332.17

		n			
		0	1	2	3
ℓ	0	4.9024	25.519	60.595	110.03
	1	21.065	52.295	97.385	156.40
	2	48.453	91.334	147.86	218.09
	3	86.630	141.29	209.54	291.40

		n			
		0	1	2	3
ℓ	1	11.509	37.185	76.982	130.93
	2	33.403	70.149	121.15	185.66
	3	66.197	114.96	177.34	253.38

Table 7.6: Numerical results of the parameter $\bar{M}^2$ for the D2/Dk brane intersections. The top left table pertains to the D2/D6 and the top right one depicts results for the D2/D4 brane intersection. The bottom table is related to the D2/D2 setup.

7.4.5 Probing the D3-background

Before we start the analysis of the fermionic modes for the background generated by a stack of N_c branes we would like to illustrate the brane intersections that we examine in this work. This is shown in table 7.7. The fermionic action in the D3-brane background is [163–165]

	x^0	x^1	x^2	x^3	x^4	x^5	x^6	x^7	x^8	x^9
Background D3-brane	—	—	—	—	•	•	•	•	•	•
Probe D3-brane	—	—	•	•	—	—	•	•	•	•
Probe D5-brane	—	—	—	•	—	—	—	•	•	•
Probe D7-brane	—	—	—	—	—	—	—	—	•	•

Table 7.7: The brane intersections that preserve eight supercharges. In the above notation — denotes that a brane extends along that particular direction, while • means that the coordinate is transverse to the brane.

$$S_{Dk} = \frac{T_{Dk}}{2} \int d^{k+1}\xi \sqrt{-\hat{g}}\, \bar{\Psi}\, \mathcal{P}_- \left(\not{D}_{Dk} + \frac{i}{2 \cdot 8 \cdot 5!} \Gamma^{\hat{M}} F_{ABCDE}\, \Gamma^{ABCDE}\, \Gamma_{\hat{M}} \right) \Psi. \tag{7.85}$$

Varying equation (7.85) with respect to the conjugate spinor $\bar{\Psi}$, we readily obtain the equation of motion of the spinor Ψ, namely it is

$$\not{D}_{Dk}\Psi + \frac{i}{2 \cdot 8 \cdot 5!} \Gamma^{\hat{M}} F_{ABCDE}\, \Gamma^{ABCDE}\, \Gamma_{\hat{M}} \Psi = 0\,. \tag{7.86}$$

In this particular scenario the dilaton field vanishes, while the R-R field strength is a self-dual 5-form, which is determined with the use of equation (7.8) for $p = 3$, namely we have [6]

$$F_{(5)} = dC_{(4)} + \star(dC_{(4)})\,. \tag{7.87}$$

[6] For more details about the Hodge star operator $\star$ see appendix C.

As it is depicted in table 7.7, there are three possibilities for the probe Dk-branes, $k = \{3, 5, 7\}$ with $d = \{1, 2, 3\}$ respectively. In case of the D3/D3-brane setup, the above relation leads to

$$F_{(5)} = \frac{4}{rR}\Bigg[e^{(0)} \wedge e^{(1)} \wedge e^{(2)} \wedge e^{(3)} \wedge \left(\rho\, e^{(\rho)} + \sum_{m=1}^{4} w^m\, e^{(w^m)}\right) - \rho\, e^{(\theta)} \wedge e^{(w^1)} \wedge e^{(w^2)} \wedge e^{(w^3)} \wedge e^{(w^4)}$$
$$- e^{(\rho)} \wedge e^{(\theta)} \wedge \Big(w^1\, e^{(w^2)} \wedge e^{(w^3)} \wedge e^{(w^4)} - w^2\, e^{(w^1)} \wedge e^{(w^3)} \wedge e^{(w^4)} + w^3\, e^{(w^1)} \wedge e^{(w^2)} \wedge e^{(w^4)}$$
$$- w^4\, e^{(w^1)} \wedge e^{(w^2)} \wedge e^{(w^3)}\Big)\Bigg]\,. \tag{7.88}$$

In case of the D3/D5-brane setup, it is

$$F_{(5)} = \frac{4}{rR}\Bigg[e^{(0)} \wedge e^{(1)} \wedge e^{(2)} \wedge e^{(3)} \wedge \left(\rho\, e^{(\rho)} + \sum_{m=1}^{3} w^m\, e^{(w^m)}\right) - \rho\, e^{(S^2)} \wedge e^{(w^1)} \wedge e^{(w^2)} \wedge e^{(w^3)}$$
$$+ e^{(\rho)} \wedge e^{(S^2)} \wedge \Big(w^1\, e^{(w^2)} \wedge e^{(w^3)} - w^2\, e^{(w^1)} \wedge e^{(w^3)} + w^3\, e^{(w^1)} \wedge e^{(w^2)}\Big)\Bigg]\,, \tag{7.89}$$

where $e^{(S^2)} = e^{(\theta_1)} \wedge e^{(\theta_2)}$. Finally, in case of the D3/D7-brane setup, we have

$$F_{(5)} = \frac{4}{rR}\Bigg[e^{(0)} \wedge e^{(1)} \wedge e^{(2)} \wedge e^{(3)} \wedge \left(\rho\, e^{(\rho)} + \sum_{m=1}^{2} w^m\, e^{(w^m)}\right) - \rho\, e^{(S^3)} \wedge e^{(w^1)} \wedge e^{(w^2)}$$
$$- e^{(\rho)} \wedge e^{(S^3)} \wedge \Big(w^1\, e^{(w^2)} - w^2\, e^{(w^1)}\Big)\Bigg]\,, \tag{7.90}$$

where $e^{(S^3)} = e^{(\theta_1)} \wedge e^{(\theta_2)} \wedge e^{(\theta_3)}$. Having in our disposal the components of the R-R field strength as well as the expression of the dilaton field it is straightforward to calculate that regardless the D3/Dk-brane system it is

$$\frac{i}{2 \cdot 8 \cdot 5!}\Gamma^{\hat{M}} F_{ABCDE}\, \Gamma^{ABCDE}\, \Gamma_{\hat{M}}\Psi = i\, \frac{\rho}{rR}\Gamma_{0123\rho}\Psi\,, \tag{7.91}$$

while by setting $p = 3$ in equation (7.55) we get

$$\not{D}_{Dk}\Psi^{\ell\pm} - \frac{\Gamma^M \partial_M \phi}{2}\,\Psi^{\ell\pm} = \left\{\frac{R}{r}\,\Gamma^\mu \partial_\mu + \frac{r}{R}\,\Gamma^\rho \partial_\rho \pm \frac{1}{\rho}\frac{r}{R}\left(\ell + \frac{m}{2}\right) + \frac{1}{R}\left(\frac{1}{2}\frac{\rho}{r} + \frac{m}{2}\frac{r}{\rho}\right)\Gamma^\rho\right\}\Psi^{\ell\pm}\,. \tag{7.92}$$

Substituting equations (7.91) and (7.92) in equation (7.86) and imposing the projection $\Gamma_{0123\rho}\Psi = -i\Psi$, we are led to the following first-order equation of motion

$$\left\{\frac{R}{r}\Gamma^\mu \partial_\mu + \frac{r}{R}\Gamma^\rho \partial_\rho + \frac{1}{R}\left[\frac{\rho}{r} \pm \left(\ell + \frac{m}{2}\right)\frac{r}{\rho}\right] + \frac{1}{2R}\left(\frac{\rho}{r} + m\,\frac{r}{\rho}\right)\Gamma^\rho\right\}\Psi^{\ell\pm} = 0\,. \tag{7.93}$$

Applying the procedure which was described in section 7.4.2 to equation (7.93), we construct the following second-order differential equation

$$\left(\mathcal{A}_1^{\pm}\partial_\varrho^2 + \mathcal{A}_2^{\pm}\partial_\varrho + \mathcal{A}_3^{\pm}\bar{M}^2 + \mathcal{A}_4^{\pm}\Gamma^\varrho + \mathcal{A}_5^{\pm}\right)\psi^{\ell\pm}(\varrho) = 0\,, \tag{7.94}$$

where

$$\begin{aligned}
&\mathcal{A}_1^{\pm} = 1, \quad \mathcal{A}_2^{\pm} = \frac{m}{\varrho} + \frac{3\varrho}{\varrho^2+1}, \quad \mathcal{A}_3^{\pm} = \frac{1}{(\varrho^2+1)^2}\,, \\
&\mathcal{A}_4^{\pm} = \frac{1 \pm 2\ell \pm m}{\varrho^2+1} \mp \frac{1}{\varrho^2}\left(\ell + \frac{m}{2}\right)\,, \\
&\mathcal{A}_5^{\pm} = \frac{1}{\varrho^2+1}\left(\frac{3m+1\mp 2m}{2} \mp 2\ell\right) - \frac{3}{4}\frac{\varrho^2}{(\varrho^2+1)^2} - \frac{1}{\varrho^2}\left(\ell^2 + m\ell + \frac{m}{2}\right)\,.
\end{aligned} \tag{7.95}$$

Employing the projection $\Gamma^{\rho}\,\psi^{\ell^{\pm}} = \psi^{\ell^{\pm}}$ and using equations (7.94) and (7.95) one can readily obtain the fermionic second-order ordinary differential equation for $\psi^{\ell^{\pm}}(\varrho)$. In case of positive spinorial harmonics (ℓ^{+}), we get the differential equation of $\psi^{\oplus}_{\mathcal{G}_\ell}(\varrho)$, while for negative spinorial harmonics (ℓ^{-}), the differential equation of $\psi^{\oplus}_{\mathcal{F}_\ell}(\varrho)$ is obtained. The corresponding bosonic equations of motion for the D3/Dk-brane setups ($k = \{3, 5, 7\}$), can be determined from equations (C.9) and (C.11) by setting $p = 3$. For all possible D3/Dk-brane systems the transformation

$$\psi^{\oplus}_{\mathcal{G}_\ell}(\varrho) = \frac{1}{(1+\varrho^2)^{3/4}}\, f_{\ell+1}(\varrho)\,, \tag{7.96}$$

maps the fermionic function $\psi^{\oplus}_{\mathcal{G}_\ell}(\varrho)$ to the bosonic function $f_{\ell+1}(\varrho)$, while the transformation

$$\psi^{\oplus}_{\mathcal{F}_\ell}(\varrho) = \frac{1}{(1+\varrho^2)^{3/4}}\, f_{\ell}(\varrho)\,, \tag{7.97}$$

maps the fermionic function $\psi^{\oplus}_{\mathcal{F}_\ell}(\varrho)$ to the bosonic function $f_{\ell}(\varrho)$. Notice as well that the above transformations can be obtained from equation (7.1) by setting $p = 3$.

Analytic solutions

The equation of motion which result from equation (7.95) admit analytic solutions. Although they have been previously derived in [1, 82] for massless and massive flavours respectively, we present them here as well for completeness. The solution of the differential equation related to the positive spinor spherical harmonics is of the following form

$$\begin{aligned}
\psi_{\mathcal{G}} = &\frac{\varrho^{\ell+1}}{(1+\varrho^2)^{\left(n+\ell+\frac{m}{2}+\frac{5}{4}\right)}}\; {}_2F_1\left(-n, -n-\ell-\frac{1}{2}(m+1); \ell+\frac{m+3}{2}; -\varrho^2\right)\chi_{+} \\
&+ \frac{\varrho^{\ell}}{(1+\varrho^2)^{\left(n+\ell+\frac{m}{2}+\frac{5}{4}\right)}}\; {}_2F_1\left(-n, -n-\ell-\frac{1}{2}(m+3); \ell+\frac{m+1}{2}; -\varrho^2\right)\chi_{-}\,.
\end{aligned} \tag{7.98}$$

In the above, the number n is directly related to the mass spectrum via the relation

$$\bar{M}^2_{\mathcal{G}} = 4\left(n + \ell + \frac{m+1}{2}\right)\left(n + \ell + \frac{m+3}{2}\right)\,, \tag{7.99}$$

where $n,\ \ell \geq 0$. The spinors $\chi_{\pm}$ are eigenstates of the Γ^{ϱ}-matrix and they obey the relation $\Gamma^{\varrho}\chi_{\pm} = \pm\chi_{\pm}$. They are related to one another via

$$\chi_{-} = \frac{i\not{k}}{M}\chi_{+}\,, \tag{7.100}$$

where k is the wave-vector from the plane-wave ansatz in the decomposition of the ten-dimensional spinor. The asymptotic behaviour of the above solution in the UV ($\varrho \to \infty$) and the IR ($\varrho \to 0$) are given below

$$\begin{aligned} \psi_{\mathcal{G}}|_{\varrho\to\infty} &\sim \varrho^{-\ell-m-3/2}\chi_+ + \varrho^{-\ell-m-5/2}\chi_- \,, \\ \psi_{\mathcal{G}}|_{\varrho\to 0} &\sim \varrho^{\ell+1}\,\chi_+ + \varrho^{\ell}\,\chi_- \,. \end{aligned} \tag{7.101}$$

We can perform the same analysis and derive the solutions describing the $\mathcal{F}$, the ones obtained by considering the negative eigenvalues on the internal manifold. They are

$$\begin{aligned} \psi_{\mathcal{F}} = &\frac{\varrho^{\ell}}{(1+\varrho^2)^{\left(n+\ell+\frac{m}{2}+\frac{1}{4}\right)}}\;{}_2F_1\left(-n,-n-\ell-\frac{1}{2}(m-1);\ell+\frac{m+1}{2};-\varrho^2\right)\chi_+ \\ &+\frac{\varrho^{\ell+1}}{(1+\varrho^2)^{\left(n+\ell+\frac{m}{2}+\frac{1}{4}\right)}}\;{}_2F_1\left(-n,-n-\ell-\frac{1}{2}(m+1);\ell+\frac{m+3}{2};-\varrho^2\right)\chi_- \,, \end{aligned} \tag{7.102}$$

leading to the discrete mass spectrum

$$\bar{M}^2_{\mathcal{F}} = 4\left(n+\ell+\frac{m-1}{2}\right)\left(n+\ell+\frac{m+1}{2}\right)\,, \tag{7.103}$$

$n,\,\ell \geq 0$. The asymptotic behaviour of the above solution in the UV ($\varrho \to \infty$) and the IR ($\varrho \to 0$) are given below

$$\begin{aligned} \psi_{\mathcal{F}}|_{\varrho\to\infty} &\sim \varrho^{-\ell-m-1/2}\,\chi_+ + \varrho^{-\ell-m+1/2}\,\chi_- \,, \\ \psi_{\mathcal{F}}|_{\varrho\to 0} &\sim \varrho^{\ell}\,\chi_+ + \varrho^{\ell+1}\,\chi_- \,. \end{aligned} \tag{7.104}$$

7.4.6 The D4 background and five dimensional SYM theories

For illustrative purposes we show explicitly the relevant brane intersections in the case of the D4 background, see table 7.8. The fermionic action is given by [163–165]

	x^0	x^1	x^2	x^3	x^4	x^5	x^6	x^7	x^8	x^9
Background D4-brane	—	—	—	—	—	•	•	•	•	•
Probe D4-brane	—	—	—	•	•	—	—	•	•	•
Probe D6-brane	—	—	—	—	•	—	—	—	•	•
Probe D8-brane	—	—	—	—	—	—	—	—	—	•

Table 7.8: The brane intersections that preserve $\mathcal{N}=2$ SUSY in a four-dimensional language. In the above notation — denotes that a brane extends along that particular direction, while • means that the coordinate is transverse to the brane.

$$S_{Dk} = \frac{T_{Dk}}{2}\int d^{k+1}\xi\sqrt{-\hat{g}}\,\bar{\Psi}\,\mathcal{P}_-\left[\not{D}_{Dk} + \frac{e^{\phi}}{8\cdot 4!}F_{ABCD}\left(\Gamma^{ABCD} - \Gamma^{\hat{M}}\Gamma^{ABCD}\Gamma_{\hat{M}}\right) - \frac{1}{2}\Gamma^M\partial_M\phi\right]\Psi\,. \tag{7.105}$$

Varying equation (7.105) with respect to the conjugate spinor $\bar{\Psi}$, we readily obtain the equation of motion of the spinor Ψ, namely it is

$$\not{D}_{Dk}\Psi + \frac{e^{\phi}}{8\cdot 4!}F_{ABCD}\left(\Gamma^{ABCD} - \Gamma^{\hat{M}}\Gamma^{ABCD}\Gamma_{\hat{M}}\right)\Psi - \frac{1}{2}(\Gamma^{M}\partial_{M}\phi)\Psi = 0\,, \tag{7.106}$$

where the dilaton field and the R-R field strength, which in this case constitutes a 4-form, can be determined from equation (7.8) with $p = 4$, thus we have

$$e^{\phi} = \left(\frac{r}{R}\right)^{\frac{3}{4}}\,, \qquad\qquad F_{(4)} = \star(dC_{(5)})\,, \tag{7.107}$$

respectively. As it is depicted in table 7.8, there are three possibilities for the probe Dk-branes, $k = \{4, 6, 8\}$ with $d = \{2, 4, 6\}$ respectively. In case of the D4/D4-brane setup, the above relation leads to

$$\begin{aligned} F_{(4)} = \frac{3}{r^2}\Big[\rho\, e^{(\theta)}\wedge e^{(w^1)}\wedge e^{(w^2)}\wedge e^{(w^3)} + e^{(\rho)}\wedge e^{(\theta)}\wedge\Big(w^1\, e^{(w^2)}\wedge e^{(w^3)} \\ - w^2\, e^{(w^1)}\wedge e^{(w^3)} + w^3\, e^{(w^1)}\wedge e^{(w^2)}\Big)\Big]\,. \end{aligned} \tag{7.108}$$

In case of the D4/D6-brane setup, it is

$$F_{(4)} = \frac{3}{r^2}\left[\rho\, e^{(S^2)}\wedge e^{(w^1)}\wedge e^{(w^2)} - e^{(\rho)}\wedge e^{(S^2)}\wedge\left(w^1\, e^{(w^2)} - w^2\, e^{(w^1)}\right)\right]\,, \tag{7.109}$$

where $e^{(S^2)} = e^{(\theta_1)}\wedge e^{(\theta_2)}$. Finally, in case of the D4/D8-brane setup, we have

$$F_{(4)} = \frac{3}{r^2}\left(\rho\, e^{(S^3)}\wedge e^{(w^1)} + w^1\, e^{(\rho)}\wedge e^{(S^3)}\right)\,, \tag{7.110}$$

where $e^{(S^3)} = e^{(\theta_1)}\wedge e^{(\theta_2)}\wedge e^{(\theta_3)}$. Having in our disposal the components of the R-R field strength as well as the expression of the dilaton field it is straightforward to calculate that for the D4/Dk-brane system it is

$$\frac{e^{\phi}}{8\cdot 4!}F_{ABCD}\left(\Gamma^{ABCD} - \Gamma^{\hat{M}}\Gamma^{ABCD}\Gamma_{\hat{M}}\right)\Psi = -\frac{3}{4}\frac{\rho}{R^{3/4}\, r^{5/4}}\Gamma_{S^{k-d-1}w^1\ldots w^{5-k+d}}\Psi\,, \tag{7.111}$$

while by setting $p = 4$ in equation (7.55) we get

$$\begin{aligned} \not{D}_{Dk}\Psi^{\ell\pm} - \frac{\Gamma^{M}\partial_{M}\phi}{2}\,\Psi^{\ell\pm} = \left(\frac{R}{r}\right)^{\frac{3}{4}}\Gamma^{\mu}\partial_{\mu}\Psi^{\ell\pm} + \left(\frac{r}{R}\right)^{\frac{3}{4}}\Gamma^{\rho}\partial_{\rho}\Psi^{\ell\pm} \pm \frac{1}{\rho}\left(\frac{r}{R}\right)^{\frac{3}{4}}\left(\ell + \frac{m}{2}\right)\Psi^{\ell\pm} \\ + \frac{1}{R^{\frac{3}{4}}}\left(\frac{3}{8}\frac{\rho}{r^{\frac{5}{4}}} + \frac{m}{2}\frac{r^{\frac{3}{4}}}{\rho}\right)\Gamma^{\rho}\Psi^{\ell\pm}\,. \end{aligned} \tag{7.112}$$

Substituting equations (7.111) and (7.112) in equation (7.106) and imposing the projection $\Gamma_{S^{k-d-1}w^1\ldots w^{5-k+d}}\Psi = -\Psi$, we are led to the following first-order equation of motion

$$\left\{\left(\frac{R}{r}\right)^{\frac{3}{4}}\Gamma^\mu\partial_\mu + \left(\frac{r}{R}\right)^{\frac{3}{4}}\Gamma^\rho\partial_\rho + \frac{1}{R^{\frac{3}{4}}}\left[\frac{3}{4}\frac{\rho}{r^{\frac{5}{4}}} \pm \left(\ell+\frac{m}{2}\right)\frac{r^{\frac{3}{4}}}{\rho}\right] + \frac{1}{R^{\frac{3}{4}}}\left(\frac{3}{8}\frac{\rho}{r^{\frac{5}{4}}} + \frac{m}{2}\frac{r^{\frac{3}{4}}}{\rho}\right)\Gamma^\rho\right\}\Psi^{\ell\pm} = 0\,. \tag{7.113}$$

Applying the procedure which was described in section 7.4.2 to equation (7.113), we construct the following second-order differential equation

$$\left(\mathcal{A}_1^\pm\partial_\varrho^2 + \mathcal{A}_2^\pm\partial_\varrho + \mathcal{A}_3^\pm\bar{M}^2 + \mathcal{A}_4^\pm\Gamma^\varrho + \mathcal{A}_5^\pm\right)\psi^{\ell\pm}(\varrho) = 0\,, \tag{7.114}$$

where

$$\begin{aligned}
&\mathcal{A}_1^\pm = 1, \quad \mathcal{A}_2^\pm = \frac{m}{\varrho} + \frac{9}{4}\frac{\varrho}{\varrho^2+1}, \quad \mathcal{A}_3^\pm = \frac{1}{(\varrho^2+1)^{3/2}}\,,\\
&\mathcal{A}_4^\pm = \frac{3}{4}\frac{1\pm 2\ell\pm m}{\varrho^2+1} \mp \frac{1}{\varrho^2}\left(\ell+\frac{m}{2}\right) - \frac{3}{8}\frac{\varrho^2}{(\varrho^2+1)^2}\,,\\
&\mathcal{A}_5^\pm = \frac{3}{8}\frac{1}{\varrho^2+1}\left(3m\mp 2m+1\mp 4\ell\right) - \frac{39}{64}\frac{\varrho^2}{(\varrho^2+1)^2} - \frac{1}{\varrho^2}\left(\ell^2+m\ell+\frac{m}{2}\right).
\end{aligned} \tag{7.115}$$

Employing the projection $\Gamma^\rho\,\psi^{\ell\pm} = \psi^{\ell\pm}$ and using equations (7.114) and (7.115) one can readily obtain the fermionic second-order ordinary differential equation for $\psi^{\ell\pm}(\varrho)$. In case of positive spinorial harmonics (ℓ^+), we get the differential equation of $\psi^{\oplus}_{\mathcal{G}_\ell}(\varrho)$, while for negative spinorial harmonics (ℓ^-), the differential equation of $\psi^{\oplus}_{\mathcal{F}_\ell}(\varrho)$ is obtained. The corresponding bosonic equations of motion for the D4/Dk-brane setups ($k = \{4,6,8\}$), can be determined from equations (C.9) and (C.11) by setting $p = 4$. For all possible D4/Dk-brane systems the transformation

$$\psi^{\oplus}_{\mathcal{G}_\ell}(\varrho) = \frac{1}{(1+\varrho^2)^{9/16}}\,f_{\ell+1}(\varrho)\,, \tag{7.116}$$

maps the fermionic function $\psi^{\oplus}_{\mathcal{G}_\ell}(\varrho)$ to the bosonic function $f_{\ell+1}(\varrho)$, while the transformation

$$\psi^{\oplus}_{\mathcal{F}_\ell}(\varrho) = \frac{1}{(1+\varrho^2)^{9/16}}\,f_{\ell}(\varrho)\,, \tag{7.117}$$

maps the fermionic function $\psi^{\oplus}_{\mathcal{F}_\ell}(\varrho)$ to the bosonic function $f_\ell(\varrho)$. Notice as well that the above transformations can be obtained from equation (7.1) by setting $p = 4$.

The above equations of motion cannot be solved analytically (as in the case of bosonic mesons) and we have to resort to numerical analysis. We show explicitly the first few numerical values of the masses in table 7.9. The numerical values for n and ℓ describe the $\mathcal{F}$ operators and one needs to shift appropriately the ℓ to read off the value of the $\mathcal{G}$ states.

ℓ \ n	0	1	2	3
0	5.0604	14.068	27.856	46.573
1	14.685	26.910	43.421	64.677
2	29.701	45.647	65.237	89.117
3	49.985	69.994	93.198	120.08

ℓ \ n	0	1	2	3
0	2.2741	9.8420	22.321	39.768
1	9.1908	19.745	34.871	54.857
2	21.527	35.556	53.543	76.084
3	39.189	57.140	78.472	103.79

ℓ \ n	0	1	2	3
1	5.0604	14.068	27.856	46.573
2	14.685	26.910	43.422	64.677
3	29.701	45.647	65.237	89.116

Table 7.9: Numerical results of the parameter $\bar{M}^2$ for the D4/Dk brane intersections. The top left table pertains to the D4/D8 and the top right one depicts results for the D4/D6 brane intersection. The bottom table is related to the D4/D4 setup.

7.5 Super(conformal) multiplet counting

We have computed the mass spectra of the spin-1/2 modes arising in the massive canonical D3/D7 system. As was first shown in [121], open string excitations of the probe D7-brane fit into massive $\mathcal{N} = 2$ supermultiplets. While the counting of the states in the super(conformal)multiplets has been performed in the past, in [156] and [121], it is useful test of our results to check the counting.

For $L \to 0$, the fundamental hypermultiplet are massless and the theory is conformal. The modes are in representations of the $SU(2)_R \times SU(2)_L \times U(1)_R$ labelled by $(j_1, j_2)_s$, where $j_{1,2}$ is an index denoting the spin under the $SU(2)_{R,L}$ respectively, and s is the eigenvalue associated with the group $U(1)_R$. The dimension of chiral primaries is given by the formula $\Delta = 2j_1 + s/2$. Two scalar fields are associated with the transverse fluctuations of the D7-brane each of which, after a Kaluza-Klein reduction on the three-sphere, will lead to tower of real scalars, ϕ^ℓ, transforming in the $\left(\frac{\ell}{2}, \frac{\ell}{2}\right)_2$, with $\ell \in \mathbb{N}_0$. The vector field admits a similar expansion, and from the bulk components on the D7-brane we obtain a tower of AdS vectors, A^ℓ, transforming in the $\left(\frac{\ell}{2}, \frac{\ell}{2}\right)_0$, with $\ell \in \mathbb{N}_0$. Finally, from the components of the vector field on the internal manifold we obtain two different Kaluza-Klein towers of real scalar fields, that we call $A^\ell_\pm$, transforming in the $\left(\frac{\ell\mp1}{2}, \frac{\ell\pm1}{2}\right)_0$, with $\ell \in \mathbb{N}$. There are also two types of fermions, which upon reduction on the three sphere will give two towers of states transforming in the $\left(\frac{\ell}{2}, \frac{\ell+1}{2}\right)_1$ - the $\mathcal{F}$ fermions - and $\left(\frac{\ell+1}{2}, \frac{\ell}{2}\right)_1$ - the $\mathcal{G}$ fermions.

Introducing a mass gap in the probe-brane setup ($L \neq 0$) breaks the $U(1)_R$ acting on the two-dimensional plane that is transverse to both the background and the probe branes and the R-symmetry group is just $SU(2)_R$.

The spectra of the modes are degenerate, namely states with the same $n + \ell$ have the same mass. It was observed that such is the case for the D3-brane background in the analysis performed in [160, 161]. We proceed to counting the number of states in a given multiplet. Since the theory has a global $\mathcal{N} = 2$ supersymmetry the modes should fill massive supermultiplets, and they have to be in the same

representation of the copy of $SU(2)$ that is inert under the supercharges. To arrange this we have to appropriately shift the angular quantum number of the sphere, such that all states fall in the same representation of the $SU(2)_L$. This is shown in table 7.10.

Modes	Fluctuation	Representations	Shifted ℓ
2 real scalars	transverse oscillations	$\left(\frac{\ell}{2},\frac{\ell}{2}\right)$	$\left(\frac{\ell}{2},\frac{\ell}{2}\right)$
1 real scalar	Type I_+ fluctuations	$\left(\frac{\ell-1}{2},\frac{\ell+1}{2}\right)$	$\left(\frac{\ell-2}{2},\frac{\ell}{2}\right)$
1 real scalar	Type I_- fluctuations	$\left(\frac{\ell+1}{2},\frac{\ell-1}{2}\right)$	$\left(\frac{\ell+2}{2},\frac{\ell}{2}\right)$
1 vector	Type II fluctuations	$\left(\frac{\ell}{2},\frac{\ell}{2}\right)$	$\left(\frac{\ell}{2},\frac{\ell}{2}\right)$
1 real scalar	Type III fluctuations	$\left(\frac{\ell}{2},\frac{\ell}{2}\right)$	$\left(\frac{\ell}{2},\frac{\ell}{2}\right)$
1 Dirac fermion	Type $\mathcal{F}$ fluctuations	$\left(\frac{\ell+1}{2},\frac{\ell}{2}\right)$	$\left(\frac{\ell+1}{2},\frac{\ell}{2}\right)$
1 Dirac fermion	Type $\mathcal{G}$ fluctuations	$\left(\frac{\ell}{2},\frac{\ell+1}{2}\right)$	$\left(\frac{\ell-1}{2},\frac{\ell}{2}\right)$

Table 7.10: The origin, degrees of freedom and quantum numbers of the fermionic and bosonic states of the $\mathcal{N}=2$ multiplets of mesinos.

Moreover, we have to account for the degeneracy under the $SU(2)_R$: we count the degrees of freedom of a given state and then multiply by $(2j_1+1)$. Then, the number of bosonic components in a given multiplet for a fixed value of ℓ is equal to

$$1\left(2\left(\frac{\ell}{2}+1\right)+1\right)+6\left(2\cdot\frac{\ell}{2}+1\right)+1\left(2\left(\frac{\ell}{2}-1\right)+1\right) \tag{7.118}$$

and the number of states for the spin-1/2 components in the same multiplet is given by

$$4\left(2\frac{\ell+1}{2}+1\right)+4\left(2\frac{\ell-1}{2}+1\right) \tag{7.119}$$

For the $\ell=0$ multiplet, we obtain eight bosonic degrees of freedom and an equal number of fermionic states.

7.6 The limit of large number of colours

In this section we would like to specify our discussion to the case of a four-dimensional strongly coupled gauge theory without defects and hence we will be focused on the D3/probe-D7 intersection. The extension of the analysis to lower dimensional gauge theories based on the D3-background geometry is straightforward and similar arguments can be given for theories with quarks confined on one and two-dimensional defects.

We have studied, thus far, the dynamics and solved for the spectra of the fermionic superpartners of mesons - dubbed mesinos - which have no counterpart in ordinary non-supersymmetric field theories. For phenomenological applications of holography, however, it is interesting to study fermionic degrees of freedom in the bulk. As it was pointed out in [1] a certain class of these mesino states, namely the $\mathcal{G}$ string modes, resemble structurally the baryons of ordinary QCD. This observation was made at

the level of the analysis of the fluctuation to operator matching. It was observed that these states are comprised out of three elementary fermionic fields, two quarks and a gaugino.

On the formal side of the analysis, the true dynamical baryonic vertex in the string theory setup has been described in [103] and it consists of our base system with the D7-probe in addition to which we add D5-branes wrapping a spherical subspace inside the initial $AdS_5 \times S^5$ background geometry and having N_c strings ending on it. One can immediately see the complications. Since in the dynamical baryonic vertex N_c strings are ending on the baryonic (D5-)brane it is unclear whether or not the probe-approximation can be made and what its regime of validity is if any. Also, since the brane intersection consists of several different branes, the topology of the system of interest is inherently complicated. Finally, baryons are half-integer fields and their dynamics are governed by the Dirac or the Rarita-Schwinger actions which have to be studied on highly curved manifolds.

Now, we would like to give additional evidence and support the notion that the $\mathcal{G}$-states (which we remind the reader are $\mathcal{G} \sim \bar{\psi}\lambda\psi$, where $\bar{\psi}, \psi$ are fundamental Fermi fields - quark like states - and λ is an adjoint fermion - a gaugino field) can be thought of as effectively describing baryonic operators. In order to amplify and re-express the argument of [1] regarding the possible baryonic interpretation of these supergravity states, we will show that their mass eigenvalues obey the correct large-N_c scaling, dictated by field theory considerations [171]. This has already been done in an effective, bottom-up approach in [82]. More precisely the case of massless quarks/overlapping branes was considered in that work.

We start the analysis of this section by recalling that the scaling dimension and the AdS_5 mass for a spin-1/2 field is given by [81]

$$\Delta_\ell = |m_\ell| + 2\,, \tag{7.120}$$

and for the states considered so far we have $m_\ell^{\mathcal{G}} = \frac{5}{2} + \ell$ and $m_\ell^{\mathcal{F}} = -\left(\frac{1}{2} + \ell\right)$ for the $\mathcal{G}$ and $\mathcal{F}$ states respectively.

Now, let us turn our attention to baryonic operators in a supersymmetric Yang-Mills theory with an $SU(N_c)$ gauge group and a certain number of flavours. We will be assuming that the theory is such that it is conformal, or perhaps more generally it possesses a regime in its phase space with walking dynamics (conformal window). There are many examples of such four-dimensional field theories that are asymptotically free, for a discussion on the phase diagram of supersymmetric $SU(N_c)$ Yang-Mills theories see [175], but here we just mention the four-dimensional $SU(3)$ super-QCD with $9/2 \leq N_f \leq 9$ flavours as an example of the theories we mentioned. The existence of the conformal phase of the theory makes sure that the holographic gravity description has an AdS_5 structure. In the aforementioned class of theories a baryon is the colour singlet composite bound state comprised out of N_c quarks, and a baryonic operator is the totally anti-symmetrized object given by

$$\mathcal{B} \sim \epsilon^{\overbrace{ijk\cdots yz}^{N_c-indices}} \underbrace{q_i q_j q_k \cdots q_y q_z}_{N_c-fields}\,, \tag{7.121}$$

where we have written the lowest entry of the super(conformal) multiplet up to an irrelevant numerical

coefficient which is a function of N_c. We can construct higher baryonic excitations in the multiplet by applying an ℓ number of times the derivative operator to the above. The associated conformal dimension is given by

$$\Delta = \frac{3}{2}N_c + \ell\,. \tag{7.122}$$

It is straightforward to use equation (7.120) and obtain

$$m_\ell^{\mathcal{B}} = \frac{3}{2}N_c + \ell - 2\,. \tag{7.123}$$

We have already seen that the positive spinor spherical harmonics give rise to states that resemble baryons of non-supersymmetric QCD. We re-write the eigenvalues of the spinor spherical harmonic in a different but equivalent form for the $\mathcal{G}$-modes

$$\not{D}_{S^3}\Psi^{\ell^+} = \left(m_\ell^{\mathcal{G}} - 1\right)\Psi^{\ell^+}\,. \tag{7.124}$$

At this point we replace in the above relation equation (7.124) the bulk-AdS mass for a baryonic operator given by equation (7.123) and hence we obtain

$$\not{D}_{S^3}\Psi = \left(m_\ell^{\mathcal{B}} - 1\right)\Psi\,. \tag{7.125}$$

It is a matter of simple algebra to derive the differential equation by using equation (7.125) and the mathematical procedure explained in the previous section. Thus, we get

$$\begin{aligned}\Big\{\partial_\varrho^2 + \left[\frac{3\varrho}{1+\varrho^2} + \frac{2(m_\ell^{\mathcal{B}} - \ell - 1)}{\varrho}\right]\partial_\varrho + \frac{\bar{M}_{\mathcal{B}}^2}{(1+\varrho^2)^2} - \frac{3}{4}\frac{\varrho^2}{(1+\varrho^2)^2} - \frac{1}{\varrho^2}\Big[m_\ell^{\mathcal{B}}(2\ell+1) - (\ell+1)^2 - \ell \\ + (m_\ell^{\mathcal{B}} - 1)\Gamma^\varrho\Big] + \frac{1}{1+\varrho^2}\left[m_\ell^{\mathcal{B}} - 3\ell - \frac{1}{2} + (2m_\ell^{\mathcal{B}} - 1)\Gamma^\varrho\right]\Big\}\Psi = 0\,.\end{aligned} \tag{7.126}$$

In order to obtain the solution to the above equation of motion representing the supergravity states we require the solution to be normalizable in the UV and regular in the IR, hence, we have

$$\begin{aligned}\psi_{\mathcal{B}} =& \frac{\varrho^{\ell+1}}{(1+\varrho^2)^{n+\ell+\frac{3N_c}{2}-\frac{7}{4}}}\;{}_2F_1\left(-n, -n-\ell-\frac{3N_c-5}{2}; \ell+\frac{3(N_c-1)}{2}; -\varrho^2\right)\chi_+ \\ &+ \frac{\varrho^{-\frac{9}{2}+\ell+\frac{3N_c}{2}}}{(1+\varrho^2)^{-\frac{7}{4}+n+\ell+\frac{3N_c}{2}}}\;{}_2F_1\left(-n, -n-\ell-\frac{3(N_c-1)}{2}; \ell+\frac{3N_c-5}{2}; -\varrho^2\right)\chi_-\,,\end{aligned} \tag{7.127}$$

while the discrete mass spectrum is shown below

$$\bar{M}_{\mathcal{B}} = 2\sqrt{\left(n+\ell+\frac{3}{2}N_c - \frac{5}{2}\right)\left(n+\ell+\frac{3}{2}(N_c-1)\right)}\,. \tag{7.128}$$

It is obvious that in the $N_c \to \infty$ limit the mass scales with N_c as desired [171]. It is quite obvious as well, that for $N_c = 3$ equations (7.127) and (7.128) reduce to the ones derived in section 7.4.5 above for the D3/probe-D7 setup.

Let us conclude the discussion of this section by stating the basic points. The large-N_c limit scaling of the mass was derived in [82] for the case of overlapping branes in a bottom-up way effectively. Here, we provide a derivation from the top-down construction in a set-up that describes massive dynamical quarks by construction. We should stress - though obvious - that our result is derived by assuming that the identification of the $\mathcal{G}$ modes as describing baryonic operators at least in some regime of the parameter space of the gauge theory is correct. The precise statement we wish to make here is the same as the one made in [82]. If one realizes and manages to solve the brane configuration that yields a dynamical baryon in the string theory side with an AdS geometric part, then the result derived in equation (7.128) should be re-obtained from the full brane intersection; it should at least hold in a certain regime of the parameter space of the full setup.

7.7 Double-trace interactions

In this section we are shifting back to the original parameterization and no longer using the dimensionless ϱ variable. This we do in order to precisely acount for some extra factors in the solutions of the supergravity eigenstates that can only be obtained using dimensional analysis. It is worthwhile stressing that qualitively we would obtain the same results even without the shift, however we have chosen to be precise.

In the ρ variable, the equations of motion for the $\mathcal{G}$-modes are given by

$$\begin{aligned}&\left[\frac{r^2}{R^2}\partial_\rho^2+\frac{1}{R^2}\left(3\rho+3\frac{r^2}{\rho}\right)\partial_\rho+\frac{M^2R^2}{r^2}+\frac{1}{R^2}\left(4+2\ell-\frac{r^2}{\rho^2}\left(\ell+\frac{3}{2}\right)\right)\gamma^\rho\right.\\&\left.+\frac{1}{R^2}\left(-\frac{3\rho^2}{4r^2}+2-2\ell\right)-\frac{r^2}{R^2\rho^2}\left(\ell^2+3\left(\ell+\frac{1}{2}\right)\right)\right]\psi^\ell_{\mathcal{G}}(\rho)=0\,,\end{aligned}\tag{7.129}$$

where $k^2=-M^2$. While the relevant expression for the $\mathcal{F}$ modes is

$$\begin{aligned}&\left[\frac{r^2}{R^2}\partial_\rho^2+\frac{1}{R^2}\left(3\rho+3\frac{r^2}{\rho}\right)\partial_\rho+\frac{M^2R^2}{r^2}+\frac{1}{R^2}\left(-2-2\ell+\frac{r^2}{\rho^2}\left(\ell+\frac{3}{2}\right)\right)\gamma^\rho\right.\\&\left.+\frac{1}{R^2}\left(-\frac{3\rho^2}{4r^2}+8+2\ell\right)-\frac{r^2}{R^2\rho^2}\left(\ell^2+3\left(\ell+\frac{1}{2}\right)\right)\right]\psi^\ell_{\mathcal{F}}(\rho)=0\,.\end{aligned}\tag{7.130}$$

In order to proceed we need to perform the large-ρ limit at the level of the equations of motion. Solving the resulting differential equations yields a solution in terms of four constants. Why though are there extra terms relative to what we were expecting with respect to the coupled first-order equations? We have seen, already, why this happens and how we can remedy that in the case of pure AdS_5. The answer is that the two second order equations duplicate the data of the first order equations - the solutions of one are tied to a particular solution of the other at leading order in M and beyond. To see this we must return to the first order equations to link the solutions. In particular we can substitute the solutions we obtained from solving the large-ρ equations into the first-order equations and then return to the decoupled second-order differential equation. In this way we can fix the solutions of the

second order equations to take the asymptotic form

$$\begin{aligned}\psi_{\mathcal{G},+}(\rho) &\sim -\frac{c_2 R^2 M}{2(2+\ell)}\ \rho^{-1/2+\ell} + c_1\ \rho^{-9/2-\ell},\\ \psi_{\mathcal{G},-}(\rho) &\sim c_2\ \rho^{1/2+\ell} - \frac{R^2 M c_1}{(6+2\ell)}\ \rho^{-11/2-\ell},\end{aligned} \tag{7.131}$$

which have the same number of degrees of freedom as the solutions of the linearized equation. Note in practice now we can solve just one of the second order equations and extract c_1 and c_2 from the asymptotics. The analysis for the $\mathcal{F}$ modes follows that for the $\mathcal{G}$ modes. The result is

$$\begin{aligned}\psi_{\mathcal{F},+}(\rho) &\sim c_2\ \rho^{-3/2+\ell} + \frac{c_1 M R^2}{2(\ell+1)}\ \rho^{-7/2-\ell},\\ \psi_{\mathcal{F},-}(\rho) &\sim \frac{c_2 M R^2}{2\ell}\ \rho^{-5/2+\ell} + c_1\ \rho^{-5/2-\ell}.\end{aligned} \tag{7.132}$$

Having fixed these constants we can straightforwardly compute the supergravity mode solutions. They are given by

$$\begin{aligned}\psi^{\ell}_{\mathcal{G}}(\rho) = \Big(-L^2\Big)^n \Bigg[&\frac{\rho^{\ell+1}}{(\rho^2+L^2)^{n+\ell+\frac{11}{4}}}\ {}_2F_1\Big(-n,-(n+\ell+2),\ell+3,-\frac{\rho^2}{L^2}\Big)\alpha_+\\ &-\frac{R^2 M(\ell+2)}{2(\ell+n+2)(\ell+n+3)}\frac{\rho^{\ell}}{(\rho^2+L^2)^{n+\ell+\frac{11}{4}}}\ {}_2F_1\Big(-n,-(n+\ell+3),\ell+2,-\frac{\rho^2}{L^2}\Big)\alpha_-\Bigg]\end{aligned} \tag{7.133}$$

and

$$\begin{aligned}\psi^{\ell}_{\mathcal{F}}(\rho) =(-L^2)^n \Bigg[&\frac{R^2 M}{2}\frac{\rho^{\ell}}{(\rho^2+L^2)^{n+\ell+\frac{7}{4}}}\ {}_2F_1\Big(-n,-(n+\ell+1),\ell+2,-\frac{\rho^2}{L^2}\Big)\alpha_+\\ &+\frac{(n+\ell+1)}{(\ell+1)}\frac{\rho^{\ell+1}}{(\rho^2+L^2)^{n+\ell+\frac{7}{4}}}\ {}_2F_1\Big(-n,-(n+\ell),\ell+3,-\frac{\rho^2}{L^2}\Big)\alpha_-\Bigg]\ .\end{aligned} \tag{7.134}$$

and of course the mass spectra are the same as the ones we have already discovered.

We proceed to a presentation of a numerical approach to solving these equations of motion which we will use since we need to find the spectrum in cases where the source for the fermionic operator does not vanish. To demonstrate the method, we consider the $\mathcal{G}$ modes and we will just concentrate on the $n=0,\ell=0$ and $n=1,\ell=0$ cases. We need to solve for the negative eigenvalue of the Γ^{ρ}-matrix (or equally we could solve for the positive one as we have already argued and obtain completely equivalent results). We have seen the solution of the differential equations near the boundary, however shooting from the IR to the UV looking for normalizability of the solutions is a much less numerically intensive procedure. We expand the analytic solutions to obtain their IR scaling behaviour and find that

$$\begin{aligned}\psi_{\mathcal{G},+}(\rho) &\sim \rho^{\ell+1}, \qquad \partial_\rho\psi_{\mathcal{G},+}(\rho) \sim (\ell+1)\rho^{\ell},\\ \psi_{\mathcal{G},-}(\rho) &\sim \rho^{\ell}, \qquad \partial_\rho\psi_{\mathcal{G},-}(\rho) \sim \ell\rho^{\ell-1}.\end{aligned} \tag{7.135}$$

Thus for $\psi_{\mathcal{G},-}$ we may use the shooting technique for the $\ell=0$ state with the boundary conditions

$\psi_{\mathcal{G},-}(0) = 1$, $\psi'_{\mathcal{G},-}(0) = 0$ to seek solutions that asymptote to the source $J = 0$ in the UV. We recall that the solution takes the asymptotic form

$$\begin{aligned}\psi_{\mathcal{G},+}(\rho) &\sim -\frac{JR^2M}{2(2+\ell)}\ \rho^{-1/2+\ell} + \mathcal{O}\ \rho^{-9/2-\ell},\\ \psi_{\mathcal{G},-}(\rho) &\sim J\ \rho^{1/2+\ell} - \frac{\mathcal{O}R^2M}{(6+2\ell)}\ \rho^{-11/2-\ell},\end{aligned} \tag{7.136}$$

where $\mathcal{O}$ is the operator value (we have absorbed factors of R into M for the numerical analysis). We find it most helpful to plot $\rho^{-1/2}\ \psi_{\mathcal{G},-}(\rho)$ since this asymptotes to J. The procedure is simply to shoot out tuning M^2 so that $J = 0$ in the UV. In this way, it is straightforward to numerically reproduce the analytic solutions in section 7.4.5 - we have been able to straightforwardly reproduce the value of M^2 of the analytic spectrum numerically to three decimal places. In figure 7.5 we show this process in action, plotting the solutions for different M^2. We repeat the analysis for the $\mathcal{F}$-modes, however, this

Figure 7.5: Shooting from the IR to the UV for different values of M^2 for the $\mathcal{G},-$ type mesinos, using the boundary conditions in equation (7.135). The left plot shows the results for $\rho^{-1/2}\psi_{\mathcal{G},-}$ for the ground state ($n = \ell = 0$) starting from $M^2 = 0$ and proceeding with steps of one to $M^2 = 24$ and the right plot corresponds to the first excited state ($n = 1, \ell = 0$) starting from $M^2 = 25$ and proceeding with steps of one to $M^2 = 48$. The solutions relevant to the supersymmetric theory asymptote to zero where the source J vanishes.

time we choose to study the differential equation associated with the positive eigenvalue of the chiral Γ-matrix. The IR scaling behaviour here is

$$\begin{aligned}\psi_{\mathcal{F},+}(\rho) &\sim \rho^{\ell}, \qquad & \partial_\rho\psi_{\mathcal{F},-}(\rho) &\sim \ell\rho^{\ell-1},\\ \psi_{\mathcal{F},-}(\rho) &\sim \rho^{\ell+1}, \qquad & \partial_\rho\psi_{\mathcal{F},+}(\rho) &\sim (\ell+1)\rho^{\ell},\end{aligned} \tag{7.137}$$

and the UV asymptotics are

$$\begin{aligned}\psi_{\mathcal{F},+}(\rho) &\sim J\ \rho^{-3/2+\ell} + \frac{\mathcal{O}MR^2}{2(\ell+1)}\ \rho^{-7/2-\ell},\\ \psi_{\mathcal{F},-}(\rho) &\sim \frac{JMR^2}{2\ell}\ \rho^{-5/2+\ell} + \mathcal{O}\ \rho^{-5/2-\ell}.\end{aligned} \tag{7.138}$$

We solve for $\psi_{\mathcal{F},+}(\rho)$ shooting out from $\psi_{\mathcal{F},+}(0) = 1$, $\psi'_{\mathcal{F},+}(0) = 0$ and seek solutions where $J = 0$. It is helpful to plot $\rho^{3/2}\ \psi_{\mathcal{F},+}(\rho)$ which asymptotes to J. Again the supersymmetric states are easily recovered - we show the process in figure 7.6. So far we have explored the fermionic bound states of

Figure 7.6: Shooting from the IR to the UV for different values of M^2 for the $\mathcal{F},+$ type mesinos, using the boundary conditions in equation (7.137). The left plot shows the results for $\rho^{3/2}\psi_{\mathcal{F},+}$ for the ground state ($n=\ell=0$) starting from $M^2=0$ and proceeding with steps of one to $M^2=8$ and the right plot corresponds to the first excited state ($n=1,\ell=0$) starting from $M^2=9$ and proceeding with steps of one to $M^2=24$. The solutions relevant to the supersymmetric theory asymptote to zero where the source J vanishes.

the supersymmetric $\mathcal{N}=2$ gauge theory dual to the D3/ probe D7 system. Our motivation is to find holographic models that give rise to anomalously light fermionic bound states, as required in composite Higgs models. What we have seen though is that the spectrum of the supersymmetric brane models is characterized by the scale $m_q/\sqrt{\lambda_{YM}}$. As the 't Hooft coupling of the gauge theory grows large, this scale is small relative to the bare quark mass, but it nevertheless sets an intrinsic scale for the strong dynamics. All states lie near that scale, up to order one numerical numbers. This of course has been known for many years, since supersymmetry ties the fermionic bound states to the mesonic bound state masses computed in [121].

How can we then obtain a baryonic bound state (denoted generically by Ψ_B associated with an operator $\mathcal{O}_B$), to be light relative to that scale? We wish to explore an answer to that question which consists of including a higher dimension operator in the field theory. These higher dimension operators should be associated with new physics at a UV scale Λ_{UV}. The precise form of the operator will be chosen so that it corresponds to a shift in the bound state mass at low energies. Generically the approach is this: we add a term to the field-theory Lagrangian of the form

$$\Delta\mathcal{L}_{UV}=\frac{g^2}{\Lambda_{UV}^p}\bar{\mathcal{O}}_B\mathcal{O}_B, \tag{7.139}$$

where the power, p of the cut off Λ_{UV} determined dependent on the UV dimension of the operator. As a very simple model, we assume that this operator leads to an RG flow such that in the IR, the baryon Ψ_B receives a mass shift of the form

$$\Delta\mathcal{L}_{IR}\propto\frac{g^2m_q^{p+1}}{\Lambda_{UV}^p}\bar{\Psi}_B\Psi_B\,. \tag{7.140}$$

Here we have assumed that the dynamics that binds the fermions occurs around the quark mass scale where the conformal symmetry is broken - hence the m_q term which is present to make the operator of dimension four in the IR. Naively if this term plays a passive role only, this could be used for a negative shift in the baryon mass that could be tuned to reduce the baryonic mass scale. In fact we will see that

such operators show a sort of critical behaviour at large g which is more than just this shift.

To include such an operator, we use Witten's multi-trace prescription [147]. This essentially says that, if the operator equation (7.139) acquires a VEV, then a source is generated with the value

$$J = \frac{g^2}{\Lambda_{UV}^p} \langle \mathcal{O}_B \rangle \,. \tag{7.141}$$

This relation is imposed on the holographic field corresponding to the operator at the UV cut-off $\rho = \Lambda_{UV}$ - there is thus a large ρ boundary of the dual space. In practice one just finds solutions with different source-operator combinations and computes g^2 at the scale Λ_{UV}. We have done most of the work for this process in previous sections.

An explicit example - the $\ell = 0$ $\mathcal{G}$ mode

Let us now study an explicit example. We are interested in driving the mass of one of the mesinos of the $\mathcal{N} = 2$ gauge theory described by the D3/probe D7 system much lighter than the characteristic scale $m_q/\sqrt{\lambda_{YM}}$. Let us pick on the lightest $\ell = 0, n = 0$ $\mathcal{G}$-type mesino discussed above. In particular the masses of this state are found by solving equation (7.129),

$$\begin{aligned} &\left[\frac{r^2}{R^2}\partial_\rho^2 + \frac{1}{R^2}\left(3\rho + 3\frac{r^2}{\rho}\right)\partial_\rho + \frac{M^2R^2}{r^2} + \frac{1}{R^2}\left(4 + 2\ell - \frac{r^2}{\rho^2}\left(\ell + \frac{3}{2}\right)\right)\gamma^\rho \right. \\ &\left. + \frac{1}{R^2}\left(-\frac{3\rho^2}{4r^2} + 2 - 2\ell\right) - \frac{r^2}{R^2\rho^2}\left(\ell^2 + 3\left(\ell + \frac{1}{2}\right)\right)\right] \psi^0_{\mathcal{G}}(\rho) = 0 \,, \end{aligned} \tag{7.142}$$

for the supergravity modes corresponding to the $\mathcal{G}$-type mesinos. We will solve for the negative eigenvalue of γ^ρ. The UV and IR behaviour of the solutions have been determined in equations (7.135) and (7.136),

$$\begin{aligned} &\psi_{\mathcal{G},-}(\rho)_{IR} \sim 1, && \partial_\rho \psi_{\mathcal{G},-}(\rho)_{IR} \sim 0, \\ &\psi_{\mathcal{G},-}(\rho)_{UV} \sim J\ \rho^{1/2} + \frac{\mathcal{O}R^2M}{6}\ \rho^{-11/2}. \end{aligned} \tag{7.143}$$

In the previous sections we gave a full numerical prescription to find these solutions. In figure 7.5 we display the full set of regular solutions for $\psi_{\mathcal{G}}$ - each line corresponds to a particular mesino mass M and predicts an associated value of the source J extracted from the UV asymptotics. In the supersymmetric model we rejected any solutions for which $J \neq 0$ but now we will consider the full set.

Remember that in the dual field theory we are looking at states that are associated with the UV operator

$$\mathcal{G}^\ell \sim \psi^\dagger \lambda \psi \,, \tag{7.144}$$

which includes a three fermion bound state; two quarks and a gaugino and the precise holographic mapping can be found in [82]. In the above, ψ is the fundamental spinor, and λ is the adjoint hypermultiplet.

Here consider adding, at the scale Λ_{UV}, the field-theory Lagrangian term

$$\Delta\mathcal{L}_{UV} = \frac{g^2}{\Lambda_{UV}^5}\bar{\mathcal{G}}^0\mathcal{G}^0\,. \tag{7.145}$$

The IR mesino Ψ_M receives a mass shift of the form

$$\Delta\mathcal{L}_{IR} \propto \frac{g^2 m_q^6}{\Lambda_{UV}^5}\bar{\Psi}_M\Psi_M\,. \tag{7.146}$$

Witten's multi-trace prescription [147] tells us to require of our regular solutions in figure 7.5

$$J = \frac{g^2}{\Lambda_{UV}^5}\langle\mathcal{G}^0\rangle\,. \tag{7.147}$$

We have already numerically computed the solutions to the fluctuation equations for different values of the mass by solving equation (7.129) for the mode $\psi^0_{\mathcal{G}-}$, using the shooting method. We obtain the supersymmetric spectrum from these numerical flows by considering the solutions that asymptote to zero for a vanishing source, $J = 0$, and disregarding all other numerical flows. Now, we allow for all the different numerical values of M^2 and consider the corresponding numerical solutions we obtained by performing the method described above. For each of those cases we then extract $\mathcal{O}$ from the UV asymptotics in equation (7.143). Here we determine J and $\mathcal{O}$ at a value of ρ that corresponds to the UV cut-off Λ_{UV} (numerically here we pick $\Lambda_{UV}/L = 10$ as an example).

Now we have a series of solutions with M, J and $\mathcal{O}$ and we may compute the higher dimension operator's coupling g from equation (7.147). The result is shown in figure 7.7 - it tracks the mass of the mesino against the strength of the coupling g. The red dots show the lightest state at each value of g^2. As g^2

Figure 7.7: The effect of double-trace interaction on the mass spectra of the D3/D7 states D3/D7-brane system: The mesino mass squared M^2 as function of the coupling strength g^2 in units of L/R^2(dots are data points whilst the line is to guide the eye) in the presence of the double-trace deformation for the $\ell = 0$ and $n = 0, 1$ radially excited modes. The $\mathcal{G}$ fermionic modes are shown on the left and the $\mathcal{F}$ modes on the right. The green points show the first, radially excited state getting lighter as the coupling is increased, and the red ones show the ground state of the modes.

increases from zero, initially the fermionic bound state mass is expected to fall linearly - the higher dimension operator is a weak perturbation and the naive analysis applies simply adding a small negative shift to the mesino mass. In fact it is numerically difficult to extract solutions in this regime because

the mesino masses must be very finely tuned close to the supersymmetric value and g^2 extracted from the noisy UV asymptotics. The lowest g^2 points we extract are consistent with this expectation though. Above $g^2 = 10$ there is a new behaviour though - the mesino mass falls sharply over a relatively small range of g^2. This is suggestive of the critical behaviour in a Nambu-Jona Lasinio type model where above a critical value the higher dimension operator is having a major role in the dynamics. Rather than then driving the mesino mass squared to zero and negative values though, above $g^2 \simeq 15$ the drop in the mesino mass plateaus before reaching $M^2 = 0$ only at infinite coupling. Note that taking the dimensionless g^2 large should be an acceptable theory provided the mesino masses do not rise above the scale Λ_{UV} which here they won't because the masses are suppressed by the large 'tHooft coupling. We believe this region of behaviour is governed by the fact that fermionic modes cannot condense and so the mass cannot be driven to become tachyonic. Mathematically, this behaviour follows from the occurrence of M in the UV solutions for the sub-leading term of the solution - at $M = 0$ if the sub-leading term is non-zero, then the operator vev is pushed to infinity and hence also g^2 goes to infinity.

Interestingly, adding the term with a negative value of g^2 does not greatly increase the mass of the mesino bound state as one would naively expect - possibly the $\mathcal{N} = 4$ dynamics is already so strong that adding additional strong interactions do not greatly change the dynamics. Such theories have unbounded potentials at the UV cut off in any case. Such a negative g^2 can be viewed as a repulsion amongst the fermions; this can also be seen by considering the operator as representing the Feynman diagram of two fermions scattering by the exchange of a massive gauge boson where repulsion is just a change in the signs.

The behaviour of the green dots that display the first radially excited state of the $\mathcal{G}^0$ modes is also interesting. These states too fall in mass as g^2 approaches the critical region, but they saturate at the value of the ground state at $g^2 = 0$, falling no lower. The reason is that for each choice of M^2, fixing the IR boundary conditions fixes the flow - if it flows to a UV boundary condition corresponding to $g^2 = 0$, then that choice of M^2 can never occur for any other value of g^2. The expectation therefore is that in this method, only a single baryonic bound state will be driven to become light, not the full tower of states.

A similar story can be told for the $\mathcal{F}$ modes made of a gaugino and a squark

$$\mathcal{F}^\ell \sim q\psi\,, \tag{7.148}$$

where in the above q denotes a scalar and the precise operator to bulk mode dictionary can also be found in [82]. The mass spectrum is shown in figure 7.7 as a function of the coupling of the higher dimension operator $g^2/\Lambda\bar{\mathcal{O}}\mathcal{O}$. The same behaviours are observed, namely the lightest state can be driven to have a light mass at intermediate g^2 and to zero as $g^2 \to \infty$. The $n = 1, \ell = 0$ state falls in mass as the coupling is approaching its critical value, but they saturate at the value of the ground state and never fall lower than that.

7.8 The avoided level crossing

The models that we have considered thus far cannot give rise to abnormally light fermionic states compared to the scale set by the vector meson mass of the brane intersection. The reason behind this, lies to the residual amount of supersymmetry - after the introduction of flavour branes - which ties these masses to the spectra of the bosonic meson states. It is, however, useful for applications of holographic models to understand if and how one is able to make certain states lighter. A neat example is the study of holographic composite Higgs models [2] where the double-trace interactions are necessary to ensure the correct mass for the top. Double-trace deformations are also used in other bottom-up applications in holography. They have been used, for example, to describe the colour superconductivity [176] where the double-trace interactions are used to generate the Cooper pair condensate.

With holographic applications in mind, the authors in [1] considered double-trace deformations of the boundary Lagrangian of "mesino" squared type. The way that this was achieved was to use the prescription for higher dimensional operators described by Witten [147]. The addition of such operators is naively a reduction to the fermionic mass in the low-energy hadronic description. It is worthwhile mentioning that the method with the double-trace interactions has been used in the past in the context of the D3/probe-D7 brane intersection to describe the Nambu-Jona-Lasinio model [148]. This model utilizes four-fermi interactions.

The precept of the exercise with double-trace operators of "mesino" squared type is that any state can be driven much lighter compared to the undeformed $\mathcal{N}=2$ theory, however it can never be made lighter than the previous one in the supermultiplet. Hence, the authors in [1] found an avoided level-crossing. This was observed only numerically and an analytic explanation is still lacking. Here we provide an analytic explanation.

The effects of adding these higher dimension operators should manifest themselves as new phenomena at some scale in the UV which we call Λ_{UV}. These operators deform the original Lagrangian in the following schematic way:

$$\mathcal{L} + \frac{g^2}{\Lambda_{UV}^q}\,\bar{\mathcal{O}}\,\mathcal{O}\,, \tag{7.149}$$

where the power q is chosen with relevance to the conformal dimension of the operator. Witten argued that if the operator obtains a non-trivial vacuum expectation value, it generates a source at the UV boundary, which is given by

$$\mathcal{J} = \frac{g^2}{\Lambda_{UV}^q}\langle\mathcal{O}\rangle\,. \tag{7.150}$$

All the spectra presented so far are solutions with a vanishing source; $\mathcal{J}=0$. In order to include the double-trace deformation of the Lagrangian, we allow for solutions to have $\mathcal{J}\neq 0$, and from the asymptotic expansions of these modes in the UV we can read off the precise values of $\mathcal{O}$ and $\mathcal{J}$. The asymptotic expansions have been obtained in the past and the precise explanation of the sources and operators in terms of these expansions are given in [1, 170] and we do not repeat the analysis here. Then, by using equation (7.150) we are able to obtain the coupling g^2. These new solutions that have $\mathcal{J}\neq 0$ are interpreted as being part of the sourceless theory in the presence of the higher dimensional

operators.

Having explained the way that these higher dimensional operators can be included in our base system, let us focus, without loss of generality, on the D3/D7 brane junction and the modes associated to the $\mathcal{G}$ operators. For a certain value of the angular momentum $\ell = 0$ we ask the question whether or not the first radially excited state of the KK tower, $n = 1$, can be driven lighter than the ground state, $n = 0$. There is numerical evidence that this does not happen.

Since we have already argued that the same arguments can be obtained from either of the Γ^{ϱ} projections we will be using the $\oplus$ states for convenience. Under the change of variables:

$$\varrho = e^{-y}, \qquad \psi(\varrho) = \frac{e^{-2y}}{(1+e^{2y})^{3/4}}\varphi(y), \tag{7.151}$$

the equations of motion can be brought in a Schrödinger form, namely

$$(\partial_y^2 - V(y))\varphi(y) = 0, \tag{7.152}$$

with the potential being given by:

$$V(y) = (\ell+2)^2 - \frac{1}{4}\,\mathrm{sech}^2\, y\ \bar{M}^2\,. \tag{7.153}$$

We drop the explicit y-dependence for notational convenience and we denote the ground state ($n = 0$, $\ell = 0$) by φ_0 and the corresponding mass eigenvalue by M_0^2. Likewise we use the subscript 1 for the $n = 1,\ \ell = 0$ state or any state that lies above the ground state ($n > 0$, $\ell = 0$) of the system and has a higher mass with a non-vanishing source in the UV. Hence, we obtain

$$\begin{aligned} \partial_y^2\varphi_0 - V_0\varphi_0 &= 0\,, \\ \partial_y^2\varphi_1 - V_1\varphi_1 &= 0\,. \end{aligned} \tag{7.154}$$

If a level-crossing is to occur it would mean that $\bar{M}_0^2 = \bar{M}_1^2$ (and $V_0 = V_1$) for some value of a specified source term. We multiply the first equation by φ_1 and the second by φ_0 and we subtract one from the other to obtain

$$\begin{aligned} \varphi_1\,\partial_y^2\varphi_0 - \varphi_0\,\partial_y^2\varphi_1 = 0 \Rightarrow \\ \partial_y\left(\varphi_1\,\partial_y\varphi_0 - \varphi_0\,\partial_y\varphi_1\right) = 0 \Rightarrow \\ \varphi_1\,\partial_y\varphi_0 - \varphi_0\,\partial_y\varphi_1 = c\,, \end{aligned} \tag{7.155}$$

where c is just a finite constant. Note that if we are dealing with the normalizable modes only, then we can use the boundary conditions at infinity to set $c = 0$ and we solve the differential equation above to obtain $\varphi_0 = \widetilde{c}\ \varphi_1$, where now $\widetilde{c}$ is a new constant. However, this would only mean that there is no deformation of the boundary Lagrangian and we have only the states of the undeformed $\mathcal{N} = 2$ theory.

If we wish to allow for a non-negligible double-trace deformation we should formally write

$$\varphi_1\,\partial_y\varphi_0 - \varphi_0\,\partial_y\varphi_1 = c\,, \tag{7.156}$$

for some finite value of the constant c. Note that while we know that φ_0 is the ground state and hence it falls off to 0 in the UV we cannot set the constant to $c = 0$ as the term with the non-vanishing source might be going to some finite value faster.

Equation (7.156) is a necessary condition for a level-crossing to occur, thus we can re-express it in terms of the ϱ coordinate and the spinorial wave-functions $\psi_{(0,1)}$ in the following way:

$$\varrho(1+\varrho^2)^{3/2}\,\partial_\varrho\left[\ln\left(\frac{\psi_0}{\psi_1}\right)\right] = \frac{c}{\psi_0\,\psi_1}. \tag{7.157}$$

We can readily obtain the form of ψ_0 by using equation (7.98) for the special values $n = \ell = 0$, $m = 3$ and taking into account the positive Γ^ϱ-projection, thus we get

$$\psi_0 = \frac{\varrho}{(1+\varrho^2)^{11/4}}. \tag{7.158}$$

However, in order to obtain the form of ψ_1 we need to reconsider the solutions of the second-order equations of motion. The difference now is that we will allow as solutions the more general form and not just the piece that falls off asymptotically to zero as $\varrho \to \infty$. For our convenience we re-state the second-order differential equation of the $\mathcal{G}$-modes for the positive Γ^ϱ-projection:

$$\left[\partial_\varrho^2 + \left(\frac{3}{\varrho} + \frac{3\varrho}{1+\varrho^2}\right)\partial_\varrho + \frac{\bar{M}^2}{(1+\varrho^2)^2} - \left(\frac{3}{4}\frac{\varrho^2}{(1+\varrho^2)^2} + \frac{1}{\varrho^2}(\ell+1)(\ell+3) - \frac{6}{1+\varrho^2}\right)\right]\psi^{\oplus}_{\mathcal{G}_\ell}(\varrho) = 0. \tag{7.159}$$

The above admits analytic solutions -without any requirements as we did previously- which are given by:

$$\begin{aligned}\psi^{\oplus}_{\mathcal{G}_\ell}(\varrho) =& (-)^{2\ell}\frac{(1+\varrho^2)^{-\frac{1}{4}+\frac{\sqrt{1+\bar{M}^2}}{2}}}{\varrho^{\ell+3}}\;{}_2F_1\left(\frac{1}{2}+\frac{\sqrt{1+\bar{M}^2}}{2}, -\frac{3}{2}-\ell+\frac{\sqrt{1+\bar{M}^2}}{2}; -(\ell+1); -\varrho^2\right)\\ &+\varrho^{\ell+1}(1+\varrho^2)^{-\frac{1}{4}+\frac{\sqrt{1+\bar{M}^2}}{2}}\;{}_2F_1\left(\frac{1}{2}+\frac{\sqrt{1+\bar{M}^2}}{2}, \frac{5}{2}+\ell+\frac{\sqrt{1+\bar{M}^2}}{2}; \ell+3; -\varrho^2\right).\end{aligned} \tag{7.160}$$

Substituting ψ_0 from equation (7.158) and ψ_1 from equation (7.160) in the condition equation (7.157), and solving for c we obtain an answer in terms of hypergeometric functions. When we fix $\ell = 0$ the solution for c simplifies to complex infinity.

Similarly, one can ask the question of whether or not the ground state ($n = \ell = 0$) of the setup can be driven to be massless or even tachyonic. Again, numerical analysis in [1] has shown that this does not happen as it requires a double-trace deformation with infinitely strong coupling. The same conclusion that we reached previously can also be drawn for this example. The only change in the computation is that now the $n = \ell = 0$ state plays the role of ψ_1 in equation (7.157) and the non-normalizable solution given by equation (7.160) plays the role of the state with a zero mass.

Consequently, we argue that we found an analytic way to see why a level crossing does not occur in these systems and furthermore why the discontinuity in the double-trace plots appeared to be going to infinite values of the coupling.

Part VI

The bottom-up method

Chapter 8

The strongly coupled sector of composite Higgs models and the top mass[1]

8.1 Introduction

As we have seen already, the AdS/CFT correspondence was first proposed for conformal field theories, such as the $\mathcal{N} = 4$ Super Yang Mills (SYM) theory [23, 106]. However, it has created a new paradigm for an effective description of gauge theory, through a five-dimensional gravitational dual, even beyond the conformal case. Non-conformal gauge/gravity dual models have been used extensively to describe theories similar to QCD. For example, chiral symmetry breaking [122, 129, 158], meson masses [41, 123, 134, 177] and baryon masses [178] have all been addressed. This modelling has been more successful than one would expect with sensible predictions of the spectrum and couplings possible at least at the 15% level, or even better. Moreover, the comparison to lattice studies turns out to be convincing. An example of this is the quark mass dependence of QCD, as realized for instance in the dependence of the ρ meson mass on the π meson mass [41, 138, 179]. The holographic techniques for QCD described above can be extended to other non-abelian gauge theories [136, 180, 181]. It is natural to apply them to strongly coupled models of physics Beyond the Standard Model (BSM) that have been proposed. For example, holographic work on technicolour includes [136, 182–188].

Another class of BSM models that have generated considerable study are composite Higgs models [189] (the idea that the Standard Model (SM) fields might be composite has a long history, see for example [190]) in these models we study the Higgs emerges as a bound state of a strongly coupled gauge theory at the 1-5 TeV scale. The composite nature of the Higgs removes the huge levels of fine tuning in the SM hierarchy problem. In this paper, we will apply holographic methods to survey the full set of gauge theories that may underpin composite Higgs models including [191, 192] and the

[1]The research presented here is based on [2, 4], which is work in collaboration with my supervisor Nick Evans as well as Johanna Erdmenger and Werner Porod. My primary contributions were to perform the analytics for the fermionic fields and performing the numerical analysis.

exhaustive listing of [144]. We predict the models' meson spectrum and investigate the properties of top partner baryons. We build on the work in our earlier, short paper [2], expanding the analysis to a much wider set of quantities in the gauge theories previously studied and hugely enlarging the set of gauge theories considered. The holographic model we use moves beyond simple holographic models such as the Randall-Sundrum [193] approach of [194, 195] by directly including the running dynamics of a particular UV completion of the model.

Holographic models of QCD-like theories split into two types: so-called top down models use the precise tools of the AdS/CFT dictionnary to study deformed versions of $\mathcal{N} = 4$ SYM that display confinement and chiral symmetry breaking. Quark fields have been rigorously included in $\mathcal{N} = 4$ SYM by adding probe D7-branes [41, 120, 121]. These models are usually highly predictive, yet an actual rigorous string dual of QCD does not exist, in particular due to the large N limit involved in holography. Thus the gravity dual theories only exemplify aspects of the dynamics. There are also bottom up models that have been constructed (often called AdS/QCD [123, 134]) which apply the basic tools of holography but are less rigorous. These models typically contain more free parameters - for example the early models imposed chiral symmetry breaking by hand and the quark condensate was a fitted parameter. More elaborate constructions such as [196] address many of these issues and fit QCD well.

The model we will use here, Dynamic AdS/YangMills [136], lies between the two extremes of top down and bottom up. The action is based on the Dirac Born Infeld (DBI) action of a D7 brane in AdS_5 which describes a quenched quark in the top down models. In examples with chiral symmetry breaking based on this action, deformations of the supersymmetric set up induce a running anomalous dimension for the quark condensate, which shows as a radially dependent mass for the scalar that describes the embedding [138, 197]. In the IR the Breitenlohner-Freedman bound [86] is violated and this scalar develops a vaccum expectation value dual to the quark condensate, which is therefore dynamically determined. The DBI action then naturally predicts the spectrum and couplings of a variety of bosonic and fermionic exitations/states. It is very natural to use this DBI action to describe the quark/meson physics for more complex models by simply feeding it the running anomalous dimension appropriate for those models - although one loses the prediction of the form of this running the spectrum remains a prediction. We will use the two loop running of the couplings in theses theories extended (beyond their formal regime of validity) into the non-perturbative regime to provide sensible ansatz for the runnings in all possible gauge groups and with quarks in all representations. The Dynamic AdS/YM theory can therefore make predictions for the spectrum of the full set of asymptotically free gauge theories proposed as composite Higgs models. A small number of previous holographic analyses of composite Higgs models exist [194, 195, 198, 199] but they do not attempt to include the particular N_c and N_f dependent runnings of the theories in the dynamics.

Recent work has also shown that it is straightforward to include higher dimension operators (HDOs), such as Nambu-Jona-Lasinio operators [200], into the Dynamic AdS/YM model [148, 201]. This is achieved by using Witten's double trace prescription [147]. We will review this mechanism and explore the role of higher dimension operators in our theories. In particular we will present a section where we study $\mathrm{N}_f = 2$ QCD to allow the reader to understand the ball-park success of the holographic model in a familiar setting. Here, to introduce the HDO work, we introduce, in the spirit of [202, 203], many

HDOs to "perfect" the predictions. This should be compared to perfecting a lattice action as introduced by Lüscher and Hasenfratz long ago [204, 205]. We introduce a UV cut-off corresponding to the scale where QCD transitions to the strong-coupling regime from the perturbative UV. Note that the gravity dual should be strongly coupled in the region where QCD becomes perturbative above this cut off. We show that HDOs, reflecting the matching at that scale, can improve the spectrum predictions, although with a growing loss of predictivity.

We will then turn to using our holographic model for composite Higgs models. The key component of composite Higgs models is that a strongly coupled gauge theory causes chiral symmetry breaking in the quark sector, generating four or more Nambu-Goldstone bosons [189]. By weakly gauging the global chiral symmetries the four then pseudo-Nambu Goldstone bosons (pNGBs) can be placed in the two-dimensional representation of $SU(2)_L$ to become the complex Higgs field. This strong dynamics is expected to happen at a scale of roughly 1-5 TeV. The Higgs Yukawa couplings must be formed by higher dimension operators from a flavour scale above the strong dynamics scale. It has been argued, for example in [206], that the electroweak gauge fields and top Yukawa interactions in the low energy effective theory of the pNGBs generates the standard model (SM) Higgs potential. We will not address the generation of the Higgs potential here, concentrating instead on the dynamics and spectrum of the strong coupled theory one level higher. The need for higher dimensional operators to give mass to the SM fermions motivates the study of related operators with a particular focus of their impact on the spectrum of the composite states.

Three theories have had particular focus in the literature. Note we will generically refer to fermions transforming under the strongly coupled gauge theory, in any representation, as quarks, in analogy to QCD (elsewhere they are referred to as hyper-quarks etc). Firstly, an $SU(2)$ model with two fundamental Dirac fermions breaks an $SU(4)/SO(6)$ global symmetry to $Sp(4)/SO(5)$ generating five Goldstones [207, 208]. Secondly, an $Sp(4)$ gauge theory with fundamental quarks has the same symmetry breaking pattern [191]. Thirdly, an $SU(4)$ theory with five quarks in the sextet representation breaks $SU(5)$ to $SO(5)$ generating fourteen Goldstone modes [192]. We will study these cases in detail and compare to lattice simulations of these theories, quenched versions or versions with slightly different fermionic content. The comparison is very favourable and leads us to place some trust in our model's predictions as flavours are unquenched or flavours added to make the precise content needed by composite Higgs models. Here we see the huge benefit of holographic models where the field content can be changed rapidly, albeit without the rigour of the lattice.

The generation of the top quark Yukawa coupling in composite Higgs models is difficult since it is so large. A possible mechanism to enhance it is for the strong dynamics to have baryons with the same symmetries as the chiral top quarks which they mix with via flavour higher dimension operators [143]. In the $Sp(4)$ model this can be achieved by adding quarks in the sextet representation [191]; and in the $SU(4)$ model by adding quarks in the fundamental representation [192] as we will explore in detail. These baryons naturally have order one couplings to the Higgs (pNGBs) generated by the strong dynamics. Even here a Yukawa coupling of order one is hard to achieve requiring anomalously light baryons (phenomenologically they must lie above 800-900 GeV or so [209, 210], dependent on the precise decay channels) and or large structure functions. Here we will investigate this dynamics

using holography. The D7-brane action, extended to its fermionic sector, naturally describes baryons (super-partners of the mesons) consisting of three fermions (a quark an anti-quark and an adjoint fermion in the root $\mathcal{N} = 2$ theory) as fermionic fields in the DBI action [1, 3, 82, 121]. We phenomenologically extend this description to describe the top partners which are also usually constructed from three constituents. We do indeed find it hard to generate a large top Yukawa coupling in the base theories. Here, as in [2], we propose a novel mechanism of adding an additional new higher dimension operator that can reduce the top partner masses. We explore the impact of this operators showing that a physical Yukawa coupling can be achieved by reducing the top partner mass relative to the vector meson mass along with simultaneous enlargements of the relevant structure functions. If the strong coupling scale is > 1 TeV then the top partner masses are still likely compatible with LHC constraints yet with a top Yukawa coupling of order one.

In particular our new results in these full theories include: meson decay constants beyond lattice analysis to date for the $SU(2)$ model; the meson spectrum and decay constants for the $Sp(4)$ model in the unquenched theory which has not been studied on the lattice; first computations of the axial meson and scalar (σ or S) meson sectors in an $SU(4)$ theory where other observables have been studied on the lattice (the theory has four Weyl sextet quarks and two flavours of Dirac fundamental quarks); and the full unquenched spectrum of the true proposed $SU(4)$ composite Higgs model (with five Weyl sextet quarks and three flavours of Dirac fundamental quarks), a theory that is beyond lattice study currently.

We will further exploit the power of holography by computing the predicted spectrum for the full class of twenty six models in the classification of [144]. Note, that we find that some of these models lie, at least based on the ansatz of the two loop running of the coupling, in the conformal window [211, 212] with an infra-red (IR) fixed point that is too small to break chiral symmetries. The scalar meson mass is particularly sensitive to the rate of running of the coupling in any given theory and some of these proposed models are walking theories with very low scalar masses (as expected from [181]; but also see [213–215] for an important discussion of the possible role of mixing with the glueball sector). The ability to see these effects is straightforward holographically but on the lattice needs both unquenched simulations and a wide separation of scales.

8.2 Dynamic AdS/YM

In this section we introduce the holographic model that we will use. The model was first suggested in [136]. Here, we refer to this model as *Dynamic AdS/YM* (Anti-de Sitter/Yang-Mills) to emphasise that it can be used to holographically describe the chiral symmetry breaking dynamics of any gauge theory (not just QCD), including with quarks in several, potentially inequivalent, representations.

The action for the model is inspired by the DBI (Dirac-Born-Infeld) action of a holographic top-down model involving a D7-brane embedded in AdS_5 or in a perturbed AdS_5 geometry. The DBI action is expanded to quadratic order in the embedding function X. A detailed description of this expansion in particular cases is described in [138, 197]. We also add an axial gauge field in the natural fashion familiar from AdS/QCD models [123]. We may think of this model as describing a single quark in the background of the gauge fields, which may include the contribution to the dynamics from any

other quarks even in the probe limit. Note here that the origin of the model at large N_c means the $U(1)_A$ flavour symmetry is not anomalous so the pNGB and so forth form part of the same $U(N_f)$ multiplet along with other flavours. In any case by placing fields in the adjoint representation of a flavour symmetry, and by tracing over the action, multiple mass degenerate quarks can be included directly.

In particular, the model has a field of dimension one, in terms of the gauge theory conformal scalings, for each of the relevant gauge invariant operators. For instance, X is dual to the complex quark bilinear - in QCD this is the operator $\bar{q}q$ but it can be any such dimension three, gauge invariant operator of the theory, as we will shortly expand on. The fluctuations of this field are dual to the σ (or S for scalar) and π mesons of the theory. We will write it as $X = Le^{i\pi}$. A_L^μ and A_R^μ are dual in QCD to the operators $\bar{q}\gamma^\mu q$ which generates the vector (the V or ρ) mesons and $\bar{q}\gamma^\mu\gamma_5 q$ which generates the axial vector (A) mesons, respectively.

Note in theories with quarks in real representations one forms a Majorana spinor from each flavour $\Psi_M = (\psi, -i\sigma^2\psi^*)$. The gauge invariant and Lorentz invariant condensates are then as in QCD written $X = \bar{\Psi}_M\Psi_M$ and one still inserts the appropriate gamma matrix structure into the operator X to describe vector and axial vector states - the former carry no charge under the broken symmetry, whilst the latter are charged. Apart from this change in meaning for X the spirit of the gravity description is then the same as in QCD.

The gravity action of Dynamic AdS/YM is

$$S_{boson} = \int d^5x\ \rho^3 \left(\frac{1}{r^2}(D^M X)^\dagger (D_M X) + \frac{\Delta m^2}{\rho^2}|X|^2 + \frac{1}{2g_5^2}\left(F_{L,MN}F_L^{MN} + (L \leftrightarrow R) \right) \right) . \tag{8.1}$$

The five-dimensional coupling may be obtained by matching to the UV vector-vector correlator [123], and is given by

$$g_5^2 = \frac{24\pi^2}{d(R)\ N_f(R)} , \tag{8.2}$$

where $d(R)$ is the dimension of the quark's representation and N_f(R) is the number of flavours in that representation.

The model lives in a five-dimensional asymptotically AdS (AAdS) spacetime, which is given by

$$ds^2 = r^2 dx^2_{(1,3)} + \frac{d\rho^2}{r^2} , \tag{8.3}$$

with $r^2 = \rho^2 + L^2$ the holographic radial direction corresponding to the energy scale, and with the AdS radius set to one. Note in D7 brane models [41, 120, 121] r is the RG scale of the gauge fields and ρ that for quark physics. The factors of ρ and L in the action and metric are implemented directly from the top-down analysis of the D3/probe-D7 brane system - there L corresponds to the direction perpendicular to the D7 in the 10 dimensional space. The factors ensure appropriate UV behaviour, such that the metric returns to pure AdS at the boundary, but also an IR behaviour where the fluctuations know about any chiral symmetry breaking through a non-zero value of L. From a bottom up perspective it is

natural for L to enter with ρ since ρ and L are both dimension one from the field theory perspective - in a sense equation (8.3) includes the backreaction of the geometry to the formation of the quark condensate. $dx^2_{(1,3)}$ is a four-dimensional Minkowski spacetime.

8.2.1 The running anomalous dimension & the vacuum

The dynamics of a particular gauge theory, including quark contributions to any running coupling, are included through the choice of Δm^2 in the action equation (8.1). In order to find the vacuum of the theory, with a non-zero chiral condensate, we set all fields to zero except for $|X| = L(\rho)$. For Δm^2 a constant, the equation of motion obtained from equation (8.1) is

$$\partial_\rho(\rho^3\partial_\rho L) - \rho\ \Delta m^2 L = 0\,. \tag{8.4}$$

When $\Delta m^2 = 0$, near the boundary of the AAdS space which corresponds to the UV, the solution is given asymptotically by $L(\rho) = m + c/\rho^2$, with $c = \langle\bar{q}q\rangle$ of dimension three and m, the mass, of dimension one (note again L and ρ have dimension one). For non-zero Δm^2, the solution takes the form $L(\rho) = m\rho^{-\gamma} + c\rho^{\gamma-2}$, with

$$\Delta m^2 = \gamma(\gamma - 2). \tag{8.5}$$

Here γ is precisely the anomalous dimension of the quark mass. The BF bound below which an instability occurs is given by $\Delta m^2 = -1$.

In the gauge theory, we expect γ to run. Therefore we impose this running at the level of equation (8.4) by allowing Δm^2 to depend on ρ. Our starting point is the perturbative results for the running of γ. Expanding equation (8.5) at small γ gives

$$\Delta m^2 = -2\gamma. \tag{8.6}$$

We proceed by determining γ from the gauge theory. Note that this relation means that the holographic model determines a theory to break chiral symmetry if the input form of γ passes through 1/2, when the BF bound is violated - we will use this criteria below (matching the assumptions in [211]).

Since the true running of γ is not known non-perturbatively, we allow ourselves to extend the perturbative results as a function of renormalization group (RG) scale μ to the non-perturbative regime. We will directly set the field theory RG scale μ equal to the holographic RG scale $r = \sqrt{\rho^2 + L^2}$. Note it is important that we let Δm^2 depend on L for the following reason. Chirally symmetry breaking occurs in the IR because the $L = 0$ state has a BF bound violation at small ρ. L then becomes non-zero, the condensate switches on, until the BF bound is not violated any more and the state becomes stable. However, if we did not have L in Δm^2 then the BF bound would remain violated even as L switches on and L would grow indefinitely. This mechanism happens naturally in the top down probe D7 systems. We consider the two-loop results for the running because this ansatz includes the possibility of conformal windows [211, 212] for ranges of N_f.

The two-loop result for the running coupling in a gauge theory with multi-representational matter is

given by

$$\mu\frac{d\alpha}{d\mu} = -b_0\alpha^2 - b_1\alpha^3\,, \tag{8.7}$$

with

$$\begin{aligned} b_0 &= \frac{1}{6\pi}\left(11C_2(G) - 2\sum_R T(R)N_f(R)\right)\,, \\ b_1 &= \frac{1}{24\pi^2}\left(34C_2^2(G) - \sum_R \left(10C_2(G) + 6C_2(R)\right)T(R)N_f(R)\right)\,. \end{aligned} \tag{8.8}$$

Here we have written the results for the number of Weyl fermion flavours in a given representation. To find the running of γ we then use the one-loop anomalous dimension

$$\gamma = \frac{3\ C_2(R)}{2\pi}\ \alpha. \tag{8.9}$$

Note we do not go beyond one loop here, since the running at large α is already a guess and moving beyond one loop in γ does not provide further features (again we are following the conventions of [211] here).

Now for a given theory we numerically solve equation (8.4) with our ansatz for Δm^2 for the function $L(\rho)$ that defines the vacuum. To do so, we need IR boundary conditions that we again import from the D3/probe D7 brane system. The initial conditions that we use are

$$L(\rho)|_{\rho=\rho_{IR}} = \rho_{\rm IR}\,, \qquad\qquad \partial_\rho L(\rho)|_{\rho=\rho_{IR}} = 0\,. \tag{8.10}$$

The first of these corresponds to an on-shell mass condition: once the IR mass, determined by $L(\rho)|_{\rho=\rho_{IR}} = L_{\rm IR}$, equals the energy scale $\rho = \rho_{IR}$, we stop the evolution of $L(\rho)$ to lower scales, since the quarks should now be integrated out. Geometrically, $\rho_{\rm IR}$ corresponds to the value of ρ at which the function $L(\rho)$ crosses a line at 45° in the L - ρ plane. The value of ρ_{IR} is fixed in each particular theory and for each choice of UV quark mass: we numerically vary ρ_{IR} until the value of L at the boundary is the desired quark mass. We refer to the corresponding configuration that describes the vacuum (for a given N_c, N_f, and quark mass) as $L_0(\rho)$ with IR value L_{IR} (this is effectively the constituent quark mass) at the IR cut off ρ_{IR}.

Note at this point we observe a crucial difference between our approach and previous papers on holgraphic composite Higgs models [194, 195], which use the boundary conditions to impose chiral symmetry breaking. Here though it is not the IR boundary conditions that cause the dynamics that we report. In our case the dynamics results from the BF bound violation (or not) for L in the bulk and the IR boundary conditions simply provide IR regularity independent of the model's dynamics.

If there are quarks in multiple representations, then we will simply replicate equation (8.1) for each representation. This ignores mixing between the mesons made of quarks in different representations, though different representations are still aware of each other through the choices of Δm^2. We will

discuss such cases and their subtleties in more specific models below.

8.2.2 The meson sectors

The mesons of the theory can be found by solving the equations of motion for fluctuations in the various fields of the model in equation (8.1). In each case a fluctuation is written as $F(\rho)e^{-ik.x}$, $M^2 = -k^2$ and IR boundary conditions $F(L_{IR}) = 1, F'(L_{IR}) = 0$ used. One seeks the values of M^2 where the UV solution falls to zero, so there is only a fluctuation in the vev of operator and not the source in the UV.

The fluctuations of $L(\rho)$ give rise to scalar mesons. They are obtained by writing $L = L_0 + S$, and where to linear order $r^2 = \rho^2 + L_0^2$. The equation of motion for the fluctuation reads

$$\partial_\rho(\rho^3\partial_\rho S(\rho)) - \rho(\Delta m^2)S(\rho) - \rho L_0(\rho)S(\rho)\frac{\partial\Delta m^2}{\partial L}|_{L_0} + M^2\frac{\rho^3}{r^4}S(\rho) = 0. \tag{8.11}$$

The vector-mesons are obtained from fluctuations of the gauge fields $V = A_L + A_R$ around the vacuum value of zero and satisfy the equation of motion

$$\partial_\rho(\rho^3\partial_\rho V(\rho)) + M_V^2\frac{\rho^3}{r^4}V(\rho) = 0. \tag{8.12}$$

To obtain a canonically normalized kinetic term for the vector meson we must impose

$$\int d\rho\ \frac{\rho^3}{g_5^2 r^4}V^2 = 1. \tag{8.13}$$

The dynamics of the axial-mesons ($A = A_L - A_R$) is described by the $\vec{x}, t$ components of A^N by the equations

$$\partial_\rho(\rho^3\partial_\rho A(\rho)) - g_5^2\frac{\rho^3 L_0^2}{r^2}A(\rho) + \frac{\rho^3 M_A^2}{r^4}A(\rho) = 0\,. \tag{8.14}$$

The difference between the V and A equations reflect that L carries axial charge so couples to A.

To compute decay constants, we must couple the meson to an external source. Those sources are described as fluctuations with a non-normalizable UV asymptotic form. Again we need to fix the coefficient of these solutions by matching to the gauge theory in the UV. External currents are associated with the non-normalizable modes of the fields in AdS. In the UV we expect $L_0(\rho) \sim 0$ and we can solve the equations of motion for the scalar, $L = K_S(\rho)e^{-iq.x}$, vector $V^\mu = \epsilon^\mu K_V(\rho)e^{-iq.x}$, and axial $A^\mu = \epsilon^\mu K_A(\rho)e^{-iq.x}$ fields. Each satisfies the same UV asymptotic equation

$$\partial_\rho[\rho^3\partial_\rho K] - \frac{q^2}{\rho}K = 0\,. \tag{8.15}$$

The solution is

$$K_i = N_i\left(1 + \frac{q^2}{4\rho^2}\ln(q^2/\rho^2)\right), \quad (i = S, V, A), \tag{8.16}$$

where N_i are normalization constants that are not fixed by the linearized equation of motion. Substituting these solutions back into the action gives the scalar correlator Π_{SS}, the vector correlator Π_{VV} and axial vector correlator Π_{AA}. Performing the usual matching to the UV gauge theory requires us to set

[123, 136]

$$N_S^2 = \frac{d(R)\ N_f(R)}{48\pi^2}, \quad N_V^2 = N_A^2 = \frac{g_5^2\ d(R)\ N_f(R)}{48\pi^2}. \tag{8.17}$$

where $d(R)$ is the dimension of the representation (note here again we write for Weyl fermions so for 2 Dirac flavours $N_f = 4$) .

The vector meson decay constant is then given by the overlap term between the meson and the external source

$$F_V^2 = \int d\rho \frac{1}{g_5^2} \partial_\rho \left[-\rho^3 \partial_\rho V \right] K_V(q^2 = 0) \,. \tag{8.18}$$

Note here that we are using the notation common in the AdS/QCD literature that the dimension two coupling between the meson and its source is called F_V^2. It is common in the phenomenology and lattice literature to call this quantity $\tilde{F}_V M_V$ (see for example [216]). Below where we compare to lattice results we must fix this choice. We have converted the lattice results to our definition of F_V in equation (8.18) which seems a purer statement of the strength of that coupling independent of the prediction of the mass. The axial meson normalization and decay constant are given by equation (8.13) and equation (8.18) with replacement $V \to A$.

The pion decay constant can be extracted from the expectation that $\Pi_{AA} = f_\pi^2$, with

$$f_\pi^2 = \int d\rho \frac{1}{g_5^2} \partial_\rho \left[\rho^3 \partial_\rho K_A(q^2 = 0) \right] K_A(q^2 = 0) \,. \tag{8.19}$$

We remind the reader that we have denoted the axial vector correlator by Π_{AA}.

To compute the pion mass in the presence of a quark mass we should formally work in the $A_\rho = 0$ gauge and write $A_\mu = A_{\mu\perp} + \partial_\mu \phi$. The ϕ and π fields (the phase of X) mix to describe the pion - we have

$$\begin{aligned} \partial_\rho(\rho^3 \partial_\rho \phi(\rho)) - g_5^2 \frac{\rho^3 L_0^2}{r^4}(\pi(\rho) - \phi(\rho)) = 0 \,, \\ q^2 \partial_\rho \phi(\rho) - g_5^2 L_0^2 \partial_\rho \pi(\rho) = 0 \,. \end{aligned} \tag{8.20}$$

Here we shoot out from the IR with $\phi(L_{IR}) = 1$, $\phi'(L_{IR}) = 0$, and then vary $\pi(L_{IR})$ and $q^2 = -M_\pi^2$ to find solutions where both ϕ, π vanish in the UV. This is numerically very intensive. Below for the non-zero quark mass cases, we will neglect the axial meson field to simplify the analysis. When substituting the lower equation of equation (8.20) into the upper one, we find

$$\partial_\rho \left(\rho^3\ L_0^2\ \partial_\rho \pi \right) + M_\pi^2 \frac{\rho^3\ L_0^2}{r^4} (\pi - \phi) = 0 \,. \tag{8.21}$$

We then assume $\phi \ll \pi$ and neglect the mixing, such that there is only the single equation for π to solve as for the other fluctuations. This is the natural description of the pion mass in the D3/probe D7 system before we added the axial field by hand. As we will see, the results below suggest that this is a sensible approximation.

In a particular $SU(4)$ model we will study below, lattice studies have identified an additional spin zero hadron (a tetraquark). Generically spinless states with UV dimension Δ can be described by adding to

the action an additional scalar field S,

$$S = S_{boson} + S_J\,, \qquad \text{with} \qquad S_J = \frac{1}{2}\int d^5x\ \rho^3\ \left(\nabla_M\nabla^M S + m^2 S^2\right)\,. \tag{8.22}$$

Fluctuations of this scalar $S = f(\rho)\ e^{ik\cdot x}$ in the background lead to the equation of motion

$$\partial_\rho^2 f(\rho) + 5\ \frac{\rho + L_0\ \partial_\rho L_0}{r^2}\partial_\rho f(\rho) + \frac{M^2}{r^4}f(\rho) - \frac{\Delta(\Delta-4)}{r^2}f(\rho) = 0, \tag{8.23}$$

where Δ is the conformal dimension of the operator that we consider.

8.2.3 The fermionic sector

One of the first new additions of this work is that we wish to allow for the inclusion of baryonic states in the Dynamic AdS/QCD theory. Here we are motivated by the mass of top partners in composite Higgs models which we will explore more below. Of course, in true large N_c holography baryons made of N_c quarks are very heavy stringy modes (for example described by a wrapped D5 with N_c strings attached in the basic AdS/CFT Correspondence [103]). However, there are fermionic bound states (baryons) described by the supergravity limit of the duality. In the D3/probe D7 system some fermionic superpartners of the mesons are made of a quark, an anti-quark and a gaugino and are described by fermionic excitations of the D7 world volume theory [82, 121]. Indeed in a preparatory paper we carefully worked through the D3/probe D7 system example [1] (see also [3]) and that work will lead us here. That a three fermion bound state can have such a description in a top down model suggests phenomenologically a proton made of 3 quarks in QCD or the top partners in the models we will discuss below could reasonable be modelled by simply placing a fermion in the bulk. The work of [178] has already trialled this in AdS/QCD with some phenomenological success.

In appendix D we provide a full derivation for placing a fermion in first AdS and then the Dynamic AdS/YM background. Here we simply summarize the results. We add to the action

$$S = S_{boson} + S_{1/2}\,, \qquad \text{with} \qquad S_{1/2} = \int d^5x\ \rho^3\ \bar{\Psi}\left(\not{D}_{\rm AAdS} - m\right)\Psi\,. \tag{8.24}$$

The four component fermion satisfies the second order equation

$$\left(\partial_\rho^2 + \mathcal{P}_1\partial_\rho + \frac{M_B^2}{r^4} + \mathcal{P}_2\frac{1}{r^4} - \frac{m^2}{r^2} - \mathcal{P}_3\frac{m}{r^3}\ \gamma^\rho\right)\psi = 0\,, \tag{8.25}$$

where M_B is the baryon mass and the pre-factors are given by

$$\begin{aligned}
\mathcal{P}_1 &= \frac{6}{r^2}\left(\rho + L_0\ \partial_\rho L_0\right)\,,\\
\mathcal{P}_2 &= 2\left((\rho^2 + L_0^2)L\partial_\rho^2 L_0 + (\rho^2 + 3L_0^2)(\partial_\rho L_0)^2 + 4\rho L_0\partial_\rho L_0 + 3\rho^2 + L_0^2\right)\,,\\
\mathcal{P}_3 &= \left(\rho + L_0\ \partial_\rho L_0\right)\,.
\end{aligned} \tag{8.26}$$

In five dimensions for the states of UV dimension 9/2, as appropriate for a three quark state, the bulk fermion mass is $m = 5/2$.

The four component spinor can then be written in terms of eigenstates of γ_ρ such that $\psi = \psi_+\alpha_+ + \psi_-\alpha_-$ where $\gamma_\rho\alpha_\pm = \pm\alpha_\pm$. The equation then becomes two equations, one for ψ_+ and one for ψ_-, obtained by replacing γ_ρ in equation (8.25) by ± 1 respectively. The two equations are though copies of the same dynamics with explicit relations between the solutions as we describe in Appendix A. Thus one need solve one only and from the UV boundary behaviour extract the source $\mathcal{J}$ and operator $\mathcal{O}$ values. The UV asymptotic form of the solutions are given by

$$\begin{aligned} \psi_+ &\sim \mathcal{J}\sqrt{\rho} + \mathcal{O}\frac{M_B}{6}\rho^{-11/2}\,, \\ \psi_- &\sim \mathcal{J}\frac{M_B}{4}\frac{1}{\sqrt{\rho}} + \mathcal{O}\rho^{-9/2}\,. \end{aligned} \tag{8.27}$$

The full solution must be found numerically - here we use the D3/probe D7 system as a guide to impose the IR boundary conditions

$$\begin{aligned} \psi_+(\rho = L_{IR}) &= 1, \qquad \partial_\rho\psi_+(\rho = L_{IR}) = 0\,, \\ \psi_-(\rho = L_{IR}) &= 0, \qquad \partial_\rho\psi_-(\rho = L_{IR}) = \frac{1}{L_{IR}}\,. \end{aligned} \tag{8.28}$$

Note that we impose these boundary conditions at $\rho = L_{IR}$ rather than at $\rho = 0$ as in the supersymmetric case in [1, 3].

8.2.4 Higher dimensional operators

Another key ingredient we wish to explore here is the inclusion of higher dimension quark operators using Witten's double trace prescription [147, 148]. This prescription amounts to introducing a cut-off at some scale Λ_{UV} in the gauge theory or an upper boundary in AdS at $\rho = \Lambda_{UV}$. In the field theory for some operator $\mathcal{O}$ we include a "double trace" higher dimensional operator (HDO) by

$$\mathcal{L}_{UV} = G\mathcal{O}^\dagger\mathcal{O},\,, \tag{8.29}$$

where G is a dimensionful coupling. Now were $\mathcal{O}$ to acquire a vacuum expectation value then via equation (8.29) there would be an effective source at the boundary

$$\mathcal{J} = G\langle\mathcal{O}^\dagger\rangle\,. \tag{8.30}$$

Note that the analysis of [147, 148] shows that adding the HDO as a boundary term in AdS and then minimizing the bulk and boundary action naturally reproduces equation (8.30).

Until now we have considered a sourceless theory and in any computation of the background ($L_0(\rho)$) or any fluctuation we have only allowed solutions where the appropriate source vanish. For example, it is precisely this prescription that picks out discrete values of the bound state masses. Now though we will allow all of the solutions with non-zero $\mathcal{J}$ and re-interpret them as part of the source free theory but with the HDO present: asymptotically we read off $\mathcal{J}, \mathcal{O}$ and then use equation (8.30) to compute G. Now we can sort through these solutions and find the masses of bound states which match the boundary condition for a particular G.

The operators we will consider in Dynamic AdS/YM, which we will explore below, are

$$\frac{g_S^2}{\Lambda_{UV}^2}|\bar{q}q|^2\,, \qquad \frac{g_V^2}{\Lambda_{UV}^2}|\bar{q}\gamma^\mu q|^2\,, \qquad \frac{g_A^2}{\Lambda_{UV}^2}|\bar{q}\gamma^\mu\gamma_5 q|^2\,, \qquad \frac{g_{\rm B}^2}{\Lambda_{UV}^5}|qqq|^2\,, \tag{8.31}$$

where the g_i are dimensionless couplings.

8.3 Two-flavour QCD

To demonstrate the Dynamic AdS/YM model and the role of HDOs, we begin with a study of $N_c = 3, N_f = 2$ QCD. We first determine the vacuum of the theory for the massless theory by finding the function $L(\rho)$ using equation (8.4). Then we compute the spectrum of the model by looking at fluctuations, study the quark mass dependence and the n dependence of excited states. Finally we consider introducing a cut off where the theory runs to a perturbative regime and include HDOs at that scale to improve the IR description.

The key input for any theory we study is the form of γ we input in equation (8.6). The formulae for the one and two-loop coefficients of the β-function and the one-loop anomalous dimension for QCD are, with N_f the number of Weyl flavours in the fundamental and $\bar{N}_f$ the number in the anti-fundamental representations

$$\begin{aligned} b_0 &= \frac{1}{6\pi}\left(11N_c - (N_f+\bar{N}_f)\right)\,, \\ b_1 &= \frac{1}{24\pi^2}\left(34{N_c}^2 - 5N_c(N_f+\bar{N}_f) - \frac{3}{2}\frac{{N_c}^2-1}{N_c}(N_f+\bar{N}_f)\right)\,, \\ \gamma &= \frac{3({N_c}^2-1)}{4N_c\pi}\alpha\,. \end{aligned} \tag{8.32}$$

We choose an initial value for $\alpha(\mu=1)=0.65$ for the numerical analysis but will set the scale with the ρ-meson mass below. The resulting running of Δm^2 in the Dynamic AdS/QCD model is shown in figure 8.1 on the left - the BF bound is violated close to the scale $r=\mu=1$.

We can now compute the vacuum for the theory by solving equation (8.4) subject to the boundary conditions in equation (8.10). We solve the equation numerically and show the results on the right in figure 8.1 for different asymptotics of $L(\rho)$ corresponding to different UV masses.

8.3.1 The meson and baryon spectrum of QCD

To compute the meson masses, we must set g_5 in equation (8.1) by matching to the UV vector-vector correlator in perturbative QCD

$$g_5^2 = \frac{48\pi^2}{N_c(N_f+\bar{N}_f)}\,. \tag{8.33}$$

Having found the massless vacuum, we can now study the spectrum as described in Section 2. We set all sources to zero in the UV. The results for the ground states in each channel are shown at the top of Table 8.1 using the ρ-meson mass to set the scale. Note we begin to use notation we will use later - labelling the holographic model as AdS/SU(3) to indicate the gauge group and $2F\ 2\ \bar{F}$ to show there are 2 Weyl fermions in the fundamental and two in the anti-fundamental representation (ie 2

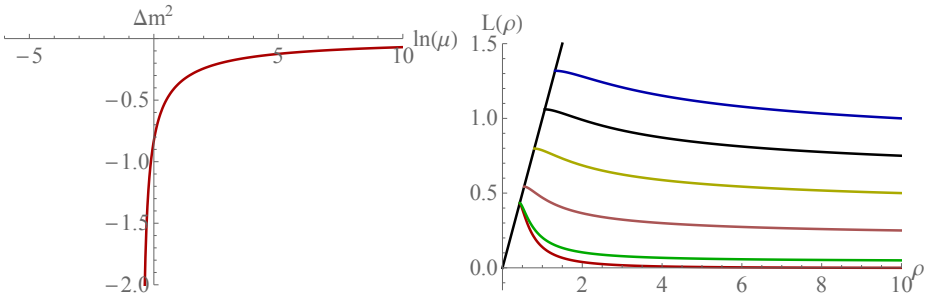

Figure 8.1: The $N_c = 3, N_f = 2$ QCD model: on the left we display the running of the AdS scalar mass Δm^2 against log RG scale (we use $\mu = \sqrt{\rho^2 + L^2}$ in the holographic model). On the right we show the the vacuum solution for $|X| = L(\rho)$ against ρ. The 45° line is where we apply the on mass shell IR boundary condition in equation (8.10). The $L(\rho)$ with a massless UV quark has $L_{IR} = 0.43$. The quark masses from top to bottom are 1, 0.75, 0.5, 0.25, 0.05, 0. Here units are set by $\alpha(\rho = 1) = 0.65$.

Dirac fermions in the fundamental). Comparing to the physically measured QCD values for the ground states, we see the ρ- and A-meson sectors are reasonably described but the pion decay constant is low (although we have not yet included a UV quark mass). The σ (S) mass is high, but possibly should be compared to the $f_0(980)$ if the $f_0(500)$ is a pion bound state [217] (in which case it fits well). The proton mass is clearly too high though.

We can compute the quark mass dependence of the meson masses also. We display the results in figure 8.2 including fits and comparisons to lattice data. The top two plots show that at low quark mass the pion mass squared is linear in m_q as required by the Gell-Mann-Oakes-Renner relation whilst at larger m_q the behaviour reverts to depending on m_q^2 as for the other mesons. In the lower plot we show the other meson masses as a function of M_π^2. The lattice data is extracted by eye from the plots in for example [218–220] so we don't give errors - they provide a guide to the expected order of magnitude. Note the coefficients are dimensionful so depend on the choice for the setting of the scale. The comparison is reasonable at the level of a factor of two except for the σ where our estimate of the mass is high and the gradient low, perhaps reflecting the difficulty with identifying the state we have already encountered.

Finally it is also interesting to look at the masses of higher excited states of the mesons. We are wary of this comparison - at infinite N_c the AdS/CFT description of excited states remains a point-like supergravity description whilst in QCD, at lower N_c, we expect, as the quarks separate, the confining strings between them to become apparent [221]. One might therefore only expect the lowest excited state(s) to be well described by the methods we are using. It has been argued that the excited state masses should scale with the excitation number n as $\sqrt{n}$ [221] whilst in standard AdS/QCD models they scale as n. In [135, 222] it was argued that rather dramatic changes to the deep IR would be needed to make highly excited states scale as $\sqrt{n}$ - this approach is not obviously reintroducing string like behaviour though. So it is interesting to look at the low lying n masses in our description. In figure 8.3 we show the wave functions for the first few excited ρ-meson states and plot the masses against n. In fact they are rather linear in n and the model, unsurprisingly, does not capture the string like behaviour. We display the values of the first excited states in Table 8.1 where they come out high. Below we will take a different approach to adding string like structure back into the model by including

Observables (MeV)	QCD	AdS/$SU(3)$ 2 F 2 $\bar{F}$	Deviation
M_ρ	775	775*	fitted
M_A	1230	1183	- 4%
M_S	500/990	973	+64%/-2%
M_B	938	1451	+43%
f_π	93	55.6	-50%
f_ρ	345	321	- 7%
f_A	433	368	-16%
$M_{\rho,n=1}$	1465	1678	+14%
$M_{A,n=1}$	1655	1922	+19%
$M_{S,n=1}$	990 /1200-1500	2009	+64%/+35%
$M_{B,n=1}$	1440	2406	+50%

Table 8.1: The predictions for masses and decay constants (in MeV) for $N_f = 2$ massless QCD. The ρ-meson mass has been used to set the scale (indicated by the *).

HDOs which does seem to improve the predictions for at least the $n = 1$ states as we will see.

8.3.2 The nucleon-σ Yukawa coupling

A further important quantity is the nucleon σ Yukawa coupling strength, which we estimate here. We must normalize the kinetic term of the scalar and the baryon using

$$\mathcal{N}_S \int d\rho \, \frac{\rho^3}{(\rho^2 + L_0^2)^2} \, S^2(\rho) = 1, \qquad \mathcal{N}_B \int d\rho \, \frac{1}{\sqrt{\rho^2 + L_0^2}} \, \psi^2(\rho) = 1 \, . \tag{8.34}$$

The precise expression for the dynamically determined Yukawa coupling would depend on the action mixing the L and ψ fields beyond quadratic order and there are a number of terms one could write on dimensional grounds with free couplings. An example term that will contribute is

$$y_{NN\sigma} = \left| \int d\rho \; \rho^3 \frac{\partial_\rho S \; \partial_\rho L_0 \; \psi^2}{(\rho^2 + L_0^2)^2} \right| . \tag{8.35}$$

For this case, we find $y_{NN\sigma} = 1.47$, which is of order one as one might expect. We stress again though that while this is indicative of the expectation that the coupling will be of order one, it is not a prediction because we can multiply by an arbitrary coupling in our holographic model.

8.3.3 Higher dimensional operators

We now turn to demonstrating the effects of the addition of higher dimensional operators to the Dynamic AdS/YM description of two-flavour QCD. The philosophy is to include a UV cut off at a scale corresponding to the transition region from strong to weak coupling - at higher scales the gravity description is expected to break down (become strongly coupled). There is an expectation that QCD will have generated HDOs at this matching scale. In addition one can consider the HDOs as potentially

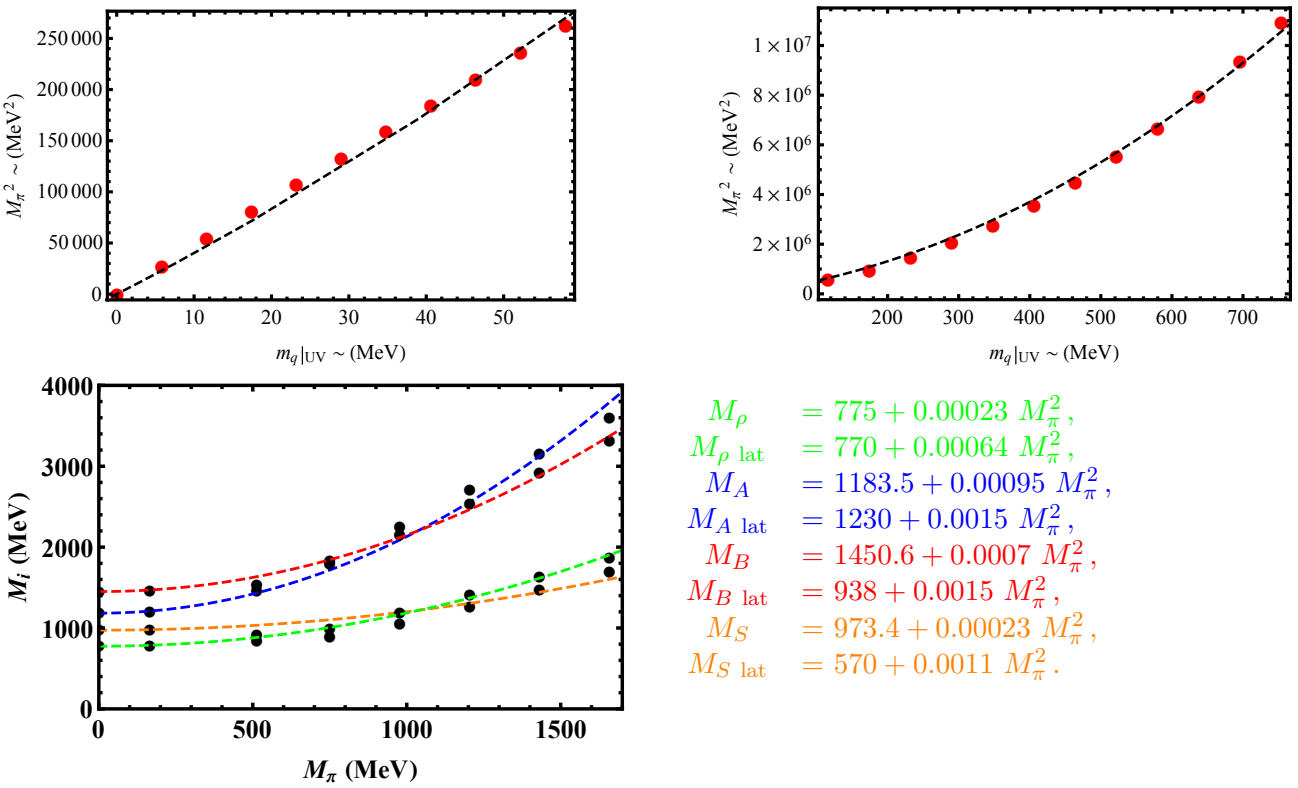

Figure 8.2: The top figures show the pion mass squared aginst the UV quark mass. The dashed black lines show the fit we obtained which is given by $M_\pi^2 = 3871 m_q + 13.45 m_q^2$. In this formula the pion mass is given in MeV. The bottom plot shows the other meson and baryon masses against M_π and the best fits obtained in our model. In these formulae the pion mass is also given in MeV. For the reader's convenience, we remind here that the lattice data is extracted by eye from the plots in for example [218–220]. This is why we do not provide errors. They are, however, important as they provide a guide to the expected order of magnitude.

including stringy effects into the gravity description as well. We enact this in the holographic model by putting a boundary at $\rho = 10$ roughly 10 times the scale of chiral symmetry breaking. Using the ρ-meson mass to set the scale this corresponds to a scale of about 6 GeV.

Let us start, as an example, with the analysis of the vector mesons. Previously we solved equation (8.12) which has UV asymptotics of the form $\mathcal{J} + \langle \mathcal{O} \rangle / \rho^2$. We only accepted solutions for values of M_V^2 where $\mathcal{J} = 0$ (see figure 8.3). Now though we will enlarge the set of available solutions to those with all values of $\mathcal{J}$ as shown on the left in figure 8.4. We now interpret these solutions as having $\mathcal{J} = 0$ but the higher dimension operator $g_V^2/\Lambda_{UV}^2 |\bar{q}\gamma^\mu q|^2$ present. We extract $\mathcal{J}$ and $\langle \mathcal{O} \rangle$ from the asymptotics and compute the four fermion operator coupling g_V^2 using equation (8.30). We can then plot the vector meson mass as a function of g_V. This is displayed on the right in figure 8.4. We see here that the mass of the bound state and the first excited state fill out the available mass values between the ground state mass and the first excited state masses at $g_V^2 = 0$ with a discontinuity between $g_V^2 = \pm\infty$. In addition positive g_V^2 drives the ground state mass below its value at $g_V^2 = 0$ and to zero as $g_V^2 \to \infty$. There is never a tachyonic state here. Note that the first excited state's mass does not fall below the mass of

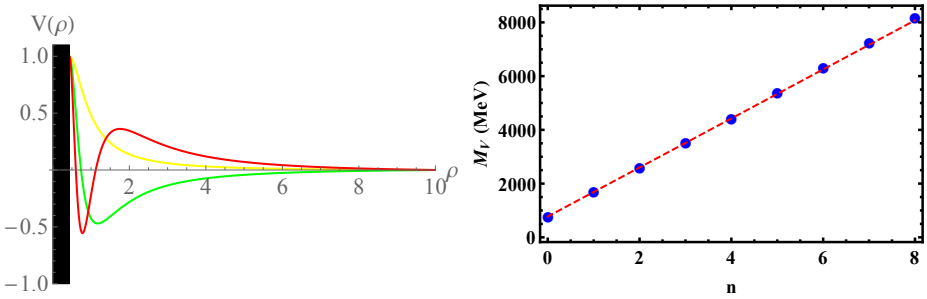

Figure 8.3: On the left, we show the normalizable solutions to the equations of motion for the vector meson (the black rectangle covers the region below the IR cut off). They are obtained for $M_V = 1.337(775\text{ MeV}), 2.895(1677.9\text{ MeV}), 4.45(2578.9\text{ MeV})$. On the right we show the numerical masses - blue dots - and the spectral curve that we obtained by fitting to the first six states and verified against the next three. Here, n is the number of nodes of the wave-functions.

the ground state at $g_V^2 = 0$. We repeat this computation for the axial vector meson and show the

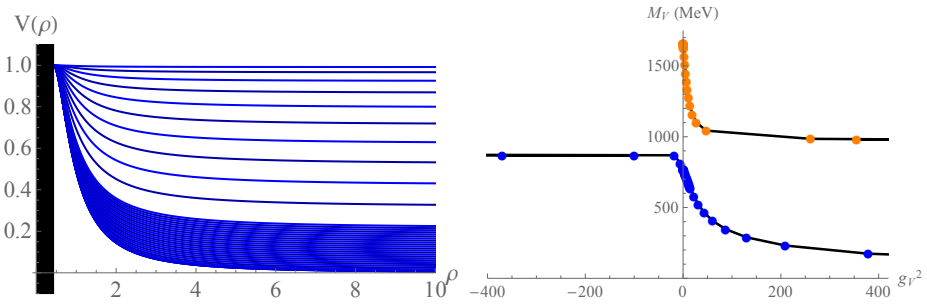

Figure 8.4: On the left the holographic wave functions of the vector meson ground state for various g_V^2 - the ground state at $g_V^2 = 0$ is the lowest curve; as M^2 decreases, g_V^2 increases and these are the higher curves. The black region represents the region below the IR cut off ρ_{IR} below which the quarks have become very massive and need to be integrated out. On the right we plot the associated masses against coupling g_V^2 extracted from those solutions - blue points are the ground state (corresponding to the left hand points), the orange points are the first excited states.

results in figure 8.5. The behaviour of the mass with g_A is very similar to that of the vector mass with g_V except that it appears to asymptote to a fixed non-zero value as $g_A^2 \to \infty$.

Next we consider the scalar meson of the theory where there is a new phenomenon. We begin by solving equation (8.11) for the scalar meson fluctuations in the background embedding with zero UV quark mass, allowing all M_S^2 values and extracting the g_s^2 coupling of the higher dimension operator

$$g_S^2/\Lambda_{UV}^2|\bar{q}q|^2. \tag{8.36}$$

We refer to this operator as a Nambu-Jona-Lasinio (NJL) operator. In figure 8.6 we show that the scalar becomes tachyonic at a finite value of g_S^2. This indicates that the vacuum has become unstable at larger g_S^2. Here though we understand this instability. Consider again the solutions of the background embedding shown in figure 8.1, including now the solutions with non-zero mass in the UV. We include all these solutions with non-zero sources as solutions of the theory with the HDO present and at the level of the background determine g_s^2. In the right hand plot in figure 8.6 we show the IR quark mass

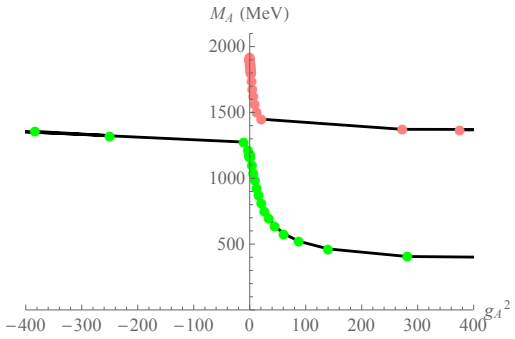

Figure 8.5: The masses of the pseudovector meson ground state and first excited state as a function of g_A^2.

L_{IR} against g_S^2. Here we interpret the $\rho = 0$ behaviour of the function $L_0(\rho)$ as the constituent quark mass. It shows that around the same critical value of g_S^2, where the scalar became tachyonic, the more massive vacua of the theory with a non-zero UV source emerge. This is the well known dynamics of the Nambu-Jona-Lasinio model [200] - this has been investigated before in a holographic context in [223]. Note it is not a pure second order transition with the IR mass rising from zero because the base QCD theory already contains chiral symmetry breaking - the NJL interaction just enhances this mass generation. If the σ mass is computed in the true vacuum, where $L_0(\rho)$ includes the effect of g_s^2, then at any g_S^2 there is no tachyonic behaviour. It is important to note that the vacuum embeddings in

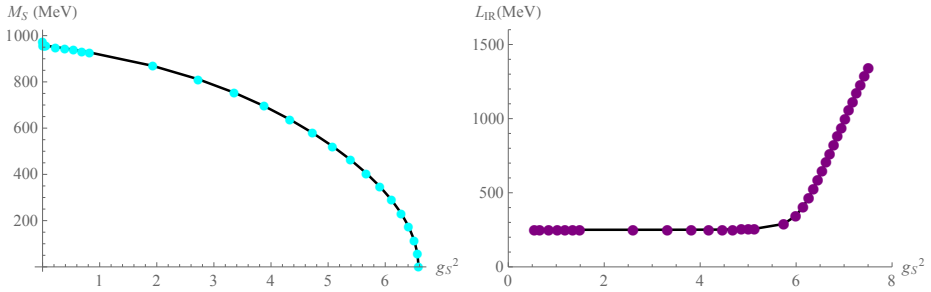

Figure 8.6: The instability of the massless embedding in the presence of an NJL interaction: on the left we show the mass of the σ scalar in the massless background of figure 8.1 (shown in red there) - it becomes tachyonic beyond a critical value of g_s^2. On the right we show the IR quark mass L_{IR} against the NJL coupling as interpreted from the embeddings with a source in figure 8.1. We see that the tachyon instability is related to the NJL interaction changing the vacuum by enhancing chiral symmetry breaking.

figure 8.1 have two interpretations - either there is an explicit UV mass for the quarks or a UV HDO is present. At the level of the solutions in figure 8.1 there is no distinction but there is at the level of the fluctuations. If there is a UV quark mass only present, then in the fluctuation calculation we must require that asymptotically in the UV there is only a vev for the operator and no $\mathcal{J}$. On the other hand, if we interpret all of the UV source in the embedding as being due to the NJL operator then we must determine the value of g_S from the background. Then we have to enforce that same value at the level of the fluctuations. Of course, most generally there can also be a mixture of quark mass and NJL operator in which case one needs to be careful to apply the appropriate g_S^2 for the fluctuation calculation.

Finally we can introduce a baryon squared HDO, $\frac{g_B^2}{\Lambda_{UV}^5}|qqq|^2$, to change the baryon mass. The results are shown in figure 8.7. In fact this plot was our initial motivation for this work since we were interested in bringing the proton mass down relative to the ρ-meson mass in AdS/QCD. As we will see later, they may be similarly used to generate light baryonic top partners in BSM models. Figure 8.7 shows similar features to the ones for the masses of the vector meson and axial-vector meson. enhances this mass

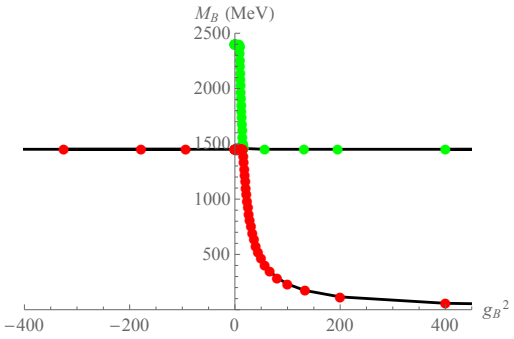

Figure 8.7: The effect of adding higher-dimensional operators on the mass spectrum of the baryon. The red dots are the results when we drive the ground state lighter and the green ones depict the first excitation.

generation. If the σ mass is computed in the true vacuum, where $L_0(\rho)$ includes the effect of g_s^2, then at any g_S^2 there is no tachyonic behaviour.

8.3.4 Perfecting two flavour QCD

Finally for two flavour QCD we will consider perfecting the holographic description [202, 203]: that is using HDOs to correct for the presence of a finite cut off. We will consider the description to only exist below $\rho = 10$ (approximately 6 GeV) and include HDOs to improve the description. These HDOs are intended to represent the physics of the perturbative regime and of the regime where the theory transitions from weak to strong coupling, which have been integrated out above the cut off. In principle one would like to explicitly match but presumably the intermediate, somewhat strongly coupled regime between perturbative QCD and where the holographic description is sensibly weakly coupled will make this matching hard. Thus we simply tune the HDOs couplings at our somewhat adhoc choice of UV cut off to match the observed mass spectrum.

To bring the decay constant f_π to its measured value we allow ourselves to move away from the L_0 corresponding vanishing quark mass. This can be interpreted either as including a small bare quark mass or a four fermion operator for $\bar{q}q$ - we find $m_q|_{UV} = 0.06576$ or equivalently $g_S^2 = 4.59$. Since we use the ρ mass to fix the scale, we can use the g_V^2 coupling to tune the ratio of F_V/M_V^2 to the observed value. We then use g_A^2, g_B^2 to arrange the masses of the axial vector, and baryon to their observed masses. The resulting spectrum is shown in table 8.2. Clearly this is a much better description of the ground state QCD spectrum than in table 8.1 if only because we have tuned most of the parameters! f_A is a prediction and lies closer to the data than before. The scalar mass is also a prediction and here, where we have interpreted the UV quark mass as the presence of g_S^2, the result has dropped closer to the mass of the $f_0(500)$ resonance. The predictions for the first excited states' masses, the final four

Observables (MeV)	QCD	Dynamic AdS/QCD	HDO coupling
M_V	775	775	sets scale
M_A	1230	1230	fitted by $g_A^2 = 5.76149$
M_S	500/990	597	prediction $+20\%/-40\%$
M_B	938	938	fitted by $g_B^2 = 25.1558$
f_π	93	93	fitted by $g_S^2 = 4.58981$
f_V	345	345	fitted by $g_V^2 = 4.64807$
f_A	433	444	prediction +2.5%
$M_{V,n=1}$	1465	1532	prediction +4.5%
$M_{A,n=1}$	1655	1789	prediction +8%
$M_{S,n=1}$	990/1200-1500	1449	prediction +46%/0%
$M_{B,n=1}$	1440	1529	prediction +6%

Table 8.2: The spectum and the decay constants for two-flavour QCD with HDOs from figure 8.7 used to improve the spectrum.

entries in the table, have all moved closer to the experimental values too - possibly this means that the HDOs are including some of the stringy effects the supergravity approximation excludes. The mass of the first excited state of the scalar is quite far off again, as in section 8.3.1, suggesting that interpreting these states is difficult. Overall though we conclude that the improvement method used is sensible. In principle one could go further and allow corrections to the UV matchings of the coupling g_5^2 and the normalization of the correlators in equation (8.17) but then we would lose essentially all predictivity.

8.4 Composite Higgs Models

The holographic model we have used above to describe QCD with higher dimension operators can naturally be extended to other non-abelian gauge theories in which a dimension three, gauge invariant quark bilinear condenses. The key idea is to simply change the running of the anomalous dimension for the quark bilinear. The bound states are then those associated with that operator with inserted gamma matrix structure. It is natural to apply this modelling to proposed strongly coupled models of physics beyond the Standard Model (BSM). In [188, 224], one of the authors has already studied predictions of such models for technicolour theories, including examples where the dynamics is enhanced by Nambu-Jona-Lasinio operators [223] and where extended technicolour interactions are included as HDOs for the generation of the top mass [225]. In this section we will apply these techniques to a further class of BSM models, the Composite Higgs Models.

8.4.1 Setting the scene

Review of composite Higgs models

The crucial ingredient in composite Higgs models is a strongly coupled sector that breaks a global symmetry generating Nambu-Goldstone bosons. By weakly gauging part of the global symmetries the Standard Model (SM) gauge groups are introduced and 4 of the then pseudo Nambu-Goldstone bosons

(pNGB) are identified with the SM Higgs. Realistic models have to contain the Higgs fields as a $(2,2)$ representation of the custodial symmetry group. Gauging the SM $SU(2)_L \times U(1)$ leads to an explicit breaking of the global group which in turn implies that a potential for the pNGBs is generated at loop-level. Moreover, in the low-energy theory one assumes that HDOs have also generated the top Yukawa coupling. The effective cut off on these loops is given by the strong coupling scale $\Lambda_S \simeq 4\pi f_\pi$ where here f_π is the pion decay constant of the $SU(4)$ gauge theory. Typically, Λ_S is assumed to be at a scale of order 1-5 TeV. The potential is of the form [206]

$$V_h = -C_{LR}(3g_1^2 + g_Y^2)\cos^2\left(\frac{h}{f}\right) + \frac{y_t^2}{2}C_t \sin^2\left(\frac{2h}{f}\right) . \tag{8.37}$$

Here C_{LR} and C_t are low-energy couplings of the effective theory below the strongly coupled group's scale, which can be expressed in terms of correlation functions within the theory (see e.g. [206] for details in the case of an explicit $SU(4)$ model). We will not revisit these low energy computations further here, but instead concentrate on the strong dynamics sector at the higher scale that generates the pNGB fields.

Explicit models of the top quark Yukawa coupling require more elaborate models. In the spirit of extended technicolour [226], one can simply include HDOs of the form where $\mathcal{F}$ are generically the composite fields that make up the Higgs. Λ_{UV} must probably be at least 5 TeV, making it hard to generate the large top mass. Such couplings also potentially suffer from Flavour Changing Neutral Currents.

$$\frac{1}{\Lambda_{UV}^2}\bar{t}_L\bar{\mathcal{F}}\mathcal{F}t_R\,, \tag{8.38}$$

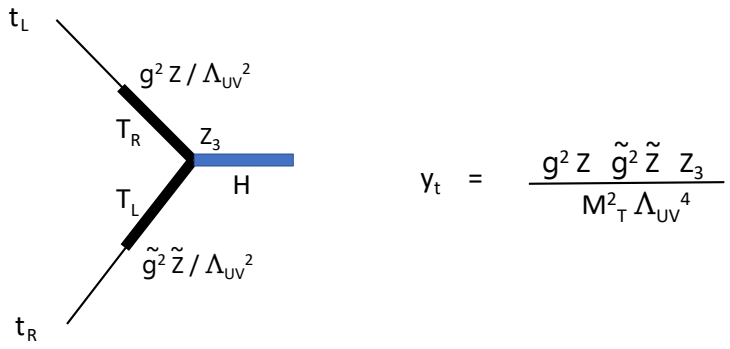

Figure 8.8: The diagram responsible for the generation of the top Yukawa coupling. t_L, t_R are the standard model top quarks, T_L, T_R the top partners - they mix via the HDOs with couplings g and $\tilde{g}$ - there are Z form factors associated with the formation of the top partner baryons. H is the pNGB that becomes the Higgs which has an order one Yukawa coupling to the top partners Z_3.

Another possibility for generating the top mass, often referred to as partial compositeness, is that the left and right-handed top particles t_L and t_R mix with baryon-like spin 1/2 states in the gauge theory T_L, T_R with the same quantum numbers [143]. These baryons are frequently called top partners. They will be involved in the strong dynamics and so have an order one Yukawa coupling to the Higgs. The

diagram in figure 8.8 then generates a contribution to the top Yukawa coupling as shown.

Here the Z factors are three structure functions that depend on the strong dynamics. The top-top partner mixing factors result from the couplings of HDOs such as

$$\frac{g^2}{\Lambda_{UV}^2}\bar{t_L}\mathcal{F}\mathcal{F}\mathcal{F}\,, \tag{8.39}$$

where the $\mathcal{F}$ are again generically representing the fermions that T_R is made from. We expect Z_3 to be of order one since it is generated by the strong dynamics - it is analogous to the nucleon-σ or π coupling in QCD. The Z and $\tilde{Z}$ factors (setting $g = \tilde{g} = 1$) will take the form $\Lambda_S^3/\Lambda_{UV}^2$ where Λ_S is the strong coupling scale. If the top partner's masses are of order Λ_S, then the Yukawa is given by

$$y_t \simeq \Lambda_S^4/\Lambda_{UV}^4 \tag{8.40}$$

which, assuming a separation of at least a factor of 3 between the flavour scale and the strong coupling scale, makes the top mass a factor of 100 too light. We will compute the Z factors and M_T holographically below where we indeed find that a large top Yukawa cannot be achieved in this way.

To combat the small Yukawa coupling size one could try to lower M_T or reduce the power of Λ_{UV} in the denominator. One proposed solution is walking dynamics [227]. In a walking theory the dimension of the fermions in equation (8.39) are lower at Λ_{UV} and then the powers of Λ_{UV} reduce (see for example [191, 228] for discussion). Here, though, we will provide a new mechanism that allows an order one top Yukawa coupling as needed for the top mass. To generate the large top mass one could hope the top partners are anomalously light relative to the strong scale Λ_S by a factor of 3 or more, but generically there is no reason to expect this. However, here we will realize such a mechanism: in particular we will include a new HDO that reduces to a shift in the top partners' mass at low energies, using the holographic HDO implementation introduced in sections 8.2.4 and 8.3.3. We show that the top Yukawa coupling can be made of order one by lowering the top partners' mass to roughly half the vector meson mass in the strongly coupled sector. This appears to be consistent with experimental constraints and provides a mechanism for generating an order one top Yukawa coupling.

A comprehensive analysis of the group theoretic possibilities for the strong sector underlying composite Higgs models with top partners was performed in [144]. We will analyze all 26 models using our holographic techniques. However, we also show that some of these models lie, at least based on the ansatz of the two loop running of the coupling, in the conformal window [211, 212] with a infra-red (IR) fixed point that is too small to break chiral symmetries. In the theories that do break symmetries dynamically we derive the values of the masses of the vector, scalar, axial mesons, and spin-1/2 baryon as well as the decay constants.

There are three scenarios that we will consider in considerable detail here, since they were already studied within lattice gauge theory [229–233]. We will start with a simple $SU(2)$ gauge theory with quarks in the fundamental representation (which in the classification of [144] is among the $Sp(2N)$ models). We will then discuss two models, one based on the gauge group $Sp(4)$, originally proposed in [191], and one based on the gauge group $SU(4)$ proposed in [192]. These models contain additional

pNGBs beyond the Higgs. We will not address their mass generation in the low-energy theory, though. Instead, we will concentrate on the bound states at the higher, strongly coupled scale.

Model classification

Since we will be discussing many different models, it is important to be able to clearly but succinctly identify them. We will label models by their gauge group and the matter content of the model. We give the number of Weyl fermions in the representations F for the fundamental, A_n for the n index antisymmetric representation, S_n for the n index symmetric representation, G for the adjoint and s for the spinor representation. We use a bar for the anti-representation. Thus, for example, we can fully specify a model as $Sp(2N_c)$ $aG,\ bF$, which means an $Sp(2N_c)$ gauge group with a Weyl flavours in the adjoint and b in the fundamental of the group. We will refer to the holographic description of such a model as $AdS/Sp(2N)$ aG, bF. We also note that we will refer to all fields in representations of the flavour group as 'quarks' in analogy to QCD.

Lattice data in a normalization adapted to holography

In the sections below, we will present data from a variety of lattice collaborations [229–233]. In order to present them in a uniform manner we have manipulated the data from some of the original papers. In particular, we choose to present all quantities as dimension one quantities (mass or decay constant) using one of the representation's vector meson mass to set the scale. Wherever possible, we give errors on the quantities we have extracted from lattice papers.[2] We propagate them using the formula:[3]

$$C = \sqrt{\frac{A}{B}}, \qquad \text{then} \qquad dC = \sqrt{\frac{dA^2}{4AB} + \frac{AdB^2}{4B^3}}. \tag{8.41}$$

We note again that we are using the notation common in the AdS/QCD literature that the dimension two coupling between the meson and its source is called F_V^2. It is common in the phenomenology and lattice literature to call this quantity $\tilde{F}_V M_V$ (see for example [216]). We have moved any lattice results we quote below to our definition of F_V as discussed in section 8.2.2.

8.4.2 $SU(2)$ gauge theory with 2 Dirac fundamental quarks - $SU(2)$ $4F$

One of the simplest gauge theories that can underlie composite Higgs models is an $SU(2)$ gauge theory with two Dirac quarks in the fundamental representation [207] (or two Weyl fermions in each of the F and $\bar{F}$). The pseudo-real nature of the fundamental of $SU(2)$ means that the naive $SU(2)_L \times SU(2)_R$ symmetry of the quarks is enhanced to an $SU(4)$ flavour symmetry [208] (the 2 and $\bar{2}$ are identical). The condensation pattern is of similar structure as in QCD ($\langle \bar{u}_L u_R + \bar{d}_L d_R + h.c. \rangle$), which then breaks the $SU(4)$ flavour symmetry to $Sp(4)$. Five generators are broken so there are 5 pNGBs.

It is straightfoward to describe the model using our AdS/YM description - we simply dial $N_c = 2, N_f = 2$

[2] Many thanks to Jonathan Flynn and Nick Evans for comments and discussions at this point.

[3] Note that the approach taken here for the computation of the errors is different compared to the published works [2, 4]. In these papers the standard formula for differentials was used, albeit modded. For example, the standard result yields $d\left(\frac{A}{B}\right) = \frac{1}{B}dA - \frac{A}{B^2}dB$, however in those two works it was taken as $d\left(\frac{A}{B}\right) = \frac{1}{B}dA + \frac{A}{B^2}dB$.

in the running of α in equation (8.8) and γ equation (8.9). These then feed into Δm^2 in equation (8.6). With these values, we repeat our computations as in holographic QCD. We have again

$$\begin{aligned} b_0 &= \frac{1}{6\pi}\left(11N_c - (N_f + \bar{N}_f)\right) , \\ b_1 &= \frac{1}{24\pi^2}\left(34{N_c}^2 - 5N_c(N_f + \bar{N}_f) - \frac{3}{2}\frac{{N_c}^2 - 1}{N_c}(N_f + \bar{N}_f)\right) , \\ \gamma &= \frac{3({N_c}^2 - 1)}{4N_c\pi}\alpha\,. \end{aligned} \tag{8.42}$$

Note that the $Sp(4)$ multiplets of mesons include the usual $SU(2)_V$ multiplets, so we compute as in QCD to find masses and decay constants. Our results for the massless theory are shown in table 8.3 normalized to the ρ/V mass. There is lattice work on this model in [229, 230], where unquenched Wilson fermions are used, i.e. the determinant of the Dirac operator is calculated instead of setting it to one, as in quenched theories. In the holographic approach this corresponds to including quark loop contributions to the gauge propagator.

We show these results in the massless limit for the V, A and σ masses also in table 8.3. Comparing to our holographic results, we see sensible agreement, as we found in the QCD analysis above. The holographic A mass is perhaps a little high. The lattice errors on the scalar mass are sufficiently large to incorporate our result. Since the lattice studies also provide fits to the quark mass dependence

Observables	Lattice	AdS/$SU(2)$ $2F$, $2\bar{F}$	
M_V	1.00(4)	1*	sets scale
M_A	1.1(3)	1.66	
M_S	1.5(7)	1.27	
f_π	0.076(45)	0.0609	
f_V		0.376	
f_A		0.474	

Table 8.3: Comparison of the lattice studies [229, 230] of the massless $SU(2)$ gauge theory to our holographic model's predictions for meson masses and decay constants in units of the vector meson mass.

in the model, we make that comparison as well. In figure 8.9 we show the small (linear) and larger (quadratic) m_q dependence of the pNGB mass squared. At larger pNGB masses, higher order terms in the expansion in m_q would be needed. We then plot the meson masses as a function of M_π^2 in figure 8.10 and present our fits and those from the lattice. The holographic model agrees rather well with the lattice fit and certainly lends strength to the view that the holographic model provides a credible and useful description of the dynamics.

8.4.3 $Sp(4)$ gauge theory with top partners - $Sp(4)$ $4F, 6A_2$

The $SU(2)$ model of the previous subsection can realize a composite pseudo-Goldstone Higgs but can not contain top partners since there are no baryons in an $SU(2)$ gauge theory. The same global

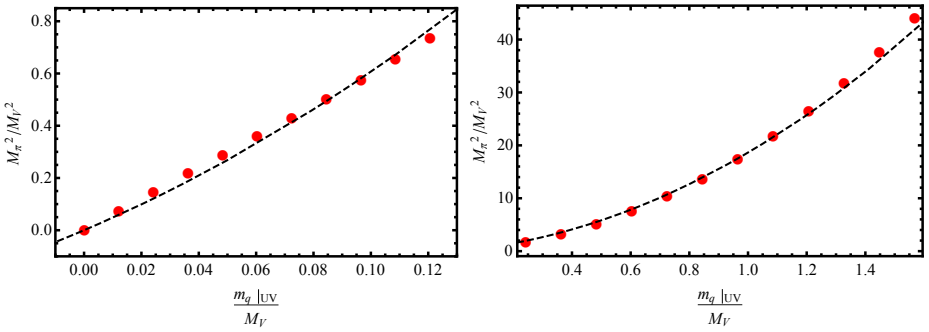

Figure 8.9: We plot the pNGB mass against the UV quark mass in the small and intermediate quark mass regions for the $SU(2)$ gauge theory (in units of the vector meson mass at $m_q|_{UV} = 0$). The red points are the numerical results. The dashed black lines are obtained as a simple analytic fit: $M_\pi^2 = 4.67\ m_q|_{UV} + 13.97\ m_q^2|_{UV}$.

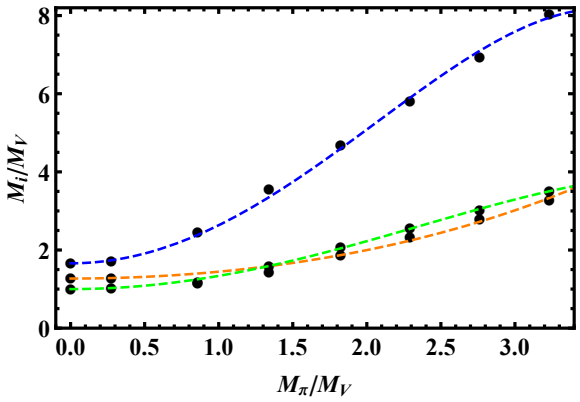

$$
\begin{aligned}
M_S &= 1.27 + 0.172\ M_\pi^2 + 0.00239 M_\pi^4\,,\\
M_{S\mathrm{lat}} &= 1.5(7) + 0.34(7)\ M_\pi^2 - 0.016(8) M_\pi^4\,,\\
M_V &= 1 + 0.348\ M_\pi^2 - 0.0104 M_\pi^4\,,\\
M_{V\mathrm{lat}} &= 1.00(4) + 0.47(3)\ M_\pi^2 - 0.039(6) M_\pi^4\,,\\
M_A &= 1.66 + 1.01\ M_\pi^2 - 0.0394 M_\pi^4\,,\\
M_{A\mathrm{lat}} &= 1.1(3) + 0.79(26)\ M_\pi^2 - 0.089(3) M_\pi^4\,.
\end{aligned}
$$

Figure 8.10: The growth of the spectra in the $SU(2)$ theory as we increase the quark mass in the UV. The masses are rescaled with respect to the vector meson mass at $m_q|_{UV} = 0$. In our analytic formulae quantities are again normalized to the vector meson mass at $m_q|_{UV} = 0$. The related lattice data can be found in [229, 230].

symmetry breaking pattern ($SU(4) \to Sp(4)$) can be achieved with any $Sp(2N)$ gauge theory with again two Dirac fermions in the fundamental representation (4 Weyl fermions in the F). It is natural to concentrate on the next most minimal $Sp(4)$ case, as $Sp(2) \simeq SU(2)$.

Top partners can be introduced [191] into the $Sp(4)$ model by the inclusion of three additional Dirac fermion in the sextet, two index anti-symmetric representation of the gauge group (we will refer to them as A_2s) (in the nomenclature of [234] this is model M8). The three copies are the three QCD colours although we drop the colour interactions since they are only weakly coupled at the energy scales we consider. The top partners are FA_2F bound states. From the point of view of the $Sp(4)$ dynamics there is an $SU(6)$ symmetry on the six Weyl fermion A_2s which are in a real representation. When the A_2 condensate forms this symmetry is broken to $SO(6)$. The full symmetry breaking pattern is characterized by

$$
SU(4) \times SU(6) \times U(1) \to \underbrace{Sp(4)}_{SU(2)_L \times U(1)} \times \underbrace{SO(6)}_{SU(3) \times U(1)} \times U(1) \tag{8.43}
$$

where the $U(1)$ factors give eventually the hypercharge.

For the holographic model we need the running of the coupling equation (8.8) and γ equation (8.9). These then feed into Δm^2 in equation (8.6) to define the model. The beta function coefficients for the running of α and γ in the UV are

$$\begin{aligned} b_0 &= \frac{1}{6\pi}\left(11(N+1) - N_{f_1} - 2(N-1)N_{f_2}\right) \\ b_1 &= \frac{1}{24\pi^2}\left(34(N+1)^2 - 5(N+1)N_{f_1} - \frac{3}{4}(2N+1)N_{f_1}\right. \\ &\quad \left. -10(N+1)(N-1)N_{f_2} - 6N(N-1)N_{f_2}\right) \end{aligned} \tag{8.44}$$

and the one-loop anomalous dimensions for the different representations are

$$\begin{aligned} \gamma_{A_2} &= \frac{3}{2\pi}N\alpha\,, \\ \gamma_F &= \frac{3}{2\pi}\frac{2N+1}{4}\alpha\,, \end{aligned} \tag{8.45}$$

In the above $N_{f_1} = 4$ denotes the flavours in the fundamental and $N_{f_2} = 6$ in the two-index antisymmetric. $N = 2$ for $Sp(4)$.

Generically one would expect the A_2 fermions to condense ahead of the fundamental fields since the critical value for α where $\gamma = 1/2$ (the criteria discussed below equation (8.6)) is smaller. If we extend the perturbative results into the non-perturbative regime we find

$$\alpha_c^{A_2} = \frac{\pi}{6} = 0.53\,, \qquad \alpha_c^{F} = \frac{4\pi}{15} = 0.84\,. \tag{8.46}$$

When the A_2s condense their condensate breaks their flavour $SU(6)$ to $SO(6)$. At this point the A_2s become massive but it is unclear how quickly they decouple from the running of α - we will investigate this point below. The usual assumption is that both species of fermion condense close to the same scale.

The holographic vacuum of the theory

Let us begin by investigating the question of the scale of the condensates in the vacuum of the theory using our holographic model. As a first run we use the AdS/YM theory with the running of α including both fermion species - that is we use equation (8.44) at all energy scales. We then track the running of the anomalous dimension γ for the two representations using equation (8.45). Note the scale where the BF bound is violated is similar for the two representations because the coupling is running quickly near the BF bound violation point. These give us two Δm^2 in equation (8.6), one for each representation, which are shown in blue (F) and orange (A_2) on the left in figure 8.11. Each of the condensates is a distinct operator which we represent by a distinct field L - in other words we run two copies of the AdS/YM equations for the vacuum expectation values of the two condensates. The results for the two resulting L functions are shown in figure 8.11 on the right - again blue (F) and orange (A_2). The A_2 fields condense at a higher scale than the F because its Δm^2 passes through the BF bound first.

There is though a tricky and interesting decoupling problem here. When the A_2 fields condense and become massive should we integrate them out of the running of α? At weak coupling massive quarks do decouple from the running but it is less clear what is appropriate at strong coupling. We have computed an example of such a possible decoupling. Here as soon as the scale L_{IR} for the A_2 fermions is reached we remove them from the running of α at lower ρ - the running of the F fields Δm^2 then deviates from the blue to the red curve on the left in figure 8.11. It runs faster than before and the condensation scale for the fundamental fields moves closer to that of the A_2s. The resulting $L(\rho)$ function for the F is shown by the red line in the right hand plot of figure 8.11.

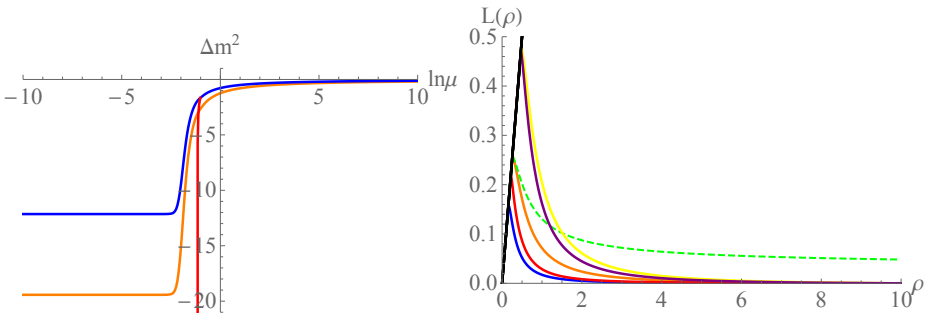

Figure 8.11: AdS/$Sp(4)$ $4F, 6A_2$. Left panel: The running of Δm^2 against RG scale for the fundamental (blue line), A_2 (orange) and in red the running of the fundamental representation after A_2 have been integrated out. Right panel: The vacuum solution $L(\rho)$: the orange line for the A_2 representation and blue the fundamental without decoupling. The red solution is when we consider the decoupling of the A_2 which condenses before the fundamental. The dashed green line is the fundamental when we consider additional NJL-terms such that it matches in the IR the A_2 representation. Finally, the yellow and purple vacuum solution correspond to the quenched models for the A_2 and fundamental representations respectively. Here units are set by $\alpha(\rho = 1) = 0.65$.

The lattice should be able to shed light on the rate of decoupling of massive flavours but to date only quenched calculations have been performed for this model as we will review below. We therefore also show results for the embeddings that result from the fully quenched (ie setting all $N_f = 0$ in equation (8.44)) running in figure 8.11 on the right - the yellow (F) and purple (A_2) curves. The coupling now runs faster at all scales and the condensation scale for both fermion species rises, with again the A_2s condensing first. The gap between the F and A_2 condensation scales is yet smaller due to the very fast running of the pure glue theory.

If the IR separation in the condensation scales for the two fermion species is undesirable then they can be brought together by including an NJL term for the F fields ($g_s^2/\Lambda_{UV}^2|\bar{F}F|^2$) that enhances the fundamental condensation scale. We have also looked at this case, adding a NJL four fermion term to make the values of L_{IR} equal for the two representations. The A_2 embedding function is our original orange curve but the embedding for the F representation becomes the green dotted curve in figure 8.11.

It is worth commenting on the size of the IR mass, L_{IR} in physical units. We will compute the spectrum in the next section but borrowing ahead we can write L_{IR} in units of the vector meson's mass in the A_2 representation for the case discussed. For the model where we do not integrate out the A_2 fields we have $L_{IR}^{A_2} = 0.304 m_V$ and $L_{IR}^{F} = 0.187 m_V$. When we integrate out the A_2s on mass shell we have

$L_{IR}^{A_2} = 0.304 m_V$ and $L_{IR}^{F} = 0.26 m_V$. For the model with the NJL interaction for the fundamental we have $L_{IR}^{A_2} = L_{IR}^{F} = 0.304 m_V$. For the quenched model we have $L_{IR}^{A_2} = 0.317 m_V$ and $L_{IR}^{F} = 0.314 m_V$.

Holographic spectrum

We now compute the spectrum of the theory holographically. We will do this for each of the scenarios we have outlined - the quenched theory; the theory where the A_2s are integrated out at their IR mass scale; the theory where A_2s are not integrated out; and the theory with a NJL term to enforce an equal scale of condensation.

We assume that there is only a small mixing between bound states made of the two fermion species so that we do not have to mix the states associated with fluctuations of each L_0 embedding (indeed to include that mixing would be hard requiring the fluctuations to know of both embeddings in some sort of non-abelian DBI action). Now we simply fluctuate around each vacuum solution separately from equation (8.1) with

$$g_5^2|_F = \frac{48\pi^2}{2N_{f_1}N_c}, \qquad g_5^2|_{A_2} = \frac{48\pi^2}{N_{f_2}(N_c(N_c-1)-1)}\,. \tag{8.47}$$

Similarly we split the normalizations for the external currents in equation (8.17). We show the resulting spectrum for each of the cases we consider in table 8.4 for the case where all fermion representations are massless.

In each case, without a NJL term, the bound states of the A_2 fields are heavier and have higher decay constants than those made of the fundamental fields F, reflecting the A_2s' higher condensation scale. The separation in scale between the two sectors does depend quite strongly on the decoupling assumptions. If the A_2s are not decoupled at all, the separation, as measured by the vector meson masses, is almost a factor of two whilst in the quenched limit it barely exists. The slowing of the running of the gauge coupling with the inclusion of flavours is important. The case where the A_2s are integrated out at their IR mass scale lies between these two extremes.

The greatest impact in the spectrum shows up in the scalar meson (S) masses. The rate of running measures the departure from conformality which shows up in the flatness of the effective potential for the quark condensates. The slower the running the lighter the resultant scalar - here there is as much as a factor of four in the prediction.When the NJL term is used to enforce equal IR mass scales for the two fermion species the bound states of the fundamental fields become just slightly heavier than those with A_2 constituents, reflecting the higher UV mass.

Finally in table 8.4 we also show results for the baryon top partner. This state is a bound state of two F and an A_2 so should know about both vacuum solutions L_{0F} and L_{0A_2}. The present holographic framework does not allow us to include two L_0 at the same time so instead we compute the mass of the baryon using each of the two embedding functions - this is as if each constituent had the same constituent mass, either that of the F or that of the A_2. We expect that the mixed state's mass will be between these two values.

	AdS/$Sp(4)$ no decouple	AdS/$Sp(4)$ A2 decouple	AdS/$Sp(4)$ quench	lattice [231] quench	lattice [232] unquench	AdS/$Sp(4)$ + NJL
$f_{\pi A_2}$	0.120	0.120	0.103	0.1453(73)		0.120
$f_{\pi F}$	0.0569	0.0701	0.0756	0.1079(85)	0.1018(253)	0.160
M_{VA_2}	1*	1*	1*	1.000(23)		1*
f_{VA_2}	0.517	0.517	0.518	0.508(43)		0.517
M_{VF}	0.61	0.814	0.962	0.83(16)	0.83(13)	1.03
f_{VF}	0.271	0.364	0.428	0.411(30)	0.43(44)	0.449
M_{AA_2}	1.35	1.35	1.28	1.75 (28)		1.35
f_{AA_2}	0.520	0.520	0.524	0.794(15)		0.520
M_{AF}	0.938	1.19	1.36	1.32(22)	1.34(11)	1.70
f_{AF}	0.303	0.399	0.462	0.54(28)	0.56(17)	0.449
M_{SA_2}	0.375	0.375	1.14	1.65(27) †		0.375
M_{SF}	0.325	0.902	1.25	1.52(25)†	1.40(13) †	0.375
M_{BA_2}	1.85	1.85	1.86			1.85
M_{BF}	1.13	1.53	1.79			1.88

Table 8.4: AdS/$Sp(4)$ $4F, 6A_2$. Ground state spectra and decay constants for our various holographic models and comparison to lattice results - we use the subscript A_2 and F for the quantity in each of the two different representation sectors. Note the lattice scalar is the a_0 not the isospin singlet σ which we compute holographically - we present the results as a guide to lattice expectations of quark anti-quark meson masses though. Note here for the unquenched lattice results, which do not include the A_2 fields, we have normalized the F vector meson mass to that of the quenched computation.

Comparison to lattice results

Lattice studies of this model, in the quenched approximation, have been made in [231]. In [232] the group followed up that work by unquenching the fundamental quark sector using Wilson fermions. We show the results of these studies in Table 8.4 for direct comparison to the holographic results. We have normalized the quenched results to the vector meson mass from the A_2 sector. For the unquenched calculation, which does not include the A_2 fields, we align the vector meson mass in the F sector to the quenched theory to allow the changes to be seen in the F sector. One notes that the variation from quenched to unquenched lattice simulations are not large. Note the lattice results for scalar masses are for the a_0 like states rather than the σ state we compute with holography - they provide a guide to the lattice expectation for scalar states though.

An initial view of the quenched results from both the lattice and the holographic model is that they show considerable correlation. As in QCD, the holographic approach appears to be a decent stab at the spectrum! This lends confidence that trends as the fields are unquenched may be trustworthy. Thus as discussed above we would expect that if the A_2 fields were included as unquenched fields the F sector would decrease in mass by 20-40%. We also expect the scalar meson masses to be considerably lower than predicted by the quenched lattice computation. Here the lattice computations to date don't provide guidance on a prescription for decoupling the A_2 fields since they have always been quenched.

Quark mass dependence

The quenched lattice study of [231] provides fits to the mass dependence of the spectrum so for comparison we reproduce the same fits in figure 8.12 . We also display the same plots and fits for the fully undecoupled model (the furthest extreme from the quenched version of our models). The fits for the quenched theory are reasonably close with gradients matching better than a factor of two in most cases. We note that our holographic model predicts that the slower the running of the coupling (the less quenched the quarks are) the sharper the slopes with M_π - this effect was previously seen for walking theories in [138]. It would be interesting to see if this result was reproduced in unquenched lattice computations.

Holography of the top partners

The top partners are FA_2F spin 1/2 baryons of the strongly coupled dynamics that play a key role in the generation of the top quark mass as described in the section 8.4.1. We have computed their masses in the Sp(4) model which are shown in Table 8.4 - we remind that we have computed the masses as if all constituents have a dynamical mass given by first the fundamental and secondly the A_2 representations. The true mass is likely to lie between these values.

For the top mass there are two key contributions as we can see in figure 8.8. The top Yukawa coupling,

$$y_t = \frac{g^2 Z\ \tilde{g}^2 \tilde{Z}\ Z_3}{M_T^2\ \Lambda_{UV}^4}\,, \tag{8.48}$$

is inversely proportional to the top partner mass squared. It is proportional to the Z_3 and $Z/\tilde{Z}$ factors which we will set equal. The Z factors, like the baryon-σ vertex in QCD, are not direct predictions of the holographic framework since they must be generated by couplings beyond the basic quadratic terms of the holographic action equation (8.1) and so in principle one can add new couplings. We can though write down holographic terms that are likely to be the dominant contributions and look at their order of magnitude behaviour.

A_2 Sector - quenched

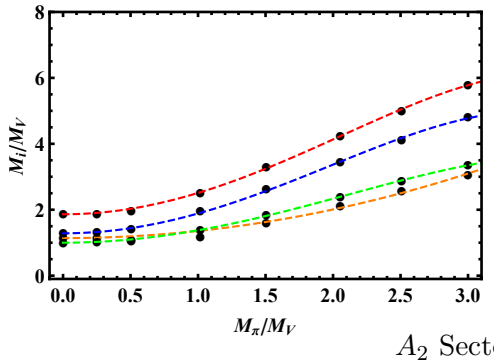

$$
\begin{aligned}
M_S &= 1.14 + 0.217\ M_\pi^2\,, \\
M_{S\text{lat}} &= 1.65(27) + 0.17(16) M_\pi^2\,, \\
M_V &= 1 + 0.392\ M_\pi^2\,, \\
M_{V\text{lat}} &= 1.000(23) + 0.45(28)\ M_\pi^2\,, \\
M_A &= 1.28 + 0.627\ M_\pi^2\,, \\
M_{A\text{lat}} &= 1.75(28) + 0.40(17)\ M_\pi^2\,, \\
M_B &= 1.86 + 0.673\ M_\pi^2\,.
\end{aligned}
$$

A_2 Sector - no decoupling

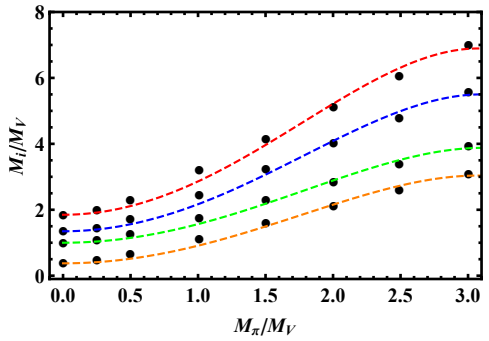

$$
\begin{aligned}
M_S &= 0.375 + 0.564\ M_\pi^2 - 0.0299\ M_\pi^4\,, \\
M_V &= 1 + 0.595\ M_\pi^2 - 0.0307\ M_\pi^4\,, \\
M_A &= 1.35 + 0.865\ M_\pi^2 - 0.0450\ M_\pi^4\,, \\
M_B &= 1.85 + 1.07\ M_\pi^2 - 0.0564\ M_\pi^4\,.
\end{aligned}
$$

F Sector - quenched

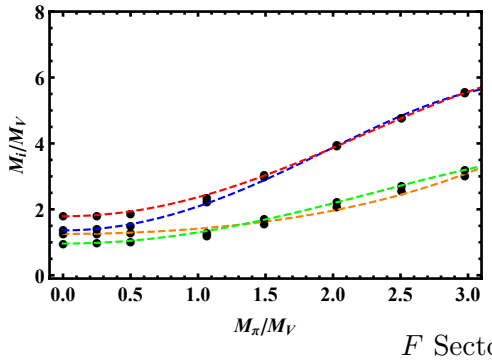

$$
\begin{aligned}
M_S &= 1.25 + 0.154\ M_\pi^2\,, \\
M_{S\text{lat}} &= 1.52(25) + 0.09(16)\ M_\pi^2\,, \\
M_V &= 0.962 + 0.349\ M_\pi^2\,, \\
M_{V\text{lat}} &= 0.83(16) + 0.50(27)\ M_\pi^2\,, \\
M_A &= 1.36 + 0.758\ M_\pi^2\,, \\
M_{A\text{lat}} &= 1.32(22) + 0.42(22)\ M_\pi^2\,, \\
M_B &= 1.79 + 0.599\ M_\pi^2\,.
\end{aligned}
$$

F Sector - no decoupling

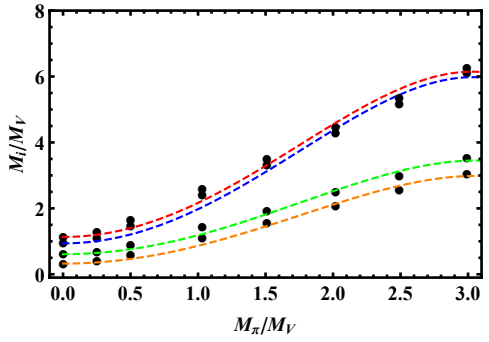

$$
\begin{aligned}
M_S &= 0.325 + 0.57\ M_\pi^2 - 0.031\ M_\pi^4\,, \\
M_V &= 0.61 + 0.61\ M_\pi^2 - 0.033\ M_\pi^4\,, \\
M_A &= 0.938 + 1.1\ M_\pi^2 - 0.06\ M_\pi^4\,, \\
M_B &= 1.13 + 1.09\ M_\pi^2 - 0.059\ M_\pi^4\,.
\end{aligned}
$$

Figure 8.12: AdS/$Sp(4)$ $4F, 6A_2$ - results for the spectrum as a function of the pNGB mass in the quenched theory and the case with no decoupling of the A_2 - lattice results from [231] are included for comparison. In our analytic formulae we use units of the vector meson mass at $m_q|_{UV} = 0$.

In particular we have

$$Z_3 \simeq \int d\rho\ \rho^3\ \frac{\partial_\rho \pi(\rho)\ \psi_B(\rho)^2}{(\rho^2+L^2)^2}\,, \tag{8.49}$$

$$Z = \tilde{Z} \simeq \int d\rho\ \rho^3 \partial_\rho \psi_B(\rho)\,. \tag{8.50}$$

Here $\pi(\rho)$ and $\psi_B(\rho)$ are the holographic wavefunctions for the pNGB and the baryon repectively. They are normalized to give canonical kinetic terms for these states as in equation (8.34).

If we naively compute the top Yukawa coupling, from the full set of factors in equation (8.48) (with $g = \tilde{g} = 1$), in the $Sp(4)$ model, with a cut off on the HDOs of roughly 6 times the vector meson mass, we find the top Yukawa coupling is only of order 0.01 which is far below the value of one needed.

The top Yukawa would be enhanced if the top partners were anomalously light relative to the strong coupling scale (roughly the scale 1 in our Table 8.4). As we have described in QCD, it is possible to drive the baryons light by including a HDO - see figure 8.7 for example. In the Sp(4) theory we can also look to include a HDO of the form

$$\mathcal{L}_{HDO} = \frac{g_T^2}{\Lambda_{UV}^5} |F A_2 F|^2\,. \tag{8.51}$$

As the operator FA_2F becomes the top partner field, this is directly a shift in the top partner mass.[4] In figure 8.13 we show the dependence of the top partner mass on g_T^2 - we show the effect using both the F and A_2 embeddings as $L_0(\rho)$ in equation (8.25). The HDO can indeed be used to reduce the top partner mass - for small g_T^2 the effect is linear and small but after a critical value the effect is much larger, as shown. One must be careful though because as the top partners' mass changes so also do the

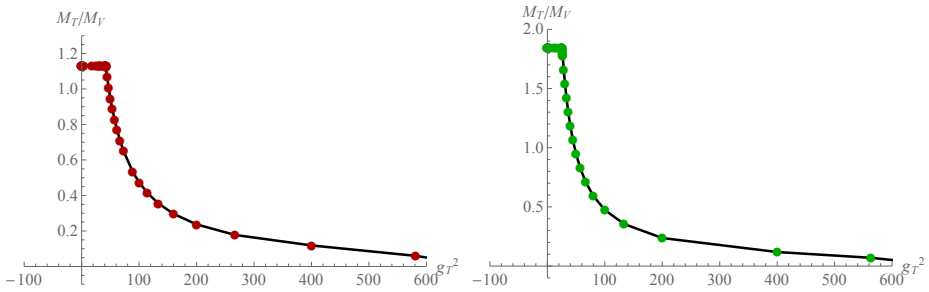

Figure 8.13: AdS/$Sp(4)$ $4F, 6A_2$ - We show the effect of adding the double-trace operator equation (8.51) to the spin-1/2 baryon's mass. On the left we use the $L_0(\rho)$ from the F representation and on the right $L_0(\rho)$ from the the A_2 representation. Note the initial linear behaviour when g_T^2 is perturbative but then as it passes a critical value the effect on the mass is much larger.

Z factors in equation (8.49) and equation (8.50). In particular as the HDO in equation (8.51) plays a large role it induces a sizeable non-normalizable piece in the UV holographic wave function of the top partner. This means that the integrals in the equivalent of the normalization factors in equation (8.34) and directly in the expressions for the Z factors are more dominated by the UV part of the integral. The overlap between different states can change substantially. We therefore plot the full expression for the Yukawa coupling from equation (8.48) against the top partner mass (which changes as we dial

[4] A similar effective operator was mentioned in [143], but there it is not included in the dynamical calculations.

g_T^2) in figure 8.14. We see that the top Yukawa does indeed grow as the top partner's mass falls and can become of order one as the top partners mass falls to about half of the vector meson mass. This suggests, that after fixing the strong coupling scale to a sensible large value in the 1-5 TeV range, we should be able to realize a top partner mass of about 1 TeV and the required top mass.

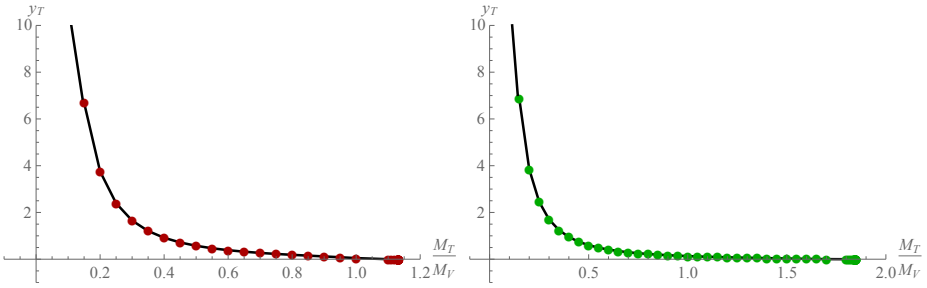

Figure 8.14: AdS/$Sp(4)$ $4F, 6A_2$ - the top Yukawa coupling, as given by equation (8.48), is plotted against the top partner mass in units of the vector meson mass. M_T is controlled by adding a HDO as in figure 8.13. We compute on the left with $L_0(\rho)$ for the fundamental quark and on the right we use the A_2 $L_0(\rho)$.

8.4.4 $SU(4)$ gauge theory with top partners - $SU(4)$ $3F, 3\bar{F}, 5A_2$

The next model we choose to study is one taken from [192, 235] for which there has been related lattice work [233, 236]. The gauge group is $SU(4)$. There are five Weyl fields in the sextet A_2 representation. When these A_2 condense they break their $SU(5)$ symmetry to $SO(5)$ - the pNGBs inlcude the Higgs.

To include top partner baryons, fermions in the fundamental representation F are added allowing FA_2F states. To make these states QCD coloured we need three Dirac spinors in the fundamental. When these fields condense the chiral $SU(3)_L \times SU(3)_R$ symmetry is broken to the vector $SU(3)$ subgroup - the $SU(3)$ sub-group is identified with weakly coupled QCD (which we will neglect since it is weak at the scales in question).

The full symmetry breaking pattern and embedding of the SM groups is

$$SU(5) \times SU(3)_L \times SU(3)_R \times U(1) \to \underbrace{SO(5)}_{SU(2)_L \times U(1)} \times \underbrace{SU(3)}_{SU(3)} \times U(1) \tag{8.52}$$

For the holographic model we need the running of the coupling equation (8.8) and γ equation (8.9). These then feed into Δm^2 in equation (8.6) to define the model. The coefficients of the one and two-loop β-function read

$$\begin{aligned} b_0 &= \frac{1}{6\pi}\Big(11N_c - N_{f_1} - (N_c-2)N_{f_2}\Big), \\ b_1 &= \frac{1}{24\pi^2}\left(34N_c^2 - 5N_cN_{f_1} - \frac{3}{2}\frac{N_c^2-1}{N_c}N_{f_1} - 5N_c(N_c-2)N_{f_2} - 3\frac{(N_c+1)(N_c-2)^2}{N_c}N_{f_2}\right). \end{aligned} \tag{8.53}$$

and the one-loop anomalous dimensions for the different representations are

$$\begin{aligned}\gamma_{A_2} &= \left(\frac{6}{4\pi}\frac{(N_c+1)(N_c-2)}{N_c}\right)\alpha\,,\\ \gamma_F &= \left(\frac{3}{4\pi}\frac{N_c^2-1}{N_c}\right)\alpha\,.\end{aligned} \tag{8.54}$$

Naively one would expect the A_2 fermions to condense ahead of the fundamental fields since the critical value for α where $\gamma = 1/2$ (the criteria discussed below equation (8.6)) is smaller. If we extend the perturbative results into the non-perturbative regime we find

$$\alpha_c^F = \frac{8\pi}{45} = 0.56\,, \qquad \alpha_c^{A_2} = \frac{2\pi}{15} = 0.42\,. \tag{8.55}$$

As in the $Sp(4)$ model we will ask how quickly the A_2 fields decouple from the running of γ below their IR mass scale.

This model is hard to simulate on the lattice because of the fermion doubling problem and the sign problem associated to chiral theories so instead lattice work [233, 236] has focused on the theory with just two Dirac A_2s and 2 Dirac fundamental quarks. In the next subsection we will switch to the holographic description of that model and the comparison to the lattice data before returning to the full model thereafter. Of course, the ability to simply switch fields in and out is one of the huge benefits of the holographic approach.

The lattice variant of the model - $SU(4)$ $2F, 2\bar{F}, 4A_2$

Here we consider a model with an $SU(4)$ gauge theory with two Dirac sextet and two Dirac fundamental quarks. We again run two separate holographic models for the F and A_2 (though linked through the different representations contributions to the running of α) which neglects mixing between the two sectors.

We set our model parameters, as defined in section 8.2, using

$$m_q|_{UV} = 0, \qquad \alpha(0) = 0.65, \qquad g_5|_4 = \frac{24\pi^2}{N_{f_1}N_c}, \qquad g_5|_6 = \frac{48\pi^2}{N_{f_2}N_c(N_c-1)}\,. \tag{8.56}$$

We run two schemes - one where the A_2s contribute to the running of α at all scales and one where we decouple them at their IR mass scale. The vacuum profiles for $L(\rho)$ are shown in figure 8.15 - here the coupling runs sufficiently quickly with or without the A_2 fields that the differences in the $L(\rho)$ function for the F quarks lies within the line width, whether the A_2 decouple or not. It would be nice if the lattice could teach us how to enact this decoupling. Here though the errors on the lattice data are still too large to distinguish these two scenarios, so again we lack data on precisely how to decouple quarks in the strong coupling regime. Finally we also compute, and display in figure 8.15, for the theory with an NJL operator ($g_s^2/\Lambda_{UV}^2|\bar{F}F|^2$) which allows us to bring the F IR mass equal to the A_2 IR mass.

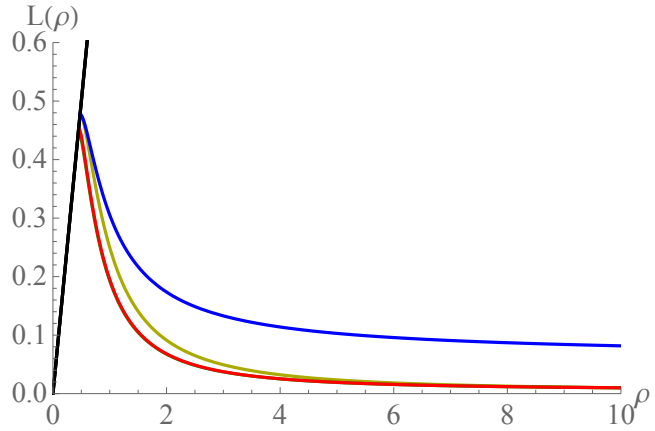

Figure 8.15: $SU(4)$ $2F, 2\bar{F}, 4A_2$ - We display the vacuum solutions $L(\rho)$: the gold line corresponds to the A_2 representation and the red is the F. The blue line is the fundamental when we consider an additional NJL-term such that it matches in the IR the A_2 representation.

Next we compute the spectrum and display the predictions in Table 8.5. We also display lattice data from [233] (also [236] and there is a relevant chiral perturbation theory analysis for the model in [237]). The holographic model and the lattice data agree well in describing the split in mass between the vector mesons of the F and A_2 sectors (the differences in decoupling choices lie within the error bars).

The top partner baryon is a mixed FA_2F state. Again we estimate the possible spread of its mass by using in turn the $L_0(\rho)$ from the F and A_2 sectors, essentially assuming the F and A_2 have the same constituent masses at either the lower F or higher A_2 scale. The holographic model over estimates the top partner mass by 30%.

	Lattice [233] $4A_2, 2F, 2\bar{F}$ unquench	AdS/$SU(4)$ $4A_2, 2F, 2\bar{F}$ no decouple	AdS/$SU(4)$ $4A_2, 2F, 2\bar{F}$ decouple	AdS/$SU(4)$ $5A_2, 3F, 3\bar{F}$ no decouple	AdS/$SU(4)$ $5A_2, 3F, 3\bar{F}$ decouple	AdS/$SU(4)$ $5A_2, 3F, 3\bar{F}$ quench	AdS/$SU(4)$ $5A_2, 3F, 3\bar{F}$ + NJL
$f_{\pi A_2}$	0.15(5)	0.0997	0.0997	0.111	0.111	0.102	0.11
$f_{\pi F}$	0.11(3)	0.0949	0.0953	0.0844	0.109	0.892	0.139
M_{VA_2}	1.00(5)	1*	1*	1*	1*	1*	1*
f_{VA_2}	0.68(3)	0.489	0.489	0.516	0.516	0.517	0.516
M_{VF}	0.93(5)	0.933	0.939	0.890	0.904	0.976	1.02
f_{VF}	0.49(4)	0.458	0.461	0.437	0.491	0.479	0.495
M_{AA_2}		1.37	1.37	1.32	1.32	1.28	1.32
f_{AA_2}		0.505	0.505	0.521	0.521	0.522	0.521
M_{AF}		1.37	1.37	1.21	1.23	1.28	1.46
f_{AF}		0.501	0.504	0.453	0.509	0.492	0.489
M_{SA_2}		0.873	0.873	0.684	0.684	1.18	0.684
M_{SF}		1.03	1.02	0.811	0.798	1.25	0.815
M_{JA_2}	3.9(18)	2.21	2.21	2.21	2.21	2.22	2.21
M_{JF}	2.0(11)	2.07	2.08	1.97	2.00	2.17	2.24
M_{BA_2}	1.4(7)	1.85	1.85	1.85	1.85	1.86	1.85
M_{BF}	1.4(7)	1.74	1.75	1.65	1.68	1.81	1.88

Table 8.5: $SU(4)$ theories - the spectrum in a variety of scenarios and lattice data for comparison.

There is lattice data for an additional spin zero state made of four quarks (either all Fs or all A_2s), that we refer to as a tetraquark, and denote as the J in table 8.5. We have computed the mass of such a state using equation (8.23) - here the holographic prediction is that the F and A_2 tetraquarks' masses lie within 10%. In contrast the lattice prediction suggests a factor of two between the masses of the states. It is hard to understand how such a large separation could occur when the constituent quark masses are very similar for the Fs and A_2 as measured by the vector meson masses. It would be interesting to look into the origin of the splitting in the lattice simulations further.

Finally in figure 8.16 we display the M_π dependence of the spectrum in the non-decoupling scenario although here we do not have lattice data for comparison.

A2 Sector

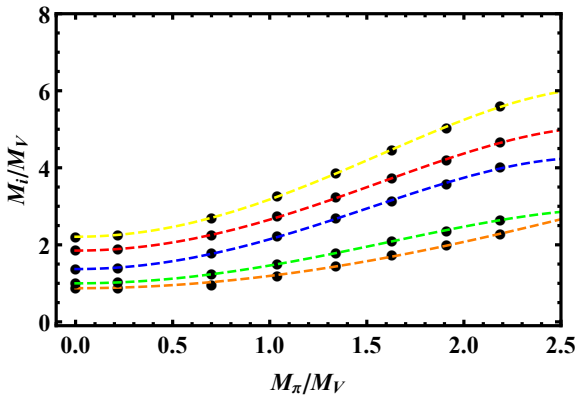

$$
\begin{aligned}
M_S &= 0.873 + 0.326\ M_\pi^2 - 0.00626\ M_\pi^4\,,\\
M_V &= 1 + 0.494\ M_\pi^2 - 0.0315\ M_\pi^4\,,\\
M_A &= 1.37 + 0.834\ M_\pi^2 - 0.0602\ M_\pi^4\,,\\
M_B &= 1.85 + 0.861\ M_\pi^2 - 0.0577\ M_\pi^4\,,\\
M_J &= 2.21 + 1.04\ M_\pi^2 - 0.0696\ M_\pi^4\,.
\end{aligned}
$$

F Sector

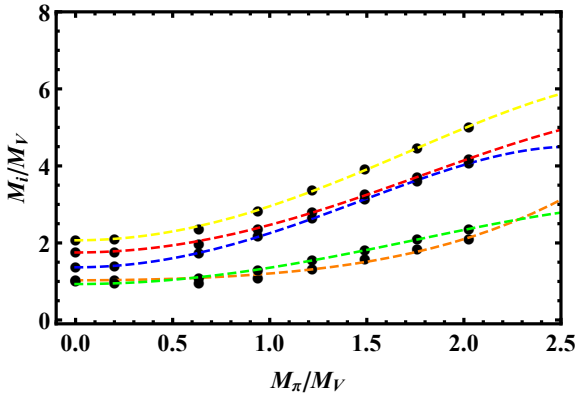

$$
\begin{aligned}
M_S &= 1.03 + 0.146\ M_\pi^2 + 0.0302\ M_\pi^4\,,\\
M_V &= 0.933 + 0.448\ M_\pi^2 - 0.0241\ M_\pi^4\,,\\
M_A &= 1.37 + 0.957\ M_\pi^2 - 0.0731\ M_\pi^4\,,\\
M_B &= 1.75 + 0.753\ M_\pi^2 - 0.039\ M_\pi^4\,,\\
M_J &= 2.07 + 0.935\ M_\pi^2 - 0.0522\ M_\pi^4\,.
\end{aligned}
$$

Figure 8.16: $SU(4)$ $2F, 2\bar{F}, 4A_2$ - The growth of the A_2 and F sectors spectra as we increase the quark mass in the UV. The masses are rescaled with respect to the vector meson mass in the A_2 representation at $m_q|_{UV} = 0$ in accord with the presentation in Table 8.5. Here M_π is the pNGB mass in units of the vector meson mass at $m_q|_{UV} = 0$.

$SU(4)$ $3F, 3\bar{F}, 5A_2$ model - vacuum configuration

After this small digression to the lattice variant, we return to the study of the model actually proposed for composite Higgs models - $SU(4)$ $3F, 3\bar{F}, 5A_2$. The coefficients of the one and two-loop β-function

are still given by equation (8.53) and the γs in equation (8.54) with appropriate choices of numbers of flavours. We choose as previously, see section 8.2,

$$m_q|_{UV} = 0, \qquad \alpha(0) = 0.65, \qquad g_5|_4 = \frac{24\pi^2}{N_{f_1} N_c}, \qquad g_5|_6 = \frac{48\pi^2}{N_{f_2} N_c (N_c - 1)}\,. \tag{8.57}$$

To address the decoupling of the A_2 we will present results for the vacuum solution, $L(\rho)$, in a number of different cases in figure 8.17. Firstly we do not decouple the A_2 from the running of α at any scale - the gold line corresponds to the A_2 representation and the green the fundamental. There is a small gap with the fundamentals a little lighter. If we decouple the A_2 fields at scales below their IR mass L_{IR} then the fundamental $L(\rho)$ becomes the red embedding. Section 8.4.4 is a zoom in showing the difference between the non-decoupled and the decoupling cases - in this model the separation barely changes when the decoupling is implemented.

It is possible to make the IR mass scales the same for both representations by including an NJL interaction for the fundamental fields ($g_s^2/\Lambda_{UV}^2 |\bar{F}F|^2$). The blue line in figure 8.17 is for the fundamental representation when we consider an additional NJL-term such that it matches in the IR the A_2 representation L_{IR}. Finally, the orange and purple vacua correspond to the quenched models for the

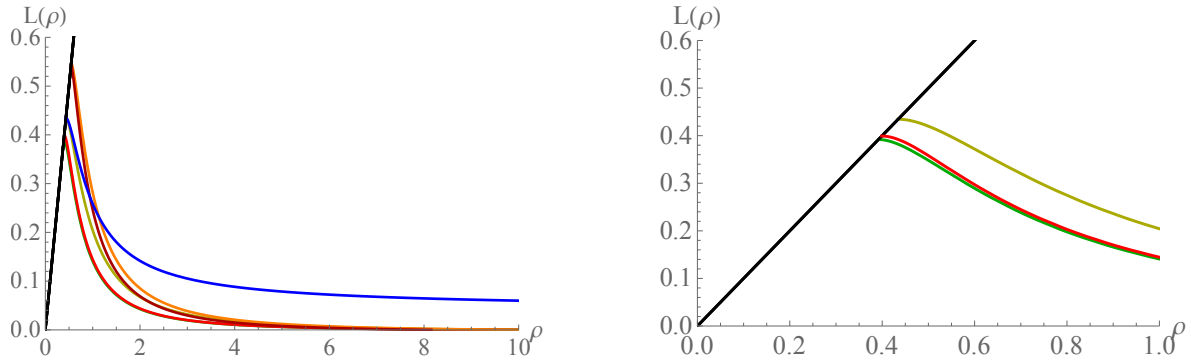

Figure 8.17: $SU(4)$ $3F, 3\bar{F}, 5A_2$ - In the left plot we display the vacuum soluions $L(\rho)$: the gold line corresponds to $AdS/SU(4)$ for the A_2 representation and the green is the fundamental. The red vacuum solution is when we consider the decoupling of the A_2 which condenses before the fundamental. The blue line is the fundamental when we consider additional NJL-terms such that it matches in the IR the A_2 representation. Finally, the orange and purple vacua correspond to the quenched models for the A_2 and fundamental representations respectively. The right hand plot is a zoom in when considering the $AdS/SU(4)$ model without decoupling and when we consider the decoupling of the A_2 quark fields.

A_2 and fundamental representations respectively - here we don't include the fermions in the running at all. We include this example because it would be relatively cheap to perform a lattice simulation of the theory in the quenched limit so our results may be of future interest.

It is worth commenting on the size of the IR mass, L_{IR} in physical units. We will compute the spectrum in the next section but borrowing ahead we can write L_{IR} in units of the vector meson's mass in the A_2 representation for the case discussed. For the model where we do not integrate out the A_2 fields we have $L_{IR}^{A_2} = 0.308 m_V$ and $L_{IR}^{F} = 0.278 m_V$. When we integrate out the A_2s on mass shell we have $L_{IR}^{A_2} = 0.308 m_V$ and $L_{IR}^{F} = 0.283 m_V$.For the model with the NJL interaction for the fundamental we

have $L^{A_2}_{IR} = L^F_{IR} = 0.308 m_V$. For the quenched model we have $L^{A_2}_{IR} = 0.318 m_V$ and $L^F_{IR} = 0.316 m_V$.

A2 Sector

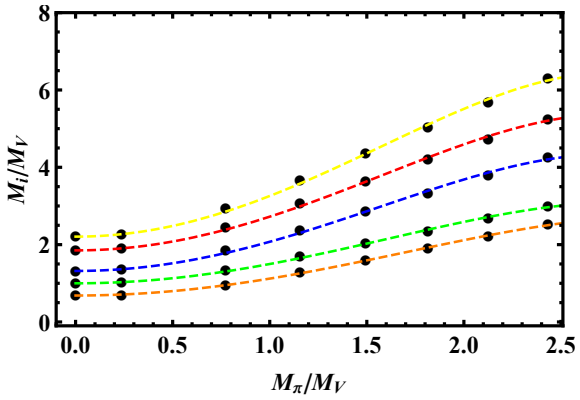

$$
\begin{aligned}
M_S &= 0.684 + 0.463\ M_\pi^2 - 0.0263\ M_\pi^4\,, \\
M_V &= 1 + 0.532\ M_\pi^2 - 0.0338\ M_\pi^4\,, \\
M_A &= 1.32 + 0.808\ M_\pi^2 - 0.0541\ M_\pi^4\,, \\
M_B &= 1.85 + 0.933\ M_\pi^2 - 0.0619\ M_\pi^4\,, \\
M_J &= 2.21 + 1.13\ M_\pi^2 - 0.0748\ M_\pi^4\,,
\end{aligned}
$$

F Sector

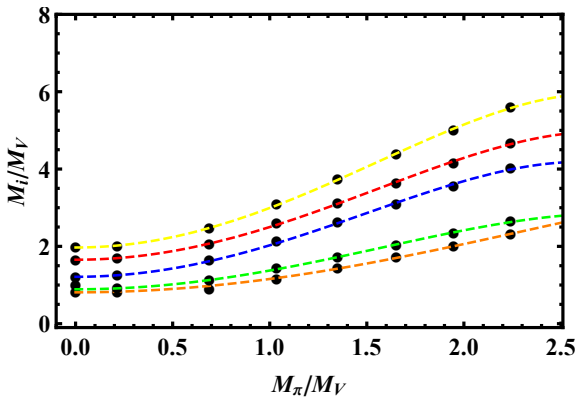

$$
\begin{aligned}
M_S &= 0.811 + 0.356\ M_\pi^2 - 0.0109\ M_\pi^4\,, \\
M_V &= 0.89 + 0.519\ M_\pi^2 - 0.0344\ M_\pi^4\,, \\
M_A &= 1.21 + 0.879\ M_\pi^2 - 0.065\ M_\pi^4\,, \\
M_B &= 1.65 + 0.907\ M_\pi^2 - 0.062\ M_\pi^4\,, \\
M_J &= 1.97 + 1.1\ M_\pi^2 - 0.0755\ M_\pi^4\,,
\end{aligned}
$$

Figure 8.18: $SU(4)$ $3F, 3\bar{F}, 5A_2$ - The growth of the spectra as we increase the quark mass in the UV. The masses are rescaled with respect to the vector meson mass in the A_2 representation at $m_q|_{UV} = 0$ in accord with the presentation in Table 8.5. In our analytic formulae the scale is again set by the A_2 vector meson mass at $m_q|_{UV} = 0$.

$SU(4)$ $3F, 3\bar{F}, 5A_2$ model - spectrum

We can now compute the spectrum of the theory in each of these cases. We display the results in table 8.5 so it is easy to compare to the lattice variant model. The spectra are fairly similar in all cases but the key changes occur as more fermions are included in the running. Thus increasing the number of fields slows the running which firstly increases the gap between the A_2 and F sectors and secondly reduces the σ scalar mass. For completeness in figure 8.18 we show the dependence of the meson and baryon masses on the pNGB mass for of the F and A_2 sectors, although there is no lattice data to compare to here.

Top partners

The top partners are FA_2F spin 1/2 baryons of the strongly coupled dynamics that play a key role in the generation of the top quark mass as described in the Section 8.4.1. We have computed their masses in the $SU(4)$ model which are shown in Table 8.5 - we remind that we have computed the masses as if all constituents have a dynamical mass given by first the fundamental and secondly the A_2 representations. The true mass is likely to lie between these values.

For the top mass there are two key contributions as we can see in figure 8.8. The top Yukawa coupling,

$$y_t = \frac{g^2 Z \ \tilde{g}^2 \tilde{Z} \ Z_3}{M_T^2 \ \Lambda_{UV}^4}\,, \tag{8.58}$$

is inversely proportional to the top partner mass squared. It is proportional to the Z_3 and $Z/\tilde{Z}$ factors. The Z factors, like the baryon-σ vertex in QCD, are not direct predictions of the holographic framework since they must be generated by couplings beyond the basic quadratic terms of the holographic action equation (8.1) and so in principle one can add new couplings. We can though write down holographic terms that are likely to be the dominant contributions and look at their order of magnitude behaviour. As in the previous model we may express the Z factors by

$$Z_3 \simeq \int d\rho \ \rho^3 \ \frac{\partial_\rho \pi(\rho) \ \psi_B(\rho)^2}{(\rho^2 + L^2)^2}\,, \tag{8.59}$$

$$Z = \tilde{Z} \simeq \int d\rho \ \rho^3 \partial_\rho \psi_B(\rho)\,, \tag{8.60}$$

Here $\pi(\rho)$ and $\psi_B(\rho)$ are the holographic wavefunctions for the pNGB and baryon repectively.They are normalized to give canonical kinetic terms for these states as in equation (8.34).

We compute the top Yukawa coupling (setting $g = \tilde{g} = 1$), from the full set of factors in equation (8.58). It is proportional to the Z_3 and $Z/\tilde{Z}$ factors which we will set equal. In this $SU(4)$ model, with a cut off on the HDOs, as an example, of roughly 6 times the vector meson mass, we find the top Yukawa coupling is only of order 0.01 which is far below the value of one needed. The top Yukawa would be

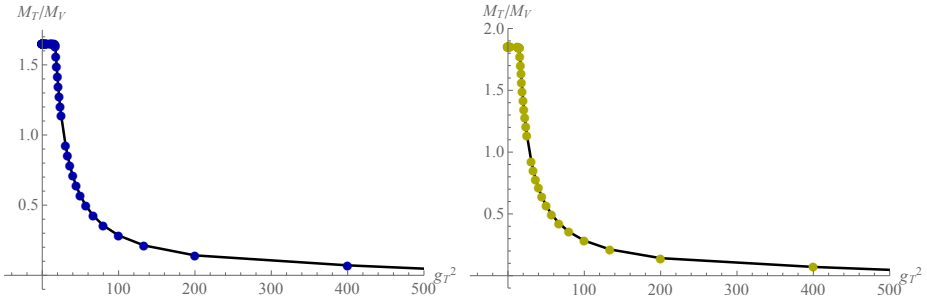

Figure 8.19: $SU(4)$ $3F, 3\bar{F}, 5A_2$ - We show the effect of adding the double-trace operator equation (8.61) to the spin-1/2 baryon's mass. On the left we use the $L_0(\rho)$ from the F representation and on the right $L_0(\rho)$ from the the A_2 representation. Note the initial linear behaviour when g_T^2 is perturbative but then as it passes a critical value the effect on the mass is much larger.

enhanced if the top partners were anomalously light relative to the strong coupling scale (roughly the

scale 1 in our Table 8.5). As we have described in QCD, it is possible to drive the baryons light by including a HDO - see figure 8.7 for example. In the SU(4) theory we can also look to include a HDO of the form

$$\mathcal{L}_{HDO} = \frac{g_T^2}{\Lambda_{UV}^5} |F A_2 F|^2 \,, \tag{8.61}$$

As the operator FA_2F becomes the top partner field this is directly a shift in the top partner mass. In figure 8.19 we show the dependence of the top partner mass on g_T^2 - we show the effect using both the F and A_2 embeddings as $L_0(\rho)$ in equation (8.25). The HDO can indeed be used to reduce the top partner mass - for small g_T^2 the effect is linear and small but after a critical value the effect is much larger, as shown.

One must be careful though because as the top partners mass changes so also do the Z factors in equation (8.59) and equation (8.60). In particular as the HDO in equation (8.51) plays a large role it induces a sizable non-normalizable piece in the UV holographic wave function of the top partner. This means that the integrals in the equivalent of the normalization factors in equation (8.34) and directly in the expressions for the Z factors are more dominated by the UV part of the integral. The overlap between different states can change substantially. We therefore plot the full expression for the Yukawa coupling from equation (8.58) against the top partner mass (which changes as we dial g_T^2) in figure 8.20. We see that the top Yukawa does indeed grow as the top partner's mass falls and can become of order one as the top partners mass falls to about half of the vector meson mass. This suggests, that after fixing the strong coupling scale to a sensible large value in the 1-5 TeV range, in this model we should be able to realize a top partner mass of about 1 TeV and the required top mass.

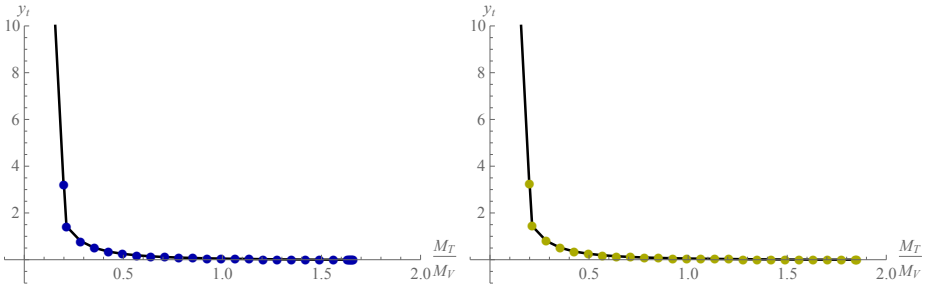

Figure 8.20: SU(4) $3F, 3\bar{F}, 5A_2$ - The top Yukawa coupling, as given by equation (8.58), is plotted against the top partner mass units of the vector meson mass. M_T is controlled by adding a HDO as in figure 8.13. We compute on the left with $L_0(\rho)$ for the fundamental quark and on the right we use the A_2 $L_0(\rho)$.

8.4.5 A catalogue of other composite Higgs models

Finally, in part to demonstrate the flexibility of the holographic method and in part as a service to model builders, we will survey many of the other gauge theories that have been proposed as composite Higgs models with top partners. In particular we will calculate their spectrum and decay constants. We are led by the proposals in [144] and will identify them by the notation of section 8.4.1. Here we do not know of any lattice data, so our results for the meson spectrum and couplings plus the top partner mass stand in isolation. We hope though they will be of potential use for future work.

All of the models proposed in [144] that we consider are asymptotically free (they have positive b_0 in equation (8.8)). However, we find that some of the models live in the conformal window [211, 212] at the level of the approximation of the two loop running results we use. To lie in the conformal window b_1 in equation (8.8) must be negative. We then compute the value of α_c, which is the value of α for $\gamma = 1/2$, the criterion discussed below equation (8.6),

$$\alpha_c = \frac{\pi}{3C_2(r)}, \tag{8.62}$$

and the (positive) value of the coupling at the IR fixed point α^* where the β-function vanishes

$$\alpha^* = -\frac{b_0}{b_1}. \tag{8.63}$$

We classify a gauge theory as lying in the conformal window if $\alpha^* < \alpha_c$. Such models do not break chiral symmetries and can not make good composite Higgs models. We will note these models below but not compute for them.

We will only compute for models that break chiral symmetries. Of course by adding NJL operators, one can force any gauge theory to break chiral symmetry. Such models, dominated by the NJL term, have spectra that will depend on the initial condition of the gauge coupling at the UV cut off (a continuous parameter) so are not easily presented. We will therefore only address models where the gauge dynamics drives the symmetry breaking.

Theories that lie close to the lower (in N_f) edge of the conformal window, yet still break chiral symmetry, have a slowly running gauge coupling and are referred to as walking theories - in these theories γ runs from zero to one over a substantial regime of RG scale μ, unlike in QCD where this running happens very quickly. The main evidence for walking in the spectrum of the theories we study is that the scalar mass (S) falls towards zero because the near conformality tends to flatten the effective potential for the quark condensate - this is the most significant result we find case by case in this section. Where theories break chiral symmetry for a range of N_c, N_f, we will display results at the extreme non-walking and walking values of the parameters. Due to their potential interest for model building, we stress walking theories below, but they are therefore over represented in the sample of theories we present.

In this sub-section we will not decouple the heavier representations from the running coupling - in most cases the two or more representations of matter condense at similar scales (within a factor of 2) and our work on the previous two models suggest the precise form of the decoupling is an interesting but small effect. We will not present as much detail as in section 8.4.3 and section 8.4.4, instead we will just display the results for the masses and couplings from the holographic description by theory. In each case we will normalize to one of the vector meson state's mass. For the numerical analysis below we fix $\alpha(0) = 0.65$ and require a massless quark in the UV, $m_q|_{UV} = 0$.

Models with exceptional gauge groups

The first models for which we compute the spectrum and decay constants are those with exceptional gauge groups that have been proposed in [144]. The gauge group can be either G_2 or F_4 with matter in

the fundamental representation. There are singlet baryons made of three quarks in these cases (see [192] for a detailed discussion). The symmetry breaking pattern with N_f Weyl fermions is $SU(N_f) \to SO(N_f)$. If $N_f \geq 11$ then the SM gauge group can be embedded in the global symmetry and a Higgs doublet and coloured top partners generated. In fact it has been argued that these models are not very promising phenomenologically [144] since there is a high number of pNGBs and some of them mediate proton decay.

The G_2 group is asymptotically free until $N_f = 22$. The theory lies in the conformal window according to the criteria discussed below equation (8.63) down to $N_f = 16$. The $N_f = 16$ theory actually has the fixed point value equal to the chiral symmetry breaking coupling so is maximally walking and would presumably have a massless scalar meson. We present results for the extreme cases we can compute, i.e. for $N_f = 11$ and $N_f = 15$, in Table 8.6.

F_4 theory is asymptotically free until $N_f = 16$. The edge of the conformal window lies between $N_f = 12$ and $N_f = 13$ flavours. We present spectra for the $N_f = 11$ and 12 cases also in Table 8.6 - both of these theories have a slowly running coupling, resulting in a very light scalar. The A and V mesons in these present models are more degenerate than in QCD.

Observables	AdS/G_2 $11F$	AdS/G_2 $15F$	AdS/F_4 $11F$	AdS/F_4 $12F$
f_π	0.0749	0.0797	0.0486	0.0489
M_V	1*	1*	1*	1*
f_V	0.456	0.488	0.49	0.501
M_A	1.15	1.11	1.03	1.03
f_A	0.438	0.470	0.483	0.494
M_S	0.288	0.114	0.000431	0.00039
M_B	1.78	1.76	1.55	1.55

Table 8.6: Holographic predictions for the spectra and decay constants of AdS/G_2, $11F$, AdS/F_4, $11F$, and AdS/F_4, $16F$.

Models with matter in two representations

Composite Higgs models with fermionic matter in two representations can only have either a $Sp(2N)$ or $SO(N_c)$ gauge group and generate the Higgs and top partners.

There are three possible scenarios with a symplectic gauge group:

$Sp(2N)$ $5S_2, 6F$	$N \geq 6$	These theories are all in the conformal window.
$Sp(2N)$ $5A_2, 6F$	$N \geq 2$	Theories with $N < 8$ are below the conformal window, and break chiral symmetry.
$Sp(2N)$ $4F, 6A_2$	$N \leq 18$	Theories with $N < 5$ are below the conformal window, and break chiral symmetry.

We present the spectra for examples of the second and third models that break chiral symmetry. In particular we present for the minimum and maximum number of colours, in Table 8.7 (note the final

model with $Sp(4)$ is the one we studied in more detail in section 8.4.3). The $Sp(14)$ case, which is the slowest walking of these theories, has a very low scalar mass. In the case of $SO(N_c)$ gauge theories,

Observables	AdS/$Sp(4)$ $5A_2, 6F$	AdS/$Sp(14)$ $5A_2, 6F$	AdS/$Sp(4)$ $4F, 6A_2$	AdS/$Sp(8)$ $4F, 6A_2$
$f_{\pi F}$	0.066	0.0521	0.057	0.115
$f_{\pi A_2}$	0.113	0.114	0.12	0.149
M_{VF}	0.618	0.364	0.61	0.913
f_{VF}	0.304	0.229	0.27	0.518
M_{VA_2}	1*	1*	1*	1*
f_{VA_2}	0.494	0.851	0.52	0.683
M_{AF}	0.862	0.414	0.938	1.13
f_{AF}	0.316	0.219	0.303	0.507
M_{AA_2}	1.4	1.02	1.35	1.12
f_{AA_2}	0.507	0.843	0.52	0.665
M_{SF}	0.348	0.000476	0.33	0.508
M_{SA_2}	0.376	0.000296	0.38	0.511
M_{BF}	1.15	0.639	1.13	1.68
M_{BA_2}	1.85	1.48	1.85	1.84

Table 8.7: Holographic results for masses and decay constants in the $Sp(2N_c)$ theories with two different matter representations that can trigger chiral symmetry breaking.

there is a discrete set of cases with two quark representations that generate both the SM Higgs and the top partners in [144]. The models have matter in the fundamental and spinor representations, and N_c and N_f are fixed. Those theories within this set that break chiral symmetry are

$$\mid SO(7)\ 5F, 6s \mid SO(7)\ 5s, 6F \mid SO(9)\ 5F, 6s \mid SO(9)\ 5s, 6F \mid$$

$$\mid SO(10)\ 5F, 6s \mid SO(11)\ 5F, 6s \mid SO(11)\ 4s, 6F \mid SO(13)\ 4s, 6F \mid .$$

We display holographic results for the masses and decay constants for these theories in Table 8.8 as well as in Table 8.9. Note that the $SO(13)$ $4s, 6F$ theory has a very light scalar meson, resulting from the slow running of the coupling. The SO(9) theories are of note since the F fields condense at a higher scale than the spinor fields s so the F bound states are heavier than the s counter parts - here the critical coupling equation (8.62) for the F lies lower than that for the s representation. In the other theories shown, the critical couplings for F is higher than that for s and the F sector is then lighter.

Observables	AdS/$SO(7)$ $5F, 6s$	AdS/$SO(7)$ $5s, 6F$	AdS/$SO(9)$ $5F, 6s$	AdS/$SO(9)$ $5s, 6F$
$f_{\pi F}$	0.125	0.132	0.115	0.121
$f_{\pi s}$	0.126	0.119	0.149	0.143
M_{VF}	1.08	1.07	0.913	0.926
f_{VF}	0.58	0.601	0.518	0.55
M_{Vs}	1*	1*	1*	1*
f_{Vi}	0.581	0.555	0.683	0.653
M_{AF}	1.39	1.33	1.13	1.11
f_{AF}	0.578	0.593	0.507	0.537
M_{As}	1.21	1.25	1.12	1.14
f_{Ai}	0.571	0.55	0.665	0.636
M_{SF}	0.744	0.687	0.508	0.579
M_{Ss}	0.728	0.725	0.511	0.568
M_{BF}	1.98	1.98	1.68	1.71
M_{Bs}	1.85	1.85	1.84	1.84

Table 8.8: Holographic results for the masses and decay constants in the two $SO(7)$ and the two $SO(9)$ theories with two matter representations that can trigger chiral symmetry breaking.

Observables	AdS/$SO(10)$ $5F, 6s$	AdS/$SO(11)$ $5F, 6s$	AdS/$SO(11)$ $4s, 6F$	AdS/$SO(13)$ $4s, 6F$
$f_{\pi F}$	0.11	0.0811	0.103	0.0615
$f_{\pi s}$	0.147	0.104	0.156	0.0878
M_{VF}	0.876	0.918	0.753	0.57
f_{VF}	0.51	0.456	0.468	0.322
M_{Vs}	1*	1*	1*	1*
f_{Vi}	0.682	0.681	0.727	0.694
M_{AF}	1.06	1.05	0.878	0.636
f_{AF}	0.5	0.432	0.455	0.308
M_{As}	1.12	1.04	1.09	1.03
f_{As}	0.664	0.666	0.708	0.684
M_{SF}	0.614	0.142	0.404	0.0453
M_{Ss}	0.578	0.154	0.44	0.0615
M_{BF}	1.61	1.33	1.38	0.884
M_{Bs}	1.83	1.46	1.82	1.34

Table 8.9: Holographic results for the masses and decay constants for the two $SO(10)$, the $SO(11)$ and the $SO(13)$ theories with two matter representations that can trigger chiral symmetry breaking.

In addition, we find the following four models to lie in the conformal window and thus do not display chiral symmetry breaking,

$$\Big|\ SO(13)\ 5F, 6s\ \Big|\ SO(14)\ 5F, 6s\ \Big|\ SO(15)\ 5G, 6F\ \Big|\ SO(55)\ 5S_2, 6F\ \Big|\ .$$

Models with matter in three representations

The $SU(4)$ model of section 8.4.4 falls into this class. In addition, there are four $SO(N_c)$ gauge theories in [144] with specific matter in the F, spinor s and the opposite chirality $\bar{s}$ representations (note the dimensions of the fundamental and the spin are equal for eight colour). Three of these break chiral symmetry,

$$SO(8)\ 5F, 3s, 3\tilde{s} \ \Big|\ SO(10)\ 5F, 3s, 3\tilde{s} \ \Big|\ SO(12)\ 5F, 3s, 3\tilde{s}$$

and one lies in the conformal window,

$$SO(14)\ 5F, 3s, 3\tilde{s}.$$

We analyze the first three in Table 8.10.

Observables	AdS/$SO(8)$ $5F, 3s, 3\tilde{s}$	AdS/$SO(10)$ $5F, 3s, 3\tilde{s}$	AdS/$SO(12)$ $5F, 3s, 3\tilde{s}$
$f_{\pi F}$	0.117	0.11	0.0796
$f_{\pi s}$	0.123	0.147	0.140
M_{VF}	1	0.876	0.608
f_{VF}	0.553	0.51	0.356
M_{Vs}	1*	1*	1*
f_{Vs}	0.579	0.682	0.732
M_{AF}	1.24	1.06	0.718
f_{AF}	0.547	0.5	0.341
M_{As}	1.21	1.12	1.06
f_{As}	0.569	0.664	0.732
M_{SF}	0.817	0.614	0.177
M_{Ss}	0.817	0.578	0.324
M_{BF}	1.85	1.61	1.08
M_{Bs}	1.85	1.83	1.68

Table 8.10: Results for the gauge theories with matter in three representations.

Models with QCD-like breaking patterns

This variety of composite Higgs models has classes with three and four representations. While we could have presented the three representation models in the previous section we chose to separate them in order to follow the classification of [192]. They each have a symmetry breaking sector for one representation where $SU(N_f)_L \times SU(N_f)_R \to SU(N_f)_V$.

In addition to the model of section 8.4.4, there are two models with three representations,

$$SO(10)\ 4s, 4\tilde{s}, 6F \ \Big|\ SU(4)\ 4F, 4\bar{F}, 6A_2 \quad ,$$

Both of these models allow chiral symmetry breaking to occur. We display our results for the masses and decay constants in these cases in Table 8.11.

Moreover, there are the following models with four representations: the isolated model

$$SU(7)\ 4F, 4\bar{F}, 3A_3, 3\bar{A}_3,$$

two classes which break chiral symmetry through the full range of N_c,

$$SU(N_c)\ 4F, 4\bar{F}, 3A_2, 3\bar{A}_2 \quad N_c \geq 5 \qquad \Big| \qquad SU(N_c)\ 3F, 3\bar{F}, 4A_2, 4\bar{A}_2) \quad N_c \geq 5$$

Observables	AdS/$SO(10)$ $4s, 4\tilde{s}, 6F$	AdS/$SU(4)$ $4F, 4\bar{F}, 6A_2$
$f_{\pi F}$	0.107	0.0922
$f_{\pi i}$	0.156	0.122
M_{VF}	0.777	0.805
f_{VF}	0.470	0.424
M_{Vs}	1*	1*
f_{Vi}	0.723	0.540
M_{AF}	0.922	1.05
f_{AF}	0.455	0.427
M_{Ai}	1.09	1.29
f_{Ai}	0.704	0.536
M_{SF}	0.311	0.494
M_{Si}	0.376	0.488
M_{BF}	1.42	1.49
M_{Bi}	1.81	1.85

Table 8.11: Holographic results for masses and decay constants in the the $SO(10)$ $4s, 4\tilde{s}, 6F$ and $SU(4)$ $4F, 4\bar{F}, 6A_2$ models. $i = s$ for the former and $i = A_2$ for the latter.

and two classes that are only outside the conformal window at large N_c,

$$SU(N_c)\ 4F, 4\bar{F}, 3S_2, 3\bar{S}_2 \quad N_c \geq 5 \quad \text{below the conformal window for } N_c > 10 \text{ and break chiral symmetry.}$$

$$SU(N_c)\ 3F, 3\bar{F}, 4S_2, 4\bar{S}_2 \quad N_c \geq 8 \quad \text{below the conformal window for } N_c > 70 \text{ and break chiral symmetry.}$$

The first theory with $N_c > 10$ and the second with $N_c > 70$ are clearly very hard to reconcile with any phenomenology. For example, the S parameter would be expected to be huge. However, for lower N_c values these models are very finely tuned to the conformal window. This leads to a very small scalar meson mass. For these classes we just present models for the smallest value of N_c, for which they break chiral symmetries in Table 8.12.

8.5 Phenomenological implications and constraints

The above analysis of the spectra of possible composite Higgs models has been a purely field theoretic exercise, without taking into account experimental constraints. Now we briefly consider their experi-

	AdS/$SU(5)$ $4F, 4\bar{F}, 3A_2, 3\bar{A}_2$	AdS/$SU(5)$ $4A_2, 4\bar{A}_2, 3F, 3\bar{F}$	AdS/$SU(7)$ $4F, 4\bar{F}, 3A_3, 3\bar{A}_3$	AdS/$SU(10)$ $4F, 4\bar{F}, 3S_2, 3\bar{S}_2$	AdS/$SU(71)$ $3F, 3\bar{F}, 4S_2, 4\bar{S}_2$
$f_{\pi F}$	0.0834	0.0598	0.0803	0.0469	0.0210
$f_{\pi i}$	0.14	0.153	0.164	0.0746	0.0192
M_{VF}	0.67	0.486	0.628	0.386	0.627
f_{VF}	0.372	0.251	0.378	0.228	0.395
M_{Vi}	1*	1*	1*	1*	1*
f_{Vi}	0.608	0.65	0.82	0.726	1.49
M_{AF}	0.845	0.661	0.741	0.434	0.63
f_{AF}	0.368	0.25	0.37	0.217	0.394
M_{Ai}	1.19	1.15	1.06	1.02	1
f_{Ai}	0.59	0.628	0.805	0.683	1.48
M_{SF}	0.338	0.13	0.534	0.000155	0.000849
M_{Si}	0.399	0.273	0.439	0.000479	0.00140
M_{BF}	1.24	0.897	1.16	0.634	0.643
M_{Bi}	1.84	1.83	1.82	1.3	0.952

Table 8.12: Results for gauge theories with matter in four representations. $i = A_2$ for the first two models. $i = A_3$ for the next one. For the final two we have $i = S_2$.

mental impact. We immediately note than many of the theories have very large field content and this is liable to be in conflict with the precision S parameter [238] constraints.

We will briefly summarize some generic phenomenological implications for searches at the LHC based on the mass hierarchies in the models presented in the previous sections. The following discussion neglects contributions to the masses arising from the gauging of the SM forces, analogous to the electric mass splitting between the charged and neutral pions in the SM. These small differences are only likely to play a role in accidentally very fine tuned cases. We will concentrate on the models in sections 8.4.3 and 8.4.4 where there are counterparts of explicit models presented in [234]. In these models the global group related to the A_2 representations contains the electroweak SM group whereas the one related to F (and in the case of $SU(4)$ also $\bar{F}$) contains $SU(3)_c$. Thus, given the measured Higgs mass is about 125 GeV and the bounds on heavy spin one resonance are well above one TeV [239], the ratio of the pion mass to the vector meson masses for the A_2 condensate shown in figures 8.12 and 8.18 is confined to small values to be consistent with the data. On the other, the other pions related to the F condensate can be substantially heavier.

Inspecting Table 8.4 we find, in the case of the $Sp(4)$ model(s), for $m_q = 0$ and negligible contributions from HDOs, that: (i) A_2 bound states are somewhat heavier than the F counterparts; (ii) The scalars are significantly lighter than the vector and axial vector states. The fermionic bound states are still heavier than the corresponding vector bound states. The EW loop corrections mentioned above will tentatively reduce the mass splitting between the corresponding A_2 and F bound states. We also recall from figure 8.12 that a finite but small hyperquark mass hardly changes the relative mass ratios yielding the same overall picture.

One expects that the scalar mesons will dominantly decay into the corresponding pNGB. There could

also be decays into a pair of top quarks arising from the mixing of the top partners with the top quark. The next heavier states are the vector mesons as can be seen from Table 8.4. In the searches for these states it is usually assumed that the decay dominantly into SM-particles. However, due to the quite large mass difference between scalars and these vector states we also expect sizeable branching ratios for the decay $V_{A_2} \to S_{A_2}\, S_{A_2}$ leading to a final state with four pNGB which will decay further. Thus we expect actually an enhancement of the multiplicity of the SM particles compared to the standard LHC searches. The top partners, which are the FA_2F states, should have about the same mass or might be even be lighter than the vector state due to the requirement of a large top Yukawa coupling as discussed in section 8.4.3. Thus we expect that in addition to the standard decays such as

$$T \to t\,\Pi \tag{8.64}$$

(where Π is one of the pNGB which belong either to the electroweak or to the strong sector) there may also be sizeable branching ratios into final states like

$$T \to t\,S\,. \tag{8.65}$$

The subsequent decay of the S into two pNGB results, also in this case, to a more complicated final state compared to the one used in the standard searches by the LHC collaboration. This affects for example the phenomenology of the models M5 and M8 presented in [234].

Turning now to the $SU(4)$ models we focus on the main differences compared to the $Sp(4)$ ones. Comparing Tables 8.4 and 8.5 we notice that in the case of $SU(4)$ the masses of the mesons and baryons depend less on the underlying hyperquarks' mass compared to the $Sp(4)$ models. Secondly, the scalars are significantly heavier than in the case of $Sp(4)$ implying that they will be less frequently produced at the LHC in both, direct production and from cascade decays from heavier states, which affects for example the LHC phenomenology of model M6 in ref. [234]. More generically one finds from these tables and the ones in section 8.4.5, that the ratio M_S/M_V is an important quantity to identify possible underlying gauge groups. However, we note for completeness that this ratio depends to some extent also on the matter content of the underlying theory.

Finally we note that many of the theories presented in section 8.4.5 have very slow running resulting in very light scalar resonances. We expect that the loop induced effective potential due to explicit symmetry breaking effects like the gauging of the SM-group will give sizeable contributions to their masses. This is beyond the realm of this paper and requires a model-by-model investigation of the spectrum of the light states. In these cases one needs also to check to which extent direct searches already constrain them. This will also depend on the precise quantum numbers of these light scalars.

8.6 Regarding the validity of the approximation

As it is obvious from the the formulae of the anomalous dimension that is utilized in this holographic bottom-up model, we have used the one-loop result. A natural question that arises has to do with the validity of the approximation and another one with regards to the error estimate.

In order to shed some light, we will repeat the computations for some of the quantities, however this time we will use a two-loop result for the anomalous dimension, which is given by

$$\gamma_{2l} = \frac{\alpha}{2\pi^2}\left(\frac{3}{2}C_2(R)^2 + \frac{97}{6}C_2(R)C_2(G) - \frac{10N_f}{3}C_2(R)T(R)\right), \tag{8.66}$$

and in this brief subsection we use γ_{1l} to denote the one-loop anomalous dimension. The presentation of the results here is chosen in accord with [2].

In order to give a solid estimate for the differences between the two approaches, we average the results obtained by each method and use half the range as the error. We present these new numerical estimates for our observables in Table 8.13.[5]

	AdS/$Sp(4)$ unquench	AdS/$Sp(4)$ quench	lattice [231] quench	lattice [232] unquench
$f_{\pi A_2}$	0.118 (02)	0.104 (02)	0.1453(12)	
$f_{\pi F}$	0.068 (02)	0.0736 (02)	0.1079(52)	0.1018(83)
M_{VA_2}	1*	1*	1.000(32)	
M_{VF}	0.783 (31)	0.920 (04)	0.83(19)	0.83(27)
M_{AA_2}	1.35 (01)	1.29 (02)	1.75 (13)	
M_{AF}	1.16 (03)	1.32 (04)	1.32(18)	1.34(14)
M_{SA_2}	0.37 (01)	0.982 (16)	1.65(15)†	
M_{SF}	0.77 (13)	1.1 (15)	1.52 (11)†	1.40(19)†
M_{TA_2}	1.85 (01)	1.85 (05)		
M_{TF}	1.46 (07)	1.71 (0)		

Table 8.13: AdS/$Sp(4)$ $4F, 6A_2$. Ground state masses for the vector, axial-vector, and scalar mesons for the two representations, F and A_2, from holography (errors show the range in using γ_{1l} and γ_{2l}) and the lattice. Also the pion decay constant and two estimates of the top partner baryon mass. We have rescaled the lattice data to the M_{VA_2} mass in the quenched case - we have already discussed how we translate errors, see section 8.4.1 - and for the unquenched case, where no A_2 states are included, rescaled so M_{VF} matches the quenched case for comparison. Note the lattice scalar results are for the α_0, namely the isospin singlet, not for the σ we compute in the holographic model. We chose to include them as they provide a guide to the lattice expectation for scalar states.

[5]The error digits are related to the last two digits of the relevant result; i.e 1.46 (07)=1.46 $\pm$ 0.07.

Part VII

Some final thoughts and remarks

Chapter 9

Epilogue

In chapter 7 we considered BPS brane intersections in Type IIA/B theories in static equilibrium that include fields in the fundamental representation of the gauge group. We studied and derived systematically the equations of motion from the fermionic completion of the DBI action. We showed the degeneration between the bosonic and fermionic states by providing the necessary transformations to map the equations of motion from the latter to the former ones. We state the transformation rules once more. The map is given by:

$$\psi^{\oplus}_{\mathcal{G}_\ell}(\varrho) = \frac{1}{(1+\varrho^2)^{\frac{3}{16}(7-p)}} f_{\ell+1}(\varrho), \qquad \psi^{\oplus}_{\mathcal{F}_\ell}(\varrho) = \frac{1}{(1+\varrho^2)^{\frac{3}{16}(7-p)}} f_{\ell}(\varrho),$$

where in the above we denote by $\oplus$ superscript the supergravity modes obtained by considering the projection $\Gamma^\rho \Psi^{\oplus} = \Psi^{\oplus}$ and we reserve the $\ominus$ for the negative eigenvalue of the projection.

In addition to that, we checked the supersymmetric degeneracy of the bosonic and fermionic masses numerically in each probe-brane system. We explicitly computed the value of $\bar{M}^2$ by solving the bosonic as well as the fermionic equations of motion and derived the same masses as expected. We remind at this stage and for the final time, that we have already performed the appropriate shifts in the ℓ quantum number as described in [121] in order to keep the presentation of our tables brief. We have included our numerical estimations for the masses in the various sections of the main body of the paper, see tables 7.2 to 7.9. Hence, we have derived the necessary equations to study the dynamics of world-volume fermions in holographic top-down systems and performed crucial checks regarding their validity.

As a by-product of our studies we managed to show that these states obey the field theory mass scaling relation that baryons have in the large-N_c limit when we fix the other quantum numbers (n which counts the nodes of the wavefunction and ℓ which is the angular momentum of the fields)

$$M^2 \sim N_c^2.$$

We also discussed what we consider to be the precise interpretation of this result. Namely we concluded that this result should be valid if one manages to solve the true dynamic string baryon vertex in the

limit where the field theory is at the conformal window (exhibits walking dynamics).

We would like to comment on further new possible directions below: The most straightforward generalisation of our considerations can be performed in the context of eleven-dimensional supergravity. The supersymmetric M-brane junctions are M2/probe-M5, M5/probe-M5 and M2/probe-M2. The bosonic cases have been performed already in [161] where it was found that the equations of motion coincide with the D1/probe-D5, D4/probe-D4 and the F1/probe-D2 systems respectively. In this notation by F1 we denote the fundamental string. We believe that the approach we developed here is directly applicable in these systems.

One of the approaches that has been followed in order to construct gravity duals of more realistic gauge theories with a reduced amount of symmetry is to replace the five-dimensional sphere of the $AdS_5 \times S^5$ background with a five-dimensional Sasaki-Einstein space. We denote the latter generically by $\mathcal{M}^5$. Doing so we obtain a duality between string theory in $AdS_5 \times \mathcal{M}^5$ and a super-conformal quiver theory. By now we know many such models explicitly. The first example that was studied in the literature is the so-called Klebanov-Witten model where we have $\mathcal{M}^5 = T^{1,1}$ [240]. We also have at our disposal infinite five (and also higher) dimensional spaces of cohomogeneity 1 and 2. These manifolds are called $Y^{p,q}$ [241] and $L^{p,q,r}$ [242, 243] respectively, with already existing work on supersymmetric brane embeddings in these backgrounds [244, 245]. It would be an interesting project to derive the corresponding mass spectra of mesonic states in these cases.

It would also be interesting to derive the fermionic spectra of gravity duals that describe chiral symmetry breaking (χSB). The most straightforward example of χSB in the context of holography is provided by the D3/probe-D7 with a non-trivial NS flux (Kalb-Ramond field) on the probe-brane [246]. The main conceptual difference between this system of χSB and the systems that we have considered here, is the non-trivial dependence of the embedding function on the holographic radial coordinate. In the magnetic field example instead of having the separation of the background and the probe branes to be a constant, it is a non-trivial function $L(\rho)$ that depends on the holographic radial coordinate. Geometrically this means that the probe-brane is curved. The practical issue in cases with such embeddings is the manipulation of the Γ-matrix projections in order to construct an ordinary second-order differential equation to apply the general steps we developed here.

Finally, it would be interesting to understand the dynamics of world-volume fermions in anisotropic RG flows in type IIB supergravity. These RG flows are solutions from the isotropic fixed points to the anisotropic ones. There are solutions in the literature [247] that describe the D3/D7 brane setup which extend from the familiar AdS_5 solution in the UV to the anisotropic solution in the IR. This generalisation of the AdS/CFT duality to include the description of Lifshitz-like fixed points was initiated in [248] and is interesting in the context of condensed matter theory and applications thereof. We believe that the general approach we developed here is applicable in these systems as well, and might also make computations more feasible.

In chapter 8 we adapted the holographic model of [136] to describe composite Higgs models, including fermionic bound states as in [1], as well as multiple representations of matter. Our holographic approach is inspired by string theory realizations of gauge/gravity duality; the holographic gravity action is based

on the top-down DBI action for a probe D7-brane. As a novel feature compared to previous holographic composite Higgs models, the spontaneous symmetry breaking is induced by the dynamics of the gravity theory, just as in the stringy top-down models. Within these models, in a phenomenological approach we directly impose the running of the quark anomalous dimension. We have used the two-loop running of the gauge coupling, extending it naively to the non-perturbative regime, to predict the running of γ. The model then predicts the light meson and nucleon spectrum for given numbers of colours and flavours for chosen groups and representations.

We also included higher dimension operators into the holographic model to describe Nambu-Jona-Lasinio-like interaction terms. We have demonstrated this in two-flavour QCD, where we 'perfected' the model in the spirit of lattice QCD by including HDOs at the UV scale where the theory transitions to weak coupling. We have shown that the spectrum can be brought closer to the observed spectrum in this way (see table 8.2).

After grounding the holographic model with the QCD predictions, we then moved to studying the underlying gauge theory dynamics in composite Higgs models. We studied three theories in particular detail that have associated lattice results - $SU(2)$ $4F$; $Sp(4)$ $4F, 6A_2$; and $SU(4)$ $3F, 3\bar{F}, 5A_2$. The results and comparisons to lattice data are in tables 8.3, 8.4 and 8.5. The holographic techniques describe the lattice data sensibly. This encouraged us to extended the results beyond known lattice results. In particular, we straightforwardly computed a wider range of observables and crucially had the ability to quench, unquench and change the number of flavours of quarks without the troubles of lattice doubling or sign problems. Indeed in section 8.4.5, we have surveyed the full set of possible gauge theories for composite Higgs models proposed in [144]. We expect that this will provide a useful resource for model builders.

In a holographic realization of models with "partial compositeness", we have also computed the top Yukawa coupling, using HDOs to impose the required mixing between the top quark and top partner baryons in the strong coupling sector. Extending this approach by including an additional HDO of the form $|FA_2F|^2$ both reduces the top partners' masses and raises the structure functions sufficiently to allow for a top Yukawa coupling of order $y_t \simeq 1$, consistent with the Standard Model. This value is obtained for a top partner mass of half the value of the vector meson mass in the strongly coupled sector. For a choice of the strong coupling scale between 1-5 TeV, this is likely to be compatible with current experimental bounds on these states.

The holographic modelling does depend on assumptions about the IR dynamics. We expect to be able to improve the tuning of the model to the dynamics as more lattice results become available, similarly to the results for QCD of [196]. An example of an IR assumption that we have made is the input for the running of the quark anomalous dimension γ. We have considered models of [144] where the two-loop ansatz for the running of γ places the theory in the conformal window. If the IR fixed point value in these theories turns out to be higher, the ansatz for the running could be easily modified. The holographic techniques also seem likely to remain useful for chiral models that cannot be studied on the lattice easily - we anticipate a constructive dialogue with future lattice work.

There is also substantial room for future exchanges with model builders. For example, the addition of

NJL interactions could turn models in the conformal window into symmetry breaking theories. This is easily studied with the holographic approach presented. Moreover, models with further matter content that are closer to being conformal in the UV may be of interest [228]. In this case, the HDOs dimensions would reduce, such that enhancements of the top Yukawa coupling might be possible. Generically, all of these ideas are quick to apply using holographic techniques in any such model. We hope holography will become a common-place tool for model builders.

Part VIII

Appendix

Appendix A

(Super)conformal algebra

A.1 The conformal algebra

Here we demonstrate the validity of the commutation relations that specify the conformal algebra as spelled out in section 4.1.2.

- $[D, P_M] = P_M$.

  We have:

$$[D, P_M] = [x^N \partial_N, -\partial_M] = -x^N \partial_N \partial_M + \left(\partial_M x^N\right) \partial_N + x^N \partial_M \partial_N = \delta^N_M \partial_N = \partial_M = P_M \quad \text{(A.1)}$$

The next commutator is

- $[D, K_M] = -K_M$.

We have:

$$\begin{aligned} [D, K_M] &= [x^N \partial_N, -2x_M x^P \partial_P + x^2 \partial_M] \,, \\ &= -x^N \partial_N \left(2x_M x^P \partial_P\right) + \eta_{AB} x^N \partial_N \left(x^A x^B \partial_M\right) + 2x_M x^P \partial_P \left(x^N \partial_N\right) \\ &- \eta_{AB} x^A x^B \partial_M \left(x^N \partial_N\right) \,. \end{aligned} \quad \text{(A.2)}$$

We will calculate the first term explicitly

$$\begin{aligned} -2x^N \left(\partial_N x_M\right) x^P \partial_P - 2x^N \left(\partial_N x^P\right) x_M \partial_P - 2x^N x_M x^P \partial_N \partial_P = \\ -2x^N \left(\frac{\partial x_M}{\partial x^N}\right) x^P \partial_P - 2x^N x_M \left(\frac{\partial x^P}{\partial x^N}\right) \partial_P - 2x^N x_M x^P \partial_N \partial_P = \\ -2x^N \eta_{NK} \frac{\partial x_M}{\partial x_K} x^P \partial_P - 2x^N x_M \delta^P_N \partial_P - 2x^N x_M x^P \partial_N \partial_P = \\ -2x^N \eta_{NK} \delta^M_K x^P \partial_P - 2x^P x_M \partial_P - 2x^N x_M x^P \partial_N \partial_P = \\ -2x^N \eta_{NM} \delta^M_K x^P \partial_P - 2x^P x_M \partial_P - 2x^N x_M x^P \partial_N \partial_P \end{aligned} \quad \text{(A.3)}$$

Likewise, we can compute the rest of the terms and we obtain

$$\eta_{AB}x^N\partial_N\left(x^Ax^B\partial_M\right) = \eta_{NB}x^Nx^B\partial_M + \eta_{AN}x^Nx^A\partial_M + \eta_{AB}x^Ax^Bx^N\partial_M\partial_N \tag{A.4a}$$

$$2x_Mx^P\partial_P\left(x^N\partial_N\right) = 2x_Mx^N\partial_N + 2x_Mx^Nx^P\partial_N\partial_P \tag{A.4b}$$

$$-\eta_{AB}x^Ax^B\partial_M\left(x^N\partial_N\right) = -\eta_{AB}x^Ax^B\partial_M - \eta_{AB}x^Ax^Bx^N\partial_M\partial_N\,. \tag{A.4c}$$

It is straightforward now to gather the results from equation (A.3) and equations (A.4a) to (A.4c) and insert them into equation (A.2) to obtain

$$[D, K_M] = -2x_Mx^N\partial_N + x^2\partial_M = -K_M\,. \tag{A.5}$$

We proceed to examine

- $[K_M, P_N] = 2\left(\eta_{MN}D - \Lambda_{MN}\right)$.

Firstly, we expand the commutator fully

$$\begin{aligned}[K_M, P_N] = &-2x_Mx^A\partial_A\left(-\partial_N\right) + \eta_{BC}x^Bx^C\partial_M\left(-\partial_N\right)\\ &-\left(\left(-\partial_N\right)\left(-2x_Mx^A\partial_A\right) + \left(-\partial_N\right)\left(\eta_{BC}x^Bx^C\partial_M\right)\right)\,.\end{aligned} \tag{A.6}$$

All of the terms above can be computed in the same way as we have seen previously. Below we giv the results

$$-2x_Mx^A\partial_A\left(-\partial_N\right) = 2x_Mx^A\partial_A\partial_N \tag{A.7a}$$

$$\eta_{BC}x^Bx^C\partial_M\left(-\partial_N\right) = -\eta_{BC}x^Bx^C\partial_M\partial_N \tag{A.7b}$$

$$\left(-\partial_N\right)\left(-2x_Mx^A\partial_A\right) = 2\left(\eta_{MN}x^A\partial_A + x_M\partial_N + x_Mx^A\partial_N\partial_A\right) \tag{A.7c}$$

$$\left(-\partial_N\right)\left(\eta_{BC}x^Bx^C\partial_M\right) = -x_N\partial_M - x_N\partial_M - \eta_{BC}x^Bx^C\partial_N\partial_M \tag{A.7d}$$

Finally, it is easy to see that by inserting the resuts given in equations (A.7a) to (A.7d) into equation (A.6) we obtain

$$\begin{aligned}[K_M, P_N] &= -2\eta_{MN}x^A\partial_A - 2x_M\partial_N + 2x_N\partial_M\\ &= 2\left(\eta_{MN}D - \Lambda_{MN}\right)\end{aligned} \tag{A.8}$$

The next commutation relation we wish to examine is

- $[P_P, \Lambda_{MN}] = \eta_{PM}P_N - \eta_{PN}P_M$.

We have

$$\begin{aligned}[P_P, \Lambda_{MN}] &= \left[-\partial_P, x_M\partial_N - x_N\partial_M\right]\\ &= -\partial_P\left(x_M\partial_N\right) - \left(-\partial_P\right)\left(x_N\partial_M\right)\\ &= -\eta_{PM}\partial_N + \eta_{PN}\partial_M\\ &= \eta_{PM}P_N - \eta_{PN}P_M\end{aligned} \tag{A.9}$$

We move on to examine the following

- $[K_P, \Lambda_{MN}] = \eta_{PM} K_N - \eta_{PN} K_M$.

We begin by expanding it and we get:

$$\begin{aligned}[K_P, \Lambda_{MN}] = &-2x_P x^A \partial_A \left(x_M \partial_N - x_N \partial_M\right) + \eta_{BC} x^B x^C \partial_P \left(x_M \partial_N - x_N \partial_M\right) \\ &- x_M \partial_N \left(-2x_P x^A \partial_A + \eta_{BC} x^B x^C \partial_P\right) + x_N \partial_M \left(-2x_P x^A \partial_A + \eta_{BC} x^B x^C \partial_P\right)\end{aligned} \tag{A.10}$$

We compute the individual pieces of the above which give

$$\begin{aligned}-2x_P x^A \partial_A \left(x_M \partial_N - x_N \partial_M\right) = &-2x_P x_M \partial_N - 2x_P x^A x_M \partial_A \partial_N + 2x_P x_N \partial_M \\ &+2x_P x^A x_N \partial_A \partial_M \end{aligned} \tag{A.11a}$$

$$\eta_{BC} x^B x^C \partial_P \left(x_M \partial_N - x_N \partial_M\right) = \eta_{MP} x^2 \partial_N - \eta_{NP} x^2 \partial_M + x^2 x_M \partial_P \partial_N - x^2 x_N \partial_P \partial_M \tag{A.11b}$$

$$\begin{aligned}-x_M \partial_N \left(-2x_P x^A \partial_A + \eta_{BC} x^B x^C \partial_P\right) = &2\eta_{NP} x_M x^A \partial_A + 2x_P x_M \partial_N \\ &+ 2x_M x_P x^A \partial_N \partial_A - 2x_M x_N \partial_P - x_M x^2 \partial_N \partial_P \end{aligned} \tag{A.11c}$$

$$\begin{aligned}x_N \partial_M \left(-2x_P x^A \partial_A + \eta_{BC} x^B x^C \partial_P\right) = &-2\eta_{MP} x_N x^A \partial_A - 2x_P x_N \partial_M \\ &- 2x_N x_P x^A \partial_M \partial_A - 2x_M x_N \partial_P + x_M x^2 \partial_M \partial_P \end{aligned} \tag{A.11d}$$

We plug into equation (A.10) the results obtained in equations (A.11a) to (A.11d) and we obtain the desired result and more specifically

$$\begin{aligned}[K_P, \Lambda_{MN}] &= -2\eta_{MP} x_N x^A \partial_A + \eta_{MP} x^2 \partial_N + 2\eta_{NP} x_M x^A \partial_A - \eta_{NP} x^2 \partial_M \\ &= \eta_{PM} K_N - \eta_{PN} K_M\end{aligned} \tag{A.12}$$

The final task, in order to conclude this section, is to examine the commutator

- $[\Lambda_{MN}, \Lambda_{PS}] = \eta_{NP} \Lambda_{MS} + \eta_{MS} \Lambda_{NP} - \eta_{MP} \Lambda_{NS} - \eta_{NS} \Lambda_{MP}$.

The commutator, when expanded out completely, yields

$$\begin{aligned}[\Lambda_{MN}, \Lambda_{PS}] = &x_M \partial_N \left(x_P \partial_S - x_S \partial_P\right) - x_N \partial_M \left(x_P \partial_S - x_S \partial_P\right) \\ &- x_P \partial_S \left(x_M \partial_N - x_N \partial_M\right) + x_S \partial_P \left(x_M \partial_N - \partial_N x_M\right)\end{aligned} \tag{A.13}$$

We can compute in a straightforward manner each term of the above expression. We quote the results below

$$x_M \partial_N \left(x_P \partial_S - x_S \partial_P\right) = \eta_{NP} x_M \partial_S + x_M x_P \partial_N \partial_S - \eta_{NS} x_M \partial_P - x_M x_S \partial_N \partial_P \tag{A.14a}$$

$$-x_N \partial_M \left(x_P \partial_S - x_S \partial_P\right) = -\eta_{MP} x_N \partial_S - x_N x_P \partial_M \partial_S + \eta_{MS} x_N \partial_P + x_N x_S \partial_M \partial_P \tag{A.14b}$$

$$-x_P \partial_S \left(x_M \partial_N - x_N \partial_M\right) = -\eta_{MS} x_P \partial_N - x_P x_M \partial_S \partial_N + \eta_{SN} x_P \partial_M + x_P x_N \partial_M \partial_S \tag{A.14c}$$

$$x_S \partial_P \left(x_M \partial_N - \partial_N x_M\right) = \eta_{MP} x_S \partial_N - \eta_{NP} x_S \partial_M + x_S x_M \partial_P \partial_N - x_S x_N \partial_P \partial_M \tag{A.14d}$$

We are now able to use our results equations (A.14a) to (A.14d) and plug them into equation (A.13) to

obtain

$$\begin{aligned}[\Lambda_{MN},\Lambda_{PS}] &= \eta_{NP}\left(x_M\partial_S - x_S\partial_M\right) + \eta_{MS}\left(x_N\partial_P - x_P\partial_N\right) - \eta_{MP}\left(x_N\partial_S - x_S\partial_N\right) \\ &\quad - \eta_{NS}\left(x_M\partial_P - x_P\partial_M\right) \\ &= \eta_{NP}\Lambda_{MS} + \eta_{MS}\Lambda_{NP} - \eta_{MP}\Lambda_{NS} - \eta_{NS}\Lambda_{MP}\,.\end{aligned} \tag{A.15}$$

A.2 Hermitian conjugation & the superconformal algebra

The purpose of this section is to show that the definition of the † given by equation (4.63) is consistent with the superconformal algebra as is spelled out in equation (4.60). The only property needed in this section is equation (4.62).

A.2.1 Commutators

For the commutators we have seen from equation (4.60) that there are very similar expressions for barred and unbarred quantities. Here we demonstrate how the hermitian conjugation works for the case of the unbarred quantities and it should be quite straightforward how it also works for the commutators of the barred quantities.

We begin our studies by examining the following:

$$[(\Lambda_\alpha{}^\beta)^\dagger, (\mathcal{Q}^i{}_\gamma)^\dagger] = [\Lambda_\beta{}^\alpha, \mathcal{S}_i{}^\gamma] = -\delta_\beta{}^\gamma\mathcal{S}_i{}^\alpha + \frac{1}{2}\delta_\beta{}^\alpha\mathcal{S}_i{}^\gamma\,, \tag{A.16}$$

which we have to compare with the expression

$$\Big([\mathcal{Q}^i{}_\gamma, \Lambda_\alpha{}^\beta]\Big)^\dagger = -\left(\delta_\gamma{}^\beta\mathcal{Q}^i{}_\alpha - \frac{1}{2}\delta_\alpha{}^\beta\mathcal{Q}^i{}_\gamma\right)^\dagger = -\delta_\beta{}^\gamma\mathcal{S}_i{}^\alpha + \frac{1}{2}\delta_\beta{}^\alpha\mathcal{S}_i{}^\gamma\,. \tag{A.17}$$

Equations (A.16) and (A.17) suggest that this commutator respects hermitian conjugation. The calculation for corresponding commutator with barred quanitties, $[\Lambda^{\dot\alpha}{}_{\dot\beta}, \bar{\mathcal{Q}}_{i\dot\gamma}]$, follows similarly. While it should be obvious how one can obtain the remaining commutation relation, we will demonstrate explicitly for completeness. We have

$$\begin{aligned}[(\Lambda_\alpha{}^\beta)^\dagger, (\mathcal{S}_i{}^\gamma)^\dagger] &= [\Lambda_\beta{}^\alpha, \mathcal{Q}^i{}_\gamma] = \delta_\gamma{}^\alpha\mathcal{Q}^i{}_\beta - \frac{1}{2}\delta_\beta{}^\alpha\mathcal{Q}^i{}_\gamma\,, \\ \Big([\mathcal{S}_i{}^\gamma, \Lambda_\alpha{}^\beta]\Big)^\dagger &= -\left(-\delta_\alpha{}^\gamma\mathcal{S}_i{}^\beta + \frac{1}{2}\delta_\alpha{}^\beta\mathcal{S}_i{}^\gamma\right)^\dagger = \delta_\gamma{}^\alpha\mathcal{Q}^i{}_\beta - \frac{1}{2}\delta_\beta{}^\alpha\mathcal{Q}^i{}_\gamma\,.\end{aligned} \tag{A.18}$$

Furthemore,

$$\begin{aligned}[D^\dagger, (\mathcal{Q}^i{}_\alpha)^\dagger] &= [D, \mathcal{S}_i{}^\alpha] = -\frac{1}{2}\mathcal{S}_i{}^\alpha\,, \\ \Big([\mathcal{Q}^i{}_\alpha, D]\Big)^\dagger &= -\left(\frac{1}{2}\mathcal{Q}^i{}_\alpha\right)^\dagger = -\frac{1}{2}\mathcal{S}_i{}^\alpha\,.\end{aligned} \tag{A.19}$$

Additionally,

$$\begin{aligned}[D^\dagger, (\mathcal{S}_i{}^\alpha)^\dagger] &= [D, \mathcal{Q}^i{}_\alpha] = \frac{1}{2}\mathcal{Q}^i{}_\alpha\,, \\ ([\mathcal{S}_i{}^\alpha, D])^\dagger &= -\left(-\frac{1}{2}\mathcal{S}_i{}^\alpha\right)^\dagger = \frac{1}{2}\mathcal{Q}^i{}_\alpha\,.\end{aligned} \tag{A.20}$$

Moreover,

$$\begin{aligned}[(\mathcal{R}^i{}_j)^\dagger, (\mathcal{Q}^k{}_\alpha)^\dagger] &= [\mathcal{R}^j{}_i, \mathcal{S}_k{}^\alpha] = -\delta^j{}_k\mathcal{S}_i{}^\alpha + \frac{1}{4}\delta^j{}_i\mathcal{S}_k{}^\alpha\,, \\ \left([\mathcal{Q}^k{}_\alpha, \mathcal{R}^i{}_j]\right)^\dagger &= -\left(\delta_j{}^k\mathcal{Q}^i{}_\alpha - \frac{1}{4}\delta^i{}_j\mathcal{Q}^k{}_\alpha\right)^\dagger = -\delta^j{}_k\mathcal{S}_i{}^\alpha + \frac{1}{4}\delta^j{}_i\mathcal{S}_k{}^\alpha\,.\end{aligned} \tag{A.21}$$

Also,

$$\begin{aligned}[(\mathcal{R}^i{}_j)^\dagger, (\mathcal{S}_k{}^\alpha)^\dagger] &= [\mathcal{R}^j{}_i, \mathcal{Q}^k{}_\alpha] = \delta_i{}^k\mathcal{Q}^j{}_\alpha - \frac{1}{4}\delta^j{}_i\mathcal{Q}^k{}_\alpha\,, \\ \left([\mathcal{S}_k{}^\alpha, \mathcal{R}^i{}_j]\right)^\dagger &= -\left(-\delta^i{}_k\mathcal{S}_j{}^\alpha + \frac{1}{4}\delta^i{}_j\mathcal{S}_k{}^\alpha\right)^\dagger = \delta_i{}^k\mathcal{Q}^j{}_\alpha - \frac{1}{4}\delta^j{}_i\mathcal{Q}^k{}_\alpha\,.\end{aligned} \tag{A.22}$$

Withal,

$$\begin{aligned}[(P_{\alpha\dot\alpha})^\dagger, (\mathcal{S}_i{}^\beta)^\dagger] &= [K^{\dot\alpha\alpha}, \mathcal{Q}^i{}_\beta] = 2\delta_\beta{}^\alpha\bar{\mathcal{S}}^{i\dot\alpha}\,, \\ \left([\mathcal{S}_i{}^\beta, P_{\alpha\dot\alpha}]\right)^\dagger &= -\left(-2\delta_\alpha{}^\beta\bar{\mathcal{Q}}_{i\dot\alpha}\ ,\right)^\dagger = 2\delta_\beta{}^\alpha\bar{\mathcal{S}}^{i\dot\alpha}\,.\end{aligned} \tag{A.23}$$

Finally,

$$\begin{aligned}[(K^{\dot\alpha\alpha})^\dagger, (\mathcal{Q}^i{}_\beta)^\dagger] &= [P_{\alpha\dot\alpha}\,, \mathcal{S}_i{}^\beta] = -2\delta_\alpha{}^\beta\bar{\mathcal{Q}}_{i\dot\alpha}\,, \\ \left([\mathcal{Q}^i{}_\beta, K^{\dot\alpha\alpha}]\right)^\dagger &= -\left(2\delta_\beta{}^\alpha\bar{\mathcal{S}}^{i\dot\alpha}\right)^\dagger = -2\delta_\alpha{}^\beta\bar{\mathcal{Q}}_{i\dot\alpha}\,.\end{aligned} \tag{A.24}$$

Equations (A.16) to (A.24) along with their barred counterparts which we have not explicitly demonstrated prove that the definition of hermitian conjugation equation (4.63) is consistent with the commutators of the superconformal algebra.

A.2.2 Anticommutators

We need to examine the anticommutation relations that appear in the superconformal algebra. The steps are the same as above. Firstly, we have

$$\begin{aligned}\{(\mathcal{Q}^i{}_\alpha)^\dagger, (\bar{\mathcal{Q}}_{j\dot\alpha})^\dagger\} &= \{\mathcal{S}_i{}^\alpha, \bar{\mathcal{S}}^{j\dot\alpha}\} = \frac{1}{2}\delta^j{}_iK^{\dot\alpha\alpha}\,, \\ \left(\{\mathcal{Q}^i{}_\alpha, \bar{\mathcal{Q}}_{j\dot\alpha}\}\right)^\dagger &= \left(\frac{1}{2}\delta^i{}_jP_{\alpha\dot\alpha}\right)^\dagger = \frac{1}{2}\delta^j{}_iK^{\dot\alpha\alpha}\,.\end{aligned} \tag{A.25}$$

Likewise,

$$\begin{aligned}\{(\bar{\mathcal{S}}^{i\dot\alpha})^\dagger, (\mathcal{S}_j{}^\alpha)^\dagger\} &= \{\bar{\mathcal{Q}}_{i\dot\alpha}, \mathcal{Q}^j{}_\alpha\} = \frac{1}{2}\delta^j{}_iP_{\alpha\dot\alpha}\,, \\ \left(\{\bar{\mathcal{S}}^{i\dot\alpha}, \mathcal{S}_j{}^\alpha\}\right)^\dagger &= \left(\frac{1}{2}\delta^i{}_jK^{\dot\alpha\alpha}\right)^\dagger = \frac{1}{2}\delta^j{}_iP_{\alpha\dot\alpha}\,.\end{aligned} \tag{A.26}$$

In addition to the above,

$$\begin{aligned}\{(\mathcal{Q}^i{}_\alpha)^\dagger, (\mathcal{S}_j{}^\beta)^\dagger\} &= \{\mathcal{S}_i{}^\alpha\,\mathcal{Q}^j{}_\beta\} = \delta^j{}_i\Lambda_\beta{}^\alpha + \frac{1}{2}\delta^j{}_i\delta_\beta{}^\alpha D - \delta_\beta{}^\alpha\mathcal{R}^j{}_i\,, \\ \left(\{\mathcal{Q}^i{}_\alpha, \mathcal{S}_j{}^\beta\}\right)^\dagger &= \left(\delta^i{}_j\Lambda_\alpha{}^\beta + \frac{1}{2}\delta^i{}_j\delta_\alpha{}^\beta D - \delta_\alpha{}^\beta\mathcal{R}^i{}_j\right)^\dagger = \delta^j{}_i\Lambda_\beta{}^\alpha + \frac{1}{2}\delta^j{}_i\delta_\beta{}^\alpha D - \delta_\beta{}^\alpha\mathcal{R}^j{}_i\,.\end{aligned} \tag{A.27}$$

The final anticommutator that we need to examine is shown below

$$\begin{aligned}
\{(\bar{\mathcal{S}}^{i\dot{\alpha}})^\dagger, (\bar{\mathcal{Q}}_{j\dot{\beta}})^\dagger\} &= \{\bar{\mathcal{Q}}_{i\dot{\alpha}}, \bar{\mathcal{S}}^{j\dot{\beta}}\} = \delta^j{}_i \bar{\Lambda}^{\dot{\beta}}{}_{\dot{\alpha}} + \frac{1}{2}\delta^j{}_i \delta^{\dot{\beta}}{}_{\dot{\alpha}} D + \delta^{\dot{\beta}}{}_{\dot{\alpha}} \mathcal{R}^j{}_i \,, \\
\left(\{\bar{\mathcal{S}}^{i\dot{\alpha}}, \bar{\mathcal{Q}}_{j\dot{\beta}}\}\right)^\dagger &= \left(\delta^i{}_j \bar{\Lambda}^{\dot{\alpha}}{}_{\dot{\beta}} + \frac{1}{2}\delta^i{}_j \delta^{\dot{\alpha}}{}_{\dot{\beta}} D + \delta^{\dot{\alpha}}{}_{\dot{\beta}} \mathcal{R}^i{}_j\right)^\dagger = \delta^j{}_i \bar{\Lambda}^{\dot{\beta}}{}_{\dot{\alpha}} + \frac{1}{2}\delta^j{}_i \delta^{\dot{\beta}}{}_{\dot{\alpha}} D + \delta^{\dot{\beta}}{}_{\dot{\alpha}} \mathcal{R}^j{}_i \,.
\end{aligned} \tag{A.28}$$

Appendix B

Dimensional analysis & gravity

Here we demonstrate how to perform dimensional analysis in the gravity side. We are following the book [24] and more specifically we wil solve a simpler version of a homework problem from that book; see exercise 8.1.

We start by writing the Einstein-Hilbert action in four dimensions

$$S = \int d^4x\sqrt{-G}\left(\frac{1}{2\kappa^2}G^{MN}R_{MN} + \cdots\right), \tag{B.1}$$

and the task at hand is to determine the dimensions of the constant κ which is the gravitational coupling constant. In the above by $\cdots$ we have denoted various possible matter couplings that may appear in the action.

The invariant line element $ds^2 = G_{MN}dx^M dx^N$ has $[ds^2] = L^2$ where L denotes dimensions of length. The metric itself is dimensionless, $[G_{MN}] = 0$, while we have that $[dx^M] = L$. This is very convenient as the dimensions of any curvature related tensor can be found simply by counting how many spacetime derivatives are needed in order to construct it. We count a factor of L^{-1} for each one. Hence, we have that since $d^4x = L^4$ and $[R_{MN}] = L^{-2}$ then $[\kappa^2] = L^2$.

Appendix C

Notations and conventions for top-down systems

C.1 Notations and conventions

We find it necessary to collect and clarify our conventions and notation for the various manipulations of the main body of our work in this appendix. We begin by discussing the different letters that have appeared throughout the various sections.

Capital letters A, B, C,... denote type IIA/B coordinates and they take values in the range $(0, \ldots, 9)$. The space described by the Z-coordinates corresponds to spatial coordinates which are transverse to the background Dp-branes. Its dimensionality is equal to $(9-p)$. Lower-case Greek letters μ, ν,... are the Minkowski indices which correspond to the spacetime coordinates of the Dp-brane . The letters ρ and ϱ denote the radial and the rescaled dimensionless radial coordinate, respectively. Hatted indices $\hat{A}, \hat{B}$,... parametrize the spacetime spanned by the probe Dk-brane. Y-coordinates denote the $(k-d)$-dimensional internal space to the probe brane. Finally, we use the set $\{w^1, w^2, \ldots, w^{9-p-k+d}\}$ of coordinates to specify the subspace of the original ten-dimensional geometry that is transverse to both the background and the probe branes. Indices enclosed within brackets, i.e $(A), (\mu)$, take values according the aforementioned rules and denote the passing to the vielbein basis.

For the components of a p-form we use the convention

$$\mathcal{X}_{(p)} \equiv \frac{1}{p!}\, \mathcal{X}_{\mu_1\mu_2\ldots\mu_p}\, dx^{\mu_1} \wedge dx^{\mu_2} \wedge \ldots \wedge dx^{\mu_p} = \mathcal{X}_{|\mu_1\mu_2\ldots\mu_p|}\, dx^{\mu_1} \wedge dx^{\mu_2} \wedge \ldots \wedge dx^{\mu_p}. \tag{C.1}$$

In the above relation, the vertical bars denote that only components with increasing indices are included in the summation.

Definition of the Hodge star operator: Let us consider an n-dimensional spacetime and the usual $\{dx^M\}$ basis which satisfies the relation $ds^2 = g_{\mu\nu} dx^\mu dx^\nu$, then the *dual* of the q-form (with $q < n$)

$dx^{\mu_1} \wedge \ldots \wedge dx^{\mu_q}$ is defined as

$$\begin{aligned} \star\,(dx^{\mu_1} \wedge dx^{\mu_2} \wedge \ldots \wedge dx^{\mu_q}) &\equiv \frac{\sqrt{-g^{(n)}}}{(n-q)!}\, g^{\mu_1\nu_1}\, g^{\mu_2\nu_2} \cdots g^{\mu_q\nu_q}\, \epsilon_{\nu_1\nu_2\ldots\nu_q\,\nu_{q+1}\ldots\nu_n}\, dx^{\nu_{q+1}} \wedge \ldots \wedge dx^{\nu_n} \\ &= \sqrt{-g^{(n)}}\, g^{\mu_1\nu_1}\, g^{\mu_2\nu_2} \cdots g^{\mu_q\nu_q}\, \epsilon_{\nu_1\nu_2\ldots\nu_q\,|\nu_{q+1}\ldots\nu_n|}\, dx^{\nu_{q+1}} \wedge \ldots \wedge dx^{\nu_n}\,, \end{aligned} \tag{C.2}$$

where $g^{(n)} = \det(g_{\mu\nu})$, $\epsilon_{012\ldots n} = 1$. The star $\star$ is called *Hodge star operator*. Using the above equation, we can determine the dual of a p-form $\mathcal{X}_{(p)}$, namely it is

$$\star\,\mathcal{X}_{(p)} = \sqrt{-g^{(n)}}\, \mathcal{X}_{|\mu_1\mu_2\ldots\mu_p|} g^{\mu_1\nu_1}\, g^{\mu_2\nu_2} \cdots g^{\mu_p\nu_p}\, \epsilon_{\nu_1\nu_2\ldots\nu_p\,|\nu_{p+1}\ldots\nu_n|}\, dx^{\nu_{p+1}} \wedge \ldots \wedge dx^{\nu_n}\,, \tag{C.3}$$

with $p < n$.

Let us now consider the vielbein basis $\{e^{(\mu)}\}$, which satisfies the relation $ds^2 = \eta_{(\mu)(\nu)} e^{(\mu)} e^{(\nu)}$. In this case, we would have

$$\star\left(e^{(\mu_1)} \wedge \ldots \wedge e^{(\mu_q)}\right) \equiv \eta^{(\mu_1)(\nu_1)} \cdots \eta^{(\mu_q)(\nu_q)}\, \epsilon_{(\nu_1)\ldots(\nu_q)\,|(\nu_{q+1})\ldots(\nu_n)|}\, e^{(\nu_{q+1})} \wedge \ldots \wedge e^{(\nu_n)}\,. \tag{C.4}$$

C.2 Vielbeins and spin-connection components of a unit N-sphere

The line-element which defines the geometry of a unit N-sphere is of the following form

$$ds^2 = d\Omega_N^2 = d\theta_1^2 + \sum_{i=2}^{N} \left(\prod_{j=1}^{i-1} \sin^2\theta_j \right) d\theta_i^2\,. \tag{C.5}$$

It is straightforward to deduce that the vielbeins for the geometry above are given by

$$e^{(\bar{m})}{}_{\bar{1}} = \delta^{\bar{m}}{}_{\bar{1}}, \qquad e^{(\bar{m})}{}_{\bar{n}} = \prod_{j=1}^{n-1} \sin\theta_j\; \delta^{\bar{m}}{}_{\bar{n}}, \quad 1 < n \leq N, \tag{C.6}$$

while the spin-connection components can be expressed in a compact form as

$$\begin{aligned} \omega_{\bar{i}}^{(\bar{m})(\bar{n})} = &\sum_{k=2}^{N} \delta^{\bar{k}}{}_{\bar{i}} \sum_{j=1}^{k-1} \delta^{\bar{m}}{}_{\bar{k}}\, \delta^{\bar{n}}{}_{\bar{j}} \cot\theta_j \prod_{\ell=j}^{k-1} \sin\theta_\ell - \sum_{k=2}^{N} \delta^{\bar{k}}{}_{\bar{i}}\, \delta^{\bar{m}}{}_{\overline{k-1}}\, \delta^{\bar{n}}{}_{\bar{k}} \cos\theta_{k-1} \\ &- \sum_{k=3}^{N} \delta^{\bar{k}}{}_{\bar{i}} \sum_{j=1}^{k-2} \delta^{\bar{m}}{}_{\bar{j}}\, \delta^{\bar{n}}{}_{\bar{k}} \cos\theta_j \prod_{\ell=j+1}^{k-1} \sin\theta_\ell\,. \end{aligned} \tag{C.7}$$

In the above expressions we kept the same bar notation to be consistent with section 7.3.3.

C.3 Scalar mesons, probe branes and numerical spectra

There has been extensive work in the literature studying the bosonic spectra and states of probe-brane setups. Here we will limit ourselves to a minimal discussion and quoting the basic relations. This we

do for convenience with our numerical approach. Original and detailed work on this can be found in [160, 161].

Firstly, it is more useful to re-organize the probe brane junction in the following way: we have Dp/Dp+4, Dp/D$p+2$, and Dp/Dp systems. In the first class of probe-brane embeddings, p is allowed to have values $0 \leq p \leq 4$. For co-dimension one defect p can be $1 \leq p \leq 4$. Finally, for Dp/Dp systems we have $2 \leq p \leq 4$.

In all of the above systems, when considering an appropriate shift in the ℓ quantum number, the dynamics of the bosonic degrees of freedom can be mapped to those of scalar orthogonal fluctuations from the DBI action of the form

$$Y^A = \delta^A_9 \; L + 2\pi\alpha' \varphi^A \tag{C.8}$$

with A ranging from $5, \cdots, 9-p$, $4, \cdots, 9-p$ and $3, \cdots, 9-p$ for the Dp/D$p+4$, Dp/D$p+2$, and Dp/Dp systems respectively. Therefore, the most basic equations of motion that needs to be solve in the one pertaining to the above modes and we have:

$$\partial^2_\varrho f_\ell(\varrho) + \frac{3}{\varrho}\partial_\varrho f_\ell(\varrho) + \left(\frac{\bar{M}^2}{(1+\varrho^2)^{(7-p)/2}} - \frac{\ell(\ell+2)}{\varrho^2} \right) f_\ell(\varrho) = 0, \qquad \textit{for the Dp/Dp+4}\,, \tag{C.9}$$

$$\partial^2_\varrho f_\ell(\varrho) + \frac{2}{\varrho}\partial_\varrho f_\ell(\varrho) + \left(\frac{\bar{M}^2}{(1+\varrho^2)^{(7-p)/2}} - \frac{\ell(\ell+1)}{\varrho^2} \right) f_\ell(\varrho) = 0, \qquad \textit{for the Dp/Dp+2}\,, \tag{C.10}$$

$$\partial^2_\varrho f_\ell(\varrho) + \frac{1}{\varrho}\partial_\varrho f_\ell(\varrho) + \left(\frac{\bar{M}^2}{(1+\varrho^2)^{(7-p)/2}} - \frac{\ell^2}{\varrho^2} \right) f_\ell(\varrho) = 0, \qquad \textit{for the Dp/Dp}\,, \tag{C.11}$$

where in the above we have considered an appropriate decomposition of the φ^A and thus f is a scalar function of the radial coordinate. The final equation does not have normalizable solutions for zero angular momentum excitation and therefore the states with $\ell = 0$ are considered non-physical.

In [160, 161] the authors have given explicitly tables for some cases. For direct comparison, convenience and completeness, here we generate the numerical results and present them in tables that are complementary to those ones.

Our numerical approach for the bosonic spectra is the following:

- We are shooting from the $\Lambda_{\rm IR}$ to the $\Lambda_{\rm UV}$ by fine-tuning $\bar{M}^2$ such that the mode solutions are normalizable in the UV and small in amplitude [121].
- We choose as initial conditions $f(\varrho)|_{\varrho\to 0} = \varrho^\ell$ and $\partial_\varrho f(\varrho)|_{\varrho\to 0} = \ell\varrho^{\ell-1}$ [160, 161].
- We use $\Lambda_{\rm IR} = 10^{-7}$ and $\Lambda_{\rm UV} = 10$.

Appendix D

A spinor in the Dynamic AdS/YM background

We can now repeat the process described in section 3.2 for the case of the AdS/YM spacetime. The invariant line element is given by

$$ds^2 = r^2 dx^2_{(1,3)} + \frac{d\rho^2}{r^2}\,, \tag{D.1}$$

from which we can readily obtain the fünfbein, e^A_M. The fünfbein and the non-vanishing components of the spin-connection are given by

$$\begin{aligned} e^I_\mu &= \sqrt{\rho^2 + L(\rho)^2}\delta^I_\mu\,, \\ e^I_\rho &= \frac{1}{\sqrt{\rho^2 + L(\rho)^2}}\delta^I_\rho\,, \\ \omega^{r\nu}_\mu &= -\omega^{\nu r}_\mu = -(\rho + L(\rho)\ \partial_\rho L(\rho))\delta^\nu_\mu\,. \end{aligned} \tag{D.2}$$

The Dirac operator in this spacetime which is asymptotically AdS_5 (AAdS)using these conventions is given by

$$\not{D}_{\rm AAdS} = \sqrt{\rho^2 + L(\rho)^2}\gamma^\rho\partial_\rho + \frac{1}{\sqrt{\rho^2 + L(\rho)^2}}\gamma^\mu\partial_\mu + 2\frac{\rho + L(\rho)\ \partial_\rho L(\rho)}{\sqrt{\rho^2 + L(\rho)^2}}\gamma^\rho\,. \tag{D.3}$$

The action for a free spinor in the above geometry is given by

$$S_{1/2} = \int d^5x\ \rho^3\ \bar\Psi\left(\not{D}_{\rm AAdS} - m\right)\Psi\,, \tag{D.4}$$

where again we have used the square root of the metirc determinant from the top-down analyses rather than the one obtianed from our spacetime -as was done in the case of the bosonic sector of the theory. It is a straightforward task to vary the above action and obtain the equations of motion. Then, we promote the first-order equations of motion to second-order by acting on them with the differential operator $\frac{1}{r}\ \gamma^\mu\ \partial_\mu + r\ \gamma^\rho\ \partial_\rho$, and in such a way we construct a Klein-Gordon problem in terms of an

ordinary scalar function of the holographic radial coordinate ρ that reads

$$\begin{aligned}&\left(\partial_\rho^2+\frac{6}{r^2}\left(\rho+L\ \partial_\rho L\right)\partial_\rho+\frac{M^2}{r^4}-\frac{m^2}{r^2}-\frac{m}{r^3}\left(\rho+L\ \partial_\rho L\right)\ \gamma^\rho\right.\\&\left.+\frac{2}{r^4}\left((\rho^2+L^2)L\partial_\rho^2 L+(\rho^2+3L^2)(\partial_\rho L)^2+4\rho L\partial_\rho L+3\rho^2+L^2\right)\right)\psi=0\,.\end{aligned}\tag{D.5}$$

As a check of the above relation let us consider the limit $L\to 0$, in which the Dynamic AdS/QCD metric becomes AdS_5 and in that limit the equations of motion equation (D.5) reduces to

$$\left(\partial_\rho^2+\frac{6}{\rho}\partial_\rho+\frac{M^2}{\rho^4}+\frac{1}{\rho^2}\left(6-m^2-m\gamma^\rho\right)\right)\psi=0\,,\tag{D.6}$$

which is precisely what we should get in pure AdS_5 [82].

Appendix E

Group theory factors

In what follows, by G we denote the adjoint representation. Other representations are displayed by their Young Tableaux. This is a matrix of the group theory factors of the $SU(N)$ gauge group.

R	T(R)	C_2(R)	d(R)
G	N	N	N^2-1
$\square$	$1/2$	$(N^2-1)/2N$	N
$\square\square$	$(N+2)/2$	$(N-1)(N+2)/N$	$N(N+1)/2$
$\begin{smallmatrix}\square\\\square\end{smallmatrix}$	$(N-2)/2$	$(N+1)(N-2)/N$	$N(N-1)/2$
$\begin{smallmatrix}\square\\\square\\\square\end{smallmatrix}$	$(N-3)(N-2)/4$	$3(N-3)(N+1)/2N$	$N(N-1)(N-2)/6$

This is a matrix of the group theory factors of the $Sp(2N)$ gauge group.

R	T(R)	C_2(R)	d(R)
$\square$	$1/2$	$(2N+1)/4$	$2N$
G= $\square\square$	$N+1$	$N+1$	$N(2N+1)$
$\begin{smallmatrix}\square\\\square\end{smallmatrix}$	$N-1$	N	$N(2N-1)-1$

We present here the matrix of the group theory factors of the $SO(N)$ gauge group.

R	T(R)	C_2(R)	d(R)
$\square$	1	$(N-1)/2$	N
$\square\square$	$N+2$	N	$(N-1)(N+2)/2$
G = $\begin{smallmatrix}\square\\\square\end{smallmatrix}$	$N-2$	$N-2$	$N(N-1)/2$
spin(N: even)	$2^{\frac{N-8}{2}}$	$N(N-1)/16$	$2^{\frac{N-2}{2}}$
spin(N: odd)	$2^{\frac{N-7}{2}}$	$N(N-1)/16$	$2^{\frac{N-1}{2}}$

Finally, we include the group theory factors for the exceptional gauge theories G_2 and F_4 which are relevant to composite Higgs models with matter in a single representation of the gauge group.

Groups	$d(G)$	$T(G)$	$C_2(G)$	$d(F)$	$T(F)$	$C_2(F)$
F_4	52	9	9	26	3	6
G_2	14	4	4	7	1	2

In the above tables, T is half the Dynkin index, C_2 is the quadratic Casimir, and d is the dimension of the representation. The usual relation holds

$$C_2(R)d(R) = T(R)d(G)\,, \tag{E.1}$$

where by R we mean a sepcific representation. We also have that

$$T(R) = -T(\bar{R})\,. \tag{E.2}$$

References

[1] R. Abt, J. Erdmenger, N. Evans, and K. S. Rigatos, "Light composite fermions from holography," *JHEP* **11** (2019) 160, arXiv:1907.09489 [hep-th].

[2] J. Erdmenger, N. Evans, W. Porod, and K. S. Rigatos, "Gauge/gravity dynamics for composite Higgs models and the top mass," *Phys. Rev. Lett.* **126** no. 7, (2021) 071602, arXiv:2009.10737 [hep-ph].

[3] T. Nakas and K. S. Rigatos, "Fermions and baryons as open-string states from brane junctions," *JHEP* **12** (2020) 157, arXiv:2010.00025 [hep-th].

[4] J. Erdmenger, N. Evans, W. Porod, and K. S. Rigatos, "Gauge/gravity dual dynamics for the strongly coupled sector of composite Higgs models," *JHEP* **02** (2021) 058, arXiv:2010.10279 [hep-ph].

[5] J. M. Drummond, D. Nandan, H. Paul, and K. S. Rigatos, "String corrections to AdS amplitudes and the double-trace spectrum of $\mathcal{N} = 4$ SYM," *JHEP* **12** (2019) 173, arXiv:1907.00992 [hep-th].

[6] N. Evans and K. S. Rigatos, "Chiral symmetry breaking and confinement: separating the scales," *Phys. Rev. D* **103** (2021) 094022, arXiv:2012.00032 [hep-ph].

[7] K. S. Rigatos, "Nonintegrability of $L^{a,b,c}$ quiver gauge theories," *Phys. Rev. D* **102** no. 10, (2020) 106022, arXiv:2009.11878 [hep-th].

[8] K. S. Rigatos, "Non-integrability in AdS_3 vacua," *JHEP* **02** (2021) 032, arXiv:2011.08224 [hep-th].

[9] T. DeGrand and C. E. Detar, *Lattice methods for quantum chromodynamics*. 2006.

[10] J. Terning, *Modern supersymmetry: Dynamics and duality*. 2006.

[11] V. Pestun, "Localization of gauge theory on a four-sphere and supersymmetric Wilson loops," *Commun. Math. Phys.* **313** (2012) 71–129, arXiv:0712.2824 [hep-th].

[12] A. M. Polyakov, "Nonhamiltonian approach to conformal quantum field theory," *Zh. Eksp. Teor. Fiz.* **66** (1974) 23–42.

[13] S. Ferrara, A. F. Grillo, and R. Gatto, "Tensor representations of conformal algebra and conformally covariant operator product expansion," *Annals Phys.* **76** (1973) 161–188.

[14] G. Mack, "Duality in quantum field theory," *Nucl. Phys. B* **118** (1977) 445–457.

[15] R. Rattazzi, V. S. Rychkov, E. Tonni, and A. Vichi, "Bounding scalar operator dimensions in 4D CFT," *JHEP* **12** (2008) 031, arXiv:0807.0004 [hep-th].

[16] S. El-Showk, M. F. Paulos, D. Poland, S. Rychkov, D. Simmons-Duffin, and A. Vichi, "Solving the 3D Ising Model with the Conformal Bootstrap," *Phys. Rev. D* **86** (2012) 025022, arXiv:1203.6064 [hep-th].

[17] F. Kos, D. Poland, D. Simmons-Duffin, and A. Vichi, "Precision Islands in the Ising and $O(N)$ Models," *JHEP* **08** (2016) 036, arXiv:1603.04436 [hep-th].

[18] M. Lemos, "Lectures on chiral algebras of $\mathcal{N} \geqslant 2$ superconformal field theories," arXiv:2006.13892 [hep-th].

[19] M. Martone, "The constraining power of Coulomb Branch Geometry: lectures on Seiberg-Witten theory," in *Young Researchers Integrability School and Workshop 2020: A modern primer for superconformal field theories*. 6, 2020. arXiv:2006.14038 [hep-th].

[20] N. Gromov, "Introduction to the Spectrum of $N = 4$ SYM and the Quantum Spectral Curve," arXiv:1708.03648 [hep-th].

[21] S. R. Coleman, "The Quantum Sine-Gordon Equation as the Massive Thirring Model," *Phys. Rev. D* **11** (1975) 2088.

[22] J. Polchinski, "Dirichlet Branes and Ramond-Ramond charges," *Phys. Rev. Lett.* **75** (1995) 4724–4727, arXiv:hep-th/9510017.

[23] J. M. Maldacena, "The Large N limit of superconformal field theories and supergravity," *Adv. Theor. Math. Phys.* **2** (1998) 231–252, arXiv:hep-th/9711200.

[24] D. Z. Freedman and A. Van Proeyen, *Supergravity*. Cambridge Univ. Press, Cambridge, UK, 5, 2012.

[25] K. Becker, M. Becker, and J. H. Schwarz, *String theory and M-theory: A modern introduction*. Cambridge University Press, 12, 2006.

[26] E. Kiritsis, *String theory in a nutshell*. Princeton University Press, USA, 2019.

[27] L. J. Romans, "Massive N=2a Supergravity in Ten-Dimensions," *Phys. Lett. B* **169** (1986) 374.

[28] E. D'Hoker and D. Z. Freedman, "Supersymmetric gauge theories and the AdS / CFT correspondence," in *Theoretical Advanced Study Institute in Elementary Particle Physics (TASI 2001): Strings, Branes and EXTRA Dimensions*, pp. 3–158. 1, 2002. arXiv:hep-th/0201253.

[29] L. H. Ryder, *QUANTUM FIELD THEORY*. Cambridge University Press, 6, 1996.

[30] M. E. Peskin and D. V. Schroeder, *An Introduction to quantum field theory*. Addison-Wesley, Reading, USA, 1995.

[31] wiki, "Timeline of particle discoveries." https://en.wikipedia.org/wiki/Timeline_of_particle_discoveries.

[32] T. Regge, "Introduction to complex orbital momenta," *Nuovo Cim.* **14** (1959) 951.

[33] G. F. Chew and S. C. Frautschi, "Principle of Equivalence for All Strongly Interacting Particles Within the S Matrix Framework," *Phys. Rev. Lett.* **7** (1961) 394–397.

[34] G. Veneziano, "Construction of a crossing - symmetric, Regge behaved amplitude for linearly rising trajectories," *Nuovo Cim. A* **57** (1968) 190–197.

[35] L. Susskind, "Harmonic-oscillator analogy for the veneziano model," *Phys. Rev. Lett.* **23** (1969) 545–547.

[36] L. Susskind, "Structure of hadrons implied by duality," *Phys. Rev. D* **1** (1970) 1182–1186.

[37] H. Fritzsch, M. Gell-Mann, and H. Leutwyler, "Advantages of the Color Octet Gluon Picture," *Phys. Lett. B* **47** (1973) 365–368.

[38] D. J. Gross and F. Wilczek, "Ultraviolet Behavior of Nonabelian Gauge Theories," *Phys. Rev. Lett.* **30** (1973) 1343–1346.

[39] H. D. Politzer, "Reliable Perturbative Results for Strong Interactions?," *Phys. Rev. Lett.* **30** (1973) 1346–1349.

[40] I. J. R. Aitchison and A. J. G. Hey, *Gauge theories in particle physics: A practical introduction. Vol. 2: Non-Abelian gauge theories: QCD and the electroweak theory.* CRC Press, 2012.

[41] J. Erdmenger, N. Evans, I. Kirsch, and E. Threlfall, "Mesons in Gauge/Gravity Duals - A Review," *Eur. Phys. J. A* **35** (2008) 81–133, arXiv:0711.4467 [hep-th].

[42] P. W. Higgs, "Broken Symmetries and the Masses of Gauge Bosons," *Phys. Rev. Lett.* **13** (1964) 508–509.

[43] F. Englert and R. Brout, "Broken Symmetry and the Mass of Gauge Vector Mesons," *Phys. Rev. Lett.* **13** (1964) 321–323.

[44] G. S. Guralnik, C. R. Hagen, and T. W. B. Kibble, "Global Conservation Laws and Massless Particles," *Phys. Rev. Lett.* **13** (1964) 585–587.

[45] Z. Koba and H. B. Nielsen, "Reaction amplitude for n mesons: A Generalization of the Veneziano-Bardakci-Ruegg-Virasora model," *Nucl. Phys. B* **10** (1969) 633–655.

[46] M. A. Virasoro, "Alternative constructions of crossing-symmetric amplitudes with regge behavior," *Phys. Rev.* **177** (1969) 2309–2311.

[47] J. A. Shapiro, "Electrostatic analog for the virasoro model," *Phys. Lett. B* **33** (1970) 361–362.

[48] J. E. Paton and H.-M. Chan, "Generalized veneziano model with isospin," *Nucl. Phys. B* **10** (1969) 516–520.

[49] P. Ramond, "Dual Theory for Free Fermions," *Phys. Rev. D* **3** (1971) 2415–2418.

[50] A. Neveu and J. H. Schwarz, "Tachyon-free dual model with a positive-intercept trajectory," *Phys. Lett. B* **34** (1971) 517–518.

[51] J. Scherk and J. H. Schwarz, "Dual Models for Nonhadrons," *Nucl. Phys. B* **81** (1974) 118–144.

[52] T. Yoneya, "Connection of Dual Models to Electrodynamics and Gravidynamics," *Prog. Theor. Phys.* **51** (1974) 1907–1920.

[53] L. Brink, P. Di Vecchia, and P. S. Howe, "A Locally Supersymmetric and Reparametrization Invariant Action for the Spinning String," *Phys. Lett. B* **65** (1976) 471–474.

[54] S. Deser and B. Zumino, "A Complete Action for the Spinning String," *Phys. Lett. B* **65** (1976) 369–373.

[55] A. M. Polyakov, "Quantum Geometry of Bosonic Strings," *Phys. Lett. B* **103** (1981) 207–210.

[56] F. Gliozzi, J. Scherk, and D. I. Olive, "Supersymmetry, Supergravity Theories and the Dual Spinor Model," *Nucl. Phys. B* **122** (1977) 253–290.

[57] M. B. Green and J. H. Schwarz, "Anomaly Cancellation in Supersymmetric D=10 Gauge Theory and Superstring Theory," *Phys. Lett. B* **149** (1984) 117–122.

[58] D. J. Gross, J. A. Harvey, E. J. Martinec, and R. Rohm, "The Heterotic String," *Phys. Rev. Lett.* **54** (1985) 502–505.

[59] P. Candelas, G. T. Horowitz, A. Strominger, and E. Witten, "Vacuum Configurations for Superstrings," *Nucl. Phys. B* **258** (1985) 46–74.

[60] M. B. Green and J. H. Schwarz, "Supersymmetrical String Theories," *Phys. Lett. B* **109** (1982) 444–448.

[61] E. Bergshoeff, E. Sezgin, and P. K. Townsend, "Supermembranes and Eleven-Dimensional Supergravity," *Phys. Lett. B* **189** (1987) 75–78.

[62] E. Witten, "String theory dynamics in various dimensions," *Nucl. Phys. B* **443** (1995) 85–126, `arXiv:hep-th/9503124`.

[63] A. Sen, "Strong - weak coupling duality in four-dimensional string theory," *Int. J. Mod. Phys. A* **9** (1994) 3707–3750, `arXiv:hep-th/9402002`.

[64] B. Sathiapalan, "Duality in Statistical Mechanics and String Theory," *Phys. Rev. Lett.* **58** (1987) 1597.

[65] T. H. Buscher, "A Symmetry of the String Background Field Equations," *Phys. Lett. B* **194** (1987) 59–62.

[66] A. Giveon, E. Rabinovici, and G. Veneziano, "Duality in String Background Space," *Nucl. Phys. B* **322** (1989) 167–184.

[67] C. M. Hull and P. K. Townsend, "Unity of superstring dualities," *Nucl. Phys. B* **438** (1995) 109–137, `arXiv:hep-th/9410167`.

[68] L. J. Dixon, "SOME WORLD SHEET PROPERTIES OF SUPERSTRING COMPACTIFICATIONS, ON ORBIFOLDS AND OTHERWISE," in *Summer Workshop in High-energy Physics and Cosmology*. 10, 1987.

[69] W. Lerche, C. Vafa, and N. P. Warner, "Chiral Rings in N=2 Superconformal Theories," *Nucl. Phys. B* **324** (1989) 427–474.

[70] A. Strominger, S.-T. Yau, and E. Zaslow, "Mirror symmetry is T duality," *Nucl. Phys. B* **479** (1996) 243–259, arXiv:hep-th/9606040.

[71] A. Hanany and E. Witten, "Type IIB superstrings, BPS monopoles, and three-dimensional gauge dynamics," *Nucl. Phys. B* **492** (1997) 152–190, arXiv:hep-th/9611230.

[72] A. Giveon and D. Kutasov, "Brane Dynamics and Gauge Theory," *Rev. Mod. Phys.* **71** (1999) 983–1084, arXiv:hep-th/9802067.

[73] W. Nahm, "Supersymmetries and their Representations," *Nucl. Phys. B* **135** (1978) 149.

[74] E. Cremmer, B. Julia, and J. Scherk, "Supergravity Theory in Eleven-Dimensions," *Phys. Lett. B* **76** (1978) 409–412.

[75] I. C. G. Campbell and P. C. West, "N=2 D=10 Nonchiral Supergravity and Its Spontaneous Compactification," *Nucl. Phys. B* **243** (1984) 112–124.

[76] F. Giani and M. Pernici, "N=2 SUPERGRAVITY IN TEN-DIMENSIONS," *Phys. Rev. D* **30** (1984) 325–333.

[77] M. Huq and M. A. Namazie, "Kaluza-Klein Supergravity in Ten-dimensions," *Class. Quant. Grav.* **2** (1985) 293. [Erratum: Class.Quant.Grav. 2, 597 (1985)].

[78] A. Sagnotti, "Open Strings and their Symmetry Groups," in *NATO Advanced Summer Institute on Nonperturbative Quantum Field Theory (Cargese Summer Institute)*. 9, 1987. arXiv:hep-th/0208020.

[79] J. McGreevy, "String theory." https://ocw.mit.edu/courses/physics/8-821-string-theory-fall-2008/.

[80] A. Zaffaroni, "Introduction to the ads/cft correspondence." https://virgilio.mib.infn.it/~zaffaron/lezioniLosannafin.pdf.

[81] M. Henningson and K. Sfetsos, "Spinors and the AdS / CFT correspondence," *Phys. Lett. B* **431** (1998) 63–68, arXiv:hep-th/9803251.

[82] I. Kirsch, "Spectroscopy of fermionic operators in AdS/CFT," *JHEP* **09** (2006) 052, arXiv:hep-th/0607205.

[83] I. R. Klebanov and E. Witten, "AdS / CFT correspondence and symmetry breaking," *Nucl. Phys. B* **556** (1999) 89–114, arXiv:hep-th/9905104.

[84] M. Baggioli, *Applied Holography: A Practical Mini-Course*. SpringerBriefs in Physics. Springer, 2019. arXiv:1908.02667 [hep-th].

[85] P. Breitenlohner and D. Z. Freedman, "Positive Energy in anti-De Sitter Backgrounds and Gauged Extended Supergravity," *Phys. Lett. B* **115** (1982) 197–201.

[86] P. Breitenlohner and D. Z. Freedman, "Stability in Gauged Extended Supergravity," *Annals Phys.* **144** (1982) 249.

[87] J. D. Qualls, "Lectures on Conformal Field Theory," arXiv:1511.04074 [hep-th].

[88] S. Rychkov, *EPFL Lectures on Conformal Field Theory in D>= 3 Dimensions*. SpringerBriefs in Physics. 1, 2016. arXiv:1601.05000 [hep-th].

[89] L. Eberhardt, "Superconformal symmetry and representations," *J. Phys. A* **54** no. 6, (2021) 063002, arXiv:2006.13280 [hep-th].

[90] D. Poland, S. Rychkov, and A. Vichi, "The Conformal Bootstrap: Theory, Numerical Techniques, and Applications," *Rev. Mod. Phys.* **91** (2019) 015002, arXiv:1805.04405 [hep-th].

[91] M. Yamazaki, "Comments on Determinant Formulas for General CFTs," *JHEP* **10** (2016) 035, arXiv:1601.04072 [hep-th].

[92] G. Mack, "All unitary ray representations of the conformal group SU(2,2) with positive energy," *Commun. Math. Phys.* **55** (1977) 1.

[93] J. Kinney, J. M. Maldacena, S. Minwalla, and S. Raju, "An Index for 4 dimensional super conformal theories," *Commun. Math. Phys.* **275** (2007) 209–254, arXiv:hep-th/0510251.

[94] C. Cordova, T. T. Dumitrescu, and K. Intriligator, "Multiplets of Superconformal Symmetry in Diverse Dimensions," *JHEP* **03** (2019) 163, arXiv:1612.00809 [hep-th].

[95] F. A. Dolan and H. Osborn, "Superconformal symmetry, correlation functions and the operator product expansion," *Nucl. Phys. B* **629** (2002) 3–73, arXiv:hep-th/0112251.

[96] F. A. Dolan and H. Osborn, "On short and semi-short representations for four-dimensional superconformal symmetry," *Annals Phys.* **307** (2003) 41–89, arXiv:hep-th/0209056.

[97] S. Minwalla, "Restrictions imposed by superconformal invariance on quantum field theories," *Adv. Theor. Math. Phys.* **2** (1998) 783–851, arXiv:hep-th/9712074.

[98] L. Bianchi and M. Lemos, "Superconformal surfaces in four dimensions," *JHEP* **06** (2020) 056, arXiv:1911.05082 [hep-th].

[99] E. Pomoni, "4D $\mathcal{N} = 2$ SCFTs and spin chains," *J. Phys. A* **53** no. 28, (2020) 283005, arXiv:1912.00870 [hep-th].

[100] O. Aharony, S. S. Gubser, J. M. Maldacena, H. Ooguri, and Y. Oz, "Large N field theories, string theory and gravity," *Phys. Rept.* **323** (2000) 183–386, arXiv:hep-th/9905111.

[101] L. Brink, J. H. Schwarz, and J. Scherk, "Supersymmetric Yang-Mills Theories," *Nucl. Phys. B* **121** (1977) 77–92.

[102] G. T. Horowitz and A. Strominger, "Black strings and P-branes," *Nucl. Phys. B* **360** (1991) 197–209.

[103] E. Witten, "Baryons and branes in anti-de Sitter space," *JHEP* **07** (1998) 006, arXiv:hep-th/9805112.

[104] G. 't Hooft, "Dimensional reduction in quantum gravity," *Conf. Proc. C* **930308** (1993) 284–296, arXiv:gr-qc/9310026.

[105] S. S. Gubser, I. R. Klebanov, and A. M. Polyakov, "Gauge theory correlators from noncritical string theory," *Phys. Lett. B* **428** (1998) 105–114, arXiv:hep-th/9802109.

[106] E. Witten, "Anti-de Sitter space and holography," *Adv. Theor. Math. Phys.* **2** (1998) 253–291, arXiv:hep-th/9802150.

[107] D. Z. Freedman, S. D. Mathur, A. Matusis, and L. Rastelli, "Correlation functions in the CFT(d) / AdS(d+1) correspondence," *Nucl. Phys. B* **546** (1999) 96–118, arXiv:hep-th/9804058.

[108] S. Lee, S. Minwalla, M. Rangamani, and N. Seiberg, "Three point functions of chiral operators in D = 4, N=4 SYM at large N," *Adv. Theor. Math. Phys.* **2** (1998) 697–718, arXiv:hep-th/9806074.

[109] L. Rastelli and X. Zhou, "Mellin amplitudes for $AdS_5 \times S^5$," *Phys. Rev. Lett.* **118** no. 9, (2017) 091602, arXiv:1608.06624 [hep-th].

[110] G. Arutyunov, R. Klabbers, and S. Savin, "Four-point functions of 1/2-BPS operators of any weights in the supergravity approximation," *JHEP* **09** (2018) 118, arXiv:1808.06788 [hep-th].

[111] M. Henningson and K. Skenderis, "The Holographic Weyl anomaly," *JHEP* **07** (1998) 023, arXiv:hep-th/9806087.

[112] N. Beisert *et al.*, "Review of AdS/CFT Integrability: An Overview," *Lett. Math. Phys.* **99** (2012) 3–32, arXiv:1012.3982 [hep-th].

[113] N. Beisert, "The Dilatation operator of N=4 super Yang-Mills theory and integrability," *Phys. Rept.* **405** (2004) 1–202, arXiv:hep-th/0407277.

[114] P. Kraus, F. Larsen, and S. P. Trivedi, "The Coulomb branch of gauge theory from rotating branes," *JHEP* **03** (1999) 003, arXiv:hep-th/9811120.

[115] K. Skenderis and M. Taylor, "Kaluza-Klein holography," *JHEP* **05** (2006) 057, arXiv:hep-th/0603016.

[116] K. Skenderis and M. Taylor, "Holographic Coulomb branch vevs," *JHEP* **08** (2006) 001, arXiv:hep-th/0604169.

[117] K. A. Intriligator, "Maximally supersymmetric RG flows and AdS duality," *Nucl. Phys. B* **580** (2000) 99–120, arXiv:hep-th/9909082.

[118] N. R. Constable and R. C. Myers, "Exotic scalar states in the AdS / CFT correspondence," *JHEP* **11** (1999) 020, arXiv:hep-th/9905081.

[119] D. Z. Freedman, S. S. Gubser, K. Pilch, and N. P. Warner, "Continuous distributions of D3-branes and gauged supergravity," *JHEP* **07** (2000) 038, arXiv:hep-th/9906194.

[120] A. Karch and E. Katz, "Adding flavor to AdS / CFT," *JHEP* **06** (2002) 043, arXiv:hep-th/0205236.

[121] M. Kruczenski, D. Mateos, R. C. Myers, and D. J. Winters, "Meson spectroscopy in AdS / CFT with flavor," *JHEP* **07** (2003) 049, arXiv:hep-th/0304032.

[122] J. Babington, J. Erdmenger, N. J. Evans, Z. Guralnik, and I. Kirsch, "Chiral symmetry breaking and pions in nonsupersymmetric gauge / gravity duals," *Phys. Rev. D* **69** (2004) 066007, arXiv:hep-th/0306018.

[123] J. Erlich, E. Katz, D. T. Son, and M. A. Stephanov, "QCD and a holographic model of hadrons," *Phys. Rev. Lett.* **95** (2005) 261602, arXiv:hep-ph/0501128.

[124] C. V. Johnson, "D-brane primer," in *Theoretical Advanced Study Institute in Elementary Particle Physics (TASI 99): Strings, Branes, and Gravity*. 7, 2000. arXiv:hep-th/0007170.

[125] A. Karch, A. O'Bannon, and K. Skenderis, "Holographic renormalization of probe D-branes in AdS/CFT," *JHEP* **04** (2006) 015, arXiv:hep-th/0512125.

[126] K. Skenderis, "Lecture notes on holographic renormalization," *Class. Quant. Grav.* **19** (2002) 5849–5876, arXiv:hep-th/0209067.

[127] E. Witten, "Current Algebra Theorems for the U(1) Goldstone Boson," *Nucl. Phys. B* **156** (1979) 269–283.

[128] G. 't Hooft, "How Instantons Solve the U(1) Problem," *Phys. Rept.* **142** (1986) 357–387.

[129] T. Sakai and S. Sugimoto, "Low energy hadron physics in holographic QCD," *Prog. Theor. Phys.* **113** (2005) 843–882, arXiv:hep-th/0412141.

[130] T. Sakai and S. Sugimoto, "More on a holographic dual of QCD," *Prog. Theor. Phys.* **114** (2005) 1083–1118, arXiv:hep-th/0507073.

[131] A. Kehagias and K. Sfetsos, "The Black hole and FRW geometries of non-relativistic gravity," *Phys. Lett. B* **678** (2009) 123–126, arXiv:0905.0477 [hep-th].

[132] S. S. Gubser, "Dilaton driven confinement," arXiv:hep-th/9902155.

[133] S. Scherer and M. R. Schindler, "A Chiral perturbation theory primer," arXiv:hep-ph/0505265.

[134] L. Da Rold and A. Pomarol, "Chiral symmetry breaking from five dimensional spaces," *Nucl. Phys. B* **721** (2005) 79–97, arXiv:hep-ph/0501218.

[135] A. Karch, E. Katz, D. T. Son, and M. A. Stephanov, "Linear confinement and AdS/QCD," *Phys. Rev. D* **74** (2006) 015005, arXiv:hep-ph/0602229.

[136] T. Alho, N. Evans, and K. Tuominen, "Dynamic AdS/QCD and the Spectrum of Walking Gauge Theories," *Phys. Rev. D* **88** (2013) 105016, arXiv:1307.4896 [hep-ph].

[137] N. Evans and M. Scott, "Hyper-Scaling Relations in the Conformal Window from Dynamic AdS/QCD," *Phys. Rev. D* **90** no. 6, (2014) 065025, arXiv:1405.5373 [hep-ph].

[138] J. Erdmenger, N. Evans, and M. Scott, "Meson spectra of asymptotically free gauge theories from holography," *Phys. Rev. D* **91** no. 8, (2015) 085004, arXiv:1412.3165 [hep-ph].

[139] M. Scott, "Dynamic ads/qcd: A holographic approach to asymptotically free gauge theories." https://eprints.soton.ac.uk/410312/1/Thesis.pdf.

[140] M. Ammon and J. Erdmenger, *Gauge/gravity duality: Foundations and applications*. Cambridge University Press, Cambridge, 4, 2015.

[141] M. A. Shifman, A. I. Vainshtein, and V. I. Zakharov, "QCD and Resonance Physics. Theoretical Foundations," *Nucl. Phys. B* **147** (1979) 385–447.

[142] S. Dimopoulos, S. Raby, and L. Susskind, "Light Composite Fermions," *Nucl. Phys. B* **173** (1980) 208–228.

[143] D. B. Kaplan, "Flavor at SSC energies: A New mechanism for dynamically generated fermion masses," *Nucl. Phys. B* **365** (1991) 259–278.

[144] G. Ferretti and D. Karateev, "Fermionic UV completions of Composite Higgs models," *JHEP* **03** (2014) 077, arXiv:1312.5330 [hep-ph].

[145] A. V. R. Daniel Areán, Imgo Kirsch, "Private notes.".

[146] A. Faraggi and L. A. Pando Zayas, "The Spectrum of Excitations of Holographic Wilson Loops," *JHEP* **05** (2011) 018, arXiv:1101.5145 [hep-th].

[147] E. Witten, "Multitrace operators, boundary conditions, and AdS / CFT correspondence," arXiv:hep-th/0112258.

[148] N. Evans and K.-Y. Kim, "Holographic Nambu–Jona-Lasinio interactions," *Phys. Rev. D* **93** no. 6, (2016) 066002, arXiv:1601.02824 [hep-th].

[149] N. Itzhaki, J. M. Maldacena, J. Sonnenschein, and S. Yankielowicz, "Supergravity and the large N limit of theories with sixteen supercharges," *Phys. Rev. D* **58** (1998) 046004, arXiv:hep-th/9802042.

[150] E. Witten, "Anti-de Sitter space, thermal phase transition, and confinement in gauge theories," *Adv. Theor. Math. Phys.* **2** (1998) 505–532, arXiv:hep-th/9803131.

[151] C. Csaki, H. Ooguri, Y. Oz, and J. Terning, "Glueball mass spectrum from supergravity," *JHEP* **01** (1999) 017, arXiv:hep-th/9806021.

[152] R. C. Brower, S. D. Mathur, and C.-I. Tan, "Glueball spectrum for QCD from AdS supergravity duality," *Nucl. Phys. B* **587** (2000) 249–276, arXiv:hep-th/0003115.

[153] N. R. Constable and R. C. Myers, "Spin two glueballs, positive energy theorems and the AdS / CFT correspondence," *JHEP* **10** (1999) 037, arXiv:hep-th/9908175.

[154] E. Caceres and C. Nunez, "Glueballs of super Yang-Mills from wrapped branes," *JHEP* **09** (2005) 027, arXiv:hep-th/0506051.

[155] A. Fayyazuddin and M. Spalinski, "Large N superconformal gauge theories and supergravity orientifolds," *Nucl. Phys. B* **535** (1998) 219–232, arXiv:hep-th/9805096.

[156] O. Aharony, A. Fayyazuddin, and J. M. Maldacena, "The Large N limit of N=2, N=1 field theories from three-branes in F theory," *JHEP* **07** (1998) 013, arXiv:hep-th/9806159.

[157] M. Bertolini, P. Di Vecchia, M. Frau, A. Lerda, and R. Marotta, "N=2 gauge theories on systems of fractional D3/D7 branes," *Nucl. Phys. B* **621** (2002) 157–178, arXiv:hep-th/0107057.

[158] M. Kruczenski, D. Mateos, R. C. Myers, and D. J. Winters, "Towards a holographic dual of large N(c) QCD," *JHEP* **05** (2004) 041, arXiv:hep-th/0311270.

[159] I. R. Klebanov and M. J. Strassler, "Supergravity and a confining gauge theory: Duality cascades and chi SB resolution of naked singularities," *JHEP* **08** (2000) 052, arXiv:hep-th/0007191.

[160] R. C. Myers and R. M. Thomson, "Holographic mesons in various dimensions," *JHEP* **09** (2006) 066, arXiv:hep-th/0605017.

[161] D. Arean and A. V. Ramallo, "Open string modes at brane intersections," *JHEP* **04** (2006) 037, arXiv:hep-th/0602174.

[162] C. Nunez, A. Paredes, and A. V. Ramallo, "Unquenched Flavor in the Gauge/Gravity Correspondence," *Adv. High Energy Phys.* **2010** (2010) 196714, arXiv:1002.1088 [hep-th].

[163] D. Marolf, L. Martucci, and P. J. Silva, "Actions and Fermionic symmetries for D-branes in bosonic backgrounds," *JHEP* **07** (2003) 019, arXiv:hep-th/0306066.

[164] D. Marolf, L. Martucci, and P. J. Silva, "Fermions, T duality and effective actions for D-branes in bosonic backgrounds," *JHEP* **04** (2003) 051, arXiv:hep-th/0303209.

[165] L. Martucci, J. Rosseel, D. Van den Bleeken, and A. Van Proeyen, "Dirac actions for D-branes on backgrounds with fluxes," *Class. Quant. Grav.* **22** (2005) 2745–2764, arXiv:hep-th/0504041.

[166] M. Cederwall, A. von Gussich, B. E. W. Nilsson, P. Sundell, and A. Westerberg, "The Dirichlet super p-branes in ten-dimensional type IIA and IIB supergravity," *Nucl. Phys. B* **490** (1997) 179–201, arXiv:hep-th/9611159.

[167] E. Bergshoeff and P. K. Townsend, "Super D-branes," *Nucl. Phys. B* **490** (1997) 145–162, arXiv:hep-th/9611173.

[168] M. Ammon, J. Erdmenger, M. Kaminski, and A. O'Bannon, "Fermionic Operator Mixing in Holographic p-wave Superfluids," *JHEP* **05** (2010) 053, arXiv:1003.1134 [hep-th].

[169] R. Heise and H. G. Svendsen, "A Note on fermions in holographic QCD," *JHEP* **08** (2007) 065, arXiv:0706.2253 [hep-th].

[170] J. N. Laia and D. Tong, "Flowing Between Fermionic Fixed Points," *JHEP* **11** (2011) 131, arXiv:1108.2216 [hep-th].

[171] E. Witten, "Baryons in the 1/n Expansion," *Nucl. Phys. B* **160** (1979) 57–115.

[172] J. Erdmenger, J. Grosse, and Z. Guralnik, "Spectral flow on the Higgs branch and AdS / CFT duality," *JHEP* **06** (2005) 052, arXiv:hep-th/0502224.

[173] R. Camporesi and A. Higuchi, "On the Eigen functions of the Dirac operator on spheres and real hyperbolic spaces," *J. Geom. Phys.* **20** (1996) 1–18, arXiv:gr-qc/9505009.

[174] J. Erdmenger and I. Kirsch, "Mesons in gauge / gravity dual with large number of fundamental fields," *JHEP* **12** (2004) 025, arXiv:hep-th/0408113.

[175] T. A. Ryttov and F. Sannino, "Conformal Windows of SU(N) Gauge Theories, Higher Dimensional Representations and The Size of The Unparticle World," *Phys. Rev. D* **76** (2007) 105004, arXiv:0707.3166 [hep-th].

[176] K. Bitaghsir Fadafan, J. Cruz Rojas, and N. Evans, "Holographic description of color superconductivity," *Phys. Rev. D* **98** no. 6, (2018) 066010, arXiv:1803.03107 [hep-ph].

[177] D. Arean, I. Iatrakis, M. Järvinen, and E. Kiritsis, "V-QCD: Spectra, the dilaton and the S-parameter," *Phys. Lett. B* **720** (2013) 219–223, arXiv:1211.6125 [hep-ph].

[178] G. F. de Teramond and S. J. Brodsky, "Hadronic spectrum of a holographic dual of QCD," *Phys. Rev. Lett.* **94** (2005) 201601, arXiv:hep-th/0501022.

[179] G. Bali and F. Bursa, "Meson masses at large N(c)," *PoS* **LATTICE2007** (2007) 050, arXiv:0708.3427 [hep-lat].

[180] M. Jarvinen and E. Kiritsis, "Holographic Models for QCD in the Veneziano Limit," *JHEP* **03** (2012) 002, arXiv:1112.1261 [hep-ph].

[181] N. Evans and K. Tuominen, "Holographic modelling of a light technidilaton," *Phys. Rev. D* **87** no. 8, (2013) 086003, arXiv:1302.4553 [hep-ph].

[182] D. K. Hong and H.-U. Yee, "Holographic estimate of oblique corrections for technicolor," *Phys. Rev. D* **74** (2006) 015011, arXiv:hep-ph/0602177.

[183] J. Hirn and V. Sanz, "A Negative S parameter from holographic technicolor," *Phys. Rev. Lett.* **97** (2006) 121803, arXiv:hep-ph/0606086.

[184] C. D. Carone, J. Erlich, and J. A. Tan, "Holographic Bosonic Technicolor," *Phys. Rev. D* **75** (2007) 075005, arXiv:hep-ph/0612242.

[185] K. Agashe, C. Csaki, C. Grojean, and M. Reece, "The S-parameter in holographic technicolor models," *JHEP* **12** (2007) 003, arXiv:0704.1821 [hep-ph].

[186] K. Haba, S. Matsuzaki, and K. Yamawaki, "S Parameter in the Holographic Walking/Conformal Technicolor," *Prog. Theor. Phys.* **120** (2008) 691–721, arXiv:0804.3668 [hep-ph].

[187] A. Belyaev, A. Coupe, N. Evans, D. Locke, and M. Scott, "Any Room Left for Technicolor? Dilepton Searches at the LHC and Beyond," *Phys. Rev. D* **99** no. 9, (2019) 095006, arXiv:1812.09052 [hep-ph].

[188] A. Belyaev, K. Bitaghsir Fadafan, N. Evans, and M. Gholamzadeh, "Any room left for technicolor? Holographic studies of NJL assisted technicolor," *Phys. Rev. D* **101** no. 8, (2020) 086013, arXiv:1910.10928 [hep-ph].

[189] N. Arkani-Hamed, A. Cohen, E. Katz, and A. Nelson, "The Littlest Higgs," *JHEP* **07** (2002) 034, arXiv:hep-ph/0206021.

[190] H. Terazawa, K. Akama, and Y. Chikashige, "Unified Model of the Nambu-Jona-Lasinio Type for All Elementary Particle Forces," *Phys. Rev. D* **15** (1977) 480.

[191] J. Barnard, T. Gherghetta, and T. S. Ray, "UV descriptions of composite Higgs models without elementary scalars," *JHEP* **02** (2014) 002, arXiv:1311.6562 [hep-ph].

[192] G. Ferretti, "UV Completions of Partial Compositeness: The Case for a SU(4) Gauge Group," *JHEP* **06** (2014) 142, arXiv:1404.7137 [hep-ph].

[193] L. Randall and R. Sundrum, "A Large mass hierarchy from a small extra dimension," *Phys. Rev. Lett.* **83** (1999) 3370–3373, arXiv:hep-ph/9905221.

[194] R. Contino, Y. Nomura, and A. Pomarol, "Higgs as a holographic pseudoGoldstone boson," *Nucl. Phys. B* **671** (2003) 148–174, arXiv:hep-ph/0306259.

[195] K. Agashe, R. Contino, and A. Pomarol, "The Minimal composite Higgs model," *Nucl. Phys. B* **719** (2005) 165–187, arXiv:hep-ph/0412089.

[196] U. Gursoy, E. Kiritsis, L. Mazzanti, and F. Nitti, "Deconfinement and Gluon Plasma Dynamics in Improved Holographic QCD," *Phys. Rev. Lett.* **101** (2008) 181601, arXiv:0804.0899 [hep-th].

[197] R. Alvares, N. Evans, and K.-Y. Kim, "Holography of the Conformal Window," *Phys. Rev. D* **86** (2012) 026008, arXiv:1204.2474 [hep-ph].

[198] D. Croon, B. M. Dillon, S. J. Huber, and V. Sanz, "Exploring holographic Composite Higgs models," *JHEP* **07** (2016) 072, arXiv:1510.08482 [hep-ph].

[199] B. M. Dillon, "Neutral-naturalness from a holographic $SO(6)/SO(5)$ composite Higgs model," *Phys. Rev. D* **99** no. 11, (2019) 115008, arXiv:1806.10702 [hep-ph].

[200] Y. Nambu and G. Jona-Lasinio, "Dynamical Model of Elementary Particles Based on an Analogy with Superconductivity. 1.," *Phys. Rev.* **122** (1961) 345–358.

[201] M. Jarvinen, "Massive holographic QCD in the Veneziano limit," *JHEP* **07** (2015) 033, arXiv:1501.07272 [hep-ph].

[202] N. Evans, J. P. Shock, and T. Waterson, "Towards a perfect QCD gravity dual," *Phys. Lett. B* **622** (2005) 165–171, arXiv:hep-th/0505250.

[203] N. Evans and A. Tedder, "Perfecting the Ultra-violet of Holographic Descriptions of QCD," *Phys. Lett. B* **642** (2006) 546–550, arXiv:hep-ph/0609112.

[204] M. Luscher, "IMPROVED LATTICE GAUGE THEORIES," in *Summer School in Theoretical Physics, Session XLIII*, pp. 359–374. 1984.

[205] P. Hasenfratz and F. Niedermayer, "Perfect lattice action for asymptotically free theories," *Nucl. Phys. B* **414** (1994) 785–814, arXiv:hep-lat/9308004.

[206] M. Golterman and Y. Shamir, "Top quark induced effective potential in a composite Higgs model," *Phys. Rev. D* **91** no. 9, (2015) 094506, arXiv:1502.00390 [hep-ph].

[207] T. Appelquist, P. Rodrigues da Silva, and F. Sannino, "Enhanced global symmetries and the chiral phase transition," *Phys. Rev. D* **60** (1999) 116007, arXiv:hep-ph/9906555.

[208] R. Lewis, C. Pica, and F. Sannino, "Light Asymmetric Dark Matter on the Lattice: SU(2) Technicolor with Two Fundamental Flavors," *Phys. Rev. D* **85** (2012) 014504, arXiv:1109.3513 [hep-ph].

[209] G. Cacciapaglia, T. Flacke, M. Park, and M. Zhang, "Exotic decays of top partners: mind the search gap," *Phys. Lett. B* **798** (2019) 135015, arXiv:1908.07524 [hep-ph].

[210] G. Brooijmans *et al.*, "Les Houches 2019 Physics at TeV Colliders: New Physics Working Group Report," in *11th Les Houches Workshop on Physics at TeV Colliders: PhysTeV Les Houches: Contribution 8*. 2, 2020. arXiv:2002.12220 [hep-ph].

[211] T. Appelquist, J. Terning, and L. Wijewardhana, "The Zero temperature chiral phase transition in SU(N) gauge theories," *Phys. Rev. Lett.* **77** (1996) 1214–1217, arXiv:hep-ph/9602385.

[212] D. D. Dietrich and F. Sannino, "Conformal window of SU(N) gauge theories with fermions in higher dimensional representations," *Phys. Rev. D* **75** (2007) 085018, arXiv:hep-ph/0611341.

[213] D. Elander, M. Piai, and J. Roughley, "Probing the holographic dilaton," *JHEP* **06** (2020) 177, arXiv:2004.05656 [hep-th].

[214] D. Elander, M. Piai, and J. Roughley, "Dilatonic states near holographic phase transitions," arXiv:2010.04100 [hep-th].

[215] A. Pomarol, O. Pujolas, and L. Salas, "Holographic conformal transition and light scalars," *JHEP* **10** (2019) 202, arXiv:1905.02653 [hep-th].

[216] E. Bennett, D. K. Hong, J.-W. Lee, C. J. D. Lin, B. Lucini, M. Piai, and D. Vadacchino, "Sp(4) gauge theory on the lattice: towards SU(4)/Sp(4) composite Higgs (and beyond)," *JHEP* **03** (2018) 185, arXiv:1712.04220 [hep-lat].

[217] J. Londergan, J. Nebreda, J. Pelaez, and A. Szczepaniak, "Identification of non-ordinary mesons from the dispersive connection between their poles and their Regge trajectories: The $f_0(500)$ resonance," *Phys. Lett. B* **729** (2014) 9–14, arXiv:1311.7552 [hep-ph].

[218] **Hadron Spectrum** Collaboration, H.-W. Lin *et al.*, "First results from 2+1 dynamical quark flavors on an anisotropic lattice: Light-hadron spectroscopy and setting the strange-quark mass," *Phys. Rev. D* **79** (2009) 034502, arXiv:0810.3588 [hep-lat].

[219] R. A. Briceno, J. J. Dudek, R. G. Edwards, and D. J. Wilson, "Isoscalar $\pi\pi$ scattering and the σ meson resonance from QCD," *Phys. Rev. Lett.* **118** no. 2, (2017) 022002, arXiv:1607.05900 [hep-ph].

[220] **Extended Twisted Mass** Collaboration, M. Werner *et al.*, "Hadron-Hadron Interactions from $N_f = 2 + 1 + 1$ Lattice QCD: The ρ-resonance," *Eur. Phys. J. A* **56** no. 2, (2020) 61, arXiv:1907.01237 [hep-lat].

[221] M. Shifman, "Highly excited hadrons in QCD and beyond," in *1st Workshop on Quark-Hadron Duality and the Transition to pQCD*, pp. 171–191. 7, 2005. arXiv:hep-ph/0507246.

[222] N. Evans, P. Jones, and M. Scott, "Soft walls in dynamic AdS/QCD and the technidilaton," *Phys. Rev. D* **92** no. 10, (2015) 106003, arXiv:1508.06540 [hep-ph].

[223] W. Clemens and N. Evans, "A Holographic Study of the Gauged NJL Model," *Phys. Lett. B* **771** (2017) 1–4, arXiv:1702.08693 [hep-th].

[224] K. Bitaghsir Fadafan, W. Clemens, and N. Evans, "Holographic Gauged NJL Model: the Conformal Window and Ideal Walking," *Phys. Rev. D* **98** no. 6, (2018) 066015, arXiv:1807.04548 [hep-ph].

[225] W. Clemens, N. Evans, and M. Scott, "Holograms of a Dynamical Top Quark," *Phys. Rev. D* **96** no. 5, (2017) 055016, arXiv:1703.08330 [hep-ph].

[226] E. Eichten and K. D. Lane, "Dynamical Breaking of Weak Interaction Symmetries," *Phys. Lett. B* **90** (1980) 125–130.

[227] B. Holdom, "Raising the Sideways Scale," *Phys. Rev. D* **24** (1981) 1441.

[228] B. S. Kim, D. K. Hong, and J.-W. Lee, "Into the conformal window: Multirepresentation gauge theories," *Phys. Rev. D* **101** no. 5, (2020) 056008, arXiv:2001.02690 [hep-ph].

[229] R. Arthur, V. Drach, M. Hansen, A. Hietanen, C. Pica, and F. Sannino, "SU(2) gauge theory with two fundamental flavors: A minimal template for model building," *Phys. Rev. D* **94** no. 9, (2016) 094507, arXiv:1602.06559 [hep-lat].

[230] R. Arthur, V. Drach, A. Hietanen, C. Pica, and F. Sannino, "$SU(2)$ Gauge Theory with Two Fundamental Flavours: Scalar and Pseudoscalar Spectrum," arXiv:1607.06654 [hep-lat].

[231] E. Bennett, D. K. Hong, J.-W. Lee, C.-J. D. Lin, B. Lucini, M. Mesiti, M. Piai, J. Rantaharju,

and D. Vadacchino, "Sp(4) gauge theories on the lattice: quenched fundamental and antisymmetric fermions," arXiv:1912.06505 [hep-lat].

[232] E. Bennett, D. K. Hong, J.-W. Lee, C.-J. D. Lin, B. Lucini, M. Piai, and D. Vadacchino, "Sp(4) gauge theories on the lattice: $N_f = 2$ dynamical fundamental fermions," *JHEP* **12** (2019) 053, arXiv:1909.12662 [hep-lat].

[233] V. Ayyar, T. Degrand, D. C. Hackett, W. I. Jay, E. T. Neil, Y. Shamir, and B. Svetitsky, "Baryon spectrum of SU(4) composite Higgs theory with two distinct fermion representations," *Phys. Rev. D* **97** no. 11, (2018) 114505, arXiv:1801.05809 [hep-ph].

[234] A. Belyaev, G. Cacciapaglia, H. Cai, G. Ferretti, T. Flacke, A. Parolini, and H. Serodio, "Di-boson signatures as Standard Candles for Partial Compositeness," *JHEP* **01** (2017) 094, arXiv:1610.06591 [hep-ph]. [Erratum: JHEP 12, 088 (2017)].

[235] G. Ferretti, "Gauge theories of Partial Compositeness: Scenarios for Run-II of the LHC," *JHEP* **06** (2016) 107, arXiv:1604.06467 [hep-ph].

[236] V. Ayyar, T. DeGrand, M. Golterman, D. C. Hackett, W. I. Jay, E. T. Neil, Y. Shamir, and B. Svetitsky, "Spectroscopy of SU(4) composite Higgs theory with two distinct fermion representations," *Phys. Rev. D* **97** no. 7, (2018) 074505, arXiv:1710.00806 [hep-lat].

[237] T. DeGrand, M. Golterman, E. T. Neil, and Y. Shamir, "One-loop Chiral Perturbation Theory with two fermion representations," *Phys. Rev. D* **94** no. 2, (2016) 025020, arXiv:1605.07738 [hep-ph].

[238] M. E. Peskin and T. Takeuchi, "Estimation of oblique electroweak corrections," *Phys. Rev. D* **46** (1992) 381–409.

[239] **Particle Data Group** Collaboration, P. Zyla *et al.*, "Review of Particle Physics," *PTEP* **2020** no. 8, (2020) 083C01.

[240] I. R. Klebanov and E. Witten, "Superconformal field theory on three-branes at a Calabi-Yau singularity," *Nucl. Phys. B* **536** (1998) 199–218, arXiv:hep-th/9807080.

[241] J. P. Gauntlett, D. Martelli, J. Sparks, and D. Waldram, "Sasaki-Einstein metrics on S**2 x S**3," *Adv. Theor. Math. Phys.* **8** no. 4, (2004) 711–734, arXiv:hep-th/0403002.

[242] M. Cvetic, H. Lu, D. N. Page, and C. N. Pope, "New Einstein-Sasaki spaces in five and higher dimensions," *Phys. Rev. Lett.* **95** (2005) 071101, arXiv:hep-th/0504225.

[243] D. Martelli and J. Sparks, "Toric Sasaki-Einstein metrics on S**2 x S**3," *Phys. Lett. B* **621** (2005) 208–212, arXiv:hep-th/0505027.

[244] F. Canoura, J. D. Edelstein, L. A. Pando Zayas, A. V. Ramallo, and D. Vaman, "Supersymmetric branes on AdS(5) x Y**p,q and their field theory duals," *JHEP* **03** (2006) 101, arXiv:hep-th/0512087.

[245] F. Canoura, J. D. Edelstein, and A. V. Ramallo, "D-brane probes on L(a,b,c) Superconformal Field Theories," *JHEP* **09** (2006) 038, arXiv:hep-th/0605260.

[246] J. Erdmenger, R. Meyer, and J. P. Shock, "AdS/CFT with flavour in electric and magnetic Kalb-Ramond fields," *JHEP* **12** (2007) 091, arXiv:0709.1551 [hep-th].

[247] T. Azeyanagi, W. Li, and T. Takayanagi, "On String Theory Duals of Lifshitz-like Fixed Points," *JHEP* **06** (2009) 084, arXiv:0905.0688 [hep-th].

[248] S. Kachru, X. Liu, and M. Mulligan, "Gravity duals of Lifshitz-like fixed points," *Phys. Rev. D* **78** (2008) 106005, arXiv:0808.1725 [hep-th].